Titre: Title:	Characterization of Phenomena Governing Oxidation of Cyanobacteria Through Metagenomics
Auteur: Author:	Saber Moradinejad
Date:	2021
Type:	Mémoire ou thèse / Dissertation or Thesis
Référence: Citation:	Moradinejad, S. (2021). Characterization of Phenomena Governing Oxidation of Cyanobacteria Through Metagenomics [Thèse de doctorat, Polytechnique Montréal]. PolyPublie. https://publications.polymtl.ca/5625/

ÉCOLE POLYTECHNIQUE DE MONTRÉAL

affiliée à l'Université de Montréal

Characterization of phenomena governing oxidation of cyanobacteria through metagenomics

SABER MORADINEJAD

Département des génies civil, géologique et des mines

Thèse présentée en vue de l'obtention du diplôme de *Philosophiae Doctor*

Génie civil

Mars 2021

ÉCOLE POLYTECHNIQUE DE MONTRÉAL

affiliée à l'Université de Montréal

Cette thèse intitulée :

Characterization of phenomena governing oxidation of cyanobacteria through metagenomics

présentée par **Saber MORADINEJAD**

en vue de l'obtention du diplôme de : *Philosophiae Doctor*

a été dûment acceptée par le jury d'examen constitué de :

Yves COMEAU, président
Michèle PRÉVOST, membre et directeur de recherche
Sarah DORNER, membre et codirecteur de recherche
Arash ZAMYADI, member et codirecteur de recherche
Nicolas TROMAS, member
Ronald HOFMANN, member extrne

DEDICATION

To MAHSA , for her indescribable love…

برای مهسا

ACKNOWLEDGEMENTS

I would like to express my sincere gratitude to my research director Professor Michèle Prévost, and co advisors Dr. Arash Zamyadi and Professor Sarah Dorner for their continued support and guidance throughout my PhD. I would like to thank you all for priceless advice and for giving me the great opportunity of being a part of your team. Also, I would like to thanks Professor Benoit Barbeau for his support in answering my questions during my PhD project.

I acknowledge the members of my committee, Professor Ronald Hofmann and Professor Nicolas Tromas for taking interest in my work and examining my thesis.

My special thanks to Dr. Hana Trigui and Juan Francisco Guerra Maldonado for their amazing support at different stages of data analysis and omics related data.

My deepest appreciation goes to the secretary, technicians and research associates in the Department of Civil, Geological and Mining Engineering, particularly Laura, Jacinthe, Julie, Tetiana, Mireille and Yves for their excellent assistance. In addition, I thank the secretary of the Department of Civil, Geological and Mining Engineering for helping us and providing us with an ideal atmosphere.

I also gratefully acknowledge the financial support by the Genome Quebec and Genome Canada (ATRAPP) which made this research work possible.

Special thanks to my Polytechnique friends, Hamed, Farhad, Sanaz, Fatemeh, Liya, Faezeh, Pegah, Vahid and Lena. I am very grateful to all my colleagues in our research group and my fellow lab mates and officemates for their cooperative manner and friendly support.

Moreover, I am especially grateful to my wife Mahsa for her unconditional support and patience and for being part of my life project. I also thank my beloved family for everything they have done in my life and for their support.

RÉSUMÉ

L'apparition fréquente de proliférations de cyanobactéries toxiques dans les ressources d'eau douce constitue une menace pour les stations d'épuration d'eau potable en raison de la libération de métabolites et de l'accumulation potentielle de cyanobactéries dans les plantes. La pré-oxydation a été largement utilisée pour amortir l'entrée de cyanobactéries dans les stations d'épuration et pour éliminer les métabolites nocifs (par exemple les cyanotoxines, les composés du goût et de l'odeur). La sélection du meilleur scénario de pré-oxydation nécessite une compréhension de la dynamique des cyanobactéries et de leur comportement complexe pendant l'oxydation. Pourtant, on sait peu de choses sur la manière dont les communautés bactériennes/cyanobactériennes et leurs capacités fonctionnelles sous-jacentes réagiront à l'oxydation chimique. Pour répondre à cette question, nous nous sommes concentrés sur le lac Champlain, Québec, Canada, à une période de floraison des cyanobactéries, du 1er au 29 août, 2018.

L'objectif principal de cette recherche est d'étudier le devenir des cyanobactéries lors de l'oxydation par la génomique. Les objectifs spécifiques sont de déterminer (1) le devenir des cyanobactéries pendant l'oxydation en utilisant la cytométrie de flux, les analyses par microscopie électronique à balayage et la détection de carbone organique par chromatographie liquide, (2) la déformation morphologique des cyanobactéries pendant l'oxydation, (3) la composition du profil taxonomique et la persistance sélective potentielle pendant l'oxydation d'eau et (4) la capacité fonctionnelle de des cyanobactéries exposées à l'oxydation.

La première partie de ce projet de recherche consiste à étudier la réponse morphologique des cyanobactéries à l'oxydation chimique ainsi que l'impact de la fraction de matière organique à l'aide de la détection de carbone organique par chromatographie liquide. Une nouvelle technique microscope été appliquée pour étudier la réponse morphologique des cellules de cyanobactéries pendant l'oxydation. Des spectres distincts de la paroi cellulaire pour *Microcystis* et *Dolichospermum* après chloration et ozonation ont confirmé une déformation morphologique différente des espèces cyanobactériennes. Les résultats de microscopie électronique à balayage ont révélé la fragmentation des liaisons cellulaires dans *Dolichospermum* avant la lyse cellulaire. Les composants de la matière organique (substances humiques, biopolymères, éléments de construction, acides et substances naturelles) ont augmenté après la chloration et l'ozonation. La forte variation des biopolymères est attribuée à la libération de matière organique algale et/ou à la

fragmentation de la membrane cellulaire. Toutes les fractions se sont dégradées sous l'effet de l'oxydation du permanganate de potassium et du peroxyde d'hydrogène.

Pour la deuxième phase, nous évaluons la persistance et l'élimination sélective potentielle et les changements de composition de la communauté cyanobactérienne suite à l'oxydation. En utilisant un séquençage à haut débit (métagénomique shotgun), un changement net des taxons dominants a été observé pendant l'échantillonnage des proliférations : de la dominance initiale des proliférations par *Dolichospermum*/*Dolichospermum Sp.90* à une dominance de fin d'été par *Microcystis/Microcystis aeruginosa*. La composition de la structure des communautés bactériennes/cyanobactériennes a été progressivement modifiée après la chloration à faible dose en fonction de l'augmentation de la concentration et temps de contact (CT). Le permanganate de potassium et le peroxyde d'hydrogène ont provoqué des changements plus importants. Une composition des communautés de cyanobactérie similaire a été trouvée pour une faible exposition au chlore, au peroxyde d'hydrogène et au permanganate. Certaines espèces productrices de toxines (*Dolichospermum sp.90*) peuvent persister après l'oxydation, indépendamment de la différence significative dans la composition de la communauté imposée par les oxydants. Parmi les oxydants utilisés, seul le peroxyde d'hydrogène (10 mg/L) apparait comme une barrière efficace contre l'entrée des cyanobactéries dans les stations de traitement d'eau potable en diminuant l'abondance relative de tous les taxons et espèces (y compris certaines espèces productrices de toxines). En outre, nos résultats ont montré que le séquençage à haut débit était capable d'identifier différentes communautés (genre, espèce) que celles observées par dénombrement taxonomique des cellules.

Au stade final, les capacités fonctionnelles bactériennes et cyanobactériennes des communautés de prolifération de cyanobactéries à l'oxydation ont été étudiées. Des différences de capacité fonctionnelle sont observées entre le début (1er août) et la fin de la période de floraison (29 août) a été détectée après l'oxydation. Pour l'échantillon du 1er août, qui correspond aux Protéobactéries en tant que taxons principaux, les catégories de sous-systèmes "Métabolisme des composés aromatiques", "Glucides", "Réponse au stress" et "Acquisition du fer" ont été regroupées avec une faible exposition relative au chlore et au peroxyde d'hydrogène. L'augmentation de l'exposition au chlore, au permanganate et au peroxyde d'hydrogène a entraîné une diminution des catégories "Glucides" et "Acides aminés et dérivés". Il est intéressant de noter que les gènes liés à la "division cellulaire et au cycle cellulaire", au "métabolisme de l'azote" et à la "photosynthèse" ont montré une corrélation positive significative avec l'embranchement des cyanobactéries, qui était dominé

par *Dolichospermum* apres chlorination. Pour les échantillons du 29 août, aucun changement notable n'a été observé entre les échantillons de contrôle et les échantillons après oxydation, à l'exception de l'augmentation des éléments prophétiques, transposables, des plasmides, sous un CT relativement plus élevé de $KMnO_4$. Trois biomarqueurs de cyanobactéries (Heterocyst formation in Cyanobacteria and Transcription factors cyanobacterial *rpoD*-Like sigma factors) ont été identifiés dans l'analyse métagénomique et ont été utilisés pour suivre la capacité fonctionnelle de la communauté cyanobactérienne. La variation de l'abondance relative des biomarqueurs de cyanobactéries après exposition au chlore et au permanganate a été limitée (en présence d'une abondante *Microcystis*). Cependant, l'abondance relative des biomarqueurs de cyanobactéries diminue après le peroxyde d'hydrogène, dans les deux dates d'échantillonnage, indépendamment de l'abondance du genre *Dolichospermum* ou *Microcystis*. En ce qui concerne les gènes liés à la production de toxines, une corrélation positive significative a été observée entre les copies de gènes *mcyD* et la microcystin (MC) totale (intra et extra) dans l'eau brute. Ces résultats ont révélé un potentiel pour prédire la concentration de MC en utilisant un test basé sur la toxicité.

Cette étude fournit de nouvelles informations sur trois facteurs importants qui influencent l'efficacité de l'oxydation au sein d'une prolifération de cyanobactéries : la réponse morphologique des cyanobactéries, l'impact de la matière organique et la dynamique des profils taxonomiques/fonctionnels. Dans ce cas, la métagénomique s'est révélée être un outil efficace pour le dépistage et l'identification des cyanobactéries, tout en offrant une capacité de diagnostic pour évaluer les capacités fonctionnelles des communautés bactériennes et cyanobactériennes à diverses conditions d'oxydation. Ces résultats devraient être pris en compte dans la surveillance future et la sélection de scénarios de pré-oxydation efficaces dans le cadre de la gestion des efflorescences cyanobactériennes dans les sources d’eau potable.

ABSTRACT

The frequent occurrence of toxic cyanobacterial blooms in the freshwater resources poses a threat to drinking water treatment plants by metabolites release and potential cyanobacteria accumulation within the plants. Pre-oxidation has been widely used to dampen cyanobacterial shock before entering treatment plants and removing harmful metabolites (e.g. cyanotoxins, taste and odor compounds). The selection of the best pre-oxidation scenario requires an understanding of cyanobacteria's dynamics and its complex behavior during oxidation. Yet, little is known about how bacterial/cyanobacterial communities and their underlying functional capacities will respond to chemical oxidation. It is unclear how each cyanobacteria species may change morphologically; which genera and species of cyanobacteria are more susceptible/resistant to the oxidation; what are the oxidation impacts on the cyanobacterial community shifts and functional subsystems. To address this question, we focused on Lake Champlain, Quebec, Canada at a cyanobacterial bloom period, from August 1st to 29th 2018.

The main objective of this research is to study the fate of cyanobacteria during oxidation through genomics.The specific objectives of this study are to determine, (1) the fate of cyanobacteria during oxidation using flow cytometry, scanning electron microscopy (SEM) and liquid chromatography – organic carbon detection – organic nitrogen detection (LC-OCD-OND) analyses, (2) morphological deformation of cyanobacteria during oxidation, (3) taxonomic profile composition and the potential selective persistence during bloom oxidation and (4) the functional capacity of the cyanobacterial bloom to the oxidation.

The first part of this research project is to study cyanobacteria's morphological response to chemical oxidation alongside the impact of organic matter fraction using liquid chromatography organic carbon detection-organic nitrogen detection (LC-OCD-OND). A novel technique enhanced darkfield microscopy/hyperspectral imaging (EDM/HSI) was applied to study cyanobacteria's morphological response (cell) during oxidation. Distinct cell wall spectra for *Microcystis* and *Dolichospermum* following chlorination and ozonation confirmed different morphological deformation of cyanobacterial species. SEM results revealed the fragmentation of cell links in *Dolichospermum* before cell lysis. Organic matter components (humic-like substances, biopolymers, building blocks, low molecular weight acids and naturals) increased following chlorination and ozonation. The high variation of biopolymers is attributed to the algal organic

matter release and/or fragmentation of the cell membrane. All the fractions degraded under both potassium permanganate and hydrogen peroxide oxidation.

For the second phase, we assess potential selective persistence/removal and community composition changes within the cyanobacterial community following oxidation. Using high throughput sequencing (shotgun metagenomics), a clear shift in dominant taxa was observed during the bloom sampling: from initial bloom dominance by *Dolichospermum/Dolichospermum Sp.90* to a late summer dominance by *Microcystis/Microcystis aeruginosa*. The composition of bacterial/cyanobacterial communities' structure was progressively shifted after soft-chlorination with increasing CT, while potassium permanganate and hydrogen peroxide caused larger changes. A similar cyanobacterial community composition was found for low chlorine, low hydrogen peroxide and low permanganate exposure. Some toxin-producing species (*Dolichospermum sp.90*) could persist following oxidation regardless of the significant difference in the community composition imposed by oxidants. Among oxidants used, only hydrogen peroxide (10 mg/L) showed an efficient barrier against entering cyanobacteria to drinking water treatment plants by declining the relative abundance of all taxa and species (including some toxin-producing species). Also, our results showed that high throughput sequencing was able to identify different communities (genus, species) compared to taxonomic cell count.

At the final stage, bacterial and cyanobacterial functional capacity of the cyanobacterial bloom communities to oxidation were studied. A differentially abundant functional capacities between the beginning (August 1st) and the end of the bloom period (August 29th) has been detected after oxidation. For August 1st sample, which corresponds to Proteobacteria as the major taxa, “Metabolism of aromatic compounds”, “Carbohydrates”, “Stress response” and “Iron acquisition” subsystem categories were clustered with low relative exposure of chlorine and hydrogen peroxide. Increasing oxidant exposure of chlorine, permanganate and hydrogen peroxide caused a decrease in “Carbohydrates” and “Amino acids and derivatives” categories. Interestingly, “Cell division and cell cycle”, “Nitrogen metabolism” and “photosynthesis” related genes have shown a significant positive correlation with cyanobacteria phylum, which was dominated by *Dolichospermum* after chlorination. For August 29th samples no markedly, change was observed between control and after oxidation samples except the increase of prophage, transposable elements, plasmids, under relatively higher CT of $KMnO_4$. Three cyanobacteria biomarkers (Heterocyst formation in Cyanobacteria and Transcription factors cyanobacterial *rpoD*-Like sigma factors) were identified

in metagenomic analysis and were used to track the functional capacity of cyanobacterial community. The relative abundance variation of cyanobacteria biomarkers following chlorine and permanganate exposure was limited (in the presence of abundant *Microcystis*). However, the relative abundance of cyanobacteria biomarkers decreases following hydrogen peroxide, in both sampling dates regardless of the abundant genus *Dolichospermum* or *Microcystis*. In terms of the genes related to toxin production, a significant positive correlation was observed between *mcyD* gene copies and microcystin (MC) total (intra and extra) in raw water. These results revealed a potential to predict the MC concentration using toxicity-based test.

This study provided new insights into three important factors influencing the oxidation efficiency within a cyanobacterial bloom: cyanobacteria morphological response, the impact of the organic matter, and the taxonomic/functional profiles' dynamics. Here, metagenomics proved to be an effective tool for screening and identifying while also providing diagnostic ability to assess bacterial and cyanobacterial communities' functional capacity to various oxidation conditions. These findings should be considered in future monitoring and selecting efficient pre-oxidation scenarios within cyanobacterial bloom managements in drinking water resources.

TABLE OF CONTENTS

LIST OF TABLES

LIST OF FIGURES

LIST OF SYMBOLS AND ABBREVIATIONS

BMAA	β-MethylAmino- l-Alanine
BB	Building Blocks
BP	Biopolymers
CCL	Chemical Contaminant List
CYN	Cylindrospermopsin
DOC	Dissolved Organic Carbon
ddPCR	Droplet Digital Polymerase Chain Reaction
EDM	Enhanced Darkfield Microscopy
HSI	Hyper Spectral Imaging
LC- OCD-OND	Liquid Chromatography-Organic Carbon Detection-Organic Nitrogen Detection
LMW	Low Molecular Weight
MC	Microcystin
N	Nitrogen
P	Phosphorus
PCA	Principal Component Analysis
RDA	Redundancy analysis
STX	Saxitoxin
SEM	Scanning Electron Microscopy
T&O	Taste and Odor
USEPA	United States Environmental Protection Agency

LIST OF APPENDICES

CHAPTER 1 INTRODUCTION

Cyanobacteria is a group of prokaryote, photosynthetic, and gram-negative bacteria (Stanier and Cohen-Bazire, 1977; Zamyadi, 2011). Some cyanobacteria are labelled as potent producers of harmful metabolites (cyanotoxins) and taste and odor compounds (Fan et al., 2013a). Toxic metabolites can be released into the water bodies during cyanobacteria lifetime (Carmichael, 2013; Codd et al., 1994; Falconer, 2012; Fan et al., 2013a; Zamyadi et al., 2010a). Over 20 genera of cyanobacteria have been identified as toxic cyanobacteria (Health Canada, 2018). The presence of cyanotoxins in water bodies can cause serious problems for animals, fishes and humans. Liver damage, gastrointestinal and nervous system damage are examples of harmful metabolites effect on human bodies through consumption of contaminated water (Health Canada, 2018). The most problematic genera found in Canada are *Dolichospermum*, *Aphanizomenon*, *Microcystis*, *Planktothrix*, *Pseudoanabaena*, *Gleotrichia woronichina* (Health Canada, 2018).

Recently the occurrence of cyanobacterial bloom increased due to climate change (temperature increase) and eutrophication of the lakes (improper nutrient management) (Paerl and Paul, 2012; Wells et al., 2015). Several cyanobacterial bloom reported around the world, including North America, Lake Erie (Berry et al., 2017; Chaffin et al., 2019; Ho and Michalak, 2015), Lake Champlain (Fortin et al., 2015; McQuaid et al., 2011; Zamyadi et al., 2015a; Zamyadi et al., 2013b; Zamyadi et al., 2012b), Lake Winnipeg (Bishop et al., 2018; McKindles et al., 2019; Schindler et al., 2012) are the examples of the lakes which experienced cyanobacterial bloom in Canada in the recent years. Some of the reported cyanobacterial blooms occurred in drinking water sources such as Lake Erie, which provides water for drinking water treatment plants in the US and Canada. Therefore, cyanobacteria and their associated metabolites must be removed from the water through drinking water treatment processes. Due to the increasing occurrence of cyanobacterial bloom and cyanotoxin presence in freshwater bodies, a water quality guideline cyanotoxin concertation in drinking water has come into force. Canada's guideline set a threshold of 1.5 µg/L Total microcystin for the drinking water. This threshold in the US is 0.3 µg/L for children under 6 and 1.6 µg/L for adults and children older than 6 years; Australian guideline suggests 1.3 µg/L Total microcystin total (Health Canada, 2018).

The drinking water treatment process must be able to remove cyanobacterial cells and their associated dissolved metabolites. Conventional treatment processes (coagulation, flocculation and

filtration) are only efficient to remove cyanobacterial cells and the portion of the cyanotoxins which are associated within the cell (Henderson et al., 2010; Newcombe, 2009; Pivokonsky et al., 2015b; Zamyadi et al., 2013b). The conventional treatment process is not an efficient option to remove the dissolved cyanotoxins from the drinking water (Henderson et al., 2010; Newcombe, 2009; Pivokonsky et al., 2015b). In 2012, a breakthrough of cyanobacterial cells and microcystin was detected in a drinking water treatment plant in southern Quebec (Lake Champlain) (Zamyadi et al., 2012a). Besides, the chlorinated water results showed 2.4 µg/L of total microcystin. Chemical oxidation has been widely used as pre-oxidation and post-oxidation to remove cyanobacteria (Zamyadi et al., 2012a). Chlorine, ozone, potassium permanganate, hydrogen peroxide, chloramine and Ferrate are the oxidants that have been used against cyanobacterial bloom (Fan et al., 2013b).

Chemical oxidation may cause cell lysis/damage and cyanotoxin release into the water. Studies have shown oxidation efficiency may vary depending on the presence of different species of cyanobacteria and background water quality (e.g. organic matter, pH). It is unclear how each cyanobacteria species may change morphologically; which genera and species of cyanobacteria are more susceptible/resistant to the oxidation; what are the oxidation impacts on the cyanobacterial community shifts and functional subsystems (which controls the metabolites of the cells using genes). Answering these questions will shed light on the chemical oxidation process in the battle against cyanobacteria and associated metabolites.

This thesis is divided into nine chapters. Chapter 1 presents a general background on cyanobacteria and their metabolites and treatment options. Chapter 2 presents a comprehensive literature review on the oxidation of cyanobacteria and its effectiveness alongside genomic studies in the cyanobacteria context. Chapter 3 includes the research objectives, hypotheses and methodology of this study. Chapter 4 contains the first published paper in the Journal of *Toxins*, followed by chapter 5 as a second paper in the form of a published manuscript in *Toxins*. The results of the functional capacity during oxidation is in chapter 6. Chapter 7 presents the general discussion followed by conclusions and recommendations in chapter 8. Supplementary results of this study are presented in Chapter 9.

CHAPTER 2 LITERATURE REVIEW

The literature review chapter is divided into five sections. The sections address the occurrence of cyanobacteria and associated cyanotoxin (Section 2.1), treatment options of cyanobacteria and cyanotoxins (Section 2.2), chemical oxidation of cyanobacteria (Section 2.3), oxidation models (Section 2.4), and cyanobacteria and genomics (Section 2.5).

2.1 Occurrence of cyanobacteria, growth and, associated cyanotoxins

2.1.1 Cyanobacteria and associated cyanotoxins

As cyanobacteria may produce and release cyanotoxin, cyanobacterial bloom management includes cyanotoxin removal (United States Environmental Protection Agency (USEPA), 2009). USEPA listed cyanotoxins in Chemical Contaminant List 4 (CCL4), which includes anatoxin-a, cylindrospermopsin, microcystins, and saxitoxin (United States Environmental Protection Agency (USEPA), 2009). Different cyanotoxins may produce by different species of cyanobacteria. Table 2.1 represents different cyanotoxins, related species, and examples of toxic cyanobacterial bloom from 2001 worldwide.

Table 2.1 Cyanotoxins, examples of occurrence and their associated health problem

Toxin	Cyanobacteria	Example of Cyanobacteria or Toxin presence in the fresh water (reference)		Target organism, health problem
Microcystin **MC-LR** **MC-RR** **MC-LF** **MC-LW** **MC-LY** **MC-LA** **MC-YR**	*Dolichospermum sp., Microcystis spp., Nostoc, Oscillatoria, Planktothrix, Phorimidium sp., Arthaspira fusiformis, Hapalosiphon*	Lake Taihu, China, 2007 Carrol township, Ohio, USA, 2013 Toledo, Ohio, USA, 2014 Nile River, Egypt, 2013	(Zhang et al., 2010) (Bullerjahn et al., 2016) (Ndlela et al., 2016a; Ndlela et al., 2016b)	Liver, tumor promoter and chronic damage of liver
Anatoxin	*Aphanizomenon sp., Anabaena sp., Cylindrospermopsis sp., Oscillatoria spp.*	lake Aydat, France (2011-13) Tapacura reservoir, Brazil 2002	(Sabart et al., 2015) (Molica et al., 2005)	Nervous system, blocking neuromuscle
Cylindrospermopsin	*Aphanizomenon sp., Dolichospermum sp., Cylindrospermopsis sp., Umezakia, C. Phillipinesis, Rhaphidiopsis*	Lake Valrico and Little Lake Florida, USA, 2008 Constance Lake, Ontario, Canada 2001	(Yilmaz and Phlips, 2011) (Hamilton et al., 2005)	Liver, tissue damage and gastrointestinal problem
Saxitoxin	*Aphanizomenon sp., Dolichospermum sp., Cylindrospermopsis sp., Phorimidium spp., Lyngbya , Planktothrix*	Finland 2002 and 2003 Waikato River, New Zealand	(Rapala et al., 2005) (Kouzminov et al., 2007)	Nervous system, damage neuromuscle
BMAA	Wide range of species	Lake Winnipeg, Canada, 2016 Waterways of rural and urban, New South Wales, Australia, 2015-2017	(Bishop et al., 2018) (Main et al., 2018)	Brian, alzheimer (Hypothesized)

2.1.2 Cyanobacteria occurrence and growth

Fresh-water bodies are facing a higher frequency of cyanobacterial blooms due to an increase in temperature pattern (caused by climate change) and nutrients (Nitrogen (N) and Phosphorus (P)) enrichment (Paerl et al., 2011). The growth phase, production and release of intracellular metabolites such as cyanotoxin and taste and odor compounds are also attributed to the concertation of nutrients (Bortoli et al., 2014). Table 2.2 illustrates a summary of the selected papers in which the favorable N:P ratio for cyanobacteria (*Microcystis*) growth was studied. No clear correlation can be driven for the relationship of the N:P ratio and growth phase of cultured *Microcystis*.

Table 2.2 Summary of selected papers on nutrients relationship with cyanobacteria growth

Study	**N:P Ratio**	**Condition and comment**
(Lee et al., 2000)	10:16	*Microcystis* cultured
(Downing et al., 2005)	31.1:1	*Microcystis* cultured
(Marinho and de Oliveira e Azevedo, 2007)	3:1, 10:1, 15:1	*Microcystis* cultured (no significant change observed)
(Bortoli et al., 2014)	10:1, 20:1	*Microcystis* cultured (no significant change observed)

The relation of cyanotoxin production/release and the growth phase of cyanobacteria were previously studied. An experimental study (Marinho and de Oliveira e Azevedo, 2007) revealed that cyanotoxin release by *Microcystis aeruginosa* happened right after exponential growth and at the beginning of the stationary phase; the same results were obtained by (Lee et al., 2000; Marinho and de Oliveira e Azevedo, 2007). Cyanotoxin production under different nutrients conditions (different types of media) was studied by Bortoli et al. (2014) . Higher microcystin concertation was detected at low (1) and high (100) N:P ratio; the same results were reported by Vézie et al. (2002). Also, the correlation results showed no correlation between the growth phase and cyanotoxin production Bortoli et al. (2014). Cyanotoxin production phosphate limitation condition was studied by Krüger et al. (2012). At a favourable N:P ratio for the cyanobacteria growth, higher cyanotoxin (microcystin) was detected. Also, excess nitrogen was available due to limited phosphate, which caused provocation of the nitrogen-rich substances such as microcystins (Krüger

et al., 2012). Nitrite concentration may enhance due to the transformation of excess nitrogen (such as nitrate) to nitrite and causing cell membrane damage and cyanotoxin release, subsequently.

Cyanotoxin production and release might be affected by the variation of environmental variables such as pH, temperature. Qian et al. (2014) reported higher concentration of cyanotoxins (MC-LR, STX, and CYN) released at lower pH (pH<5), at 30 min incubation time. Different cyanotoxin release trends were reported for two different strains of *Microcystis aeruginosa* under 15^{o}c Ding et al. (2017). Temperature increase from 15^{o}C to 35^{o}C caused an increase in *Microcystis aeruginosa* growth. However, MC production decrease by increasing temperature from 25 ^{o}C to 35^{o}C (Celeste et al., 2017).

2.2 Summary of treatment options for cyanobacteria and cyanotoxin

Drinking water treatment processes are responsible for removing cyanobacteria and their associated cyanotoxins to control their adverse health effect from the water. Table 2.3 exhibits a summary of different drinking water treatment processes effect on the removal of cyanobacteria cells and their associated toxins.

Table 2.3 Different treatment processes efficiency on cyanobacteria and cyanotoxin removal

Treatment process	Effect on cells and dissolved toxin	Reference
Coagulation, Sedimentation	Efficient for cyanobacteria cell removal	(Gonzalez-Torres et al., 2014; Henderson et al., 2010; Newcombe, 2009; Pivokonsky et al., 2015a; Zamyadi et al., 2013b)
Dissolved Air Flotation	Efficient for cyanobacteria cell removal	(Henderson et al., 2008; Henderson et al., 2010; Teixeira et al., 2010)
Sand filtration	Efficient for cyanobacteria cell removal	(Grutzmacher et al., 2002; Ho et al., 2012; Ho et al., 2007)
Membrane processes	Efficient for cyanobacteria cell and dissolved toxin removal (except Micro Filtration)	(Alvarez, 2010; Campinas and Rosa, 2010; Dixon et al., 2011; Ho et al., 2011; Sorlini et al., 2013; Westrick et al., 2010)
Granular and Powder Activated Carbon	Efficient for dissolved metabolites removal (except MC-LA with PAC)	(Alvarez, 2010; Ho et al., 2011; Newcombe, 2009; Wang et al., 2007; Yan et al., 2012)
Oxidation	A comprehensive review of cyanobacteria efficiency is presented in the following section.	

Despite the efficiency of treatment processes on the removal of cyanobacteria and dissolved metabolites, Zamyadi et al. (2012b) reported cyanotoxin breakthrough (2.47 µg/L in chlorinated drinking water) and cell accumulation in a full-scale treatment plant following a cyanobacterial bloom. Also, Zamyadi et al. (2013c) reported cell accumulation on sludge bed of clarifier (1.5×10^6cells/mL) and 5.5 µg/L of MC-LR on the filter basin while the raw water cell concentration at intake point was lower than 400 cells/mL and toxin concentration was below detection limit. This example manifests the potential of cell/toxin breakthrough and cells accumulation in drinking water treatment plant even at low-risk water sources (low cell number). Thus, best treatment practices for both high/low cyanobacteria cell number in raw water are required to decrease breakthrough potential. Oxidation is widely used against cyanobacteria and its harmful metabolites. In the following section, the oxidation practices to remove cyanobacteria cells and associated cyanotoxins is reviewed.

2.2.1 Chemical oxidation of cyanobacteria and cyanotoxin

2.2.1.1 Chlorine (Cl_2)

Chlorine is a strong oxidant and commonly used as a disinfectant in the water industry. Negative charge and "lack of enzyme to transport OCl^- into cells" can cause cell destruction (He et al., 2016).

Daly et al. (2007) reported complete cell lysis of *Microcystis aeruginosa* at 4 mg/L, 6 mg/L, 8 mg/L, and 15 mg/L after 30 min reaction for 32×10^3 cells/mL, 37.8×10^3 cells/mL, 54×10^3 cells/mL , and 3×10^5 cells/mL, respectively. Fan et al. (2014a) and Fan et al. (2013b) showed that for 7×10^5 cells/mL, 3 mg/L of Cl_2 with 30 min of contact time is enough to achieve 97% cell lysis (*Microcystis aeruginosa*). Zamyadi et al. (2010a) found similar results for *Anabaena circinalis*. (Ding et al., 2010) reported 150 mg.min/L for complete cell lysis of 2×10^6 cells/mL of cyanobacteria. (Ma et al., 2012b) showed chlorine exposure between 20 and 80 mg.min/L increases K^+ release, which cause an enhance in cyanobacteria cell removal (*Microcystis aeruginosa*). These results stated that initial cell density and type of cyanobacteria affect the required chlorine exposure for a complete cyanobacteria cell lysis. This conclusion confirmed by Wert et al. (2013) which exhibited that *Microcystis aeruginosa* cell damage rate is higher than *Lyngbya sp*. and *Oscillatoria sp*..

Figure 2.1 manifests chlorine residual, exposure, (initial concentration 5 mg/L) for three different studies with different cell densities (*Microcystis aeruginosa*). The results revealed that chlorine decay rate is higher for higher cell density. Fan et al. (2014a) spiked cultured cyanobacteria cells into wastewater treatment plant effluent. On the other hand, Fan et al. (2013b) and Daly et al. (2007) spiked cultured cyanobacteria cells into the natural water. Results from these studies reveal that background water quality (Dissolved Organic Carbon-DOC, pH and etc.) have an impact on the chlorine decay rate as well as cyanobacteria cell density, and cyanobacteria type (Newcombe and Nicholson, 2004; Zamyadi et al., 2013d).

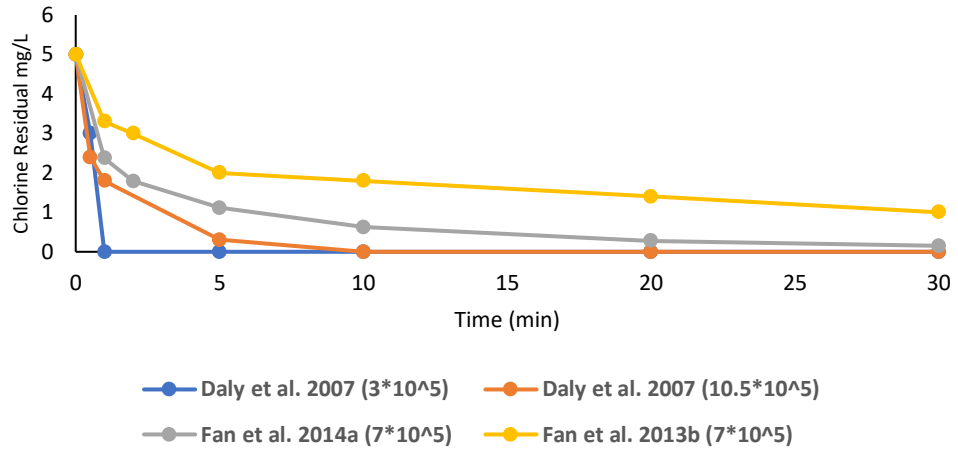

Figure 2.1 Comparison of chlorine residual for selected studies with the same cell density and cyanobacteria species

To date studies mostly focused on oxidation of unicellular cyanobacteria. (Fan et al., 2016) studied the effect of chlorination on colonial *Microcystis*. Results disclosed an increase in the required chlorine dose to decrease the intact cell percentage (for specific colonial size range). Furthermore, intact cell percentage increased as colonial size increase (for specific chlorine dosage). This observation suggests that colonial *Microcystis* are more resistant to chlorination than unicellular ones. Oxidation of colonial form of cyanobacteria required disaggregation of cells followed by unicellular fragmentation and cyanotoxin oxidation (He and Wert, 2016). To summarize, the way that cyanobacteria cells are present (colonial or unicellular) has an impact on cell lysis and cyanotoxin degradation as well as water quality characteristics, including organic matter (Figure 2.1 and Figure 2.2).

Microcystins

Chlorine is an effective oxidant agent for microcystin destruction (Acero et al., 2008; Huang et al., 2008; Zhang et al., 2016). Ho et al. (2006) studied the effect of chlorination on four variants of microcystin MC-RR, MC-LA, MC-LR, MC-YR in conventional treatment effluent. Results exhibited reaction rate as MC-YR> MC-RR> MC-LR> MC-LA. Results confirmed by Daly et al. (2007) in which a higher degradation rate for MC-LR was reported compared to the MC-LA. However, Ding et al. (2010) indicated that MC-LR oxidation rate is the lowest among different microcystin variants (MC-LW>MC-LF>MC-RR>MC-YR> MC-LA>MC-LR).

Discrete results may correspond to the background water quality which affects chlorine consumption and competition between the different MC-variants; as the chlorination of microcystin is pH and temperature dependent (Daly et al., 2007; Ding et al., 2010; Xagoraraki et al., 2005; Zamyadi et al., 2013d; Zamyadi et al., 2012a). Zamyadi et al. (2013d) revealed that MC oxidation rate in the presence of the cyanobacteria cells is lower than the absence of the cells due to lower available chlorine to reacts with the cyanotoxin (Figure 2.2).

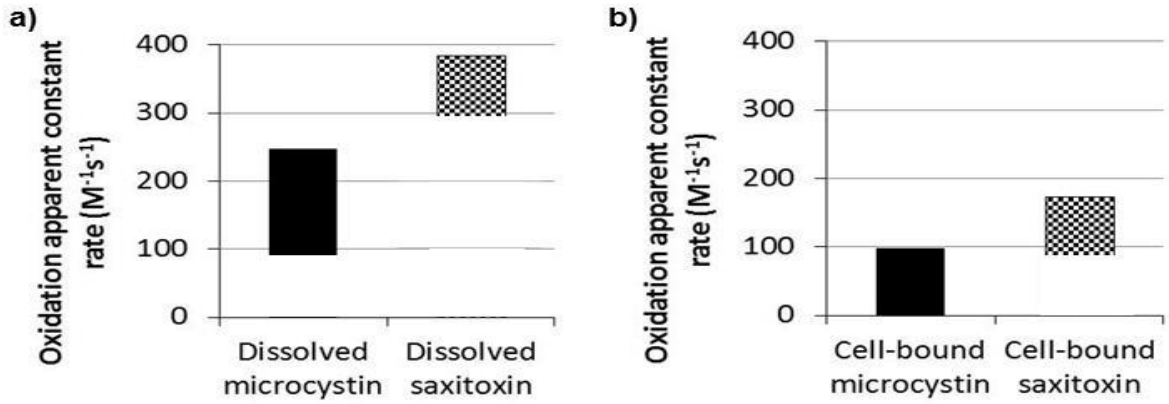

Figure 2.2 Effect of cyanobacteria presence on toxin oxidation (Zamyadi, 2014; Zamyadi et al., 2013d)

Cylindrospermopsin (CYN)

Cylindrospermopsin is reported as an easy cyanotoxin to remove using chlorination (Merel et al., 2010a). Three log CYN removal achieved by 30 min contact time of chlorine dosage of 5 mg/L, and, 4 mg/L for pH 6, and 7, respectively (Senogles et al., 2000; Senogles et al., 2002). Like microcystins, CYN oxidation in the presence of cyanobacteria cells is lower. Zamyadi et al. (2012a) reported in the presence of cyanobacteria cells (*Anabaena circinalis*, *Microcystis aeruginosa*, *Cylindrospermopsis raciborskii* and *Aphanizomenon issatsckenka*) CYN degradation

rate (8.2-186.4 $M^{-1}S^{-1}$) is much slower compared to the extracted CYN in the absence of cells (490 M^{-1} S^{-1}) from (Rodriguez et al., 2007c).

Saxitoxin

Zamyadi et al. (2010a) studied the effect of chlorination on saxitoxins (variants extracted from natural bloom) in presence and absence of *Anabaena Circinalis*. Results indicated higher chlorine decay rate in the presence of cyanobacteria cells; chlorine exposure of <15 mg.min/L degrade STX below detection limit. Zamyadi et al. (2010a) showed STX is easy to degrade using chlorine, previous studies reported higher degradation rate of STX compared to the other saxitoxin variants (STX> C2> GTX3=C1>GTX2) (Nicholson et al., 2003; Senogles-Derham et al., 2003). Zamyadi et al. (2012a) reported chlorine exposure CT> 60 mg.min/L can degrade intracellular and extracellular STX below 1µg/L (natural water, cell densities 50,000 cells/mL, and 200,000 cells/mL). Results also revealed STX degradation rate in presence of 50,000 cells/mL (170.9 $M^{-1}S^{-1}$) is slightly higher than its degradation in 200,000 cells/mL (132 $M^{-1}S^{-1}$).

Anatoxin

Previous studies showed that chlorination is not an effective option for anatoxin degradation (Newcombe and Nicholson, 2004; Rodriguez et al., 2007b; Rodriguez et al., 2007c; Vlad et al., 2014). Also, the efficiency of the anatoxin degradation using chlorine is highly dependent on pH and background water quality (Merel et al., 2010b).

Beta-MethylAmino-L-Alanine (BMAA)

Limited studies have been conducted on BMAA oxidation. Chen et al. (2017) studied BMAA chlorination and its reaction kinetics. Results demonstrated that at pH 7, BMAA decreased by 85% in the first minute of the reaction (second order, constant rate 2100 and 50000 $M^{-1}S^{-1}$ for pH 5.8 and pH 7 respectively). At the same time, free chlorine decreased by 50%. On the other hand, total chlorine decreased slightly in the first minutes of contact time. Authors stated, due to presence of alanine chain and amine group in BMAA structure, combined chlorine will be formed which explain the lower degradation rate of total chlorine. Results revealed that BMAA degradation starts with combined chlorine formation (Chen et al., 2017).

2.2.1.2 Potassium Permanganate ($KMnO_4$)

Potassium permanganate is being used as pre-oxidant to remove cyanobacteria cells. Ding et al. (2010) reported that 160 mg.min/L of permanganate exposure (CT) can cause complete cell lysis of lab-cultured *Microcystis aeruginosa* cells. Other studies, stated 10 mg/L of $KMnO_4$ with six hours of contact time is required to reach complete cell lysis of *Microcystis aeruginosa* (Fan et al., 2013a; Fan et al., 2013b; Fan et al., 2014a; Fan et al., 2014b). Ou et al. (2012) reported 2-5 mg/L $KMnO_4$ had a low influence on cell integrity of *Microcystis aeruginosa*. $KMnO_4$ reacts with the dissolved metabolites, mucilage followed by the cell wall destruction and caused cell lysis and cyanotoxin release (Gad and El-Tawel, 2016; Li et al., 2014; Naceradska et al., 2017; Piezer et al., 2020; Qi et al., 2016). Varying results indicate that the oxidation efficiency $KMnO_4$ may vary depending on the organic matter fraction in water, cyanobacteria cell density, lab-cultured or natural and, mono or mixed species (may change mucilage fraction around the cyanobacteria cells).

Microcystins

Rodriguez et al. (2007a) studied the effect of $KMnO_4$ on the degradation of microcystins. Results revealed complete microcystin (purified from a culture) oxidation in two hours contact time and dosage of 1.5 mg/L $KMnO_4$. Rodriguez et al. (2007a) reported degradation rates as MC-RR (418 $M^{-1}S^{-1}$)> MC-YR (405 $M^{-1}S^{-1}$)> MC-LR (357 $M^{-1}S^{-1}$). Also, authors stated that microcystin oxidation using $KMnO_4$ is pH depended. Such an observation is consistent with other study (Acero et al., 2008). Ding et al. (2010) reported degradation rate of different microcystin variants as MC-RR> MC-LR> MC-YR> MC-LW> MC-LF> MC-LA.

Fan et al. (2013a) studied the $KMnO_4$ oxidation of cyanobacteria cells and MC-LR with dosage 1-10 mg/L. After injecting $KMnO_4$, no increase in total MC-LR was observed (i.e. no oxidative stress to produce more toxin). However, MC-LR released in the first stages of oxidation (less than 5 min); followed by degradation of dissolved MC-LR. MC-LR release rate is lower than the degradation of dissolved MC-LR at the doses lower than 5mg/L $KMnO_4$. The reported results were confirmed by Li et al. (2014). A comparison between the Rodriguez et al. (2007a) and Fan et al. (2013a) revealed lower oxidation efficiency of microcystin in the presence of cells.

Cylindrospermopsin (CYN), Saxitoxin, Anatoxin

$KMnO_4$ oxidation is not a feasible oxidation practice against Cylindrospermopsin (Cheng et al., 2009; Rodriguez et al., 2007b). Also, negligible saxitoxin release (from *Anabaena circinalis*) and degradation of dissolved metabolites were reported by Ho et al. (2009).

$KMnO_4$ oxidation has been documented as an effective oxidation practice against Anatoxin; but pH dependent (Hall et al., 2000; Rodriguez et al., 2007c; Vlad et al., 2014). Hall et al. (2000) achieved more than 90% of anatoxin degradation with 2 mg/L $KMnO_4$ in treated water. Rodriguez et al. (2007c) observed complete anatoxin removal with 0.5 mg/L of $KMnO_4$ at pH 8 in natural water (DOC=3.6 mg/L).

(Chen et al., 2018) stated that BMAA degradation less than 10 percent, while $KMnO_4$ decreased by 5 percent. Results revealed that $KMnO_4$ had low impact on BMAA concentration (5.7×10^{-5} $M^{-1}S^{-1}$).

2.2.1.3 Ozone (O_3)

Different studies revealed ozonation potential to oxidize cyanobacteria cells (Coral et al., 2013; Ding et al., 2010; Fan et al., 2013b; Fan et al., 2014b). Wert et al. (2013) showed complete cell lysis of *Microcystis aeruginosa* at 0.63 mg/L of ozone (close to immediate demand of water background). *Lyngbya sp.* and *Oscillatoria sp.* required 5 mg/L of ozone for complete cell lysis in the same study. Also, lower cell damage rate has been reported for filamentous lab cultured *Lyngbya sp.* and *Oscillatoria sp.* than unicellular species by Wert et al. (2013). Zamyadi et al. (2015a) studied ozonation of natural bloom samples containing *Anabaena*, *Aphanizomenon*, *Microcystis aeruginosa*, and *Pseudanabaena*. Cell count based results exhibited that *Anabaena* was the most susceptible species to be oxidized with ozone while *Microcystis* had the lowest cell damage rate. This result is not in accordance with Wert et al. (2013) in which authors reported higher cell damage rate for *Microcystis*. Cell damage and oxidation could be affected by water quality characteristics, cell membrane, mixed or mono species, outer sheath thickness and growth phase (Coral et al., 2013; He and Wert, 2016; Wert et al., 2013; Zamyadi et al., 2013b; Zamyadi et al., 2013d). Coral et al. (2013) studied ozonation of a toxic strain of *Microcystis aeruginosa* and a nontoxic strain of *Anabaena flos-aquae*. Results reported a quick decrease in cell viability (CT<0.2 mg.min/L). However, at the same ozone exposure, taxonomic cell counts remained constant. This phenomenon indicates membrane damage following ozonation rather than complete cell disruption

at low ozone exposure. Also, algal organic matter released from the cyanobacteria depends on ozone dosage and pH (higher dosage and higher pH caused higher release).

Limited number of studies focused on fragmentation of cyanobacteria cells after oxidation. Wert et al. (2013) used digital flow cytometry to evaluate different cyanobacteria species following chlorination/ozonation. Results manifests cell wall damage for *Microcystis* cells. On the other hand, oxidation did not affect *Oscillatoria sp.* and *Lyngbya sp.* cell membrane while, loss of chlorophyll-a has been observed.

Microcystin

Ozone is a strong scavenger for microcystins. Several authors reported ozonation efficiency even at low dosage and contact time to degrade microcystins (Miao et al., 2010; Newcombe and Nicholson, 2004; Onstad et al., 2007; Rodriguez et al., 2007b; Wert et al., 2014). Ding et al. (2010) showed half-life of microcystin variants (MC-LW,MC-LF,MC-RR,MC-YR, MC-LA, MC-LR) are lower than 0.1 minutes for 0.5 mg/L ozone; and degradation rate is higher than 10,000 $M^{-1}S^{-1}$ at pH 7.6. Newcombe and Nicholson (2004) stated ozonation depends on the water quality background, especially Natural Organic Matter (NOM); the same conclusion was reported by (Brooke et al., 2006). Liu et al. (2010) reported 1 mg/L ozone with 5 min contact time can degrade 50% of MC-LR in filtered water. On the other hand, the same dosage and contact time could completely remove MC-LR in ultrapure water. Results revealed the competition between the NOM and MC-LR to consume ozone. Zamyadi et al. (2015a) reported degradation rate of MC-LR is lower than its degradation rate in the absence of cyanobacteria cells (Figure 2.2). The results unveil factors which may overestimate ozonation efficiency of cyanotoxins, including different nature of cultures (lab or natural, mixed or mono) and water quality matrix (Zamyadi et al., 2015a).

Cylindrospermopsin (CYN)

Digging in literature elucidates the high efficiency of CYN degradation using ozone. (Rodriguez et al., 2007b; Rodriguez et al., 2007c) reported that half-life of 0.1 min for CYN with 1 mg/L ozone dosage at pH 8. Similar results archived by (Cheng et al., 2009); complete CYN degradation with CT=1 mg.min/L. Also, no extracellular toxin increase has been observed by Cheng et al. (2009) which could be due to no CYN release or very quick oxidation of released toxin. Yan et al. (2016) reported high efficiency of ozonation on CYN degradation; whereas, no toxicity of ozonation by-products has been observed.

Saxitoxin, Anatoxin, and BMAA

Rositano et al. (2001) stated ozonation potential to degrade saxitoxin. Results demonstrated GTX3 and C2 are more susceptible to be oxidized with ozone than C1 and GTX2. Also, saxitoxin C2 had higher degradation rate compared to the MC-LR and Anatoxin.

Table 2.4 exhibits the studies on anatoxin degradation using ozone. Table 2.4 revealed the importance of pH and NOM. Anatoxin degradation is more efficient in low NOM and higher pH.

(Chen et al., 2018) reported BMAA degradation rate with ozone in natural water is lower than BMAA degradation in deionized water, 2.19×10^9 $M^{-1}S^{-1}$ and 2.82×10^9 $M^{-1}S^{-1}$, respectively.

Table 2.4 Summary of selected papers on the ozonation of Anatoxins

Reference	Ozone dose (mg/L)	Anatoxin removal %	Water condition
(Hall et al., 2000)	2	>90	Treated water
(Rositano et al., 2001)	1.1	100	Natural water, DOC= 5.3 mg/L
	1.7		DOC= 4.6 mg/L
	1.5		DOC= 5.7 mg/L
	>2.2		DOC= 15.5 mg/L
(Rodriguez et al., 2007c)	0.75	95	Natural water, DOC= 3.6 mg/L ,pH 8
(Onstad et al., 2007)	>2.0	95	Natural water, DOC= 13.1 mg/L ,30 min
(Al Momani, 2007)	1.8	46	Ultrapure water, pH=7
	2	63	pH=11

2.2.1.4 Hydrogen Peroxide (H_2O_2)

Zhou et al. (2013) reported intact cell decline for *Microcystis aeruginosa* 4 hours after H_2O_2 (10 mg/L) injection. Zhou et al. (2013) revealed that H_2O_2 will increase extracellular MC-LR concentration due to cell lysis and cyanotoxin release. However, Fan et al. (2013b) disclosed intact cell increase after two days of contact time (cell growth started to increase). This is the case because

there is no oxidant residue remains after the second day of the experiment while the cyanobacteria are still alive. Fan et al. (2014a) reported 91% and 93% decrease in intact cells of *Microcystis* after two days contact time; for 10 mg/L and 51 mg/L H_2O_2 respectively. Fan et al. (2013b) used same species, cell density, and H_2O_2 dosage with wastewater effluent; outcomes were 84% and 69%. In another study Matthijs et al. (2012) reached 2 log removal of *Planktothrix agardhiio* by applying 2 mg/L of H_2O_2 after 10 days contact time; microcystin oxidation revealed minimum concentration achieved after 12 days contact time. Burson et al. (2014) reported 3 log removal of *Alexandrium ostenfeldii* by injecting 50 mg/L and 27h contact time (real bloom). At the same time saxitoxin concentration decrease by 78%. To summarize, results from different studies revealed that H_2O_2 is able to inhibit the cell growth, however, the efficiency may vary depends on background water quality background, growth phase, type of species, mono or mixed species.

2.3 Oxidation models

The scientific, mechanistic model will help water utilities design the oxidation process and react appropriately against cyanobacteria cell and/or toxin breakthroughs in treated water. A review of studies on the oxidation of cyanobacteria and cyanotoxin revealed the negative effect of the cell presence on cyanotoxin oxidation (Figure 2.2). Zamyadi et al. (2013d) used following model to estimate cyanobacterial oxidation efficiency. Although, they reported the model overestimates oxidation efficiency in comparison with the experimental data (Figure 2.3).

$$A \rightarrow B \rightarrow C \qquad \text{Eq. 2-1}$$

$$A = A_0 e^{-k_r CT} \qquad \text{Eq. 2-2}$$

$$B = B_0 e^{-k_d CT} \times \frac{A_0}{1 - \frac{k_d}{k_r}} (e^{-k_d CT} - e^{-k_r CT}) \qquad \text{Eq. 2-3}$$

A_0 and A are the concentration of intracellular toxin at CT=0 and a given CT; B_0 and B are the concentration of dissolved toxin at CT=0 and a given CT, respectively; C is the degraded toxin at

given CT; K_r is the release rate of intracellular toxin; K_d is the degradation rate of dissolved toxin. Figure 2.3 exhibits difference between the current model and experimental oxidation efficiency for microcystin degradation in presence of *Microsystis* cells with $KMnO_4$. The bias source of model estimation accuracy could be related to water quality characteristics which have an effect on the oxidant degradation rate (Rodriguez et al., 2007a; Zamyadi et al., 2013d). Kim et al. (2018b) revealed that the most eminent water quality parameter during oxidation (permanganate) of microcystin are types and concentration of organic matter.

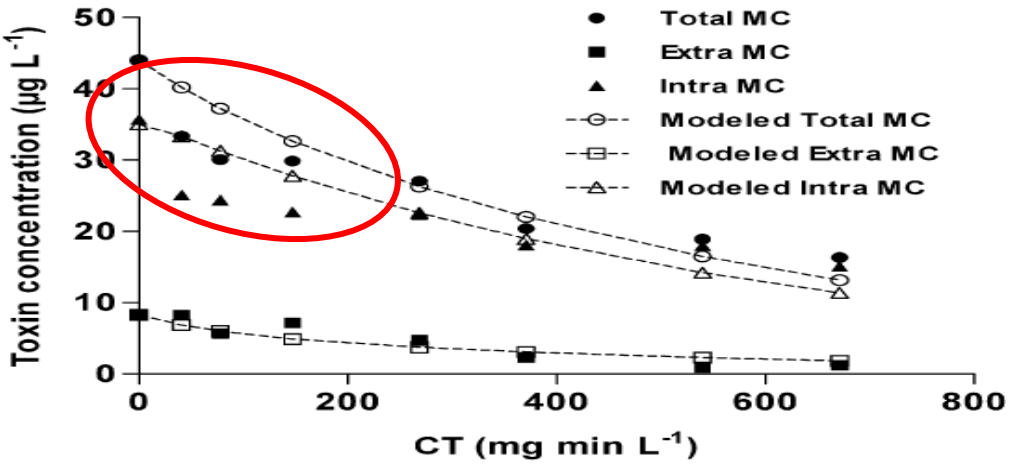

Figure 2.3 Comparison between the modeled and experimental MC concentration following $KMnO_4$ oxidation adapted from (Fan et al., 2013a)

2.4 High-throughput metagenomics sequencing technologies in cyanobacteria studies

In recent years, advances in sequencing technologies and statistical analysis tools to assess taxonomic dynamics of cyanobacterial communities have supported an extensive number of microbial-diversity studies. the studies unveiled new findings about the role of these organisms in the functioning and maintenance of aquatic ecosystems (Caporaso et al., 2012; Gonzalez et al., 2012; Großkopf and Soyer, 2014; Ininbergs et al., 2015; Logares et al., 2009; Raes and Bork, 2008). In particular, metagenomic analyses have improved the accuracy of quantitative approaches of cyanobacterial communities. High-throughput metagenomics analysis includes 16S rRNA sequencing and shotgun metagenomics sequencing. 16S rRNA sequencing produces hundreds of thousands of 16S rRNA fragments that enable taxonomic analysis into microbial communities simultaneously. However, it is noteworthy to mention that 16S rRNA analysis is less precise in

analyzing taxa (genus and species level) compared to the metagenomics (Quince et al., 2009; Ranjan et al., 2016). Alternatively, Shotgun metagenomic sequencing does not rely on a single diagnostic gene, it allows more in-depth analysis of taxonomy, metabolic pathways and functional capacities (Chen and Pachter, 2005). The majority of the cyanobacterial metagenomics related studies applied 16s rRNA gene sequencing to track the cyanobacterial community composition in several lakes and drinking water treatment plants (Berry et al., 2017; Casero et al., 2019; Eldridge and Wood, 2019; Fortin et al., 2015; Hou et al., 2018; Kim et al., 2018a; Pei et al., 2017; Tromas et al., 2017; Xu et al., 2018). Tromas et al. (2017) used 16S rRNA sequencing data of 8 years (between 2006 and 2013) to predict the occurrence of cyanobacterial bloom based on time course sequence data in Missisquoi Bay (Lake Champlain, Quebec, Canada). Lusty and Gobler (2020) used 16S rRNA to evaluate the mitigation of cyanobacterial bloom using H_2O_2. Results showed relative resistance of *Cyanobium* and *Cylindrospermopsis* to moderate H_2O_2 dose (4 mg/l); *Planktothrix* and *Microcystis* (abundant genus) were the most sensitive genera, respectively (Lusty and Gobler, 2020). Studies using shotgun metagenomic approach to assess the diversity and functional ability of cyanobacteria in bloom ecosystems are mainly focused on water resources such as lakes and reservoirs (Table 2.5). They significantly contributed to our understanding of cyanobacterial ecology and potential mechanisms of control (Affe et al., 2018; Cissell and McCoy, 2020; Lorenzi et al., 2019; Walter et al., 2018). Table 2.5 summarize the selected recent studies that used metagenomics approaches to study cyanobacteria under different environmental conditions. In this study, Shotgun metagenomic technology will help us to fully understand cyanobacterial community dynamics, then, to better predict the cyanobacterial fitness towards oxidation, according to the bacterial community composition shifts, persistence/removal ability, dynamics within functional subsystems and cyanotoxin production and release.

Table 2.5 Summary of selected recent studies on metagenomic/amplicon sequencing studies in cyanobacteria

Reference	Objective	Condition	Summary of results
(Pei et al., 2017)	Microbial community of sludge at different storage times	Lab cultured *Microcystis* Lab sludge, Natural water Coagulants $FeCl_3$, $AlCl_3$, PAFC	• *Microcystis* relative abundance in $AlCl_3$ lower than $FeCl_3$ and PAFC; consistent with intracellular MC • Genus *Microcystis* decline rate in $AlCl_3$ higher than $FeCl_3$ and PAFC • $FeCl_3$ sludge (8 days) is correlated with TN,TP
(Xu et al., 2018)	Microbial community of sludge	The sludge of sedimentation in six plants in China	• Cyanobacteria were dominant in two sites with high TN, TP • Dominant species *Microcystis, Cylindrospermopsis* and *Planktothrix* (higher CYN and MC in raw water); non-toxic *Synechococcus* for the second site • All species correlated with TN,TP, in raw water except *Synechococcus* which was correlated with Cl^- and SO_4
(Berry et al., 2017)	Spatiotemporal dynamics of cyanobacterial populations	Lake Erie, USA	• Dynamic fluctuation of cyanobacterial community during the bloom • Large shift in non-cyanobacterial community coincided with bloom • Correlation between bloom dynamics and Actinobacteria
(Affe et al., 2018)	Composition and functional profile of cyanobacteria	Camamu Bay, Brazil (Rain and dry seasons)	• Highest relative abundance: *Synechococcus* and *Prochlorococcus* • High *Prochlorococcus* during high tidal Limited variation in functional analysis
(Cissell and McCoy, 2020)	Taxonomic and functional diversity of benthic cyanobacterial mat	Benthic cyanobacterial mat Bonaire, Caribbean Netherlands	• Cyanobacteria (47.57%) and other bacteria (45.785) • Identifying regulatory genes for nitrogen, sulfur, phosphorus and iron metabolisms
(Walter et al., 2018)	Water quality and toxicity potential of three reservoirs	Campina Grande (Paraíba, Brazil)	• Cytometry analysis reported high relative abundance of cyanobacteria, while metagenomic showed only 10.6% • High abundance of cyanobacteria and their associated cyanotoxins under extremely drought condition
(Lorenzi et al., 2019)	biodiversity of cyanobacteria in drinking water reservoirs	Ingazeira and Munda Reservoirs, Northeastern Brazil	• Ingazeira: *Microcystis* abundant in dry season, *Cylindrospermopsis raciborskii* was abundant in rainy season • *mcyE* detected in both reservoirs and had correlation with MC concertation • *cyrJ* was not detected in the reservoirs

CHAPTER 3 RESEARCH OBJECTIVES, HYPOTHESES AND METHODOLOGY

3.1 Critical review and problem statement

Even though several studies address the oxidation of cyanobacteria and their harmful metabolites, there are still rooms to explore. Oxidation impact may vary for cell damage, metabolites release/removal due to slime layer, different strains of cyanobacteria and background water quality (e.g. pH and organic matter). Discrepancy of the results were documented for the metabolites released and removed during the oxidation. Understanding of morphological deformation caused by oxidation might help fill the gap between the expected and actual release. No quantitative information is available for cyanobacteria cell morphology during oxidation. Digital flowcytometry and Scanning Electron Microscopy (SEM) provide qualitative information on morphological changes.

High throughput sequencing has been used to study bacterial/cyanobacterial community diversity. However, limited studies focused on the cyanobacterial community's shifts during water treatment processes. Also, the cyanobacterial community's functional profile following oxidation will determine how cyanobacteria may respond to the oxidation stress. The functional capacity may help optimize the treatment process and decision making for bloom management in drinking water resources. To the best of our knowledge, no study has focused on understanding community shifts, potential selective resistance/removal and functional structure during chemical oxidation of cyanobacteria.

3.2 Objectives and hypotheses

3.2.1 General objective

The main objective of this research effort is to characterize phenomena governing oxidation of cyanobacteria through metagenomics.

3.2.2 Specific objectives

On a detailed level, specific objectives were:

1) Assess fate of cyanobacteria following oxidation via chlorine, ozone, potassium permanganate, and hydrogen peroxide using flowcytometry, SEM, and Liquid Chromatography with Organic Carbon and Nitrogen Detection (LC-OCD-OND).
2) Evaluate morphological deformation of cyanobacteria using Enhanced Dark Field Microscopy/Hyper Spectral Imaging (EDM/HSI) following oxidation with chlorine, ozone, potassium permanganate, and hydrogen peroxide.
3) Evaluate structural composition (at genus, species level) and diversity of cyanobacterial community following oxidation using high-throughput sequencing.
4) Evaluate the potential selective persistence/removal of cyanobacteria following oxidation.
5) Investigate functional capacity of cyanobacterial bloom to the oxidation stress caused by chlorine, potassium permanganate, and hydrogen peroxide.

The objectives of this study were based on the following hypothesis:

1) Morphological deformation of cyanobacteria species are different following oxidation and its quantification will unveil how oxidant reacts with cells; the concentrations of different types of organic matter (background water-algal) changes during oxidation and have an effect on the oxidation efficiency;

Originality: *This is the first study to quantify the morphological deformation/changes of cyanobacteria cells using EDM/HSI and LC-OCD-OND*

2) Bacterial/cyanobacterial community composition/diversity change/shift during the oxidation.

Originality: *This is the first study to show cyanobacterial community composition following oxidation*

3) Oxidation cause a selective persistence/removal of cyanobacteria species;

Originality: *This is the first study to assess potential persistence/removal of cyanobacteria species using high-throughput sequencing*

4) Oxidation stress cause a shift in cyanobacterial bloom functional capacity;

Originality: *This is the first study to assess functional capacity of the cyanobacterial bloom following oxidation stress*.

The results of this study were presented in three sections. The first article which was published in *Toxins* journal (May 2019) is using advanced spectroscopy and organic matter characterization to evaluate the impact of oxidation on cyanobacteria. The second article which was published in *Toxins* journal (Nov 2020) is focused on diversity assessment of the toxic cyanobacterial bloom during oxidation. The third article is submitted to Chemical Engineering Journal Advances (Feb 2021 highlight the functional capacity of the cyanobacterial bloom during oxidation.

3.3 Research Strategy and Methodology

Chemical oxidation is commonly used to manage cyanobacterial bloom in drinking water treatment plants. To fulfill the specific objectives, two different aspects of the experimental plan have been chosen to tackle cyanobacteria's fate during chemical oxidation.

These two approaches include cell-cultured based experiments and natural bloom experiments. Toxic cyanobacteria strains (including *Microcystis aeruginosa* CPCC 300 and *Dolichospermum sp.* CPCC 554) were cultured in BG-11 medium. The culture room is a part of CREDEAU facilities at Ecole Polytechnqiue Montreal. Cultures were incubated at 21^{o}C under 12-hr rotating light-darkness at an intensity of 70 µmol S^{-1} m^{-2}. Cultures were harvested at stationary phase (Figure 3.1). Cyanobacterial bloom happened in summer 2018 in Lake Champlain (Southern Quebec) and Lemieux reservoir in Granby (Quebec). Both sites are providing raw water for drinking water treatment plants. Cyanobacterial bloom samples were collected and transferred to the laboratory for oxidation experiments. The composition and characteristics of the sampled bloom is summarized in chapter 5. Chemical oxidation tests were performed using chlorine, ozone, potassium permanganate and hydrogen peroxide. The experimental procedure, therefore, was organized and summarized in each chapter.

The oxidation experiments were performed at CREDEAU laboratory. LC-OCD-OND samples were analyzed at water research center and University of Waterloo. Cyanotoxin samples were analyzed at Environmental Chemistry lab at Université de Montreal. Taxonomic cell count samples were analyzed at Polytechnique Montreal and Université du Quebec à Montreal. EDM/HSI samples were measured at at Polytechnique Montreal, chemical engineering department (Tavares

lab). Omics samples were extracted at Polytechnique Montreal and analyzed with the close collaboration of Genome Quebec/Canada and Shapiro lab (department of biology) at Universite de Montreal. Detailed methodology to analysis each parameters is presented in the following chapters.

Figure 3.1 Culture room at CREDEAU, Polytechnique Montreal

Table 3.1 Experimental approach to validate/in-validate of the hypothesis and related chapter in thesis

Specific objective	Hypothesis	Experimental Approach	Chapter
Assess fate of cyanobacteria following oxidation using flowcytometry, SEM, and Liquid Chromatography with Organic Carbon and Nitrogen Detection (LC-OCD-OND)	The concentrations of different types of organic matter (background water-algal) changes during oxidation and have an effect on the oxidation efficiency	Cultured based: *Microcystis* and *Dolichospermum* Oxidants: Cl_2, O_3, $KMnO_4$ and H_2O_2 Samples: LC-OCD-OND, DOC, SEM, EDM/HSI, Flowcytometry, Taxonomic cell count	4
Evaluate morphological deformation of cyanobacteria using Enhanced Dark Field Microscopy/Hyper Spectral Imaging (EDM/HSI) following oxidation	Morphological deformation of cyanobacteria species are different following oxidation and its quantification will unveil how oxidant reacts with cells		4
Evaluate structural composition (at genus, species level) and diversity of cyanobacterial community following oxidation using high-throughput sequencing	Bacterial/cyanobacterial community composition/diversity change/shift during the oxidation	Natural bloom: Lake Champlain, Granby reservoir Oxidants: Cl_2, O_3, $KMnO_4$ and H_2O_2 Samples: Omics, Taxonomic cell count, DOC, Flow cytometry, Cyanotoxins	5
Evaluate the potential selective persistence/removal of cyanobacteria following oxidation	Oxidation cause a selective persistence/removal of cyanobacteria species		5
Investigate functional capacity of cyanobacterial bloom to the oxidation stress	Oxidation stress cause a shift in cyanobacterial bloom functional capacity		6

CHAPTER 4 ARTICLE 1 - USING ADVANCED SPECTROSCOPY AND ORGANIC MATTER CHARACTERIZATION TO EVALUATE THE IMPACT OF OXIDATION ON CYANOBACTERIA

In this chapter, we discussed the morphological response of cyanobacteria (cultured-based) during oxidation using advanced spectroscopy. Also, the organic matter fractions during oxidation (algal and background) were characterized using liquid chromatography. The results showed a distinct morphological response of cyanobacteria species during oxidation. Such results alongside the organic matter characterization will help identify the potential bias source of different results between the oxidation models and full-scale oxidations. This chapter was published as a research paper in the Journal of *Toxins* on May 17th 2019. Supplementary information is presented in Appendix A.

USING ADVANCED SPECTROSCOPY AND ORGANIC MATTER CHARACTERIZATION TO EVALUATE THE IMPACT OF OXIDATION ON CYANOBACTERIA

Saber Moradinejad[1], Caitlin M. Glover[1], Jacinthe Mailly[1], Tahere Zadfathollah Seighalani[1], Sigrid Peldszus[2], Benoit Barbeau[1], Sarah Dorner[1], Michèle Prévost[1], Arash Zamyadi[1*]

1: Department of Civil, Geological & Mining Engineering, Ecole Polytechnique de Montréal, 2900 boulevard Édouard-Montpetit, Montréal, Québec, Canada H3T 1J4

2: Department of Civil & Environmental Engineering, University of Waterloo, Waterloo, Canada

* corresponding author: Arash.zamyadi@polymtl.ca

Abstract

Drinking water treatment plants throughout the world are increasingly facing the presence of toxic cyanobacteria in their source waters. During treatment, the oxidation of cyanobacteria changes cell morphology and can potentially lyse cells thereby release intracellular metabolites. In this study, a combination of techniques was applied to better understand the effect of oxidation with chlorine, ozone, potassium permanganate, and hydrogen peroxide on two cell cultures (*Microcystis aeruginosa*, *Dolichospermum sp.*) in Lake Champlain water. Flow cytometry and cell counting showed that cell lysis overestimates cell viability; this discrepancy was more pronounced for hydrogen peroxide and potassium permanganate than ozone and chlorine. Liquid chromatography with organic carbon and nitrogen detection was applied to monitor the changes in dissolved organic matter fractions following oxidation. Increases in the biopolymer fraction after oxidation with chlorine and ozone were attributed to the release of intracellular algal organic matter and/or fragmentation of the cell membrane. A novel technique, Enhanced Darkfield Microscopy with Hyperspectral Imaging (EDM/HSI), was applied to chlorinated and ozonated samples. Significant changes in the peak maxima and number of peaks were observed for the cell walls post-oxidation, but this effect was muted for the cell bound material, which remained relatively unaltered.

Keywords

cyanobacteria; oxidation; cell morphology; enhanced darkfield microscopy/hyperspectral imaging; intracellular organic matter

Key Contribution

This study is the first to use Enhanced Darkfield Microscopy with Hyperspectral Imaging to characterize the changes in cell spectra following oxidation with chlorine and ozone.

4.1 Introduction

Rising temperatures and the eutrophication of freshwaters have contributed to an increase in the frequency of cyanobacterial blooms (J. Alex, 2012; Paerl and Paul, 2012). Cyanobacterial cells are of concern because they can produce and release cyanotoxins as well as taste and odor (T&O) compounds. T&O compounds affect the aesthetic water quality, result in customer complaints, and

lower the trust customers have in their water (Watson, 2004). If ingested, cyanotoxins can cause gastroenteritis, cytotoxicity, liver damage, neurological effects and they have been linked to cancer, Alzheimer's disease and Motor Neurone Disease (Chernoff et al., 2017; Lévesque et al., 2014). To protect customers, regulatory agencies have proposed and in some cases set health-based guidelines and threshold alert levels for both cells and their metabolites (Chorus and Bartram, 1999; Health Canada and Federal-Provincial-Territorial Commitee on Drinking Water, 2016; United States Environmental Protection Agency (USEPA), 2015).

The removal of cyanobacteria and their metabolites is often a challenge for conventional water treatment (i.e., coagulation, flocculation, sedimentation and filtration) with both cyanotoxins and/or T&O compounds observed in finished drinking water (Pazouki et al., 2016; Zamyadi et al., 2015b; Zamyadi et al., 2012b). However, cyanobacteria can also breakthrough filtration in water treatment plants considered to be low-risk, i.e., with low intake cell concentrations in their source waters, and high-risk, i.e., during bloom events (Almuhtaram et al., 2018; Zamyadi et al., 2013c; Zamyadi et al., 2012b). Cyanobacterial breakthrough, particularly for low-risk plants, has been attributed to the accumulation of cells during treatment, e.g., in filter beds, in the sludge bed of sedimentation tanks, and in sludge thickeners (Pestana et al., 2016; Zamyadi et al., 2013c; Zamyadi et al., 2012b). Apart from the breakthrough of cyanobacteria and their metabolites, the presence of intracellular and extracellular organic matter (IOM and EOM) in treatment, increases the coagulant demand and the formation of disinfection by-products (Pivokonsky et al., 2015b).

A number of studies have evaluated the oxidation (e.g., ozone, chlorine, potassium permanganate, and hydrogen peroxide) of cyanobacteria and their metabolites (Coral et al., 2013; Ding et al., 2010; Fan et al., 2013a; Fan et al., 2014a; Zamyadi et al., 2015a). The impact of these oxidants ranges from cell damage to the release of metabolites through diffusion or cell lysis; the level of impact varies depending on the species of cyanobacteria present, presence of a slime layer, and the background water matrix, i.e., pH and background organic matter (Coral et al., 2013; Ding et al., 2010; Fan et al., 2016; He and Wert, 2016). To model the release of metabolites, previous work has applied pseudo first-order sequential reaction rates to track the release of intracellular metabolites and the subsequent oxidation of the extracellular metabolites, i.e., intracellular -- rate of release -- extracellular -- rate of oxidation -- oxidized metabolites (Zamyadi et al., 2013b; Jones, 1970). However, when model results have been compared with laboratory and full-scale oxidation data, models often overestimate the oxidation efficiency (Fan et al., 2013a; Zamyadi et al., 2013d).

In addition, the release of cyanotoxins and/or T&O compounds, can occur at very low doses (e.g., at detection limit for chlorine), making it very difficult to assess the potential risk during treatment (Zamyadi et al., 2016b; Zhang et al., 2017).

To better understand the changes in morphology that may be causing the discrepancy between expected release and actual release, previous work has used both Scanning Electron Microscopy (SEM) and Digital Flow Cytometry (Daly et al., 2007; Ding et al., 2010; Plummer and Edzwald, 2002; Wert et al., 2013). However, these techniques are qualitative and do not provide quantitative results. Enhanced Darkfield Microscopy with Hyperspectral Imaging (EDM/HSI) not only captures images of the sample, but also measures the visible wavelength spectrum (400 – 1000 nm) of each pixel. The black background in EDM allows the instrument to collect scattered light from the desired (i.e., cells) pixels of a sample. HSI has been used successfully to identify cyanobacteria blooms in laboratory and remote sensing applications (Paine et al., 2018; Randolph et al., 2008; Simis et al., 2005; Vincent et al., 2004); however, it has not yet been applied to evaluate the impact of oxidation on cyanobacteria cells.

In this study, a combination of techniques was used to explore the impact of oxidation on cyanobacteria cells. The objectives of this study were as follows: (1) to quantify changes of two cyanobacteria in natural water following oxidation with chlorine, ozone, hydrogen peroxide, and potassium permanganate with flow cytometry, SEM, and liquid chromatography with organic carbon and nitrogen detection (LC-OCD-OND) and (2) to compare these results against the morphological changes observed with EDM/HSI after oxidation with chlorine and ozone. To the best of the author's knowledge, this study presents the first assessment of morphological deformation of cyanobacteria after oxidation with EDM/HSI.

4.2 Materials and methods

4.2.1 Cyanobacteria culture sample preparation

Microcystis aeruginosa strain CPCC 300 (referred to as *Microcystis* in the manuscript) and *Anabaena sp.* strain CPCC 544 (referred to as *Dolichospermum* in the manuscript due to recent nomenclature changes) were cultured in BG-11 medium. Cultures were incubated at 21^{o}C under 12-hr rotating light-darkness at an intensity of 70 µmol S-1 m-2. Cultures were harvested at stationary phase and spiked into water from Lake Champlain to reach a concentration of 4×10^5

cells/mL. The Lake Champlain sample was collected from a water treatment plant intake (filtered before spiking the cells into the water) in southern Quebec, Canada in late October and early November of 2018. During this time, the utility measured its intake as having 5 – 6 mg/L dissolved organic carbon (DOC) and a pH of 6.5 – 7.

4.2.2 Preparation of oxidants and calculation of exposure

A 2000 mg/L as free chlorine stock solution was prepared from sodium hypochlorite (5.25%) on the day of the experiment. N,N-diethyl-p-phenylenediamine (DPD) colorimetric method was used to measure free chlorine concentration according to Standard Methods (SM) 4500-Cl G (American Public Health Association (APHA) et al., 2012). Chlorine doses of 1 mg/L, 2 mg/L, and 3 mg/L were added to the two cultures and exposed for 10-min, 20-min and 30-min of contact time. Samples were exposed at room temperature (22 °C) and chlorine residual measurements were taken to estimate oxidant exposure. Samples were quenched sodium thiosulfate at a dose of 1.1 mg/L per 1 mg/L chlorine from a stock solution of 3000 mg/L.

An ozone stock solution (50-60 mg/L) was prepared with gaseous ozone using bench scale ozone generator (additional details in Zamyadi et al. (2015a)). Ozone stock concentration and residual ozone in water samples were measured using SM 4500-O_3 (American Public Health Association (APHA) et al., 2012). Ozonation experiments were conducted with doses of 0.5 mg/L, 1 mg/L, and 2 mg/L with 5-min and 10-min contact time. Again, samples were quenched with 1.6 mg/L sodium thiosulfate per 1 mg/L ozone. Due to the rapid decay of ozone, residuals were below detection for the 0.5 mg/L and 1 mg/L doses.

Potassium permanganate ($KMnO_4$) crystals were dissolved in ultrapure water to prepare a stock solution of 5000 mg/L. Experiments were conducted with 2 mg/L and 5 mg/L with 120 min contact time. Samples were taken at specific times to measure potassium permanganate residual and measured according to the DPD colorimetric method ratio of 0.891 $KMnO_4/Cl_2$ SM 4500-Cl G (American Public Health Association (APHA) et al., 2012). After 120-min of contact time, 1.2 mg/L sodium thiosulfate per 1 mg/L $KMnO_4$ was used to quench further oxidation.

Hydrogen peroxide (H_2O_2) stock (10 g/L) was prepared from purchased solution of stabilized hydrogen peroxide (30%). Cyanobacteria suspension were dosed with 5 mg/L and 10 mg/L of hydrogen peroxide and exposed for 6-hrs of contact time. The hydrogen peroxide residual was

measured using colorimetric test kit (Chemetrics K-5510, Midlands, VA, U.S.). After the contact time, the residual was quenched with 1.2 mg/L sodium thiosulfate per 1 mg/L H_2O_2.

Oxidant exposures (CT) were calculated using Eq. 4-1:

$$CT = \int_0^t [Oxidant]dt = \frac{C_0}{k_{decay}}(e^{k_{decay}t} - 1) \qquad \text{Eq. 4-1}$$

where k_{decay} (min^{-1}) is the first order decay rate, t (min) is the exposure time, and C_0 (mg/L) is the initial concentration of oxidant at time zero. CT values for chlorine, ozone, potassium permanganate, and hydrogen peroxide are shown in the Table A.1 of the Supporting Information (SI).

CT values were subsequently used to calculate the cell lysis rate:

$$C = C_0 \times e^{-kR} \qquad \text{Eq. 4-2}$$

where C was concentration [total cell number (cells/mL)] at a given time, C_0 was the starting concentration [cell number (cells/mL) prior to oxidant exposure], *k* was the rate [$M^{-1}S^{-1}$], and R was the oxidant exposure [CT (mg-min/L)].

4.2.3 DOC and LC-OCD-OND

DOC and LC-OCD-OND samples were filtered via pre-rinsed 0.45µm membrane (Supor 45µm, 47m, PES PALL, Port Washington, NY, U.S.) and stored in carbon free glass vials. A 5310 total organic carbon analyser (Sievers Analytical Instruments, Boulder, CO, U.S.) was used to measure DOC. LC was coupled with OCD, OND, and UVD (254 nm) to track the DOC, DON, and UV responses over chromatographic retention times with various peaks identified and integrated according to (Huber et al., 2011). From the LC-OCD, the concentrations of biopolymers (e.g., high molecular weight (> 10 kDa) polysaccharides, proteins, amino-acids, and other components in extracellular polymeric substance), humic substances, building blocks (e.g., low molecular weight humic substances), low molecular weight (LMW) acids, and LMW neutrals were determined. An example chromatogram with peaks labeled can be found in Figure A.4. The added data from LC-OND and UVD provided the concentration of biopolymer DON and N/C ratio as well as humic substances DON, N/C ratio, and specific UV absorption (SUVA) at 254 nm.

4.2.4 Cell counts, morphology and integrity

Taxonomic cell counts were determined using an inverted microscope in a Sedgwick-Rafter chamber with 20X magnification on cells preserved with Lugol's Iodine (Baker and Larelle, 1999; Planas et al., 2002). Images of cyanobacteria during oxidation were captured using a SEM (JSM-7600 TFE, JEOL, Japan) according to the methods applied in Coral et al. (2013). Cell integrity was determined using flow cytometry (BD Accuri C6 Flow Cytometer, San Jose, CA, U.S.) and samples were stained with SYBR Green I (SG) and SG propidium iodide to determine total and compromised/dead cells (Buskey and Hyatt, 2006; Wert et al., 2013). A pre-test with pure cultures (*Microcystis* and *Dolichospermum*) was performed to define a suitable gating to differentiate cyanobacteria cells from other bacteria. This modified gating was used in all subsequent flow cytometry analysis.

Sample morphology was analyzed under optical microscope equipped with darkfield illumination and hyperspectral analysis or EDM/HSI (CytoViva, Auburn, Alabama, U.S.) (Théoret and Wilkinson, 2017). HSI was equipped to monitor wavelengths from 400 – 1000 nm for every pixel of the image, which was captured at 40X magnification. Pixel sizes were estimated to be 265 nm x 265 nm. Quenched samples were put on a microscope slide (500µL) and then dried under the fume hood to avoid the movement of liquid during EDM/HSI. A spot on the slide containing both cyanobacteria species (*Microcystis* and *Dolichospermum*) was selected to capture image and acquire spectral data.

4.3 Results and discussion

4.3.1 Cell viability post oxidation

Cultured cells (*Microcystis* and *Dolichospermum*) were spiked into Lake Champlain surface water prior to their exposure to chlorine, ozone, potassium permanganate, and hydrogen peroxide. Oxidant exposures (CTs) were calculated via decay rates according to Eq. 4-1 with the rates and CTs shown in Table A.1. The CT values for the five chlorine doses ranged from 6.9 – 36.7 mg-min/L. The two highest ozone exposures had CT values of 2.15 – 2.94 mg-min/L, but given the immediate decay of ozone, doses of 0.5 mg/L and 1 mg/L (at 5-min) had nominal CT values of 0 mg-min/L. Potassium permanganate was dosed at 2 mg/L and 5 mg/L for 120 mins or CT values of 172 mg-min/L and 456 mg-min/L and hydrogen peroxide was dosed at 5 mg/L and 10 mg/L for

6-hrs or CT values of 837 mg-min/L and 2168 mg-min/L. The impact of this oxidation on the fraction of viable vs. injured/dead cells (as determined with flow cytometry) with the cell numbers are shown in Figure 4.1. Across all oxidants, the control sample initially contained 4×10^5 cells/mL split equally between the *Microcystis* and *Dolichospermum*.

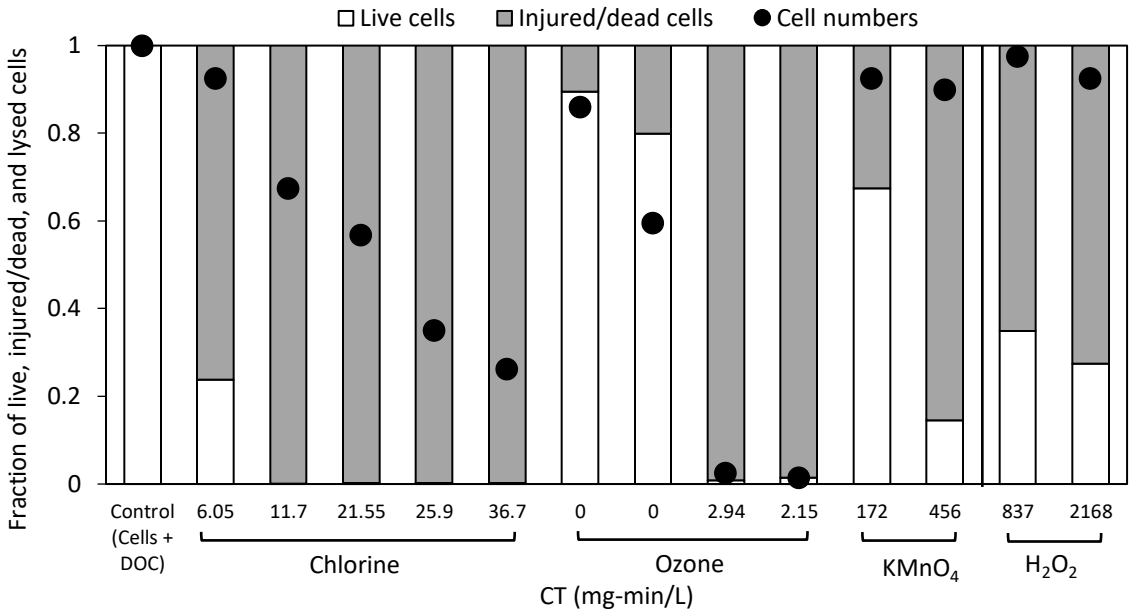

Figure 4.1 Impact of chlorine, ozone, potassium permanganate, and hydrogen peroxide on the fraction of viable cells relative to the injured/dead cells and cell number. The control sample contained 4×10^5 cells/mL of *Microcystis* and *Dolichospermum* in Lake Champlain water. Viable vs. injured/dead cell concentrations were determined with flow cytometry.

For chlorine, 24% of the cells remained viable at the CT of 6.9 mg-min/L whereas the taxonomic cell count had only dropped to 98%. CT values of 11.7 – 36.7 mg-min/L all had less than 1% viable cells, but the cell numbers continued to decrease until they reached 26% at which point 2×10^4 cells/mL of *Dolichospermum* and 7×10^4 cells/mL of *Microcysis* remained (Figure 4.1). In order to compare results with previous work, a rate of cell lysis was calculated from the taxonomic cell count results according to pseudo-first order reaction kinetics (Equation 2) and found to be 53 $M^{-1}S^{-1}$ ($R^2 = 0.91$) and 24 $M^{-1}S^{-1}$ ($R^2 = 0.90$) for *Dolichospermum* and *Microcystis*, respectively. The efficacy of chlorine here was similar both in the CT required (7 – 29 mg-min/L) and the lysis rates (30 – 170 $M^{-1}S^{-1}$; pH 7 – 8.6 with 5 – 20 $\times 10^4$ cells/mL in surface waters) with differences

attributed to the pH, specific background organic matter, and the presence of mixed species (Daly et al., 2007; Ding et al., 2010; Zamyadi et al., 2013c).

With ozone doses of 0.5 mg/L and 1 mg/L, cell viability was reduced by 10% and 20% and cell numbers decreased to 3.4 and 2.4 $\times$ 10^5 cells/mL, respectively (Figure 4.1). At 2 mg/L for both 5 and 10 mins, the cell numbers decreased to 1 $\times$ 10^3 cells/mL for *Dolichospermum* and 5 $\times$ 10^3 cells/mL for *Microcystis* with the total viable cells < 1%. This is in-line with previous work in the absence of background organic matter in which a rapid reduction in cell viability was observed (Coral et al., 2013; Ding et al., 2010; Fan et al., 2013b; Zamyadi et al., 2015a). Even with potential scavenging from background organic matter, Zamyadi et al. (2019) observed that 90% of cells were no longer viable following pre-ozonation (1.2 mg/L, with 20 min of contact time) of a cyanobacterial bloom in a full-scale WTP.

The two doses of potassium permanganate and hydrogen peroxide saw very limited changes in cell numbers with less than 5% reduction in *Dolichospermum* and *Microcystis*. For potassium permanganate, the flow cytometry results showed that only 67% and 15% of total cells were viable at 172 mg-min/L and 456 mg-min/L, respectively. Compared to previous work without background organic matter, lower CTs were required to achieve 90% loss of cell viability (Ding et al., 2010; Fan et al., 2014a). After dosing with hydrogen peroxide, viable cells were reduced to 35% with 5 mg/L and 27% with 10 mg/L. In previous work with *Microcystis*, hydrogen peroxide didn't affect the cell membrane until high concentrations, e.g., > 10 mg/L with more than 2-days of contact time lysed >80% of cells (Fan et al., 2014a; Mikula et al., 2012).

The discrepancy between the reduction in cell numbers (generated from taxonomic cell count) vs. cell-viability (determined via flow-cytometry) was significantly smaller after ozone relative to chlorine, potassium permanganate and hydrogen peroxide. This is reflective of the type of damage imparted by the oxidant as well as exposure dose. SEM was used to generate images of cells before and after oxidation with ozone, chlorine, and hydrogen peroxide (Figure A.1 and Figure A.2). Though a very limited data set, these images provide insight into the impact of chlorine, ozone, and hydrogen peroxide on the morphology. Under chlorine (37 mg-min/L) and ozone (0.5 mg/L, 5 min), the cell links between *Dolichospermum* cells were the first part of the cell damaged; hydrogen peroxide (837 mg-min/L) shrank and deformed the cells, but fragmentation of the filaments did not occur. *Microcystis* cells appeared deformed under ozone and chlorine, but not fragmented. These

results are similar to those observed in past studies with SEM where ozone and chlorine produced similar breakup of filaments and deformation of cells (Coral et al., 2013; Lin et al., 2009).

As shown with flow cytometry, taxonomic cell count and SEM images, ozone produced fragmentation and the release of intracellular material, but potassium chlorine, permanganate and hydrogen peroxide damaged cell walls and viability. This result was further supported by the negligible (< 0.1 mg/L) releases of dissolved organic carbon (DOC) after oxidation with potassium permanganate and hydrogen peroxide relative to the 0.55 mg/L released after chlorination (max across all CT values) and 1.26 mg/L after ozonation (2 mg/L with 5- or 10-min contact times).

4.3.2 LC-OCD-OND

To evaluate the changes in DOC induced by oxidation, the organic matter fractions were determined with LC-OCD-OND. Although cell viability was monitored at multiple CT values, the max CT for each oxidant was used for LC-OCD-OND, i.e., chlorine at 37 mg-min/L, ozone at 2.15 mg-min/L, potassium permanganate at 456 mg-min/L, and hydrogen peroxide at 2168 mg-min/L. From the OCD peaks, the concentration of biopolymers, humic-substances, building blocks, LMW acids, and LMW neutrals were determined (Figure 4.2; Figure A.2). Biopolymers include high molecular weight (>10 kDa) polysaccharides, proteins, amino-acids, and extracellular polymeric substances. OND provided information regarding the nitrogen content of a subset of the DOC including biopolymer DON, biopolymer N/C ratio, humic-substances DON and humic-substances N/C ratio. Based on the UVD and the OCD signal, the specific UV absorption (SUVA) at 254 nm of humic-substances was also determined (Table A.2). Algal organic matter is generally divided into intracellular organic matter (IOM) and extracellular organic matter (EOM). IOM is primarily composed of proteins, polysaccharides, lipids and humic-like substances (Pivokonsky et al., 2015b). (Henderson et al., 2010) showed that the EOM of *Microcystis* contains primarily hydrophilic polysaccharides and proteins.

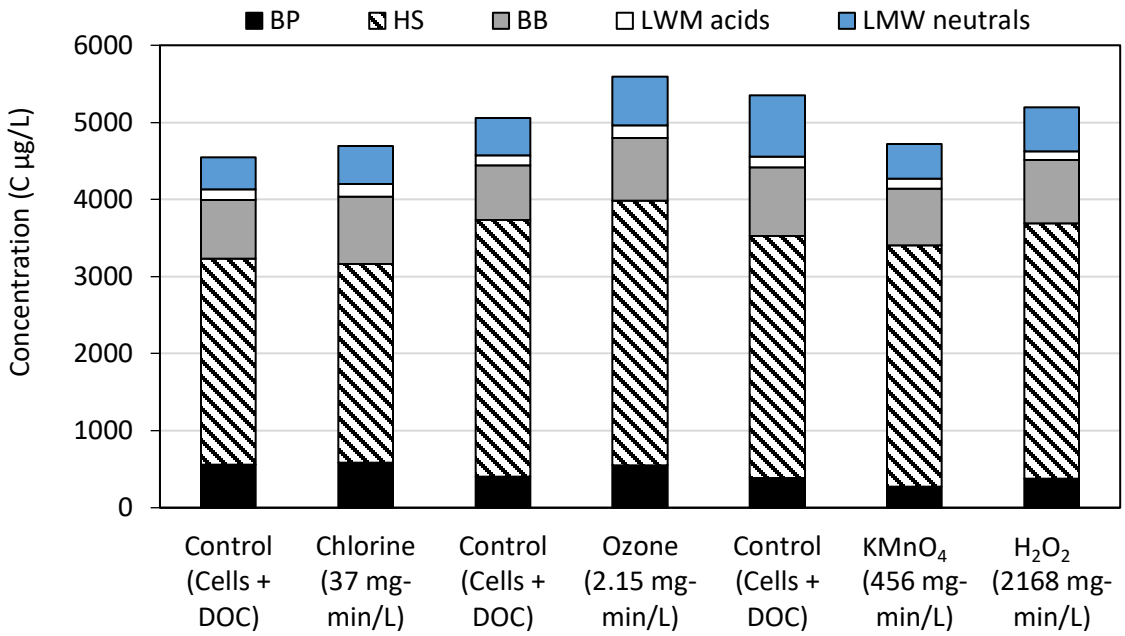

Figure 4.2 Organic matter fractions before (control) and after oxidation of *Microcystis* and *Dolichospermum* in Lake Champlain water. The three different control samples are the same matrix, conducted as separate experiments. Components were identified via LC-OCD-OND (Huber et al., 2011): BB = building blocks; HS = humic-substances; BP = Biopolymer; LMW = low molecular weight.

The control sample contained both the background organic matter from Lake Champlain and any cell fragments able to pass through the 0.45 µm filter. Across all oxidants, humic-substances $SUVA_{254}$ values were lower after exposure due to oxidation reactions with the aromatic rings (Weishaar et al., 2003) (Figure A.2). Decreases of the number-averaged molecular weight of humic-substances also occurred across all waters from the breakdown of organic matter present and in the case of ozone, the integration of oxygen resulting in more soluble components (Hammes et al., 2007) (Table A.2 and Table A.3). The humic-substances fraction generally saw minimal change (< 5%) after oxidation. This was likely due to the background organic matter, which makes up the majority of this fraction and would have been oxidized, but not mineralized at these doses.

Ozonation increased the fraction of humic-substances by 3%, biopolymers by 36%, building blocks by 15%, LMW acids by 28% and LMW neutrals by 31% (Figure 4.2). Chlorination also increased these fractions, though to a lower extent at 4.8% for biopolymers, 14% for building blocks, 13% LMW acids, and 20% for LMW neutrals. Biopolymers likely increased due to the release of IOM,

but may also have come from fragments of the cell membrane or extracellular material (e.g., amino-acids, polysaccharides and proteins) (Villacorte et al., 2015). The DON results supported this conclusion as ozonation also increased the concentration of DON biopolymers from 56 ppb-N to 216 ppb-N and the ratio of N/C from 0.14 to 0.40. An important caveat to these results is that the formation of building blocks and LMW acids/neutrals could also have come from the degradation of humic-substances.

Potassium permanganate and hydrogen peroxide produced the degradation of all fractions (biopolymer, building blocks, LMW acids/neutrals) and a minor loss of the total carbon, which was attributed to biological consumption during the reaction period (Figure 4.2). However, DON biopolymers increased in concentration from 10 ppb-N to 54 ppb-N (after H_2O_2) and to 26 ppb-N (after $KMnO_4$) indicative of select IOM release not detected in the bulk DOC. These releases coincided with a change in the fraction of N/C from 0.03 in the control to 0.09 after potassium permanganate and to 0.14 after hydrogen peroxide indicative of the presence of added material from biomass.

The LC-OCD-OND results helped to identify the fractions found in EOM and IOM, which are potential components that could scavenge oxidants and hinder the effective modeling of the oxidation of cyanotoxin and T&O compounds. Although these fractions have been analyzed as a potential source of disinfection by-products and interference to coagulants, they have only been included in a limited set of competition kinetic studies to evaluate its impact on the degradation of cyanotoxins and T&O compounds (Laszakovits and MacKay, 2019).

4.3.3 EDM/HSI

The flow cytometry, SEM, and LC-OCD-OND results were compared against the spectra generated with EDM/HSI. EDM/HSI allows for spectra (400 – 1000 nm) to be generated from a specific pixel (containing a cell component of interest). In this case, the components of interest for oxidation were the cell wall and cell bound material for *Microcystis* and cell wall, cell bound material, and the links between cells for *Dolichospermum*. Figure 4.3 (*Dolichospermum*) and Figure A.3 (*Microcystis*) are labeled EDM images that show examples of where the cell component spectra were collected. During the experiments, three pixels were selected from each cell component to minimize cell specific variability. The collected spectra were smoothed using a moving average to minimize the noise within the spectra and signal responses were normalized to the maximum value

within each spectrum for comparison. EDM/HSI was only conducted for samples oxidized with chlorine (CT of 37 mg-min/L) and ozone (0.5 mg/L for 5 min). After this chlorine exposure (37 mg-min/L), >99% of cells were not viable and only 26% of total cells remained from taxonomic cell count. The 0.5 mg/L and 5-min ozone exposure resulted in a 20% and 40% reduction in the viable cells and cell numbers, respectively.

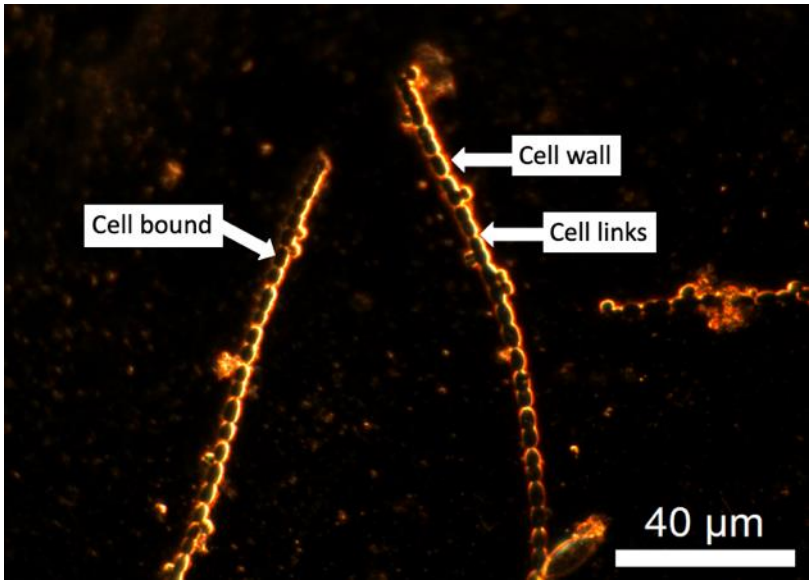

Figure 4.3 EDM image of *Dolichospermum* before oxidation illustrating different pixels targeted for spectral analysis: intracellular or cell bound material, cell links, and cell wall. The EDM image for *Microcystis* with labels for intracellular or cell bound material and cell wall is shown in Figure A.3

The two species had uniquely shaped spectra regardless of cell component (Figure A.5 and Figure A.6). However, the specific cell components shared common peaks/shoulders for both species, even if the peaks were slightly higher or lower in their maximum wavelength. For *Microcystis* cells, the spectra had two peaks at approximately 600 – 650 nm and 705 – 715 nm. *Dolichospermum* had three main features with two peaks at 650 – 665 nm and 695 – 705 nm and a shoulder at 530 – 550 nm. For *Microcystis*, the cell bound material did not show a dramatic change following chlorination and ozonation (Figure 4.4a). The ozonated cell bound material was still dominated by one peak at ~620 nm. After chlorination, the two cell-bound peaks remained, but a shoulder emerged centered around ~500 nm. In contrast to the cell bound material, the cell wall spectra were significantly impacted by the two oxidants showing that both oxidants impact the cell membrane before other components of the cell (Figure 4.4b). The ozonated cell wall retained a single peak at

660 nm, though significantly broader than the control. The chlorinated cell wall produced a new peak at ~500 nm and the removal of the two peaks originally exhibited by the control sample at ~660 nm and ~715 nm.

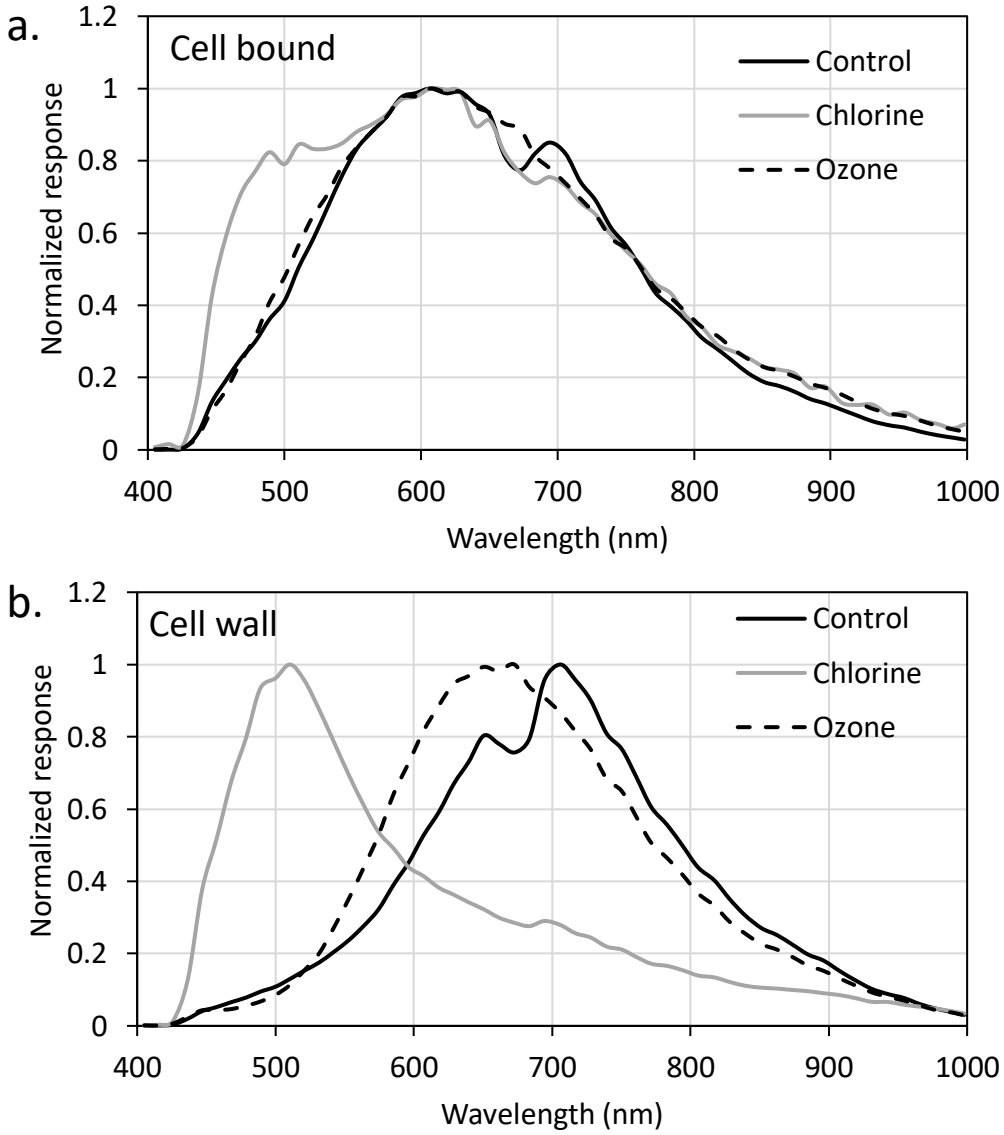

Figure 4.4 Impact of chlorine (CT = 37.5 mg-min/L) and ozone (0.5 mg/L, 5 min) on *Microcystis* a) cell bound and b) cell wall. EDM was used to find a pixel containing only the cell bound bulk material or cell wall where HSI spectra was collected. Instrument responses were normalized to the maximum value of each spectra for comparison.

SEM images of *Dolichospermum* cells showed that the cell links were targeted first by ozone and chlorine, but the EDM/HSI spectra did not show this result. When the cell links were oxidized

(Figure 4.5c), the ozonated spectra was very similar to the control sample with the same peaks observed. The chlorination of the cell links produced a new shoulder with a max around 595 nm, but it smoothed the two other peaks observed in the control. The ozonated cell bound material retained the two peaks of the control, though the ~660 nm peak was lower than the ~700 nm peak; the control shoulder remained, though shifted to lower energy wavelengths (~550nm at max). Chlorination had peaks at ~660 nm and ~700 nm, and the shoulder remained intact with a max of ~590 nm. For the cell wall, the ozonated water response mirrored those observed in the control at ~520 nm (shoulder), ~660 nm (peak), and ~700 nm (peak). As was observed with *Microcystis*, chlorine resulted in the formation of a peak centered at ~500 nm, a peak at ~660 nm and the removal of the peak at ~700 nm.

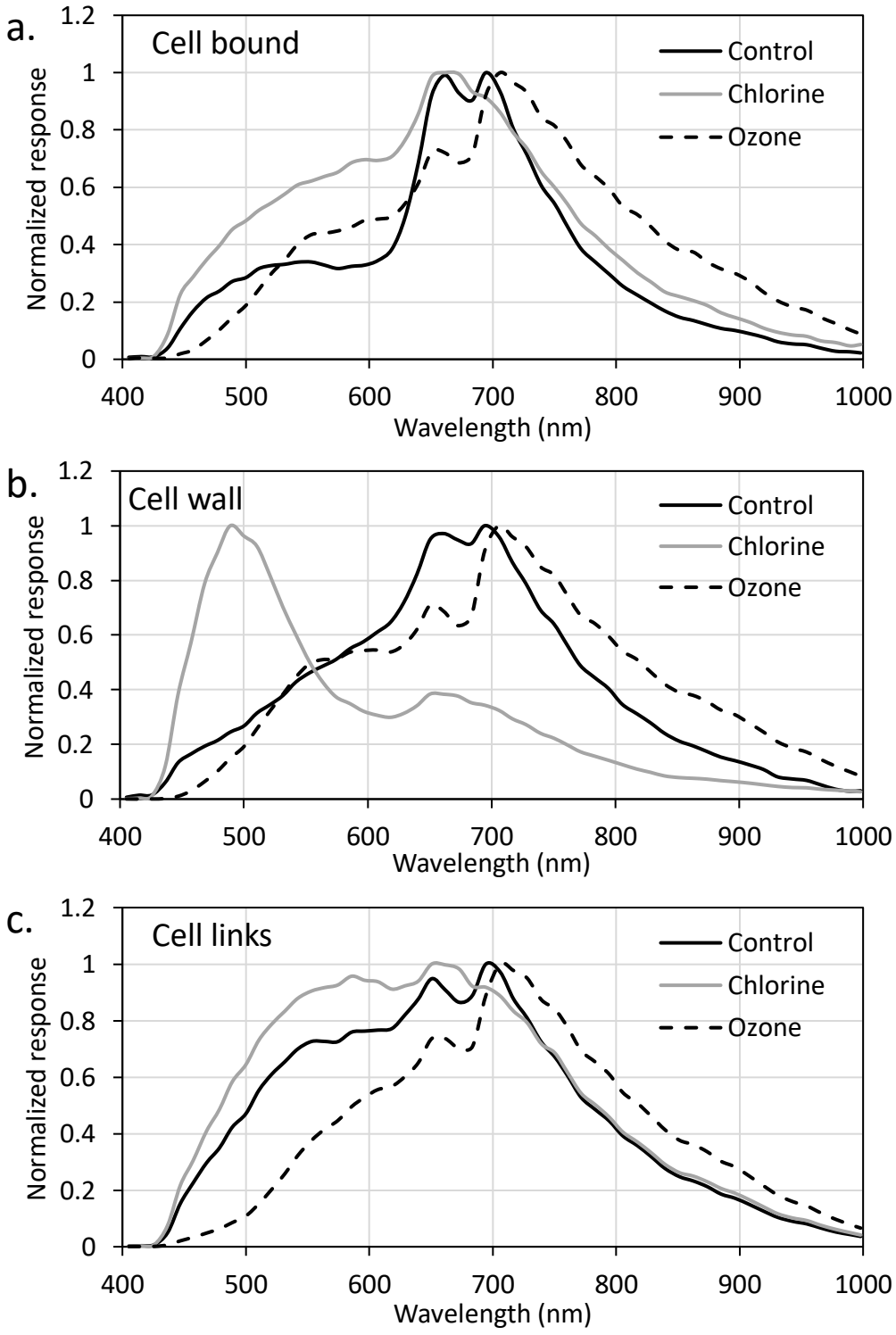

Figure 4.5 Impact of chlorine (CT = 37.5 mg-min/L) and ozone (0.5 mg/L, 5 min) on *Dolichospermum* a) cell bound, b) cell wall, and c) cell links. EDM was used to find a pixel containing only the cell bound, cell wall, or links between cells where HSI spectra was collected. Instrument responses were normalized to the maximum value of each spectra for comparison.

The presence of all the peaks identified within these culture samples were likely due to the overlapping absorption of pigments within the cells (e.g., phycocyanin, chlorophyll). The shifts in their absorption to a single peak would appear to indicate a change in the pigments present within the cell wall, cell links or cell bound material as a result of oxidation. In remote sensing applications, HSI peaks of 620 nm, and 665 nm were found to corelate with on-the ground levels of phycocyanin and chlorophyll-*a*, respectively (Randolph et al., 2008; Simis et al., 2005). The ~700 nm peak is not used in remote sensing applications because of the interference from water; this interference comes from the application of HSI in reflectance mode as opposed to transmittance mode, which is typically applied at the bench-scale (Simis et al., 2005). However, the differences in spectra shape have been taken advantage of to differentiate between *Aphanizomenon flos-aqua* and *Microcystis* at the bench-scale (Paine et al., 2018). This was accomplished with a spectral shape algorithm applied to the derivative of the spectrum to obtain meaningful results, which is beyond the scope of this work.

4.4 Conclusion

Flow cytometry and taxonomic cell count after oxidation with ozone, chlorine, potassium permanganate and hydrogen peroxide highlighted the discrepancy between cell viability vs. cell lysis and fragmentation. These differences were also observed visually via SEM, which showed the shrinking/deformation of *Microcystis* and *Dolichospermum*, but not complete lysis. SEM results also showed the fragmentation of *Dolichospermum* cell links prior to cell lysis, which has been observed in previous work (Coral et al., 2013; Lin et al., 2009; Wert et al., 2013).

LC-OCD-OND was used to identify the fractions of IOM and EOM released after oxidation of *Microcystis* and *Dolichospermum* in addition to the changes in bulk organic matter from Lake Champlain. Following ozonation and chlorination, increases in the biopolymer fraction were attributed to the release of IOM and potentially fragments of the cell membrane (e.g., amino-acids, polysaccharides, and proteins). Future work should aim to better understand how this fraction of released IOM and oxidized EOM impacts the degradation of the compounds of interest.

EDM/HSI revealed the unique spectra of both the *Dolichospermum* and *Microcystis*. Both cultures had spectra with peaks at ~660 nm and ~700 nm, but *Dolichospermum* had a shoulder with a peak at ~550 nm. The oxidation of these cells shifted the responses, which was attributed to the decrease

in concentration of pigments present. Both cell wall spectra revealed the formation of a peak after chlorination at ~ 500 nm, but limited changes were observed following ozonation

Acknowledgements

The authors gratefully acknowledge support from Algal Blooms, Treatment, Risk Assessment, Prediction and Prevention through Genomics (ATRAPP) − Genome Quebec and Genome Canada, Natural Sciences and Engineering Research Council of Canada (NSERC), and Fonds de recherche du Québec – Nature et technologies (FRQNT). The authors thank the staff at NSERC Industrial Chair on Drinking Water at Polytechnique Montreal. LC-OCD measurements were performed at the NSERC Cahir in Water Treatment at the University of Waterloo by Lin Shen.

CHAPTER 5 ARTICLE 2 - DIVERSITY ASSESSMENT OF THE TOXIC CYANOBACTERIAL BLOOM DURING OXIDATION

Our objective was to assess the diversity, changes, shifts and potential persistence in cyanobacterial community during bloom oxidation using high throughput sequencing. High throughput sequencing gives us the opportunity to study the impact of oxidation in a deep and precise manner on whole cyanobacterial community. The results highlights the importance of community shifts and persistence of toxin producing species in the pre-oxidant selection. This chapter was published as a research paper in the Journal of *Toxins* on Nov 18th 2020. Supplementary information is presented in Appendix B.

DIVERSITY ASSESSMENT OF THE TOXIC CYANOBACTERIAL BLOOM DURING OXIDATION

Saber Moradinejad[1], Hana Trigui[1], Juan Francisco Guerra Maldonado[1], Jesse Shapiro[2], Yves Terrat[2], Arash Zamyadi[3,4], Sarah Dorner[1], Michèle Prévost[1]

1: Department of Civil, Geological & Mining Engineering, Ecole Polytechnique de Montréal, 2900 boulevard Édouard-Montpetit, Montréal, Québec, H3T 1J4, Canada

2: Department of biological science, Université de Montréal, Montréal, Québec, H2V 0B3, Canada

3: Water Research Australia (WaterRA), Adelaide, SA 5001, Australia

4: BGA Innovation Hub and Water Research Centre, School of Civil and Environmental Engineering, University of New South Wales (UNSW), Sydney, NSW 2052, Australia

* corresponding author: Saber.moradinejad@polymtl.ca

Abstract

Fresh-water sources of drinking water are experiencing toxic cyanobacterial blooms more frequently. Chemical oxidation is a common approach to treat cyanobacteria and their toxins. This study systematically investigates the bacterial/cyanobacterial community following chemical oxidation (Cl_2, $KMnO_4$, O_3, H_2O_2) using high throughput sequencing. Raw water results from high throughput sequencing show that *Proteobacteria*, *Actinobacteria*, *Cyanobacteria* and *Bacteroidetes* were the most abundant phyla. *Dolichospermum, Synechococcus, Microcystis* and *Nostoc* were the most dominant genera. In terms of species, *Dolichospermum sp.90* and *Microcystis aeruginosa* were the most abundant species at the beginning and end of the sampling, respectively. A comparison between the results of high throughput sequencing and taxonomic cell counts highlighted the robustness of high throughput sequencing to thoroughly reveal a wide diversity of bacterial and cyanobacterial communities. Principal component analysis of the oxidation samples results showed a progressive shift in the composition of bacterial/cyanobacterial communities following soft-chlorination with increasing common exposure units (CTs) (0–3.8 mg·min/L). Close cyanobacterial community composition (*Dolichospermum* dominant genus) was observed following low chlorine and mid-$KMnO_4$ (287.7 mg·min/L) exposure. Our results showed that some toxin producing species may persist after oxidation whether they were dominant species or not. Relative persistence of *Dolichospermum sp.90* was observed following soft-chlorination (0.2–0.6 mg/L) and permanganate (5 mg/L) oxidation with increasing oxidant exposure. Pre-oxidation using H_2O_2 (10 mg/L and one day contact time) caused a clear decrease in the relative abundance of all the taxa and some species including the toxin producing taxa. These observations suggest selectivity of H_2O_2 to provide an efficient barrier against toxin producing cyanobacteria entering a water treatment plant.

Keywords

Cyanobacteria, Diversity, Oxidation, High throughput sequencing, *Dolichospermum, Microcystis*

Key Contribution

This study provides a diversity assessment of cyanobacterial bloom following oxidation. Changes, shifts and oxidant persistence potential of cyanobacterial community during oxidation were quantified and reported.

5.1 Introduction

The occurrence of cyanobacterial blooms in fresh-water bodies has been enhanced due to eutrophication and temperature increases (Paerl and Paul, 2012; Wells et al., 2015). Cyanobacterial blooms may produce and release taste and odor compounds as well as cyanotoxins into water bodies. More than 40 species of cyanobacteria are known as potentially toxic species (Al-Sammak et al., 2014; Westrick et al., 2010). microcystin (MC), anatoxin (ATX-a), saxitoxin (STX), cylindrospermopsin (CYN) and β-Methylamino-L-alanine (BMAA) are the five major groups of cyanotoxins due to their toxicity and frequent occurrence around the world (Casero et al., 2019).

Conventional drinking water treatment plants are often challenged by the removal of cyanobacteria and cyanotoxins (Almuhtaram et al., 2018; Pazouki et al., 2016; Zamyadi et al., 2013c; Zamyadi et al., 2012a) including both low risk (low cell numbers in the source) and high-risk water treatment plants (high cell numbers in the source). Several studies have evaluated the removal of the cyanobacteria and their harmful metabolites using different oxidants such as chlorine, ozone and, potassium permanganate (Coral et al., 2013; Ding et al., 2010; Fan et al., 2013a; Fan et al., 2014a; Zamyadi et al., 2015a; Zamyadi et al., 2020). Pre-oxidation dampens the cyanobacterial shock before entering the drinking water treatment plant and can limit the accumulation of cyanobacteria within the plant. Chlorine and ozone are also used as primary disinfectants providing an additional oxidation barrier after the filtration to remove cyanobacterial harmful metabolites (cyanotoxins) (Vlad et al., 2014; Zamyadi et al., 2010a).

Dynamic and complex behaviour of cyanobacterial blooms, including cyanotoxin production and release under various environmental conditions represents a treatment challenge. The oxidation efficiency of cyanobacteria blooms may vary according to water quality parameters (such as pH, Dissolved Organic Carbon (DOC) and the presence of other bacterial communities), cyanobacterial community shape, potential agglomeration, and the growth phase (He and Wert, 2016; Merel et al., 2013; Wert et al., 2013; Zamyadi et al., 2015a). Cyanobacteria treatment efficiency improvement requires an understanding of the cyanobacterial composition structure in response to treatment processes (Zamyadi et al., 2013b). Molecular methods have been used to study the fate of the microbial community, including cyanobacteria, within different conditions (Casero et al., 2019; Zhu et al., 2016). Molecular methods can overcome the challenges of microscopic cell counts such

as time and qualified person requirements, as well as changes in biovolumes during analyses (American Water Works Association (AWWA), 2010; Hawkins et al., 2005; Zamyadi et al., 2019).

Molecular methods such as high throughput sequencing have been deployed to study cyanobacterial communities and identify cyanotoxin biosynthesis genes (Berry et al., 2017; Casero et al., 2014; Casero et al., 2019; Eldridge and Wood, 2019; Kim et al., 2018a; Lezcano et al., 2017; Pessi et al., 2016; Scherer et al., 2017; Willis and Woodhouse, 2020; Woodhouse et al., 2015). Diversity of the cyanobacterial community and toxigenic cyanobacteria was assessed based on the Operational Taxonomy Units (OTUs) derived from 16S rRNA gene amplification (metabarcoding) (Casero et al., 2019). Limited studies have applied high throughput sequencing to monitor the fate of cyanobacteria during the treatment processes. Xu et al. (2018) studied the microbial community of the sludge in six different drinking water treatment plants using high throughput sequencing. Results showed that cyanobacteria were the most dominant phylum in two treatment plants with a higher level of nutrients in raw water. *Planktothrix, Microcystis* and *Cyindrospermopsis* were the most abundant genera and were positively correlated with the nutrient levels in raw water. Pei et al. (2017) used 16S rRNA sequencing to study the shifts in the microbial community in clarifier sludge following coagulation by $FeCl_3$, $AlCl_3$ and PAFC (Polyaluminium Ferric Chloride). Results revealed selective removal of the different bacterial species, as the relative abundance of the *Microcystis, Rhodobacter, Phenylobacterium* and *Hydrogenophaga* decreased in $AlCl_3$ sludge compare to the $FeCl_3$ and PAFC. Lower *Microcystis* abundance could be related to high Al toxicity or large and high-density floc in $FeCl_3$ and PAFC, which plays a protective role for microorganisms (Pei et al., 2017). Lusty and Gobler (2020) used 16S rRNA to evaluate the mitigation of cyanobacterial blooms using H_2O_2. Results showed relative persistence of *Cyanobium* and *Cylindrospermopsis* to a moderate H_2O_2 dose (4 mg/L); *Plankthotrix* and *Microcystis* (abundant genus) were the most sensitive genera, respectively (Lusty and Gobler, 2020).

High throughput sequencing has been widely applied to study bacterial/cyanobacterial communities. Fewer studies focused on the diversity of bacterial/cyanobacterial communities during water treatment processes. However, no study has focused on the cyanobacterial community following chemical oxidation using high throughput sequencing. Understanding the shifts and the potential selective persistence in cyanobacterial communities following oxidation is important for choosing an efficient oxidant. Thus, the objective of this study was to assess the structural

composition of the cyanobacteria community following oxidation (with Cl_2, O_3, $KMnO_4$, H_2O_2) using high throughput metagenomic shotgun sequencing over the seasonal bloom period.

5.2 Materials and methods

5.2.1 Sampling site description

The oxidation tests were conducted using natural bloom samples. Cyanobacterial bloom samples were collected and transferred to the laboratory from the Bedford water treatment plant intake (Missisquoi Bay—Lake Champlain) in southern Quebec, Canada (45°02'22.0"N 73°04'40.5"W). Sampling was performed during the bloom season from 1 August to 29 August 2018. Several cyanobacterial blooms have been documented for the Lake Champlain in previous years (McQuaid et al., 2011; Zamyadi et al., 2015a; Zamyadi et al., 2013b; Zamyadi et al., 2012b).

5.2.2 Chemicals and Reagents

A free chlorine stock of 2000 mg/L was freshly prepared from sodium hypochlorite (5.25%) on the day of the experiment. Free chlorine residual was measured using an N,N-diethyl-p-phenylenediamine (DPD) colorimetric method based on Standard Methods (SM) 4500-Cl G (American Public Health Association (APHA) et al., 2012). Samples were dosed at room temperature (22 °C). A stock of sodium thiosulfate 3000 mg/L was used to quench the chlorine samples at a dose of 1.1 mg/L per 1 mg/L chlorine.

A potassium permanganate ($KMnO_4$) stock solution of 5000 mg/L was prepared by dissolving $KMnO_4$ crystals into the ultrapure water. A DPD colorimetric method ratio of 0.891 $KMnO_4/Cl_2$ SM 4500-Cl G was used to determine the $KMnO_4$ residual (American Public Health Association (APHA) et al., 2012). An amount of 1.2 mg/L sodium thiosulfate per 1 mg/L $KMnO_4$ was used to quench further oxidation with $KMnO_4$.

A bench-scale ozone generator (details in (Zamyadi et al., 2015a)) was used to prepare an ozone stock solution 50–60 mg/L. SM 4500-O_3 was used to determine the stock and ozone residual concentration (Zamyadi et al., 2015a). An ozone stock solution (50–60 mg/L) was prepared with gaseous ozone using a bench-scale ozone generator (additional details in (Zamyadi et al., 2015a)). Ozone stock concentration and residual ozone in water samples were measured using SM 4500-O_3 (Zamyadi et al., 2015a). An amount of 1.6 mg/L sodium thiosulfate per 1 mg/L ozone was used to quench the ozonation samples.

Stabilized hydrogen peroxide (30%, Sigma Aldrich, MO, USA) was used to prepare the Hydrogen peroxide (H_2O_2) stock (10 g/L). A colorimetric test kit (Chemetrics K-5510, Midlands, VA, USA) was performed to measure the hydrogen peroxide residual. Moreover, 1.2mg/L sodium thiosulfate per 1 mg/L H_2O_2 was used to quench further oxidation with H_2O_2.

The selected oxidant doses and contact times are presented in Table 5.1. The doses (concentration) and contact time have been selected based on the common pre-oxidation doses used in drinking water treatment intake.

Table 5.1 Oxidation experimental plan

Oxidant	**Water type**	**Oxidant dose (mg/L)**	**Contact time**
Cl_2	Real Bloom, Missisquoi Bay, Quebec, Canada	0.2	1min
			2min
		0.6	5min
			10min
			60min
			120min
O_3		0.1	1min
			2min
		0.3	5min
			10 min
$KMnO_4$		5	30min
			60min
			120min
H_2O_2		10	6 hours
			24 hours

Oxidant exposures (CT) were calculated for chlorine using Equation 5-1:

$$CT = \int_0^t [Oxidant]dt = \frac{C_0}{k_{decay}}(e^{k_{decay}t} - 1) \qquad \text{Eq. 5-1}$$

Where k_{decay} (min^{-1}) is the first-order decay rate, t (min) is the exposure time, and C_0 (mg/L) is the initial concentration of oxidant at time zero.

5.2.3 DNA extraction, Metagenomic preparation, sequencing and Bioinformatic analysis

Total nucleic acid was extracted from the frozen filters (after filtration, samples were quickly transferred to −80 °C before DNA extraction) using a RNeasy PowerWater Kit (Qiagen Group, Germantwon, MD, USA) with modification. Before the extraction, 200 µL of nuclease-free water and 5 µL of TATAA Universal DNA spike II (TATAA Biocenter AB) were added to the filters to evaluate DNA extraction yields using RT-qPCR. RNeasy PowerWater Isolation kit solution PM1 was used to lyse the cells along with Dithiothreitol (DTT), which prevents disulfide bonds forming residues of proteins. A total volume of 60 µL nuclease-free water provided with the kit was used to elute the total nucleic acid, of which 30 µL of DNA (with minimum 1 ng of DNA) extracts were stored at −20 °C. DNA was subsequently purified with the Zymo Kit (Zymo Research, Irvine, CA, USA) according to the manufacturer's instructions. Each DNA sample was resuspended in 60 µL of nuclease-free water and quantified with a Qubit v.2.0 fluorometer (Life Technologies, Burlington, ON, Canada). A volume of 30 µL DNA was sent for pyrosequencing (Roche 454 FLX instrumentation with Titanium chemistry) to the Genome Quebec.

An Illumina NovaSeq 6000 platform using S4 flow cells was applied to sequence DNA libraries. A home-made bioinformatic pipeline was used for further analysis of Paired-end raw reads of 150 base pairs (bp) as follows. First, raw reads trimming quality was performed using the SolexaQA v3.1.7.1, default parameters (Cox et al., 2010). Further analyses were carried out on the trimmed reads shorter than 75 nt. An in-house script, based on the screening of identical leading 20 bp, was used to remove artificial duplicates. Gene fragments were predicted using FragGeneScan-Plus v3.0 based on the trimmed high-quality reads (Kim et al., 2015). Then, predicted fragments of protein were clustered at 90% similarity level using cd-hit v4.8.1 (Fu et al., 2012). A diamond engine was used for similarity search on the M5nr database based on a representative of each cluster (https://github.com/MG-RAST/myM5NR). Best hits (minimal e-value of 1E-05) combined with the last common ancestor approach were used to assess the taxonomic affiliation of protein fragments. It should be mentioned that the annotation process uses a read-mapping process of small gene fragments of encoding proteins on a large database of proteins. One gene fragments encoding protein in the database could match with multiple species or strains.

5.2.4 DOC and cyanobacteria taxonomic cell count

Pre-rinsed 0.45µm membrane filters (Supor 45µm, 47m, PES PALL, Port Washington, NY, U.S.) and carbon-free glass vials were used for the Dissolved Organic Carbon (DOC) samples. DOC measurements were performed via 5310 total organic carbon analyzer (Sievers Analytical Instruments, Boulder, CO, U.S.). An inverted microscope with 20X magnification was used to perform cell count samples, which were preserved with Lugol's Iodine (Lund, 1959; Planas et al., 2000).

5.2.5 Statistical Analysis

All analyses were performed using a custom bioinformatics pipeline implemented in R (v.3.6,2, RStudio, Inc., Boston, MA, USA), phyloseq (V.1.28.0) to visualize the community composition at phylum (all bacteria reads), order, and genus (cyanobacteria reads) (McMurdie and Holmes, 2013). The twenty-five most abundant cyanobacteria species were visualized using pheatmap (v.1.0.12) (Raivo, 2019). Then, the alpha diversity metrics were estimated using phyloseq's estimate richness function (Shannon and Chao1). Taxonomic data were normalized by the centred log-ratio transformation using easy CODA (v.0.31.1) (Greenacre, 2018). Multiple zeros were treated by adding small constant or pseudo-count to all the elements (Calle, 2019). The beta-diversity was analyzed using the vegan package (v.2.5-6), where the similarity matrices were calculated based on the Euclidean distance (Oksanen et al., 2016). The homogeneity of variances of normalized data related to each oxidant was analyzed before building the model. A Redundancy Analysis (RDA) constrained ordination to each oxidant applied to the cyanobacteria genus and tested by the permutation test (> 95% significance). Further explanation of the permutation test can be found in Calle (2019).

5.3 Results and discussion

5.3.1 Cyanobacterial bloom characteristics throughout sampling

The cyanobacteria bloom samples were collected on 5 days of the bloom period (1, 13, 15, 21 and 29 August 2018) from Missisquoi Bay (Lake Champlain) close to the water intake of the drinking water treatment plant. Cyanobacterial bloom characteristics are presented in the Table 5.2. DOC (Dissolved Organic Carbon) and pH did not demonstrate considerable variation throughout the sampling period. Total taxonomic cell counts and biovolumes follow the same decreasing and increasing trend during the sampling period. For both parameters, the highest values were found at

the beginning of the sampling period (1 August), followed by a significant drop on 13 August, where cyanobacterial taxonomic cell counts decreased from 3.3×10^5 to 7.8×10^4 cells/mL and the biovolumes from 30.6 mm^3/L to 4.6 mm^3/L. The second drop was observed between 15 August and 21 August, from 1.4×10^5 to 6.8×10^4 cells/mL for taxonomic cell count and from 9.4 to 0.3 mm^3/L for the biovolume. According to algal cell abundance descriptors (biovolume and cell counts) during the bloom period, the main peaks of cyanobacterial bloom occurred on 1 August and to a lower extent on 15 August. The observed taxonomic cell count exceeds the alert level of the 6.5×10^4 cells/mL for drinking water treatment plants (Newcombe et al., 2010), except for the 29 August with 5.4×10^4 cells/mL.

Table 5.2 Cyanobacterial bloom characteristics

Sampling Date	**DOC (mg/L)**	**pH**	**Cell Count (cells/mL)**	**Biovolume (mm^3/L)**
1 August 2018	5.9	7.6	3.3×10^5	30.6
13 August 2018	5.8	7.3	7.8×10^4	4.6
15 August 2018	5.5	7.4	1.4×10^5	9.4
21 August 2018	4.9	7.4	6.8×10^4	0.3
29 August 2018	5.6	7.5	5.4×10^4	2.1

5.3.2 Variation of the cyanobacterial bloom composition

The diversity and community variation of bacterial and cyanobacterial communities during the bloom sampling period were studied using comparative metagenomics reads levels of phylum, order and genus. The number of reads for taxonomic data was normalized by relative abundance (Figure 5.1). Analysis of relative abundance of the bacterial community at the phylum level, based on high throughput sequencing data, showed that Proteobacteria, Actinobacteria, Cyanobacteria, Bacteroidetes, Firmicutes and Verrucomicrobia were the six most abundant phyla throughout the sampling period (Figure 5.1a). As expected, Proteobacteria was by far the most abundant phylum at the beginning of the sampling period (1 August) as has been observed by Pie et al. (2017) (Pei et al., 2017). The high relative abundance of Proteobacteria, especially in the beginning of sampling and Bacteroidetes at the end of the sampling period, may indicate contamination of the sampling

point with human/animal-associated fecal markers (Ballesté and Blanch, 2010; Lee et al., 2015; Vadde et al., 2019). For the rest of the sampling dates (13, 15 and 21 August), Proteobacteria remained the predominant phylum, but at a lower extent than what was observed in the first and last days of sampling. The cyanobacteria phylum accounts for 5 to 10% of total relative abundance assigned to the phylum level in all samples. The cyanobacteria relative abundance started at 5% of the phyla, followed by an increase in the middle of the sampling (13 August and 15 August) to 10%. By the end of August, the cyanobacterial contribution in the whole bacterial community decreased to 5%.

At the order level, the cyanobacterial community was dominated by members of the *Chroococcales*, *Nostocales* and *Oscillatoriales* during the cyanobacterial bloom period (from 1 August and 29 August) (Figure 5.1b). The relative abundance of the *Nostocales* and *Chroococcales* varied between the different dates and even within the same day (15 August). On the other hand, *Oscillatoriales* relative abundance remained steady (Figure 5.1b).

Analysis at the genus level showed that within the *Chroococcales* order, the predominant genera were *Microcystis* and *Synechococcus. Synechococcus* was the dominant genus until 21 August of the sampling period, followed by *Microcystis,* which became the dominant genus on 29 August (Figure 5.1c). The predominant genera in the *Oscillatoriales and Nostocales* orders were *Oscillatoria* and *Dolichospermum* (formerly known as *Anabaena*), respectively (Figure 5.1c). Depending on the sampling date, *Synechococcus*, *Microcystis* and *Dolichospermum* were the predominant genera during the bloom period. Our observations are consistent with short/long term investigations of cyanobacterial bloom dynamics using taxonomic cell count and metagenomics (McQuaid et al., 2011; Tromas et al., 2017; Zamyadi et al., 2015a; Zamyadi et al., 2013b; Zamyadi et al., 2012b). *Microcystis* and *Dolichospermum* share a spatio-temporal niche during blooms and often are dominant within the cyanobacterial community, but have distinct environmental preferences; for example, they have different responses to nutrients (Andersson et al., 2015; Harke et al., 2015). During this study, the abundant genus shifted from *Nostocales* members, dominated by *Dolichospermum* for the first three weeks, to the *Microcystis* genus by the end of the sampling period (29 August). The shift to *Microcystis* dominance can probably be attributed to species-specific associations between *Microcystis spp.* and associated bacteria referred to as the epibiont phenomenon. Some species within *Proteobacteria, Bacteroidetes* and other phyla can shelter in the *Microcystis* mucilage to avoid being grazed (Li et al., 2018). These species play essential roles

in enhancing the environmental adaptation of *Microcystis* within the cyanobacterial bloom, like maintaining redox balance and coping with oxidative stress (Li et al., 2018). Our results are in accordance with the previously reported results that *Proteobacteria*, *Bacteriodetes* tend to dominate in the *Microcystis* mucilage (blooms and culture-dependent studies) (Maruyama et al., 2003; Shi et al., 2009). Moreover, allelopathy may influence the successional dominance of *Microcystis* and *Dolichospermum* within aquatic systems, whereby organisms produce bioactive compounds (allelochemicals) in the environment to positively or negatively influence the growth of neighboring species (Wacklin et al., 2009). The effects of these allelochemicals on cyanobacterial community distribution within the environment are connected with nutrient availability and environmental conditions (Kardinaal et al., 2007; Li and Li, 2012; Van Wichelen et al., 2016). Competition experiments between toxic *Microcystis* and *Dolichospermum* strains, based on the lab coculture-dependent method, showed that *Microcystis* significantly inhibited the growth of *Dolichospermum*, whereas the effects of *Dolichospermum* on *Microcystis* were minimal (Li and Li, 2012; Zhang et al., 2014). *Dolichospermum* biovolume and biomass were sharply reduced after exposure to *Microcystis* strains (Chia et al., 2018). Further investigation is required to explain the interaction and succession of *Microcystis* and *Dolichospermum* in cyanobacterial blooms.

An interesting insight was gained considering within-day changes in bacterial community composition (morning—AM and afternoon—PM) for 15 August (Figure 5.1). Based on the relative abundance analysis, a shift in bacterial composition at the phylum level was observed between the two samples on 15 August. In the afternoon, *Proteobacteria* and *Actinobacteria* increased, while *Bacteroidetes* and *Cyanobacteria* decreased as compared to their initial composition at the start of the sampling in the morning. At the order level, the most abundant order shifted from *Nostocales* in the morning to *Chroococcolas* in the afternoon. At the genus level, the changes were more evident for *Synechococcus* (increase) and *Dolichospermum* (decrease). These within-day changes in bacterial composition reflect the variation in stratification and mixing patterns of the cyanobacterial community in Missisquoi bay, as shown by Ndong et al. (2014). These findings highlight the importance of timing the sample collection by considering the stratification variation in the diel cycle (morning, noon, afternoon).

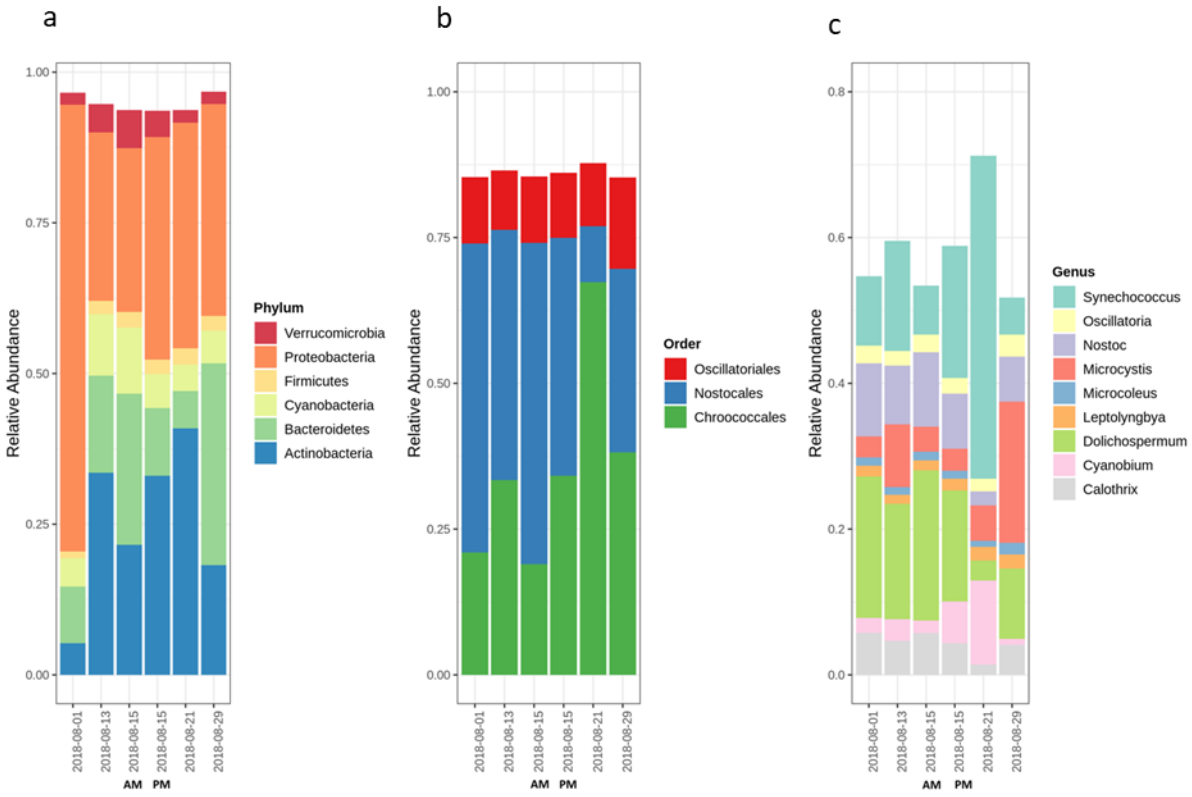

Figure 5.1 Identity of major detected bloom-associated Cyanobacterial community members during the sampling period a) Relative abundance of the different phylum b) The relative abundance of orders belonging to cyanobacterial phylum c) Relative abundance of genera belonging to the *Nostocales*, *Chrooccocales* and, *Oscillatoriales* orders

5.3.3 Impact of oxidation on cyanobacterial diversity

The impact of oxidation on cyanobacterial diversity was assessed by using the impact of increased CT (the terminology used in water treatment is CT, which represents the product of the oxidant concentration (C) and contact time (T) to inactivate microorganisms) on two different samples, first on 1 August, dominated by *Dolichospermum* and the second on 29 August dominated by the *Microcystis* genus. The oxidants considered Cl_2, $KMnO_4$, O_3, H_2O_2 differ widely in their mode of action and their persistence (Fan et al., 2014b). As a result, CT values may vary over three orders of magnitude from 0.1 mg·min/L Cl_2 and a maximum of 7035 mg·min/L for H_2O_2.

Using non-normalized data is a source of bias in statistical analyses of the effects of oxidants on the bacterial/cyanobacterial communities. Thus, the data were normalized prior to analysis. Using the common exposure unit (CT) is not representative to compare the effects of different oxidants

simultaneously. A normalized oxidant exposure (relative CT) is used to compare different oxidants among each other (Relative CT for each oxidant; max CT = 1 and min CT = 0, the exposure points in between were calculated accordingly); for example, max CT obtained for H_2O_2, on 1 August, is 7035 mg·min/L and is considered as relative CT = 1, the control condition is considered as relative CT = 0.

The doses (concentration) and contact time (T) were selected using the product CT, which is the foundation of disinfection and oxidation in drinking water. The choice of CT also considered prior evidence showing differences in species' resistance to the oxidant exposure (CT) (Coral et al., 2013; Fan et al., 2013a; Fan et al., 2013b; He and Wert, 2016; Zamyadi et al., 2015a; Zamyadi et al., 2013d; Zamyadi et al., 2020; Zamyadi et al., 2012a; Zamyadi et al., 2010a; Zamyadi et al., 2012b). However, all previously reported observations were based on taxonomic cell counts and not on high throughput sequencing. The applied dosages reflect drinking water industry practices using regulated treatment processes.

5.3.3.1 Cyanobacterial Composition

To assess the cyanobacterial bloom composition following oxidation using $KMnO_4$, Cl_2 and H_2O_2, samples were taken on 1 August (Figure 5.2) and 29 August (Figure B.1) *Dolichospermum* and *Microcystis* were the dominant genera on 1 August and 29 August, respectively.

Figure 5.2 shows the dissimilarity among groups of bacterial communities following oxidation at different exposures (relative CT) using Principal Component Analysis (PCA) on 1 August. Samples that appear more closely together within a PCA are assumed to be more similar in bacterial and cyanobacterial composition (Figure 5.2). For the bacterial community, principal axis one and principal axis two for PCA represent 51.5 and 31.4% of the variation among the samples, respectively. High-relative CT exerted clustering of two groups, the first one includes samples after Cl_2 and $KMnO_4$ oxidation and the second one encompasses $KMnO_4$ and H_2O_2 oxidation. Chlorinated samples showed a clear progressive shift (as the relative CT increased) in the bacterial community.

On the other hand, the $KMnO_4$ and H_2O_2 induce large shifts as relative CT increases. Bacterial and cyanobacterial composition similarity following the different oxidation on 29 August (*Microcystis*) is presented in Figure B.1. Like the 1 August result, a large shift in the bacterial community

composition following H_2O_2 oxidation was observed for 29 August. On the other hand, $KMnO_4$ results showed similar bacterial composition on 29 August.

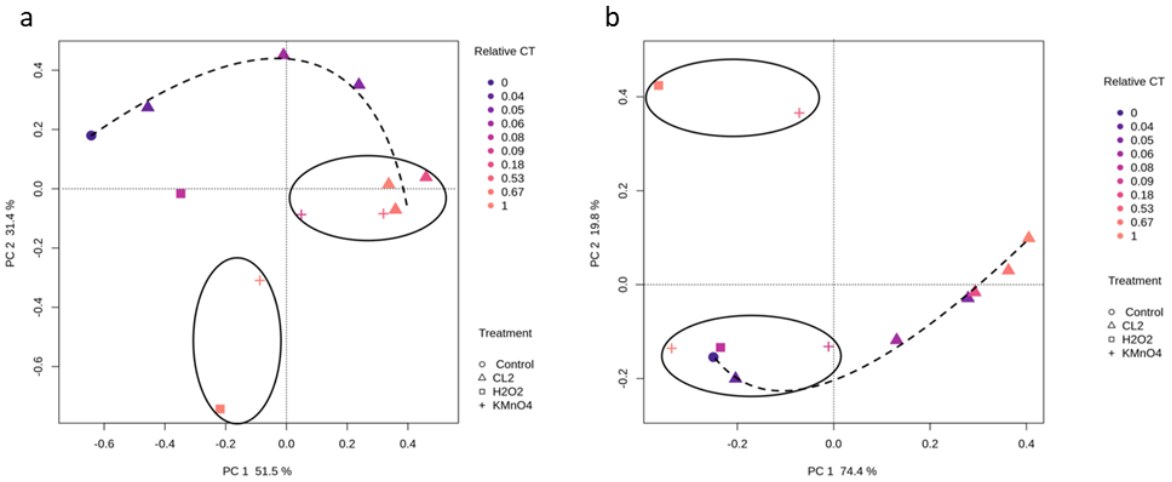

Figure 5.2 Principal components analysis (PCA) of the normalized relative abundance of comparative metagenomics reads in 1 August sample. Data are plotted following the genus-level classification (**a**) PCA analysis of bacterial community following oxidation using different common exposure units (CT), (**b**) PCA of the cyanobacterial community following oxidation using different CT.

For the cyanobacterial community (1 August), principal axis one, and principal axis two for PCA represent 74.4 and 19.8% of the variation among the samples, respectively (Figure 5.2b). A clear trend in the cyanobacterial composition variation is observed following chlorination. Cyanobacterial composition after exposure to Cl_2 (low relative CT < 0.05), $KMnO_4$ (low and high relative CT), H_2O_2 (low relative CT = 0.08) oxidation clustered in the same group with the control condition. High-relative (CT = 1) using H_2O_2 and (mid-relative = 0.53) $KMnO_4$ are grouped in a distinct second cluster, revealing similar cyanobacterial assemblages. This is in contrast with cyanobacterial/bacterial community trends following chlorination that display a progressive shift. Differences between the observed trends for the three oxidants were expected because of different mechanisms of actions and kinetics, persistence and selectivity. Taxonomic cell count based studies show progressive shifts following oxidation (Coral et al., 2013; Zamyadi et al., 2015a). Moreover, selective cyanobacteria oxidation has been demonstrated in the lab (Fan et al., 2013b; Fan et al., 2014a), in the field (Lusty and Gobler, 2020; Matthijs et al., 2012), and in drinking water treatment plants (Zamyadi et al., 2013c; Zamyadi et al., 2016b).

Our results enlighten the different oxidation impacts on the bacterial community between the Cl_2 and H_2O_2 oxidation. For 29 August, which was dominated by the *Microcystis* genus, $KMnO_4$ results revealed similar cyanobacterial composition. However, a large variation in cyanobacterial composition following H_2O_2 was observed (e.g., the samples from the 1 August).

Redundancy analysis (RDA) was used to explore the correlation between the relative abundance of nine dominant cyanobacterial genera (60% of the cyanobacterial community) observed in 1 August or 29 August samples and the different oxidant exposures (Figure 5.3). The relationship between the CT and diversity indexes (Shannon and Chao1) varies between the two dates. On 1 August, both diversity indices increase with CT, while on 29 August only the Richness index (Chao1) increased with CT. In general, the diversity of the cyanobacterial community increased due to oxidation of the dominated genus, as discussed further in detail for each oxidant.

For 1 August (*Dolichospermum* dominant), RDA analysis establishes an inverse correlation between the *Dolichospermum* genus and a wide range of chlorine exposures with relative CT > 0.04. Chlorination appears to have a lesser impact on the *Dolichospermum* genus than the *Microcystis*, possibly because of its abundance. On the other hand, no such relationship is observed between *Dolichospermum* and $KMnO_4$ exposure (relative CT = 1) and high H_2O_2 exposure (relative CT = 1), suggesting that these oxidants at these exposure levels had a negative impact on the *Dolichospermum* genus persistence within the community. Furthermore, for $KMnO_4$ at relative CT > 0.53, *Microcystis*, *Synechococcus*, and *Leptolyngbya* are less impacted by oxidation. Figure 5.3b shows the effect of the different oxidants on the cyanobacterial community of 29 August, when *Microcystis* genus is dominant. An immediate shift from the control is observed for all oxidants and for all relative CT. Unlike 1 August, the Shannon diversity is no longer correlated with *Dolichospermum*. These differences could reflect the morphological differences between the dominant genera (*Microcystis* vs. *Dolichospermum)* as a unicellular aggregate that are less resistant to oxidation as compared to filaments (Moradinejad et al., 2019). Chlorine and $KMnO_4$ exposures had a low impact on *Microcystis* and *Dolichospermum*. On the other hand, any H_2O_2 exposure causes a reduction in *Dolichospermum* and *Microcystis*, more so on 29 August. Removal of *Microcystis* using H_2O_2 was shown by Lusty and Gobler. (2020) and is in accordance with our observations of diverging correlation between Chao1 and *Microcystis* (Lusty and Gobler, 2020).

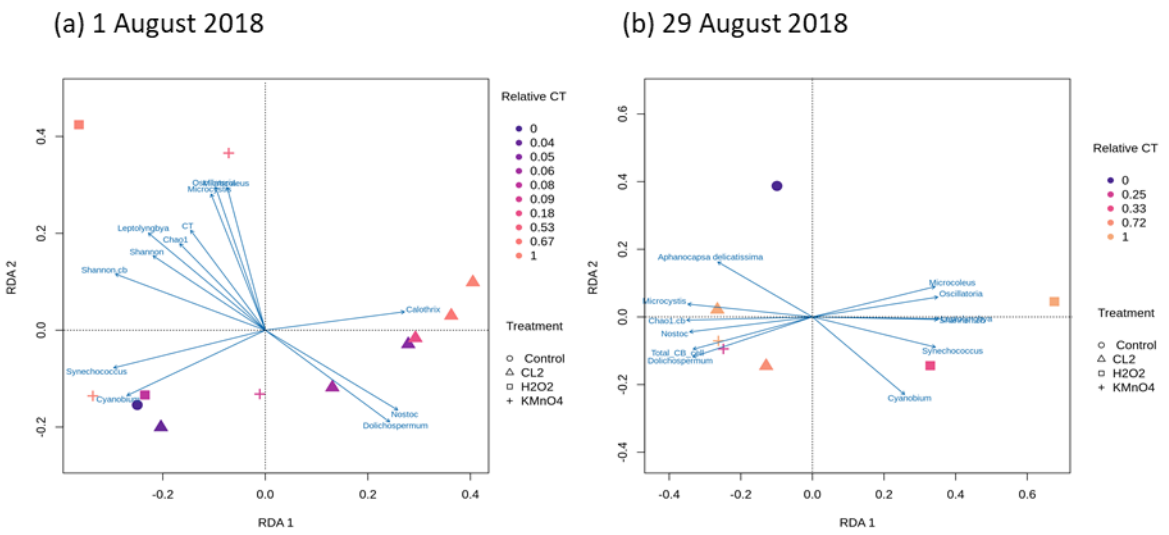

Figure 5.3 Redundancy analysis (RDA) of oxidant effect on cyanobacterial diversity and the cyanobacterial community at genus level Cl_2 (0.6 mg/L), $KMnO_4$ (5 mg/L), H_2O_2 (10 mg/L) (**a**) 1 August 2018 (**b**) 29 August 2018.

Figure B.2 shows the cyanobacterial composition following oxidation at genus level. Results show no significant variation in the relative abundance of *Dolichospermum* and *Microcystis* following Cl_2, $KMnO_4$ oxidation. Thus, no relative persistence to oxidation was observed at the genus level. On the other hand, high H_2O_2 exposure caused a decline in both *Dolichospermum* and *Microcystis* genus, which demonstrates the effect of high H_2O_2 exposure on cyanobacterial removal.

5.3.3.2 Effect of oxidation on cyanobacterial community richness and diversity

The diversity of the cyanobacterial composition following oxidation (1 August) at the species level is presented in Figure 5.4 (top 25 most abundant species). *Dolichospermum sp.90* was the dominant species in control conditions, and its relative abundance increases following chlorination and decreases after $KMnO_4$ and H_2O_2. Although no trends in relative abundance were seen at the genus level (Figure B.2), a similar trend can be seen for the three species present *Dolichospermum sp.90, Dolichospermum cylindrica* and, *Dolichospermum sp. PCC7108*. Regardless of the oxidant *Dolichospermum sp.90* remains the dominant species. Following the $KMnO_4$ and H_2O_2 oxidation, *Dolichospermum sp.90* was still the dominant species; its relative abundance declined compared to the control. The relative abundance of *Microcystis aeruginosa* is not impacted by chlorine but increases with $KMnO_4$ and H_2O_2 exposure, confirming selective removal of *Microcystis* showed by Lusty and Gobler. (2020) (Lusty and Gobler, 2020).

In the 29 August samples, *Microcystis aeruginosa* was the most abundant species (Figure B.3); its relative abundance increased after chlorination and $KMnO_4$ oxidation (as the chlorine exposure increased) and decreased after H_2O_2 oxidation as compared to the control condition. Despite the very low relative abundance of *Dolichospermum sp.90, Dolichospermum cylindrica* and D*olichospermum sp. PCC7108*, similar trends were observed on 1 August (when *Dolichospermum* was abundant).

The community richness and diversity indices for each treatment for 1 August and 29 August samples are illustrated in Figure 5.5 and Figure B.4, respectively. Shannon and Chao1 show a small decline following chlorination in comparison with the control, while they increase slightly following $KMnO_4$ exposure. The total cell numbers following $KMnO_4$ decreased by up to 63% for high $KMnO_4$ exposure (Figure B.5). A remarkable decrease in richness is observed at high relative CT of H_2O_2, while the diversity (Shannon index) increases. The decline in the richness index could be the result of some less abundant species no longer identified. Indeed, total cell counts following H_2O_2 relative CT = 1, decreased by more than 50% (Figure B.6). The same trends in the alpha diversity measurements are observed in the last week of the sampling (29 August), where the *Microcysits* were the most abundant genus.

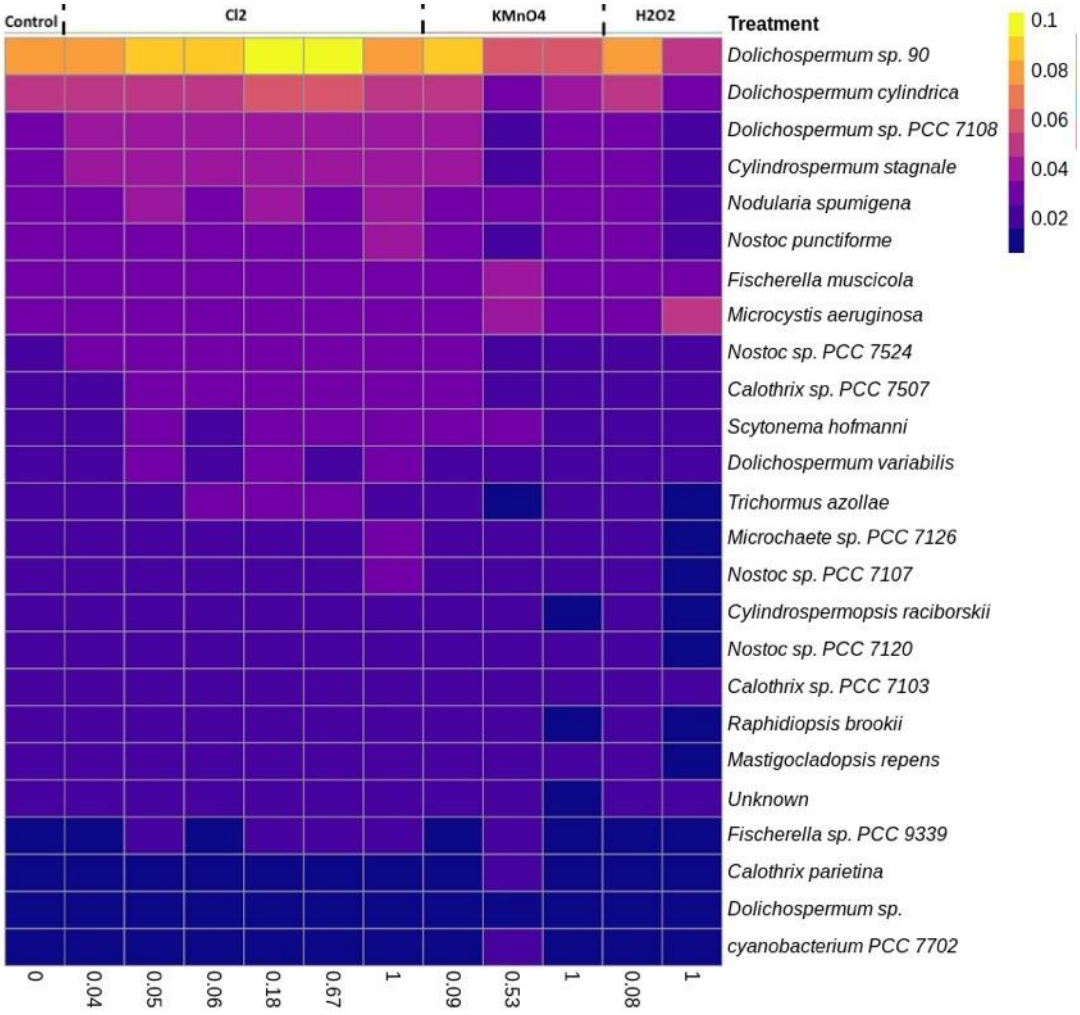

Figure 5.4 Cyanobacterial species heat map following the oxidation using Cl_2 (0.6 mg/L), $KMnO_4$ (5 mg/L), H_2O_2 (10 mg/L) (1 August 2018).

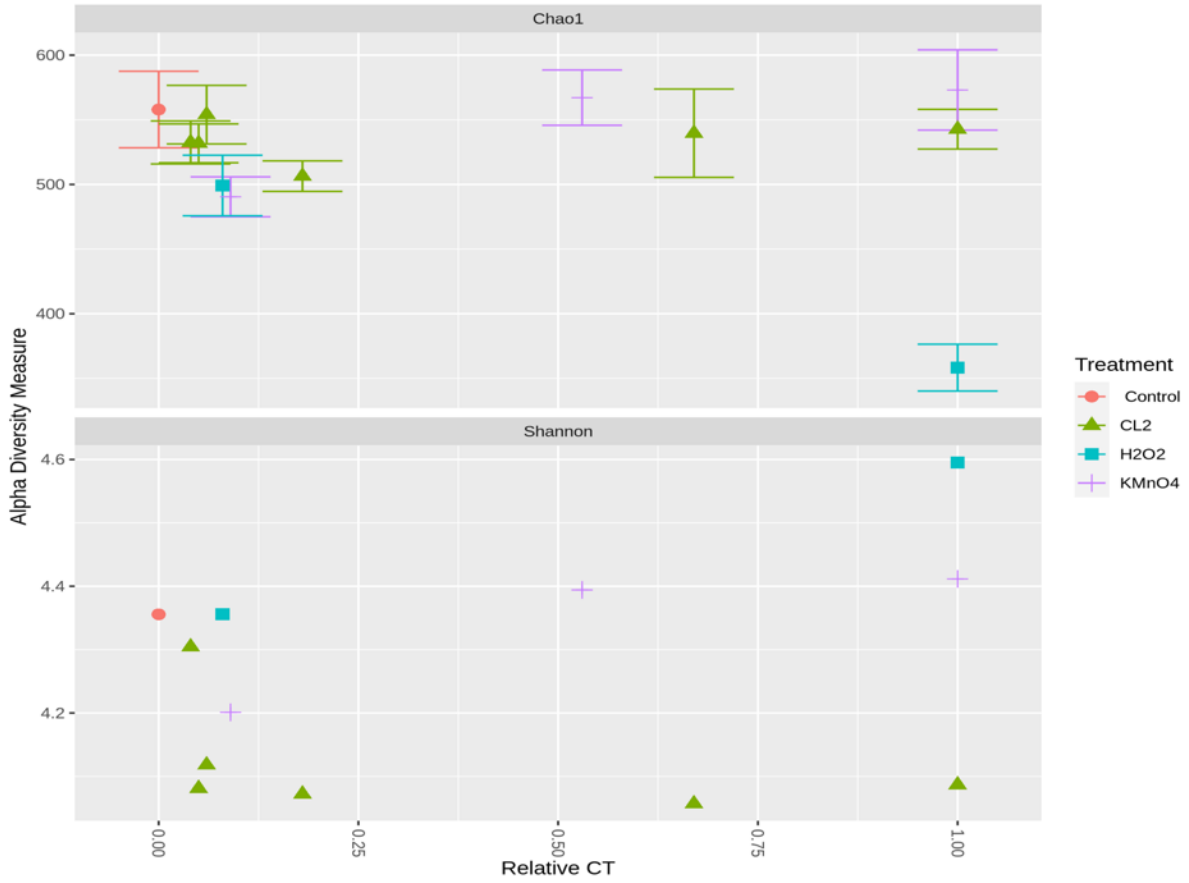

Figure 5.5 Alpha diversity measures of the cyanobacterial community following oxidation Cl_2 (0.6 mg/L), $KMnO_4$ (5 mg/L), H_2O_2 (10 mg/L) (1 August 2018).

5.3.4 Cyanobacterial community assessment following oxidation; Longitudinal study

The induced changes of cyanobacterial composition structure following the oxidation (Cl_2, $KMnO_4$, O_3 and, H_2O_2) are assessed separately. The analysis was performed at the genus and species level.

5.3.4.1 Chlorination

The chlorination experiments were conducted on 1 August Figure 5.6a, and 29 August (Figure 5.6b). In the first chlorination trial (1 August), the abundant genera were *Dolichospermum* and *Nostoc*, representing approximatively 20% and 10% of the cyanobacterial community, respectively (Figure 5.6a). Figure 5.6 shows a limited effect of chlorination on the relative abundance of all cyanobacteria genera except *Synechococcus*. In addition, taxonomic cell counts show decrease (up

to 30%) in total cyanobacteria taxonomic cell counts for the trial on 1 August and limited variation for the 29 August trial (15% variation) (Figure B.5). In terms of the species, *Dolichospermum sp.90* and *Dolichospermum cylindrica* were dominant for the 1 August trial. For the 29 August trial, *Microcystis aeruginosa* was the dominant species, followed by *Dolichospermum sp.90* (Figure B.6). In all trials, as chlorination exposure increased, the relative abundance of the abundant species, either *Dolichospermum sp.90 or Microcystis aeruginosa,* increased slightly. Moreover, the relative abundance of *Dolichospermum sp.*90 increased as *Microcystis aeruginosa* did on 29 August. Chlorination results show that *Dolichospermum* species and *Microcystis aeruginosa* are relatively more persistent than the other species.

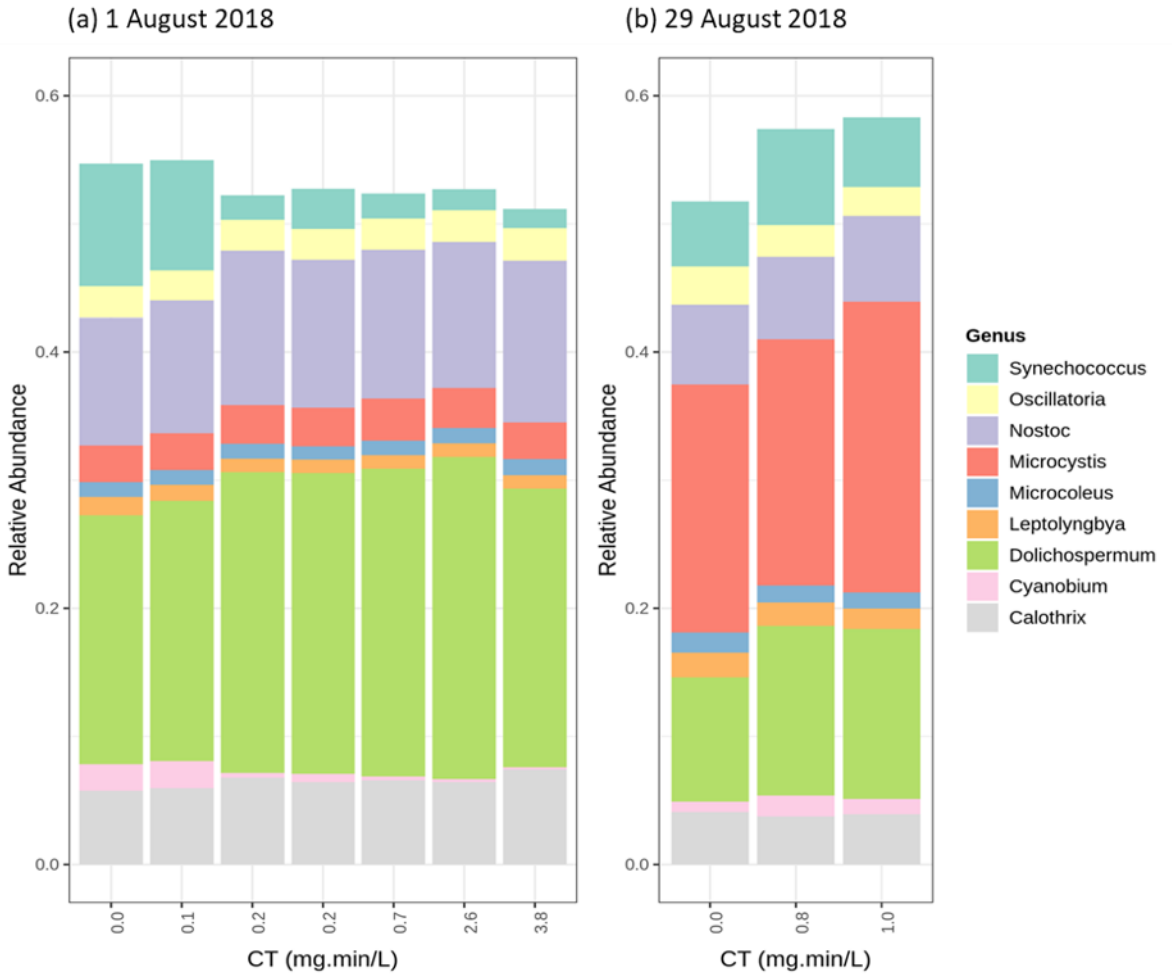

Figure 5.6 The relative abundance of the most abundant genus following chlorination (0.6 mg/L and 0.2 mg/L) (**a**) 1 August 2018 (*Dolichospermum* genus abundant) (**b**) 29 August 2018 (*Microcystis* genus abundant).

5.3.4.2 Potassium Permanganate ($KMnO_4$)

The relative abundance of the different genera following oxidation using permanganate shows limited variation for both $KMnO_4$ tests (Figure 5.7). Total taxonomic cell counts decreased (up to 57%) in the first trial (1 August) and remained stable in the second $KMnO_4$ trial (less than 1% variation) (29 August). Total taxonomic cell counts following the first $KMnO_4$ trial showed a decrease at 278 mg·min/L (Figure B.7). The relative abundance of the *Dolichospermum sp.90* increased slightly, whether it was the abundant species or not, suggesting the relative persistence of the *Dolichospermum sp.90* during $KMnO_4$ oxidation (Figure B.8).

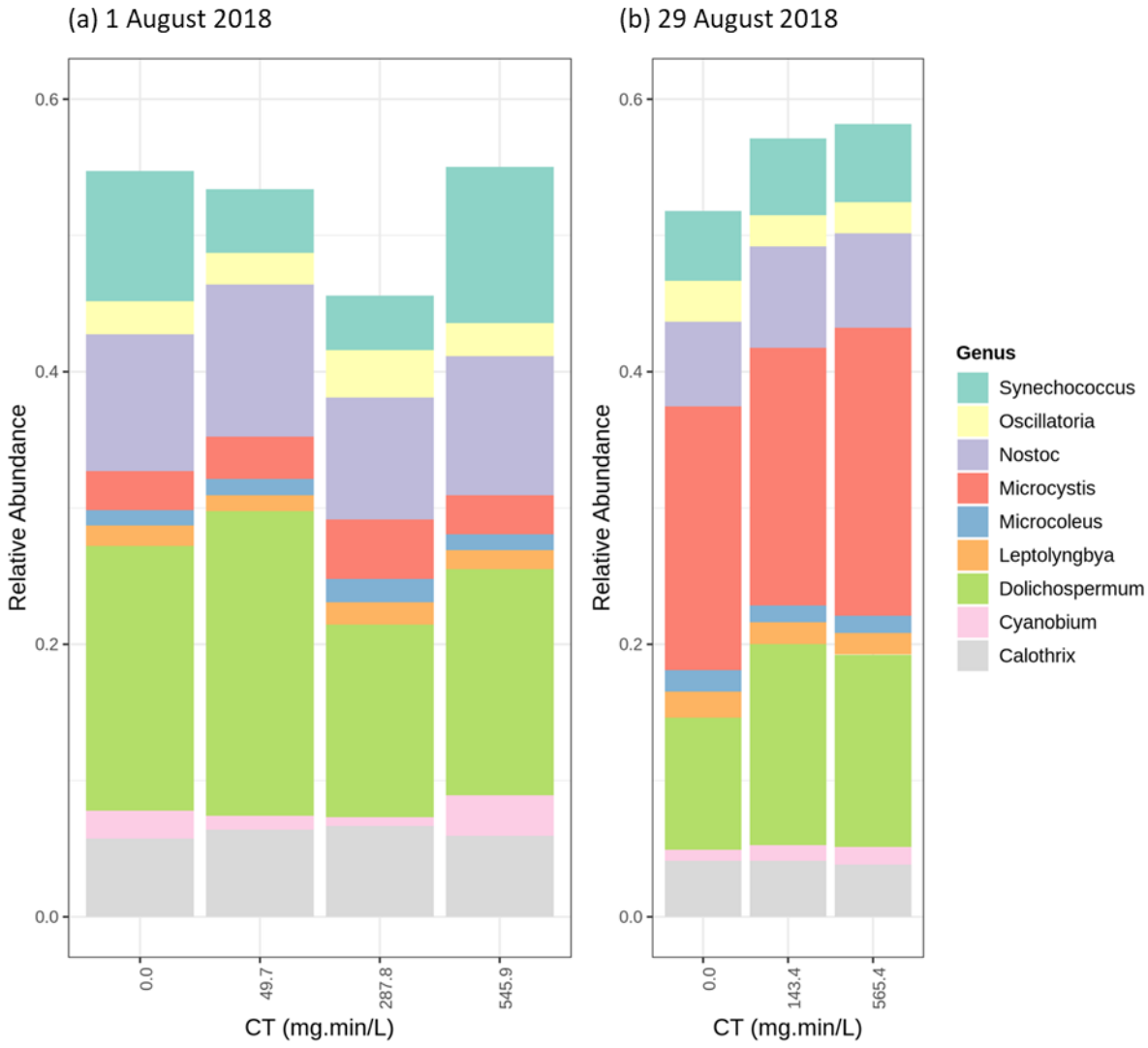

Figure 5.7 Relative abundance of the most abundant genus following $KMnO_4$ (5 mg/L) oxidation (**a**) 1 August 2018 (*Dolichospermum* genus abundant) (**b**) 29 August 2018 (*Microcystis* genus abundant).

5.3.4.3 Ozonation (O_3)

The first and second ozonation trials were performed on 15 August (*Dolichospermum* most abundant genus) and 21 August (*Synechococcus* most abundant genus). Cyanobacterial community results following ozonation in the second trial (at genus level—Figure 5.8) showed a decline of the relative abundance of *Synechococcus,* followed by an increase for *Microcystis*, as compared to the control condition. However, no significant variation was observed for the relative abundance of the different genera in the first ozonation trials. Furthermore, total cyanobacteria taxonomic cell counts revealed no significant change for both ozonation tests (up to 15%) (Figure B.9). In the control condition of the 15 August ozonation trial, *Microcystis aeruginosa* was the dominant species, followed by *Dolichospermum sp.90* (Figure B.10). *Dolichospermum sp.90* was not the dominant species, but it remained intact following ozonation. Although *Cyanobioum gracil* and *Synechococcus sp.* were the dominant species in the 21 August trial control, *Microcystis aeruginosa* became the dominant species following ozonation. At the low dosage applied, only secondary oxidation radical by-products are likely to react with cyanobacterial cells. Under these soft ozonation conditions, unicellular *Cyanobium gracil* and *Synechococcus sp.* cells were more susceptible than *Microcystis aeruginosa*.

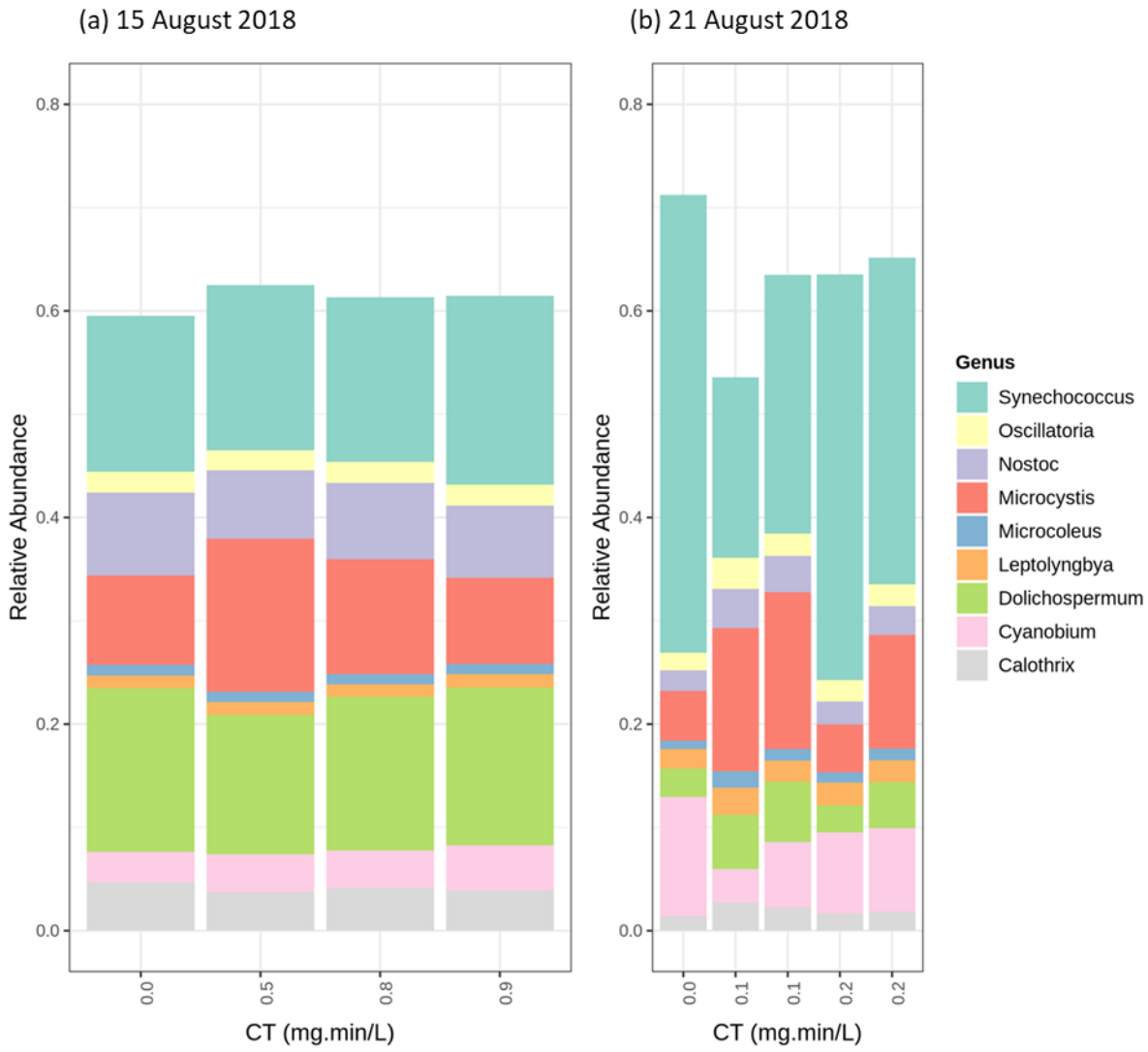

Figure 5.8 Relative abundance of the most abundant genus following O_3 (0.3 mg/L and 0.1 mg/L) oxidation (**a**) 15 August 2018 (*Dolichospermum* genus Abundant), (**b**) 21 August 2018 (*Synechococcus* genus abundant).

5.3.4.4 Hydrogen Peroxide (H_2O_2)

The *Dolichospermum*/*Dolichospermum sp.90* and *Microcystis*/*Microcystis aeruginosa* were the most abundant genus/species on 1 August and 29 August H_2O_2 oxidation, respectively. The relative abundance of the *Dolichospermum* declined following H_2O_2 exposure of CT = 7035 mg·min/L. *Microcystis* relative abundance decreases by more than 10% at 8442 mg·min/L exposure of H_2O_2 on 29 August experiment (Figure 5.9). At the same H_2O_2 exposure, *Dolichospermum* decreased by 5%. Total cyanobacteria taxonomic cell counts declined following H_2O_2 oxidation for both dates:

52% decrease on 1 August and 49% decrease on 29 August (Figure B.11). The relative abundance of the dominant species (*Dolichospermum sp.90* 1 August and *Microcystis aeruginosa* 29 August) decreases after H_2O_2 oxidation. The relative abundance of *Microcystis aeruginosa* in the H_2O_2 trial on 1 August increased after high H_2O_2 exposure. *Microcystis aeruginosa* was susceptible to H_2O_2 oxidation when abundant (as the relative abundance decreased), but it persists as an abundant species. Our results are in accordance with (Lusty and Gobler, 2020). Figure B.12 unveils higher susceptibility of *Dolichospermum* species to high H_2O_2 exposure as compared to *Microcystis aeruginosa*. Our results show the effect of high H_2O_2 exposure on the cyanobacteria species, which is in accordance with previous studies (Matthijs et al., 2012; Zhou et al., 2013).

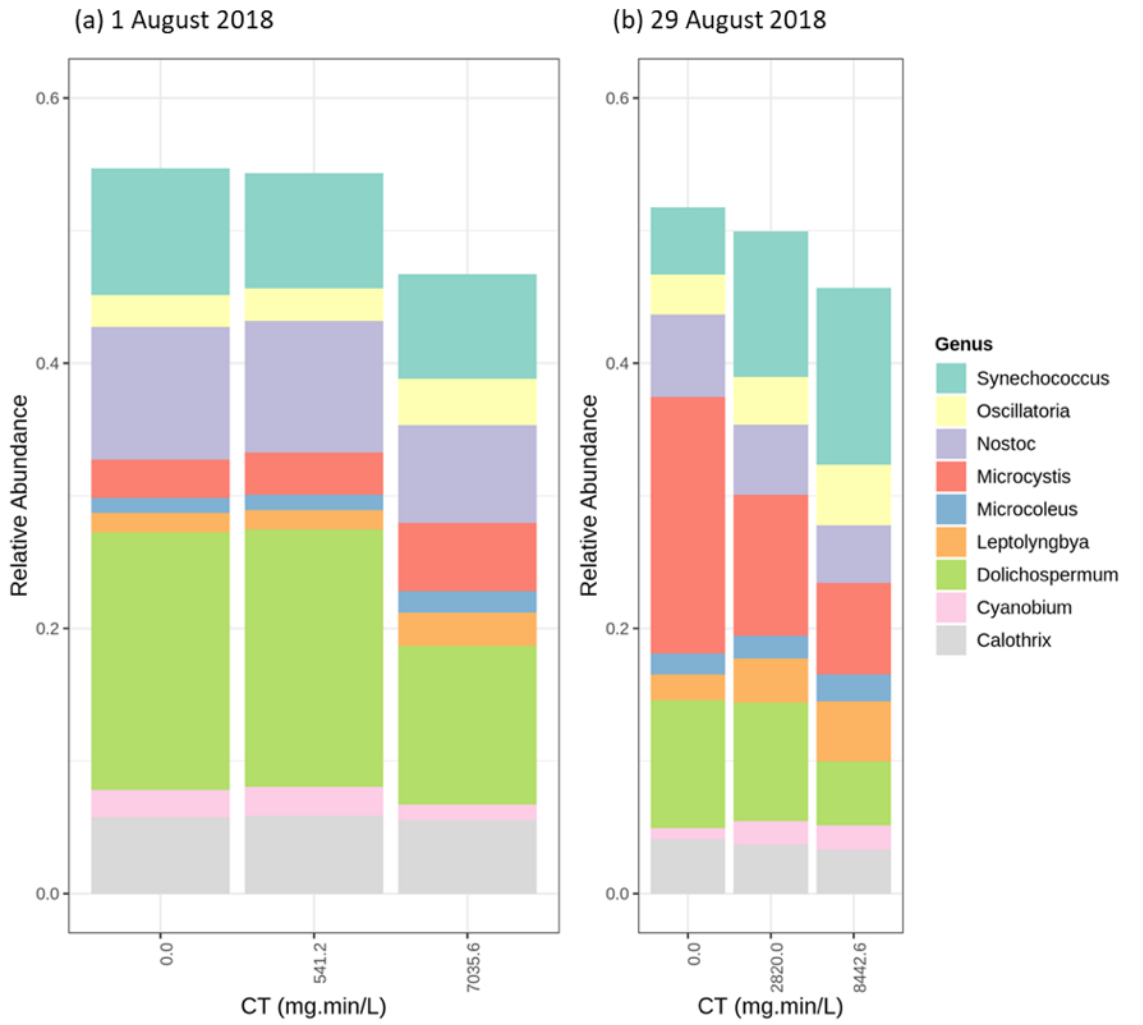

Figure 5.9 Relative abundance of the most abundant genus following H_2O_2 (10 mg/L) oxidation on (**a**) 1 August 2018 (*Dolichospermum* genus abundant) (**b**) 29 August 2018 (*Microcystis* genus abundant).

Cyanobacterial composition analysis at species level exhibits relative persistence of different *Dolichospermum* species and *Microcystis aeruginosa* when it is abundant following soft-chlorination, soft ozonation and permanganate oxidation. This result is in accordance with the previous studies, which were mainly based on the taxonomic cell count and the lab-cultured species (Coral et al., 2013; Fan et al., 2013a; Fan et al., 2014b; Zamyadi et al., 2015a; Zamyadi et al., 2013d). Our results highlight the ability of hydrogen peroxide to decrease the relative abundance of different taxa, including the toxin-producing taxa of interest. H_2O_2 selectivity provides an efficient barrier against toxic cyanobacteria entering a drinking water treatment plant.

5.3.5 Comparison of the Microscopic cell count vs Metagenomics results

The taxonomic cell count results (genus) from the chlorination on 1 August and ozonation on 15 August are presented in Figure B.13. The observed genera from microscopic cell counts do not completely match with high throughput sequencing results as *Aphanocapsa* and *Aphanothece* were only reported by taxonomic cell count. Misclassification at the genus level is less common than for species level; microscopic cell counts showed that *Dolichospermum spiroids*, *Aphanocapsa delicatissma*, *Aphanotheche clathrate brevis* and *Aphanocapsa holistca* were the most abundant species following chlorination and ozonation. However, high throughput sequencing did not identify them as an abundant species. The abundant species from high throughput sequencing were *Microcystis aeruginosa*, *Dolichospermum Sp.90* and, *Dolichospermum cylindrica* (Figure B.6 and Figure B.10). Despite the potential of the microscopic cell count to provide absolute quantitative data such as cells/mL and biovolume, it has some drawbacks.

The differences in community composition structure retrieved from the microscopic taxonomic cell counts and high throughput sequencing could be the result of the limitations inherent to these methods. For high throughput sequencing, these limitations include incomplete DNA sequencing libraries, using different libraries to identify genus and species or misclassification. In the case of microscopic taxonomic cell counts, several sources of uncertainty and error have been identified (Park et al., 2018; Xiao et al., 2014). The morphological similarity among cyanobacteria taxa may lead to overlooking or misidentifying cyanobacteria under the microscope, especially low abundant species (Casero et al., 2019; Kim et al., 2018a). Few genomes might be available for some taxa identified by taxonomic cell count (e.g., *Aphanocapsa* and *Aphanothece*), which may result in low relative abundance of these taxa using high throughput sequencing. Additionally, oxidation may

further hinder the ability to identify cells because of its impact on the cell structure. Oxidation at higher dosages can cause significant morphological deformation of the cyanobacteria species, especially for H_2O_2 and $KMnO_4$ in our study (Moradinejad et al., 2019). Flow cytometry conducted using the method described by Moradinejad et al. (2019) showed partial membrane damage (up to 80%) under the soft-oxidation conditions performed in this study (data not shown).

This study is the first to provide insights into the impact of different pre-oxidants (doses and contact time) on the diversity and cyanobacterial community composition. The experimental design focused on CTs at which the shifts occurred, in order to provide actionable results for water utilities. Additional investigation would be beneficial to extend our observations to other water bodies. In addition, using assembly/binning method is suggested for future studies to provide a more accurate view of cyanobacterial genus/species.

5.4 Conclusion

A comparison of the microscopic vs. high throughput sequencing results demonstrates the ability and robustness of high throughput sequencing to fully reveal a wide diversity of cyanobacterial communities in response to oxidant stress.

Results from longitudinal sampling over a bloom period of 4 weeks by high throughput sequencing highlight quick composition and abundance shifts in the cyanobacterial communities that occur within a day. High throughput sequencing revealed clearer shifts during a bloom from an initial dominance of *Dolichospermum*/*Dolichospermum Sp.90* toward a late summer dominance by *Microcystis*/*Microcystis aeruginosa.*

Overall, pre-oxidation caused deeper changes in the diversity of whole bacterial communities, especially proteobacteria, than was observed for the cyanobacterial community. Such changes should be considered when assessing the impact of using oxidants for onsite source control.

Depending on the oxidants used, alpha diversity indexes (Shannon and Chao1) showed that oxidation resulted in different structural composition shifts within bacterial and cyanobacterial communities.

Soft-chlorination using dosages 0.2 and 0.6 mg/L that were typically used for pre-oxidation caused a progressive shift in the bacterial and cyanobacterial communities with increasing CTs (0–3.8

mg·min/L). The results using $KMnO_4$ (5 mg/L) and H_2O_2 (10 mg/L) induced larger and distinct shifts in the structural composition of bacterial and cyanobacterial communities.

Regardless of the significant differences in community distribution shifts caused by different oxidants, some toxin producing species could persist after oxidation whether they were dominant species or not.

Soft-chlorination results revealed that *Dolichospermum sp.90* was relatively persistent with increasing CTs whether it was the dominant species or not. Relative persistence of *Dolichospermum sp.90* was also observed within $KMnO_4$ oxidation with increasing $KMnO_4$ exposure, regardless of the dominant species.

Soft-ozonation using dosage 0.1–0.3 mg/L results showed the relative persistence of *Microcystis aeruginosa* (the dominant species) with increasing ozone exposures (0–0.9 mg·min/L).

Only pre-oxidation with H_2O_2 (10 mg/L) caused a clear decrease in the relative abundance of all taxa and some species including the toxin-producing taxa of interest. As such, H_2O_2 would provide an effective first barrier against toxin producing cyanobacteria entering the drinking water treatment plant.

Selection of the most effective pre-oxidant for drinking water purposes should be made considering its impact on the cyanobacterial community structure/diversity, prevention of disinfection by-product formation and other drivers such as color and the presence of taste odor compounds.

Funding

This research was funded by Genome Canada and Genome Quebec: Algal Blooms, Treatment, Risk Assessment, Prediction and Prevention through Genomics (ATRAPP) Project, Grant number Genome Canada/UM RQ000607 and the APC was funded by Genome Canada and Genome Quebec (ATRAPP project).

Acknowledgments

The authors acknowledge support from Algal Blooms, Treatment, Risk Assessment, Prediction and Prevention through Genomics (ATRAPP), The authors thank the staff at NSERC Industrial Chair on Drinking Water at Polytechnique Montreal. The authors thank the staff at Microbial Evolutionary Genomics (Shapiro lab) at Universite de Montreal.

CHAPTER 6 ARTICLE 3 - EVALUATION OF FUNCTIONAL CAPACITY OF A CYANOBACTERIAL BLOOM DURING OXIDATION

Our objective was to assess the changes and variation of functions before and after chemical oxidation, using high throughput sequencing. High throughput sequencing gives us the opportunity to study impact of oxidation on functional capacity of the cyanobacterial bloom for the first time. The results highlight the importance of the functions following oxidation and their correlation with different phyla. This chapter was submitted as a research paper to the Chemical Engineering Journal Advances in February 2021. Supplementary information is presented in Appendix C.

EVALUATION OF FUNCTIONAL CAPACITY OF A CYANOBACTERIAL BLOOM DURING OXIDATION

Saber Moradinejad[1*],Hana Trigui[1], Juan Francisco Guerra Maldonado[1], B. Jesse Shapiro[2,3,4], Yves Terrat[2], Sébastien Sauvé[5], Nathalie Fortin[6], Arash Zamyadi[7,8], Sarah Dorner[1], Michèle Prévost[1]

[1]NSERC Industrial Chair on Drinking Water, Department of Civil, Geological, and Mining Engineering, Polytechnique Montréal, Montréal, Québec H3T 1J4, Canada

[2]Department of biological science, Université de Montréal, Montréal, Québec, H2V 0B3, Canada

[3]Department of Microbiology and Immunology, McGill University, Canada

[4]McGill Genome Centre, McGill University, Canada

[5]Département de Chimie, Université de Montréal, Montréal, QC, Canada

[6]National Research Council Canada, Energy, Mining and Environment, 6100 Royalmount Avenue, Montreal, QC H4P 2R2, Canada

[7]Water Research Australia (WaterRA), Adelaide, SA 5001, Australia

[8]BGA Innovation Hub and Water Research Centre, School of Civil and Environmental Engineering, University of New South Wales (UNSW), Sydney, NSW 2052, Australia

* corresponding author: Saber.moradinejad@polymtl.ca

Abstract

Pre-oxidation is widely used against cyanobacteria at the water treatment plant intake to improve cell removal efficiency in down flow processes (coagulation, flocculation, sedimentation) and reduce the cyanotoxins concentration. In this study, shotgun metagenomic sequencing was used to describe the bacterial community's functional capacity within cyanobacterial bloom (at Lake Champlain, southern Quebec, Canada) before and after oxidation using Cl_2, $KMnO_4$ and H_2O_2. The bloom samples were associated with two functional profile assemblages: that of August 1st (onset of the bloom) characterized by enrichment of genes related to nutrient uptake and that of August 13th-29th (towards the end of the sampling) associated with competition for resources and repair such as Photosynthesis, Protein metabolism and DNA metabolism. Different functional profile responses to oxidation with Cl_2, $KMnO_4$ and H_2O_2 was also identified as two-time points during the bloom (at the beginning-August 1st, and at the end of the bloom August 29th). On August 1st, chlorinated samples showed a progressive shift in functional profile: starting by acquiring and sequestering nutrient sources (e.g. Iron acquisition, carbohydrates) at low chlorine exposure (CT, concentration-contact time) level, followed by regulation and cell signaling pathways for nutrients acquisition at mid-relative CT to finally, showing a stronger tendency toward dormancy and sporulation genes at high CT. High relative CTs of $KMnO_4$ and H_2O_2 showed close functional composition to that of with relative high CT of Cl_2. Correlation analysis highlighted the main functional profile (level 1) following Cl_2 oxidation on beginning of the sampling. *Proteobacteria* contributed to energy acquisition (e.g. carbohydrates, iron) and usage (e.g. motility). *Bacteroidetes* were more correlated with the genes related to stressful conditions (RNA metabolism, Dormancy and Sporulation). Cyanobacteria appeared to maintain their ability for growth, photosynthesis and nitrogen/phosphorus metabolism after exposure to Cl_2. To trace the footsteps of cyanobacteria in functional capacity following oxidation, the variation of cyanobacterial biomarkers was investigated. Our results showed that following high CT of H_2O_2, the relative abundance of the cyanobacterial biomarkers decreased, regardless of the dominant cyanobacterial genus. The toxicity of the bloom and after oxidation samples were assessed by droplet digital PCR (ddPCR) to measure the *mcyD* gene. Our results showed significant positive correlation between the *mcyD* gene copies number and microcystin concentrations in the bloom samples (before the oxidation). However, such correlation was not captured in the after the oxidation samples. These results suggest that ddPCR can only be used to evaluate bloom toxicity before the oxidation.

Keywords

Cyanobacteria; Oxidation; Function; Biomarker; Stress

6.1 Introduction

Cyanobacterial blooms and water bodies eutrophication are happening more frequently due to increasing temperatures (climate change) and human activities (nutrient management in the watershed) (Paerl and Paul, 2012; Wells et al., 2015). Over 40 toxic cyanobacterial species are known to produce five major groups of cyanotoxins (microcystin, anatoxin, saxitoxin, cylindrospermopsin and β-Methylamino-L-alanine) (Al-Sammak et al., 2014; Casero et al., 2019; Westrick et al., 2010). Cyanotoxins bioaccumulate in fish and shellfish and are poisonous to nearly all livestock, wildlife and humans (Backer et al., 2013; Bukaveckas et al., 2017). Cyanobacteria metabolites can also lead to taste and odor (T&O) problems (Wert et al., 2014; Yao et al., 2017; Zamyadi et al., 2015b). The most commonly detected T&O compounds are Geosmin and 2-methylisoborneol (MIB).

Cyanobacterial cells and their metabolites (cyanotoxins-T&O) pose a challenge to drinking water treatment processes (Pazouki et al., 2016; Zamyadi et al., 2015b; Zamyadi et al., 2012b). Cyanobacteria entering and accumulating within the plant can be dampened using pre-oxidation. Pre-oxidation has been proposed as a tool to prevent the accumulation of cyanobacteria and cell-bound toxin in sludge using ozone (Zamyadi et al., 2013a; Zamyadi et al., 2013c), H_2O_2 (Matthijs et al., 2012; Zhou et al., 2013), $KMnO_4$ (Fan et al., 2013a; Fan et al., 2013b; Naceradska et al., 2017) and Cl_2 (Fan et al., 2013b; Wert et al., 2014; Zamyadi et al., 2013d). The oxidation efficiency to degrade cyanobacterial cells and their associated harmful metabolites may vary according to the presence of different bacterial communities, growth phase, cell agglomeration and background water quality parameters such as pH and dissolved organic matter (He and Wert, 2016; Merel et al., 2013; Wert et al., 2013; Zamyadi et al., 2015a). Considering cyanobacterial blooms' complex dynamics, the improvement of oxidation efficiency requires an understanding of the cyanobacterial structural and functional profile in response to oxidation processes. The fate of bacterial and cyanobacterial communities have been studied using cell count based methods and molecular tools such as high throughput sequencing and 16S rRNA and and real-time PCR (Berry et al., 2017; Casero et al., 2014; Eldridge and Wood, 2019; Kim et al., 2018a; Lezcano et al., 2017; Lusty and

Gobler, 2020; Pei et al., 2017; Scherer et al., 2017; Willis and Woodhouse, 2020; Woodhouse et al., 2015; Xu et al., 2018).

The analysis of functional structures of bacterial community using high throughput metagenomic shotgun sequencing can provide insights on how a community may respond and adapt to the imposed stress (chemical oxidation). Gomez-Smith et al. (2017) (Gomez-Smith et al., 2016) highlighted the importance of microbial functions (e.g. nitrification) in drinking water treatment. For the cyanobacterial community, several studies have focused on succession and co-presence of nitrogen fixation, inorganic phosphorus scavenging, and toxin-producing strains in cyanobacterial blooms (Harke et al., 2015). Limited studies have focused on the functional structure of bacterial community and metabolic functions such as phosphorus and nitrogen metabolisms, cell division and cell cycle (Hörnlein et al., 2020; Li et al., 2020a; Lu et al., 2019; Taton et al., 2020). A high relative abundance of nitrite/nitrate reductase was identified in an early summer bloom dominated by *Aphanizomenon*/*Dolichospermum* in lake Utah (Li et al., 2020a). At the same time, severe nutrient starvation was observed for phosphorus and carbohydrate metabolisms (Li et al., 2020a). Shi et al. (2017) studied the functional structure of a cyanobacterial bloom (Lake Taihu) during a 95-day microcosm experiment. Results showed an increase in nitrogen, amino acid-related, pyruvate and methane metabolisms during lysis of the cyanobacterial community (Shi et al., 2017). The microbial functional composition has been studied in a stratified drinking water reservoir (Shilei et al., 2020), ice-covered lakes (Zhou et al., 2020) sewage sludge (Wang et al., 2018) and a river (Li et al., 2020b). Shilei et al. (2020) (Shilei et al., 2020) reported that dissolved oxygen, pH, temperature, nitrate, ammonia, total phosphorus, and chlorophyll-a were the critical factors in the drinking water reservoir's structural and functional composition. Shilei et al. (2020) (Shilei et al., 2020) observed that metabolic functions such as cell growth and death, energy metabolism and environmental adaptation were enriched in the reservoir's mixing period compared to the stratified condition (Shilei et al., 2020). Also, results from Shilei et al. (2020) (Shilei et al., 2020) suggested that total dissolved phosphorus, $NH4^{+}$, pH, dissolved oxygen, and temperature have an impact on the functional bacterial profile of a stratified reservoir.

To our knowledge, no study has focused on the functional capacity of the cyanobacterial bloom following drinking water treatment processes such as chemical oxidation. Understanding the cyanobacterial bloom functional composition before and after oxidation can provide insights into the mechanism of oxidation and provide a stronger basis to predict treatment efficacy. The main

objective of this study was to determine how the functional abilities of bacterial community within a cyanobacterial bloom were impacted by oxidation (with Cl_2, $KMnO_4$, H_2O_2) using high throughput metagenomic shotgun sequencing. Also, we investigated potential correlation between the ddPCR results (*mcyD* gene copies number) with the concentration of microcystin to use ddPCR to evaluate cyanobacterial bloom toxicity.

6.2 Material and Methods

6.2.1 Sampling site description

Cyanobacterial bloom samples were collected from the intake (surface) of the Bedford drinking water production plant (Missisquoi Bay, Lake Champlain) in southern Quebec, Canada. Samples were collected on August 1st, 13th, 15th, 21st, 29th of 2018. Cyanobacterial blooms have been previously reported from this site (McQuaid et al., 2011; Zamyadi et al., 2015a; Zamyadi et al., 2013b; Zamyadi et al., 2012b).

6.2.2 Chemicals and Reagents

The oxidation assays were performed using chlorine (0.2 and 0.6 mg/L), permanganate (5 mg/L), and hydrogen peroxide (10 mg/L). Detailed protocols to prepare the stock solutions and quenching reagents can be found in (Moradinejad et al., 2020). The selection of doses (concentration) and contact time was based on the common pre-oxidation doses and contact time used in the operation of the drinking water treatment plant.

Oxidant exposures, concentration (C) vs contact time (T), (CT) were calculated using following Equation:

$$CT = \int_0^t [Oxidant]dt = \frac{C_0}{k_{decay}}(e^{k_{decay}t} - 1) \qquad \text{Eq. 6-1}$$

Where k_{decay} (min^{-1}) is the first-order decay rate of the oxidant, t (min) is the contact time, and C_0 (mg/L) is the initial concentration of oxidant at time zero. The oxidation assays were conducted separately but at the same day (same cyanobacterial bloom for each day) for two different dates (August 1st and August 29th).

6.2.3 DNA extraction, metagenomics preparation, bioinformatics and statistical analysis

Nucleic acid was extracted from the filters using DNeasy power kits (Qiagen Group, Germantwon, MD, USA). 200 µL of nuclease-free water and 5µL of TATAA Universal DNA spike II (TATAA Biocenter AB) were added to evaluate extraction yields using real time qPCR. More details in DNA extraction and metagenomics sequencing procedure are presented in Moradinejad et al. (2020). Variations in species community and diversity were evaluated with heat trees using the Metacoder (0.3.3) (Foster et al., 2017). The function of protein fragments were identified by retrieving the best hits through SEED Subsystems (Overbeek et al., 2014), KEGG (Kanehisa et al., 2012) and COG (Tatusov et al., 2000) databases. The Pearson correlation coefficient for binary data was calculated to measure the association within taxa and between taxa-and-functional reads, according to Pearson (1896) and Janson and Vegelius (1981). Detailed methodology for statistical analysis and permutation test is is presented in Moradinejad et al. (2020).

6.2.4 ddPCR

Detection primers of the *mcyD* gene involved in microcystin production were as follows: *mcyD*(KS)F1: 5'-TGGGGATGGACTCTCTCACTTC-3' and *mcyD*(KS)R1: 5' GGCTTCAACATTCGGAAAACG-3' (Fortin et al., 2010). Equal concentrations of DNA 1.0 ng/µL were used for ddPCR analysis. The PCR mixture consisted of 12. 5 µL Bio-Rad 2x QX200 ddPCR EvaGreen^{R} Supermix (SM) (BioRad Laboratories Ltd, Mississauga, ON), *mcyD* (KS) primers at a final concentration of 0.1 µM, 0.2 mg/mL BSA and genomic DNA input concentrations ranging from 1 to 5 ng DNA per 25µL ddPCR reaction. Sample mixtures were vortexed gently avoiding the formation of bubbles, centrifuged for 20 sec, then kept on ice until droplet generation. Samples were packaged into droplets by adding 20 µL of the PCR mixture in each sample well of the single-use DG8 cartridge followed by addition of 70 µL of droplet generation oil for EvaGreen^{R} to each of the corresponding oil wells. The cartridge was then placed into the QX200 droplet generator for droplet production. Forty microliters of generated droplets were transferred from the cartridge to a semi-skirted ddPCR 96-well plate (Bio-Rad). Samples were successively prepared in cartridges by groups of eight, transferred to the PCR plate and subsequently heat sealed with a pierceable foil seal. The plate was transferred to a thermal cycler and reactions were run under the following standard cycling conditions: 95°C for 10 min followed by 40 cycles of 94°C for 30 sec;

55°C for 60 sec, 98°C for 10 min, and 4°C hold; ramp rate = 50% (2°C/sec). Upon completion of the PCR phase, plates were loaded onto the QX200 Droplet Digital reader, which automatically reads the droplets from each well of the plate (17 000 droplets/well). Data analysis was performed using QuantasoftTM software (Bio-Rad). Negative droplets, lacking target and/or reference gene DNA, and positive droplets, containing either or both DNAs, were counted to give the fraction of positive droplets. Using Poisson statistics, the concentrations of both DNA species were determined, and copies/ng calculated.

6.2.5 Microcystin analysis

Microcystin concentrations (intracellular and extracellular) were measured using an on-line solid-phase extraction ultra-high-performance liquid chromatography coupled to tandem mass spectrometry (On-line SPE-UHPLC-MS/MS, Thermo TSQ Quantiva). Microcystin separation was performed on a Thermo Hypersil Gold C18 column (100mm x 2.1mm, 1.9 µm particle size). Further details on the cyanotoxin measurement methods can be found in Munoz et al. (2017) and Roy-Lachapelle et al. (2019).

6.2.6 Analysis of RNA integrity following exposure to oxidants

The impact of oxidants on the integrity of nucleic acids was analyzed by measuring total RNA (cultured cyanobacteria) after exposure to oxidants. *Microcystis aeruginosa* strain CPCC 300 and *Dolichospermum* strain CPCC 544 were cultured in BG-11 medium at 21°C under 12-hr rotating light-darkness at an intensity of 70 µmol S^{-1} m^{-2}. Cultures were harvested at stationary phase and spiked into intake water from the Saint Jean Sur Richelieu (Quebec, Canada) water treatment plant (6-7 mg/L of dissolved organic carbon (DOC) and pH of 7 – 7.5). A mix of 200,000 cell/mL of *Microcystis* (50%) and *Dolichospermum* (50%) was used. Cl_2 was added at 3 mg/L for contact times of 2 min, 5 min, 30 min, 1 h, 2 h) and KMnO4 at 10mg/L for contact times of 30 min, 1 h, 2 h, 4 h. RNA was extracted by the RNeasy PowerWater Kit (Qiagen). DNA was removed using the Turbo DNA free Kit from Ambion (ThermoFisher, Saint-Laurent, QC). 1% Formaldehyde-agarose gel was used to evaluate total RNA profiles. Thirty µl of total RNA were run in each lane. RiboRuler High Range RNA Ladder (ThermoFisher, Saint-Laurent, QC) was run in parallel with the samples to determine the size of the RNA bands. RNA profiles showed the 23S, 16S and 5S

ribosomal RNA corresponding respectively, to 2900, 1500 and 120 base pairs (bp). Detailed oxidation experimental design is presented in supplementary information (Table C.1).

6.3 Results and discussion

6.3.1 Bacterial functional profile of the cyanobacterial bloom metagenome

Cyanobacterial bloom samples were collected at the intake of water treatment plant from the lake Champlain. Cyanobacterial taxonomic cell count results showed maximum $3.3x10^3$ cells/mL on August 1st and minimum $5.4x10^4$ cells/mL on August 29th. Taxonomic cell count and biovolume results is presented in the Table 5.2. Taxonomic cell count results were higher than the cell number alert level for drinking water treatment plants $6.5x10^4$ except the last day of sampling. The bacterial and cyanobacterial community composition has been described recently in Lake Champlain during the bloom sampling period (from August 1st to 29th) using metagenomic shotgun sequencing (Figure C.1) (Moradinejad et al., 2020). Proteobacteria was the most abundant phylum within the whole bacterial community, with more than 70% relative abundance on August 1st. From August 13th to 29th, the major bacterial phyla were Proteobacteria, Bacteroidetes, and Actinobacteria, followed by Cyanobacteria, which accounted between 5 to 10% of the total relative abundance in all samples (Figure C.1-a). The first bloom period was on August 1st to August 15th and corresponded to the dominance of *Dolichospermum* with the contribution of *Synechococcus* (Figure C.1-c). The second period was on August 21st and it corresponded to the dominance of *Synechococcus* and the higher abundance of *Microcystis.* The last cyanobacteria bloom sample was taken on August 29th and coincided with *Microcystis* dominance (Figure C.1).

In the current study, the functional profile of these samples was explored to correlate it with the taxonomic pattern described above. Figure 6.1 illustrates 29 most dominant functional categories (level 1) based on the relative abundance of assigned reads within the clustering-based subsystems within bloom samples retrieved from Lake Champlain from August 1st to August 29th. On August 1st, "Carbohydrates" was the most abundant functional category, followed by "Protein metabolism" and "Amino acids and derivatives", suggesting that the microbial populations on August 1st were well adapted to degrade accessible carbon substrates such as soluble carbohydrates or polysaccharides and amino acid derivatives. On August 13th, the most relative abundant reads shifted to the "Protein metabolism" category, and it remained abundant until the end of the

sampling date, on August 29th (Figure 6.1). Genes related to "DNA metabolism", "RNA metabolism", "Phage, Prophage Transposable elements, Plasmids", "Photosynthesis" and "Secondary metabolism" also showed slightly higher abundance during the period of August 13th-29th in comparison with August 1st. Interestingly, an opposite trend has been observed for "Membrane transport", "Metabolism of aromatic compounds" and "Motility and chemotaxis", "Iron acquisition and metabolism", "Sulfur metabolism", "Cofactors, Vitamins", "Prosthetic groups, Pigments", "Potassium metabolism" "Stress response" categories. Their relative abundance were lower on August 13th-29th compared to those on August 1st. Song et al. (2017) used functional metagenome analysis of natural soils in laboratory microcosms to characterize different ecological strategies adopted by the microbial community. Gong et al. (2017) showed that nutrient acquisition systems were highly upregulated during cyanobacterial bloom condition Building on their findings, we suggest that the conditions of the August 1st bloom were associated with lower nutrient availability and early successional stage (bacteria developing early and ready to use available resources and replication/repair) due to the higher abundance of genes involved in the regulation of amino acids, carbohydrates, sulfur, iron acquisition, potassium and aromatic compounds metabolisms. The period of August 13th-29th was more associated with a late successional stage (sustained crowding and intense competition for resources) since "Photosynthesis, "Protein metabolism" and "DNA metabolism" categories were relatively more abundant.

Interestingly, genes belonging to the "Phage, Prophage Transposable elements, Plasmids" subsystem were much more abundant, indicating that the bloom community structure on August 13th -29th acquired more genome plasticity (Figure 6.1). It has been reported that the activity of transposable elements in bacteria generates genome plasticity, leading to genetic variability and subsequently, strong fitness benefit to environmental changes (Zambrano et al., 1993). For cyanobacteria, genome plasticity is an important adaptive driver of evolution, unveiling the means of their persistence (Willis and Woodhouse, 2020; Zhaxybayeva et al., 2006). The genome of *Microcystis aeruginosa* was described as, containing the highest record of transposase frequencies (Kaneko et al., 2007). Moreover, the taxonomic profile at the end of the bloom period exhibited higher diversity, where Proteobacteria, Actinobacteria and Bacteroidetes shared the bacterial dominance (Figure C.1a). Song et al. (2017) suggested that the high taxonomic diversity was

associated with more functional diversity, which may be relevant to the overall bacterial adaptation strategies.

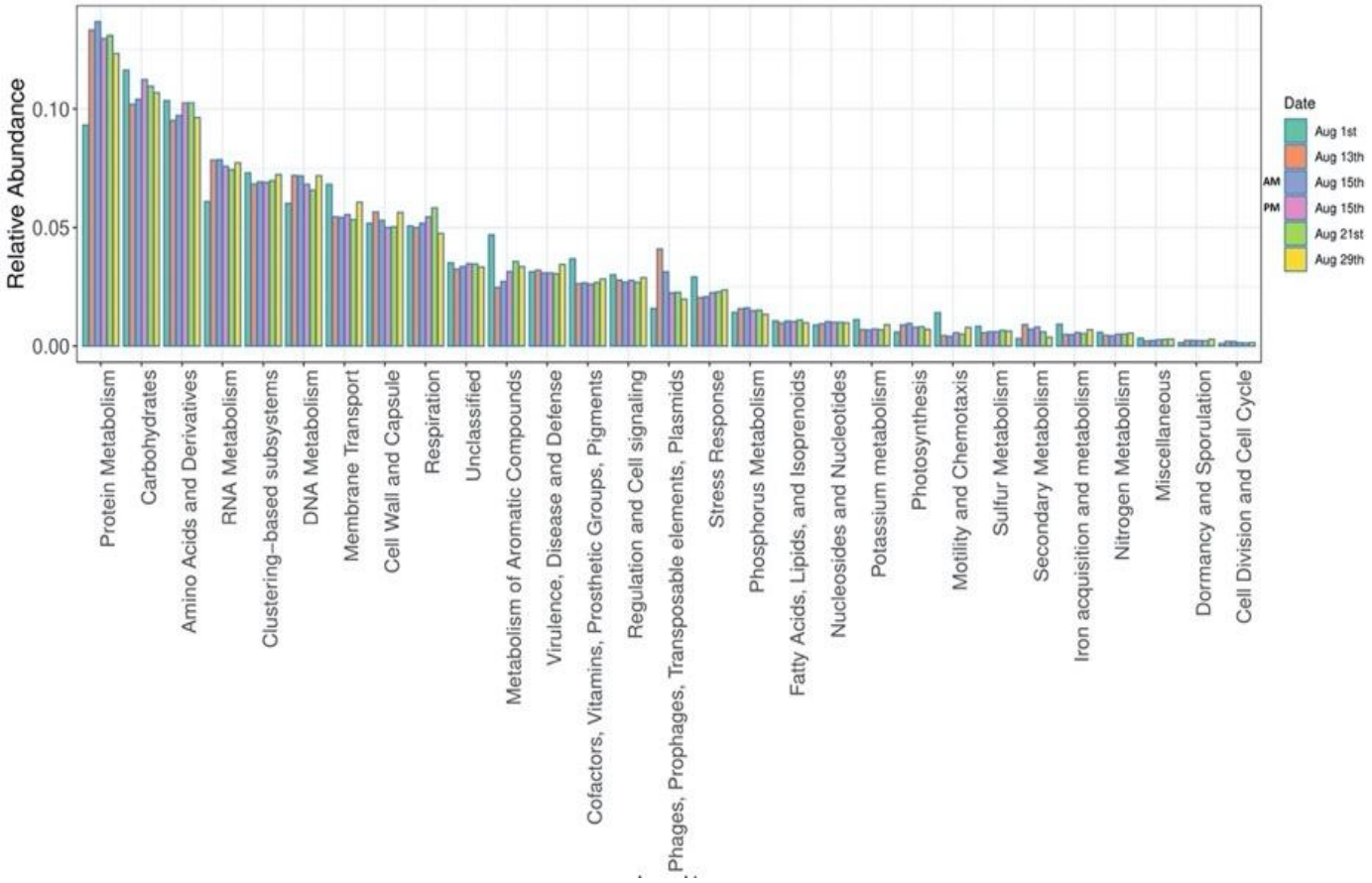

Figure 6.1 Functional profiles of the cyanobacterial bloom samples collected at the intake of the drinking water production plant in Missisquoi Bay, Lake Champlain during the month of August, 2018.

6.3.2 Oxidation impact on the bacterial functional capacity

The functional profile dynamics observed in the bloom samples (before oxidation) led us to hypothesize that these bacterial communities may have different functional capacity to in response to chemical oxidation. This hypothesis was investigated by comparing the functional profile, upon oxidation of bloom samples retrieved on two different days (August 1st and 29th).

To assess the impact of chemical oxidation on the community composition dynamics, principal component analysis (PCA) was conducted on cyanobacterial bloom samples before and after oxidation (Figure 2). The samples were those of August 1st, corresponding to *Proteobacteria* as

the most abundant phyla (accounting 70% of relative abundance), and of August 29th, corresponding to *Proteobacteria*, *Bacteroidetes* followed by *Actinobacteria* as the most abundant phyla (Figure C.1-a). On both sampling dates, cyanobacteria accounted for 5% of the relative abundance, but exhibited different composition structure; *Dolichospermum* dominated the August 1st sample, while *Microcystis* dominated on August 29th (Figure C.1-c). Exposure to oxidant was expressed as relative CT (rCT), a normalized oxidant exposure (concentration, contact time) that was used to compare the impact of the three oxidants (Cl_2, $KMnO_4$ and H_2O_2). More details can be found in Moradinejad et al. (2020).

As presented by the PCA, the differential functional structure of August 1st and August 29th bloom samples were associated with distinct microbial functional profiles after oxidation, signifying variability in microbial community fitness toward oxidation (Sharma et al., 2020). For the August 1st bloom sample, three cluster groups were detected based on the similarity of the functional composition before and after oxidation. The first group, which corresponds to control conditions and low relative CT of both Cl_2 and H_2O_2 exposure, clustered with "Metabolism of aromatic compounds", "Respiration", "Stress response", "Carbohydrates", "Iron acquisition and metabolism", "Amino acids and derivatives", "Motility and Chemotaxis" and "Membrane transport" related gene categories. The low relative CT (Cl_2 and H_2O_2) did not cause a change in the relative abundance of the genes associated with acquiring and sequestering nutrient sources such as carbohydrates. The second cluster emerged with increasing exposure to Cl_2 and was associated with the functional categories: "Sulfur metabolism", "cofactors vitamin", "Miscellaneous", "Regulation and cell signaling ", "Phosphorus metabolism ", "Nitrogen metabolism ", "Prosthetic group, Pigments". These gene-related categories correspond to the pattern of bacterial adaptation for survival in aquatic systems, encompassing various regulation and cell signaling pathways for nutrient acquisition (Song et al., 2017).

The third group included the relatively high CT of Cl_2, $KMnO_4$ and H_2O_2 exposures, and positively correlated with "Protein, DNA and RNA metabolisms", "Dormancy and sporulation", "Cell wall and capsule" and "Nucleosides and Nucleotides" related genes (Figure 6.2a). This suggests that bacterial persistence after high oxidant exposure (CT) was associated with the presence of stress response genes. Furthermore, the association of H_2O_2 with the "Nucleosides and Nucleotides" suggests a specific mode of action when compared to Cl_2 and $KMnO_4$, reflecting the differences in reactivity towards to nucleic acids and other key membrane components (Moradinejad et al., 2019).

In the present study, the surviving bacterial community also showed a strong association with dormancy and sporulation genes compared to other genes.

To better understand the shifts within the functional gene categories following oxidation for August 1st and August 29th samples, the relative CT-related changes in the functional metagenome effect is shown for each oxidant separately in Figure C.2, C.3 and C.4. For August 1st, "Carbohydrates", "Amino acids and derivatives" markedly decreased with the increase of CT of Cl_2, $KMnO_4$ and H_2O_2 exposures, suggesting that genes involved in energy metabolism were relatively less abundant. The relative abundance of the genes related to "Protein metabolism, "RNA metabolism", "DNA metabolism", "Cell wall and capsule" increased with increasing the exposure of Cl_2, $KMnO_4$ and H_2O_2. These functional profiles (August 1st) are in agreement with several studies showing that bacteria must synthesize stress response-related factors or metabolize excess nutrients in the environment to survive from harsh conditions imposed on the ecosystem (Cheriaa et al., 2012; Polek and Godočíková, 2012). This means that bacteria must increase protein synthesis and, in consequence, increase RNA and DNA synthesis (Humayun, 1998; Krämer, 2010). Our results demonstrated that metagenomes have more abundant housekeeping genes (protein, DNA and RNA metabolisms) at a high CT of Cl_2, $KMnO_4$ and H_2O_2 compared to the more permissive oxidation strategies (relatively mid/low CT).

The PCA of functional capacity following oxidation on August 29th showed different functional profiles compared to August 1st (Figure 6.2b). Some of the functions such as "Nitrogen metabolism", "DNA and RNA metabolism" were not identified in the PCA analysis (results of permutation test) following oxidation on the August 29th sample. We distinguished two cluster groups in the PCA of August 29th. The first cluster group encompassed control condition and the low relative CT of Cl_2 oxidation. The cluster was associated with "Membrane transport", "Cell wall and capsule", "Photosynthesis" and "Cell division and cell cycle" categories. Also, both $KMnO_4$ exposures (CT) were closely grouped and showed a strong association with the genes related to the "Prophage, transposable elements, plasmids" (Figure 6.2b). The second cluster group includes H_2O_2 oxidized samples and functional categories related to "Carbohydrates", "Amino acids and derivatives", "Nucleosides and Nucleotides", "Fatty acids, lipids and Isopernoids", "Miscellaneous, and "Respiration". Again, exposure to H_2O_2 resulted in distinct shifts in the functional related gene categories supporting the hypothesis of non-selective action of this oxidant (Moradinejad et al., 2020).

According to increasing relative CTs, the changes in functional profiles revealed no general trends between the control conditions and the oxidized samples on August 29th (Figure C.2, C.3 and C.4). The August 29th bacterial communities were more resilient to oxidation with Cl_2, $KMnO_4$ and H_2O_2 and demonstrated capabilities for active nutrient uptake, growth and survival to the stressful conditions in comparison with the communities inhabiting the August 1st bloom. This is coherent with our observations of a lower Shannon index on August 1st compared to the August 29th (Figure C.5).

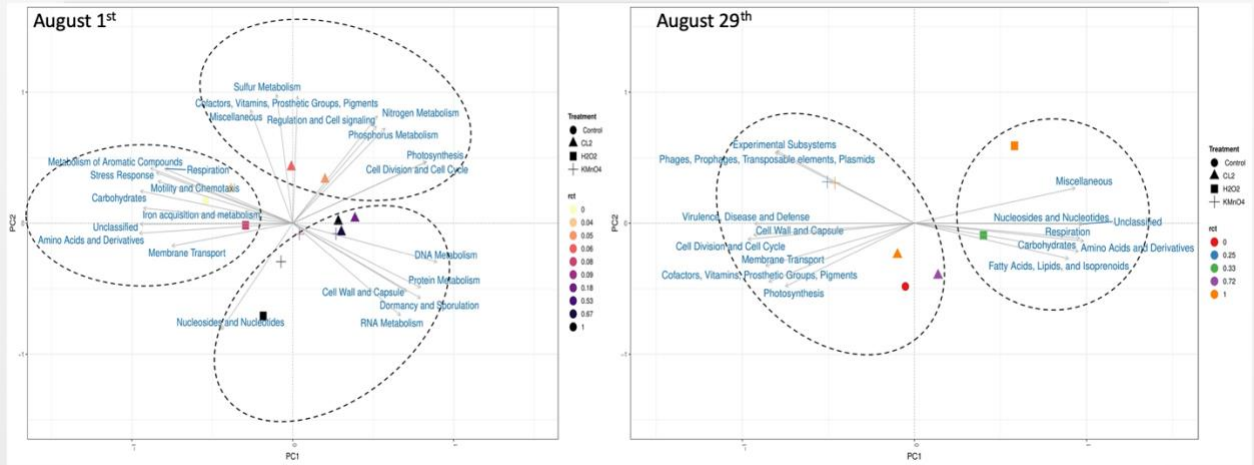

Figure 6.2 PCA of the functional structure following Cl_2, $KMnO_4$ and H_2O_2 a) August 1st (*Dolichospermum* was the most abundant genus) b) August 29th (*Microcystis* was the most abundant genus).

6.3.3 Correlation between functional subsystems and microbial taxonomic profile following chlorination

Pearson correlation coefficients (P-value <0.01) were calculated in R to determine the correlation of microbial taxa (phylum level) with the main functional subsystems (level 1) before and after chlorination. The relative abundance of both taxonomic functional responses was normalized before the correlation analysis. The correlation analysis was performed between functional categories (Level 1) and the taxonomic profile identified at the phylum level (~95% of the relative abundance). The correlation of different phyla with the five days of bloom samples' functional profiles before oxidation is presented in Figure C.6. This Figure shows that cyanobacteria had a significant positive correlation with “Cell division and cell cycle” in the bloom samples. Notably, there were no correlation with “Photosynthesis”, “Nitrogen” and “Phosphorus” metabolisms.

Photosynthesis was driven mainly by cyanobacteria as the relative abundance of the only detected photosynthetic phytoplankton, Chlorophyta, was negligible with less percentage reads ($< 10^{-5}$ %).

Correlations were also evaluated between functional and taxonomic profiles observed in August 1st water samples after oxidation with Cl_2 (Figure 3). On that date, significant positive correlations were identified between Proteobacteria and "Carbohydrates", "Iron acquisition and metabolism", "Membrane transport", "Metabolism of aromatic compounds", "Motility and chemotaxis", and "Stress response" functions. The results indicated that members of the Proteobacteria phylum had the potential to adapt to the conditions imposed by chemical oxidation and the ability for energy acquisition (e.g. carbohydrate, iron) or usage (e.g. motility), as indicated by the abundance of reads related to nutrient and energy metabolisms. Strong support of this finding was also provided by the differential heat trees using MetacodeR (Figure 4), showing the effect of Cl_2 on class abundance. *Gammaproteobacteria* was the major class within *Proteobacteria* that persisted after oxidation with Cl_2 (Figure 4). *Gammaproteobacteria* was shown in other studies to be able to win the competition for nutrients and to grow faster than the average bacterioplankton in lakes (Gasol et al., 2002; Šimek et al., 2006). Moreover, it has been often reported that iron can promote rapid growth of bacteria (Church et al., 2000). In our study, the genes involved in iron acquisition and metabolism may have been triggered to supply enough iron for continued bacterial growth in the August 1st samples after exposure to Cl_2.

Significant positive correlations were identified between *Bacteroidetes* and functional categories affiliated to "Dormancy and sporulation", "Cell wall and capsule" and housekeeping pathways such as "Protein metabolism" and "RNA metabolism" (Figure 6.3). *Bacteroidetes* was able to survive in a dormant stage after Cl_2 oxidation. Other studies have revealed that the. synthesis of stress response-associated functions or reorganization of the gene expression programs for survival under similar imposed oxidation may increase protein metabolism, thereby increasing RNA synthesis (Humayun, 1998; Krämer, 2010).

Significant positive correlations between cyanobacteria and functional categories related to "Cell division and cell cycle", "Photosynthesis" and Nitrogen metabolism", "Phosphorus metabolism" were also observed (Figure 6.3). The ability of cyanobacteria to adapt to the presence of Cl_2 was revealed through the presence of genes involved in "Cell division and cell cycle" before and after oxidation., This ability became apparent on August 1st, because members belonging to the

Cyanobacteria class persisted after oxidation with Cl_2 as compared to the *Betaroteobacteria* and *Alphaproteobacteria* (Figure 4). Positive correlations between "Photosynthesis" related genes were identified with both *Actinobacteria* and Cyanobacteria. It seems that oxidation had an impact on Cyanobacteria to acquire energy by degrading accessible amino acids substrates and performing its associated pathways related to "Iron acquisition and metabolism" as well as" Membrane transport".

A significant negative correlation between cyanobacterial and proteobacterial communities was identified on August 1st after chlorination. Previous studies have reported Proteobacteria's antagonistic activity against various Cyanobacteria (Wright and Thompson, 1985). *Rhizobiales* belonging to the *Alphaproteobacteria* phylum have been recognized to contribute to the nitrogen cycle through their contribution to the fixation of atmospheric nitrogen by plants (Newton et al., 2011). In our study, the relative abundance of *Alphaproteobacteria* dramatically declined after oxidation (Figure 6.4). Meanwhile, Cyanobacteria, which is dominated by nitrogen-fixing cyanobacteria such as *Dolichospermum*, exhibited higher relative abundance after oxidation with Cl_2 (Figure 6.4). This suggests that cyanobacteria harboring nitrogen-related genes may be better adapted to chemical oxidation and that it involved a stress response mechanism during Cl_2 exposure.

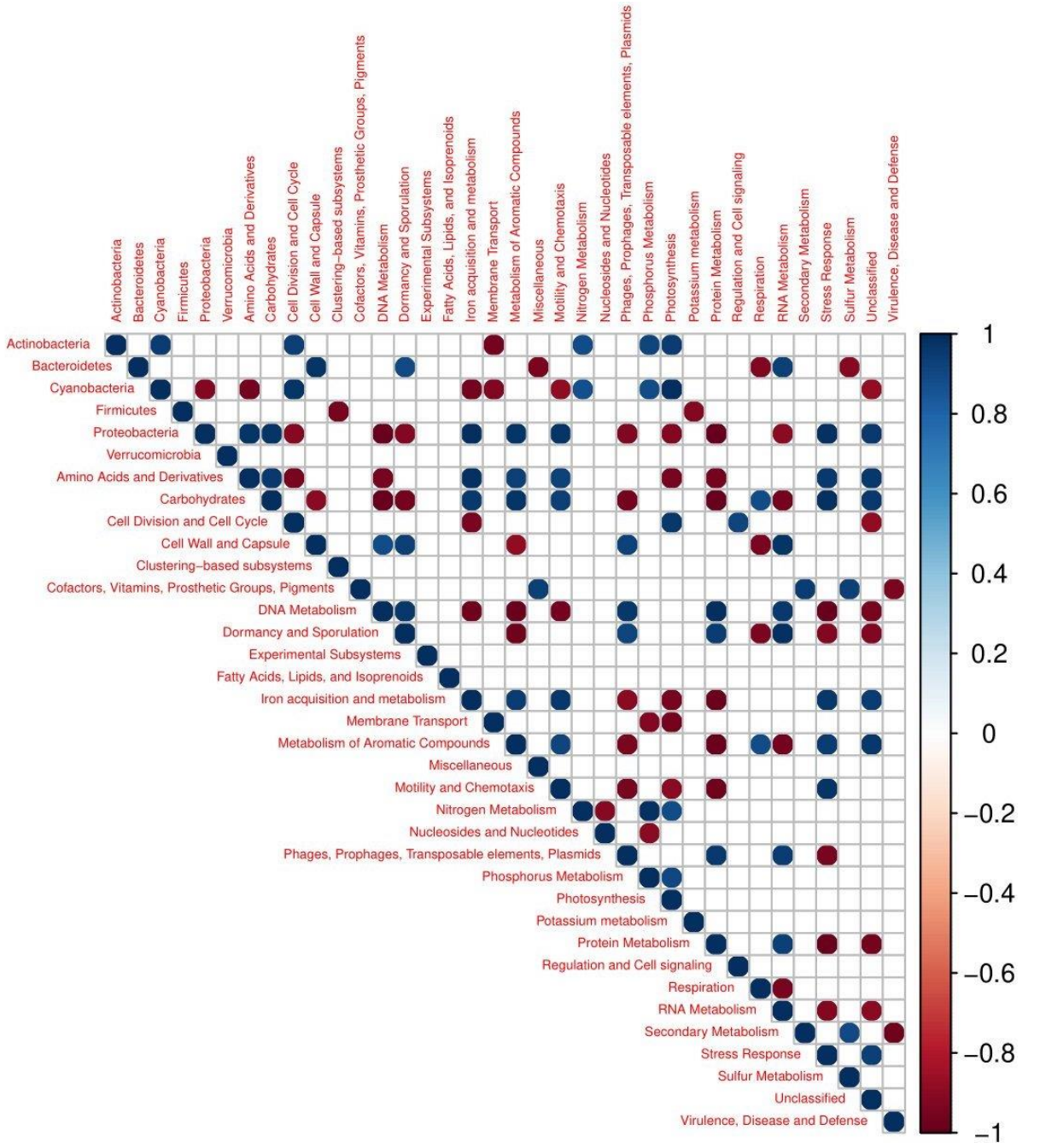

Figure 6.3 Analysis of correlations between functional and taxonomic profiles identified in the August 1st 2018 water samples after oxidation with chlorine (Cl_2). Colors represent the strength of correlations with their corresponding correlation coefficients.

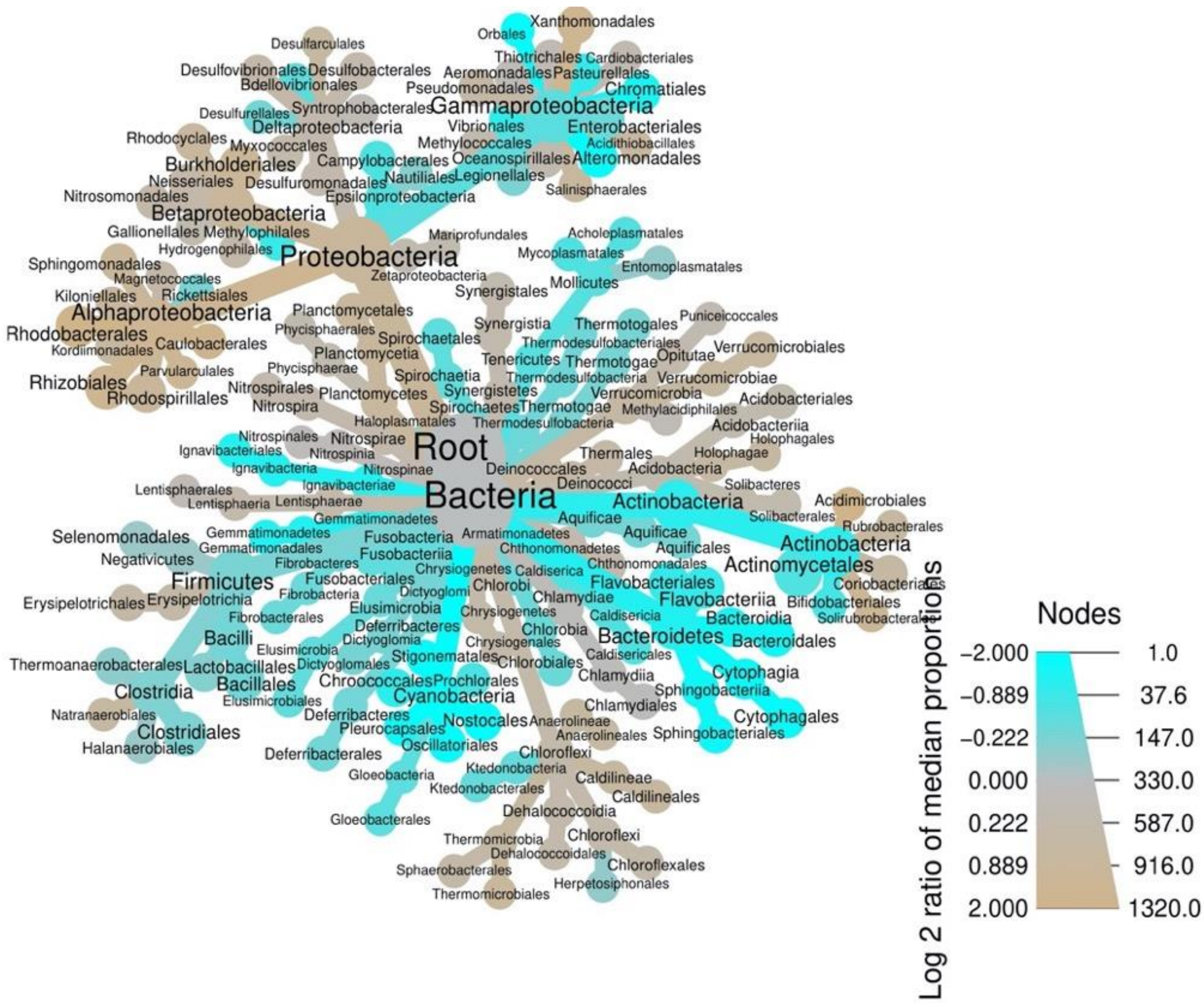

Figure 6.4 Differential heat tree demonstrating changes in taxonomic profiles the class level in the August 1st 2018 water samples after oxidation with chlorine at a concentration of 0.2 mg/L. T_0/T_{10} (August 1st), T_0=control, T_{10}= after 10 min contact time. The node size is calculated by counting the number of observations for each genus.

6.3.4 Oxidation impact on selected cyanobacterial biomarkers

In order to track the functional capacity of cyanobacteria in response to oxidation stress, three cyanobacterial biomarkers (level 3 subsystem) where selected: “Cyanobacterial circadian clock”, “Heterocyst formation in Cyanobacteria” and “Transcription factors cyanobacterial *rpoD*-Like sigma factors”, (referred in this paper as *rpoD*-Like). Cyanobacterial circadian clock and Heterocycst formation are two well documented cyanobacterial biomarkers (Bale et al., 2019;

Taton et al., 2020; Xing et al., 2020; Zhang et al., 2006). The circadian clock controls gene expression at the genome-scale and plays a role in stress response and adaptability in competitive environments (Hörnlein et al., 2020). Heterocyst formation have been associated with a wide range of roles in cyanobacteria, such as nitrogen regulation (especially during N-limited condition), cell cycle, cell size and cell division regulation (Xing et al., 2020; Zhang et al., 2006). The *rpoD*-Like factor was previously identified as a biomarker and a regulator to acclimate cyanobacteria and protect them during chemical oxidative stress (Srivastava et al., 2020). Other studies have shown that mutated *Synechocystis* cells with only *rpoD* gene have higher resistance capability to (photo)oxidative stress in comparison with the standard strain (Hakkila et al., 2019).

On August 1st, the relative abundance of the three biomarkers increased following Cl_2 oxidation, with a peak at 0.2 mg.min/L (Figure C.7-a and C.8a). However, on August 29th such trends were not observed most probably because of the very low relative abundance of these biomarkers (Figure C.7b-C.8b). Exposure to $KMnO_4$ on August 1st, was associated with an increase in the relative abundance of *rpoD*-like circadian clock and heterocyst formation which peaked at 49.7 and 287.8 mg.min/L, respectively (Figure C.9a-C.10a). At higher exposure (CT=545.9 mg/L), the relative abundance of those biomarkers returned to the initial level. A slight increase was also recorded for the relative abundance of the cyanobacterial biomarkers categories on August 29th where *Microcystis* was the most abundant genus (Figure C.9b-C.10b).

Oxidation with H_2O_2 on August 1st and 29th revealed that the relative abundance of the three biomarkers declined markedly at high H_2O_2 exposure (Figure C.11-C.12). These results are supported by the decrease of relative abundance of cyanobacterial taxa after H_2O_2 oxidation, from our previous study (Moradinejad et al., 2020).

6.3.5 ddPCR (*mcyD*) versus MC concentration

A quick response ddPCR test could provide a tool for operators to assess potential toxicity in raw water incoming to the water treatment plant and in treated water after oxidation. To be informative, the test should be predictive of toxin concentration in raw water and conservatively predict the elimination of toxins by oxidation.

Microcystin (MC) producing cyanobacteria carries the *mcy* genes. Ten *mcy* (A-J) genes were identified as MC synthesis genes (Baxa et al., 2010). Previous studies have suggested that the

monitoring of *mcyD* gene could be an appropriate approach to predict toxic cyanobacterial bloom in water resources (Davis et al., 2009; Fortin et al., 2010; Rinta-Kanto et al., 2009). Correlation analyses (p-value<0.05) for the *mcyD* gene copy numbers, assessed by ddPCR, and MC concentrations in Lake Champlain are presented in Figure 5. Results for dissolved and cell-bound total MC before and after oxidation are summarized in Figure C.13. For all oxidants (Cl_2, $KMnO_4$, H_2O_2), only partial removal of microcystin was observed ranging from 18% to 36%. Results for our raw water samples revealed a significant positive correlation between the *mcyD* gene copy numbers and extracellular MC total (R= 0.97) and intracellular MC total (R= 0.95). Also, a significant positive correlation (R=0.95) between the *mcyD* gene copies and the intracellular MC-LR was observed for the raw water samples. Our results are in accordance with previous results in Lake Champlain, in which the *mcyD* gene copies assessed by qPCR were significantly correlated with the measured MC via enzyme-linked immunosorbent assay (ELISA) (Fortin et al., 2010). Similar correlation between the *mcyD* gene and MC were also reported on other sites (Davis et al., 2009; Rinta-Kanto et al., 2009; Wood et al., 2011). Other studies did not report any correlation between the *mcyD* gene and MC concentration (Baxa et al., 2010; Hotto et al., 2008). The complexity of *mcy* cluster sequences, that could be partially deleted, rearranged or mutated (Pacheco et al., 2016), and challenges associated with DNA recovery from complex samples (Kim et al., 2013) can be issues for ddPCR analyses.

The correlation of *mcyD* gene with the detected MC was also analyzed for the oxidized samples from Lake Champlain. For chlorinated samples, a significant positive correlation (R=0.6) was observed between *mcyD* gene copies and the extracellular MC-LR variant. The KMnO4 oxidant was associated with stronger correlations between the *mcyD* gene copy numbers and total intracellular MC (R=0.98) as well as the intracellular MC-LR variant (R=0.65) (Figure 6.5). As for H_2O_2, no correlation was identified between the *mcyD* gene copies and MC concentrations. Several factors may explain these different trends in correlations. First, the mode of oxidation and reactivity of the three oxidants studied varies in terms of their impact on cell components, including nucleic acids, and toxins. Secondly, detection by ddPCR relies on the ability to detect nucleic acids while the measurements of toxins relies on the ability to detect functional groups of various analogs.

Several prior studies have documented the high reactivity of microcystin with $KMnO_4$, Cl_2 and H_2O_2 (Ding et al., 2010; Fan et al., 2013a; Zamyadi et al., 2013d; Zhou et al., 2013). Yet, in our study, limited removal (up to 36%) of microcystin was observed at the highest CTs (Figure 6.6).

However, it must be noted that relatively low concentrations of toxins were present raising potential issues with the quantification of cell-bound and free toxins. This apparent low treatment performance could be related to different water quality parameters such as lower organic matter and microcystin concentrations as compared to the previous studies.

While the reactivity of toxins with the oxidants used has been widely investigated, the reactivity of Cl_2 and $KMnO_4$ with RNA integrity is not well documented. RNA is composed of ribonucleotides (ribose and one of four nitrogenous bases) linked by phosphodiester bonds. While the oxidants react poorly with ribose, they may react readily with nucleosides (Deborde and von Gunten, 2008). Although chlorine reacts slowly with Cytidine-5'-Monophosphate (CMP) (K=negligible) and Adenosine-5'-monophosphate (AMP) (K=66 $M^{-1}S^{-1}$), it quickly reacts with Guanosine-5'-monophosphate (GMP) (K= 2.1 x 10^4 $M^{-1}S^{-1}$).) and Uridine-5'-monophosphate (UMP) (K= 5.5 x 10^3 $M^{-1}S^{-1}$) (Deborde and von Gunten, 2008). Figure 6.6 shows the impact of oxidation on the integrity of RNA extracted from a mix of cultured *Microcystis aeruginosa* strain CPCC 300 and *Dolichospermum* strain CPCC 544. RNA was poorly degraded after exposure to $KMnO_4$ (K= 1.8 x 10^{-3} $M^{-1}S^{-1}$), but Cl_2 oxidized RNA at all CTs (K= 9.6 x 10^{-1} $M^{-1}S^{-1}$). These results are coherent with the recent demonstration of the high reactivity of cytosine and thymine bases with chlorine showing nearly complete oxidation at 20 µM Cl_2 (Zhang et al., 2020). Our results shows that oxidation constants (especially $KMnO_4$) for nucleic acids (RNA) is lower than documented rate constants for MC concertation (118 $M^{-1}S^{-1}$ for the most resistant MC variant) (Piezer et al., 2020) which may explain different trends in the correlations (*mcyD* vs MC) after oxidation. Although not tested, H_2O_2 is known to be highly reactive with all cell components and to degrade RNases, a family of enzymes present in virtually all living cells (Farrell, 2010). H_2O_2 has also been shown to play a role in the degradation of bacterial DNA (Latifi et al., 2009; Wagner and Cadet, 2010; Yang et al., 2006). Therefore, some oxidants are likely to rapidly react free nucleic acids while others will not react at typical treatment dosages.

We attempted to correlate the presence of *mcyD* to the persistence of cell bound and free toxins for chlorine (0.2 and 0.6 mg/L), permanganate (5 mg/L) and hydrogen peroxide (10 mg/L). Because of the discrepancies in the kinetics of oxidation of RNA and toxins depending on the oxidant considered, the use of *mcyD* based toxicity test would best justified to estimate the potential for toxin presence in raw water prior to exposure to oxidant agents. The use of the ddPCR method as a quick response tool to predict toxin removal after oxidation is therefore not recommended.

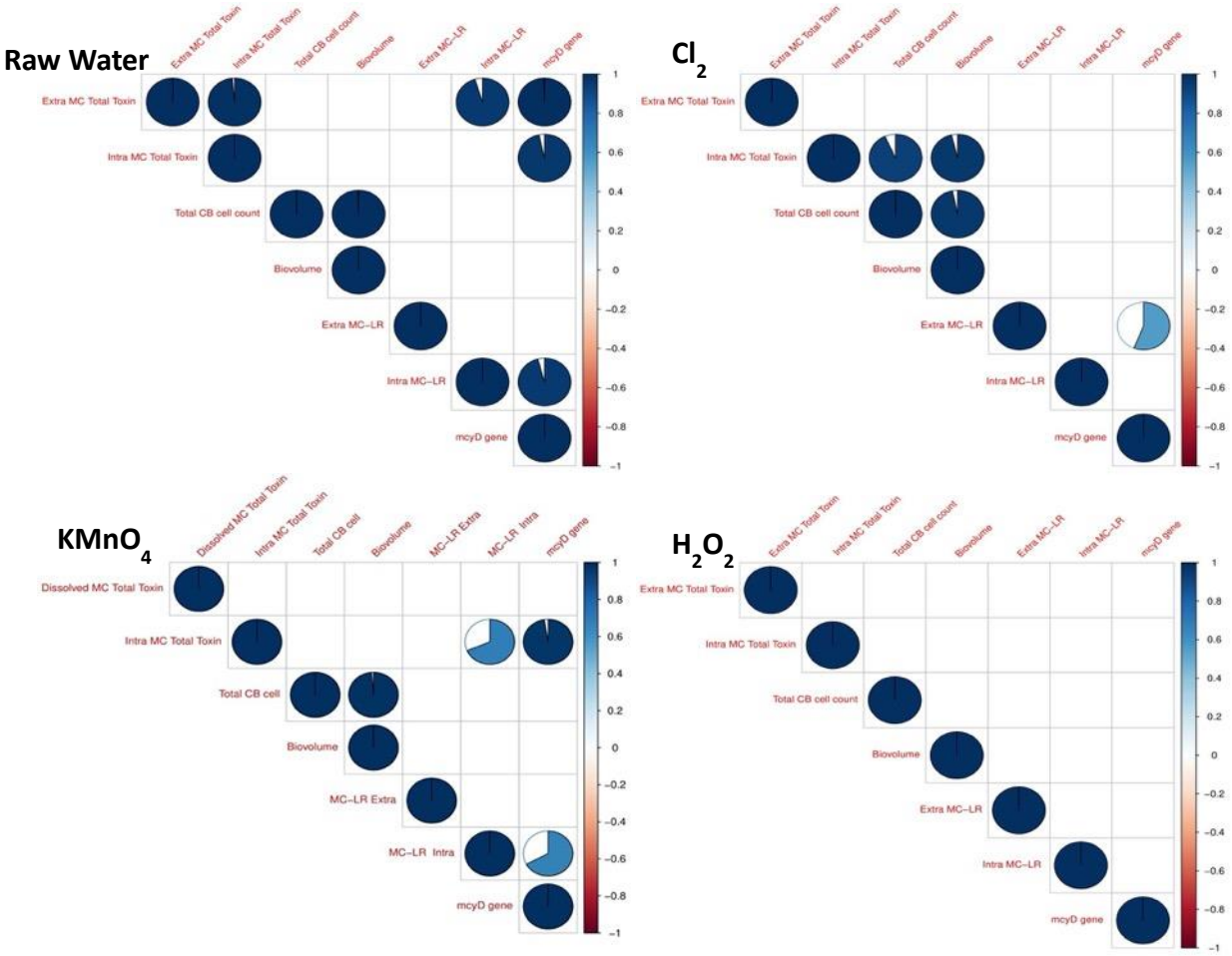

Figure 6.5 Correlation analyses of the of *mcyD* gene copy numbers with MC concentrations before and after oxidation with Cl_2, $KMnO_4$ and H_2O_2 .Colors represent the strength (blue-positive, red-negative) of correlations with their corresponding correlation coefficients. A complete circle represents the correlation coefficient equals one.

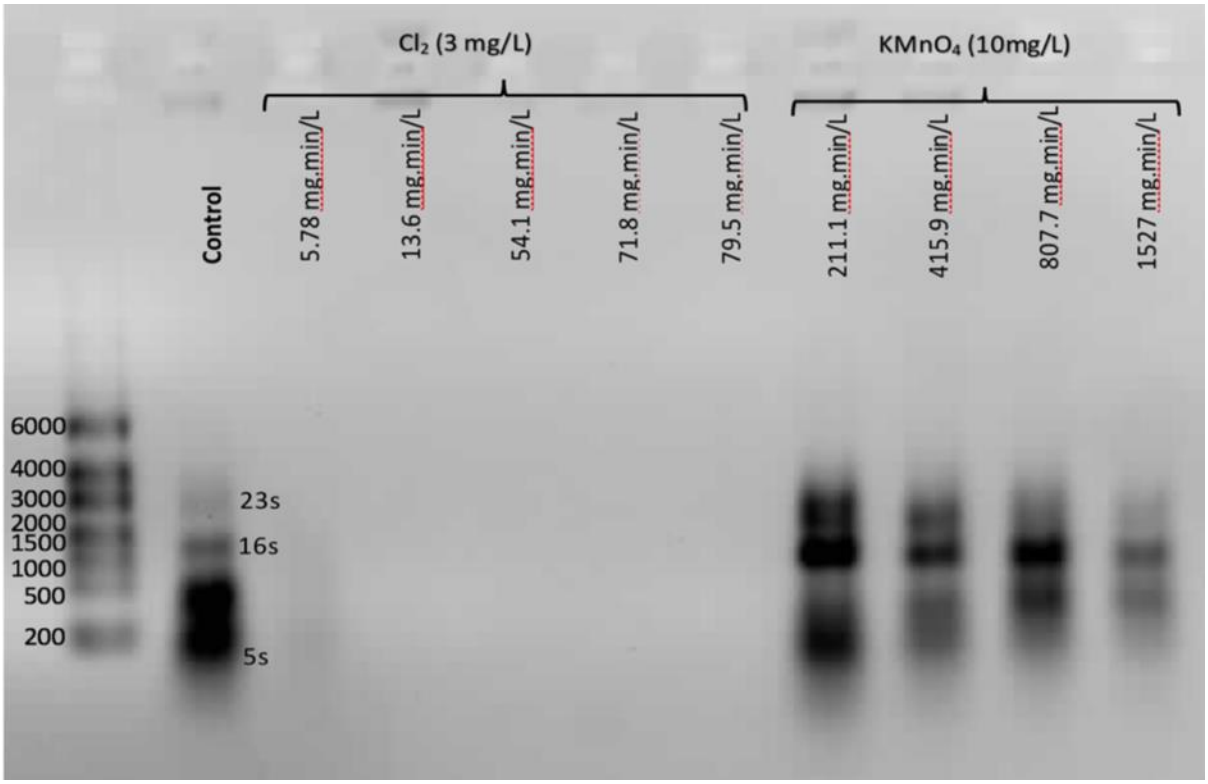

Figure 6.6 Gel electrophoresis of RNA extracted from river water spiked with a mixture of *Microcystis* and *Dolichospermum* cells as a function of CT exposure to Cl_2 and $KMnO_4$.

6.4 Conclusion

- Distinct functional assemblages were observed in bloom samples at the intake of the drinking water production plant during the month of August (August 1st to August 29th). On August 1st, the most abundant function identified in bloom samples was associated with the "Carbohydrates" category. A shift toward "Protein metabolism" was observed on August 13th which remained abundant until the end of our sampling campaign.
- Different functional clusters were observed in our water samples following oxidation with Cl_2, $KMnO_4$ and H_2O_2. On August 1st, low oxidant exposures clustered with "Carbohydrates" and "Iron acquisition" metabolic activities and higher exposure clustered with stress response related functions such as DNA metabolism and sporulation.
- The impact of oxidation was revealed through correlation analyses between different phyla and functional profiles. Positive correlations between cyanobacteria and nitrogen as well as phosphorus metabolisms showed the impact of Cl_2 since no correlation was observed in

bloom samples before oxidation. The potential of cyanobacteria to survive to Cl_2 exposure was also assessed through a positive correlation with cell division and cell cycle.

- Limited variation of cyanobacterial biomarkers such as "Cyanobacterial circadian clock", "Heterocyst formation in Cyanobacteria" and "*rpoD*-Like" was identified following Cl_2 and $KMnO_4$ oxidation on August 29th where *Microcystis* was the most abundant genus. High exposure to H_2O_2 caused a dramatic decrease in cyanobacterial biomarkers, regardless of the dominant genus. Those results confirmed the effectiveness of H_2O_2 as a pre-oxidant in cyanobacterial management of drinking water resources.
- Quick response ddPCR tests could be used to evaluate cyanobacterial bloom toxicity in drinking water resources prior to the pre-oxidation treatment. Correlation results between the *mcyD* gene and microcystin concentrations following exposure to Cl_2, $KMnO_4$ and H_2O_2 oxidants suggest that the ddPCR method or any genomic based measurement would not be appropriate to predict the removal of microcystins.
- Pre-oxidation modified the bacterial community and cyanobacteria survived after exposure to Cl_2 and $KMnO_4$ as demonstrated by functional and community composition structure. However, pre-oxidation with Cl_2, $KMnO_4$ and H_2O_2 was partially efficient in eliminating microcystins, raising the need for optimizing pre-oxidation dosages and insuring that other down-flow processes are capable of removing any toxins that would ultimately be released in potable water.

Acknowledgments

The authors are sincerely acknowledging the financial support from the Algal Blooms, Treatment, Risk Assessment, Prediction and Prevention through Genomics (ATRAPP), Génome Québec and Génome Canada grant. The authors thank the staff at NSERC Industrial Chair on Drinking Water at Polytechnique Montréal, Shapiro lab, Sung Vo Duy (University of Montréal), Irina Moukhina (Université du Québec à Montréal), Sukriye Aydin Celikkol (McGill University) and Stephanie Messina Pacheco (National Research Council) for their valuable contributions to this research.

CHAPTER 7 GENERAL DISCUSSION

This chapter presents the main findings, novelties, and limitations of this research project regarding the initial hypothesis and objective. The main objective of this Ph.D. project was to study the fate of cyanobacteria during chemical oxidation through genomics. A summary of results is presented in Table 7.1. The findings of this research study have been categorized into the following themes:

- Cyanobacteria morphological response to the oxidation
- Impact of pre-oxidation on cyanobacterial community composition
- Cyanobacteria functional capacity in response to pre-oxidation
- Management and treatment implications

Table 7.1 Overview of the results of this study

Culture	**Oxidant**	**Morphology (EDM/HSI)**	**LC-OCD**	**Taxonomic cell count**	**Cell integrity**			
	Cl_2	Unique spectrum for each species Distinct cell wall spectra for each oxidant Cell links are the first targeted during oxidation	Increase in humic like, BP, BB, LMW acids (lower than O3)	Progressive cell number reduction with CT, up to 80%	No viable cell after CT 11.7 mg.min/L			
	O_3		Increase in humic like, BP, BB, LMW acids	Low cell number at CT 2 mg.min/L (5%)	No viable cell after CT 2 mg.min/L			
	$KMnO_4$		All organic matter fraction degraded	No large variation of cell number (10%)	20% viable cell at CT 456 mg.min/L			
	H_2O_2				30% viable cell at CT 2160 mg.min/L			
Real Bloom	**Oxidant**	**Microbial diversity**	**Cyanobacteria diversity**	**Taxonomic cell count**	**Cell integrity**	**MC total Intra/extra**	**Functions**	**Toxicity (*mcyD*)**
	Bloom Sample	Abundant: Proteobacteria, Actinobacteria, Bacteroidetes and Cyanobacteria	Abundant genus 1 August: Dolichospermum 21 August: Synechococcus 29 August: Microcystis	1 August: 3.3×10^5 29 August: 5.4×10^4	-	Low toxin concentrations	Abundant function shifted from Carbohydrates to protein metabolism	Positive correlation with extra MC, intra MC and intra MC-LR
	Cl_2	Progressive shift in community with CT	Progressive shift in community with CT *Dolichospermum sp.90* relatively persisted	Up to 30% decrease	71% viable cell for the highest CT	Intra: 37% decline Extra: 25% decline	Progressive shift from basics to stress response Positive correlation with nitrogen and phosphorus metabolism	Positive correlation with extra MC-LR
	$KMnO_4$	Larger shift in the community compare to Cl_2	*Dolichospermum sp.90* relatively persisted	Up to 57% decrease	19% viable cell for the highest CT	Intra: 36% decline Extra: 27% decline	Stress response functions at high CT	Positive correlation with intra MC and intra MC-LR
	H_2O_2		All cyanobacteria taxa declined	Up to 52% decrease	41% viable cell for the highest CT	Intra: 78% decline Extra: 34% decline	Stress response functions at high CT Cyanobacteria biomarkers declined after H_2O_2	No correlation
	O_3	No significant variation in community composition	*Microcysits aeruginosa* (abundant) relatively persisted	Up to 15% decrease	69% viable cell for the highest CT	Intra: No decline Extra: 54% decline	No variation following O_3	No correlation

7.1 Cyanobacteria morphological response to the oxidation

Several studies have unveiled the morphological changes (qualitative) of cyanobacteria during oxidation by using SEM and digital flow cytometry (Daly et al., 2007; Ding et al., 2010; Wert et al., 2013). Such techniques cannot easily determine if cyanobacterial species respond differently to the oxidation. Within the oxidation mechanism, chemical molecules transport across the cell can occur with cell membrane reaction through passive or active diffusion (Wert et al., 2013). For example, it has been documented that the ozone will react with the lipid layer to remove the *E. coli* cells (Wert et al., 2013). Hydrogen peroxide can produce hydroxyl radicals to damage cells through DNA, lipids and protein degradation (Latifi et al., 2009). Oxidation using $KMnO_4$ can affect the organic compounds through oxygen donation, hydride ion abstraction and electron abstraction (Piezer et al., 2020). Permanganate can oxidize cyanobacteria cell surface, resulting in higher extracellular organic matter degradation to low molecular weight, electrostatic obstacle reduction and increasing the concentration of oxygenated groups (Naceradska et al., 2017; Piezer et al., 2020; Xie et al., 2016). Subsequently, the cell removal performance in downflow processes is enhanced by using $KMnO_4$ as a pre-oxidant.

In this thesis (chapter 4) we took advantage of EDM/HSI to quantify morphological changes by measuring visible wavelength. Our findings showed that *Microcystis* and *Dolichospermum* had a unique-shaped spectrum. Distinct cell wall spectra were observed for *Microcystis* and *Dolichospermum* following both chlorination and ozonation. Chlorine exposure (37.5 mg.min/L) caused new peaks at 500nm and removed two original peaks in the control condition. On the other hand, ozonated *Microcystis* showed one single peak at 650nm. Also, SEM results from *Dolichospermum* showed that cell links were the first targeted points by chlorine and ozone. Our results shed light on the morphological behavior of each species during oxidation, depending on the used oxidant. However, more studies are required to study the relationship between the metabolite release rate and morphological deformation to optimize oxidation efficiency.

7.2 Impact of pre-oxidation on cyanobacterial community composition

A key element when using genomic based testing is the relative efficacy of the different oxidant tested to degrade the nucleic acid components. Deoxyribonucleic acid (DNA) and ribonucleic acid (RNA) are the two types of nucleic acids. DNA nucleotides consist of a phosphate group, a ribose sugar and a base (Figure 7.1). The deoxyribose found in DNA has a hydrogen atom at the 2' carbon, while the ribose found in RNA has a hydroxyl group at the 2' carbon. Also, for RNA, thymine is replaced by uracil in the nitrogen base of RNA.

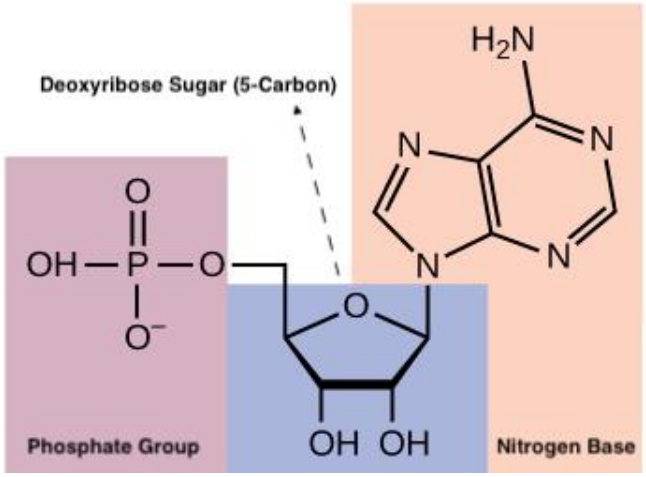

Figure 7.1 Schematic of DNA nucleotide (adapted from (Molnar and Gair, 2015))

The genomic based studies rely on DNA detection. It has been documented that tested oxidants (Cl_2, $KMnO_4$, O_3 and H_2O_2) can react with the nucleic acids differently. Studies reported high reactivity of ozone with nucleic acids (Cataldo, 2005; Cataldo, 2006; Theruvathu et al., 2001). Protonation state and pH affect the reaction of free purine and pyrimidine base with ozone (Theruvathu et al., 2001). Chlorine is able to interact with different cell components, including nucleic acids. Two main processes involved in the degradation of nucleic acids using chlorine. First, chlorine reaction with aromatic ring and giving a new carbon-chlorine bond. Second, the reaction of free chlorine with free amine groups (e.g. cytosine, adenine and guanine) results in chloramine formation (Gray et al., 2013; Hawkins et al., 2007).

H_2O_2 decomposition in water produces hydroxyl radical (OH•), that could degrade DNA and proteins (Latifi et al., 2009). Hydroxyl radicals are formed through the Fenton reaction (Eq. 7.1)

$$Fe^{2+} + H_2O_2 \rightarrow OH^- + FeO^{2+} + H^+ \rightarrow Fe^{3+} + OH^- + OH^{\cdot} \qquad \text{Eq. 7-1}$$

Hydrogen abstraction, addition and electron transfer are the main types of OH• reaction with nucleic acids. All bases of DNA can be damaged by OH•. For example, the formation of carbon-centered radicals caused hydrogen abstraction in the reaction of OH• with deoxyribose (Aust and Eveleigh, 1999; Wagner and Cadet, 2010).

RNA integrity (cell bound) test was conducted to determine the reactivity of two oxidants (Cl_2 and $KMnO_4$) with nucleic acids. RNA integrity test using Cl_2 and $KMnO_4$ shows (Figure 6.6, Figure 7.2 and 7.3) high degradation rate of RNA after chlorination. However, the RNA degradation rate following $KMnO_4$ oxidation is lower compared to Cl_2 exposure. Bui et al. (2003) observed that $KMnO_4$ selectively reacts with pyrimidine base while sugar and phosphate base remained untouched. Such a phenomenon may explain the lower reaction rate of KMnO4 with RNA in our study.

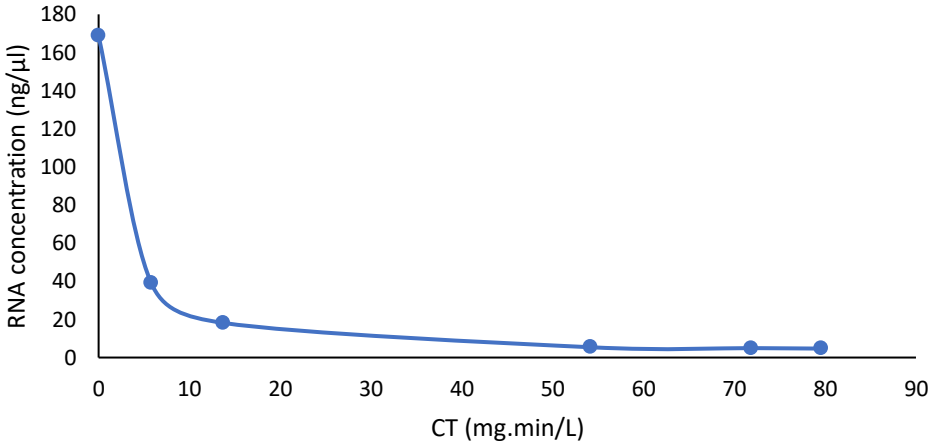

Figure 7.2 RNA concertation following the oxidation using Cl_2 (3 mg/L)

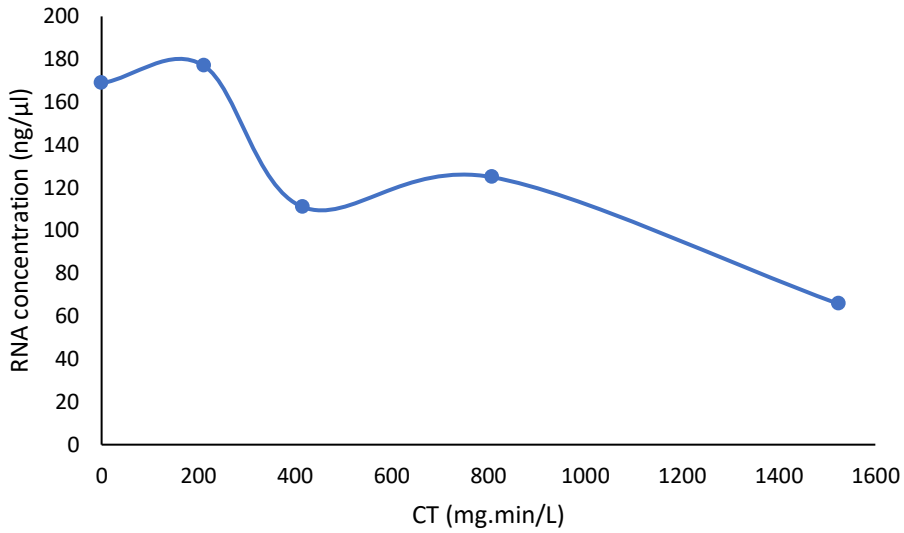

Figure 7.3 RNA concertation following the oxidation using $KMnO_4$ (10 mg/L)

Taxonomic cell count-based studies have documented the impact of various oxidants on the cyanobacterial community in the laboratory (Fan et al., 2013b; Fan et al., 2014a), in the field (Matthijs et al., 2012) and in drinking water treatment plants (Almuhtaram et al., 2018; Zamyadi et al., 2015a; Zamyadi et al., 2013c; Zamyadi et al., 2016b; Zamyadi et al., 2012a). Taxonomic cell counts have some challenges such as time consumption, qualified person requirement and biovolume changes during analysis, which could be overcome with molecular tools (Hawkins et al., 2005; Zamyadi et al., 2019). Our results in chapter 5 discussed that cyanobacteria's morphological similarities could lead to misidentifying and over-looking under microscope taxonomic cell count (Casero et al., 2019; Kim et al., 2018a). Also, potential morphological deformation of the cells following oxidation may further hinder taxonomic cell count's ability to identify cyanobacteria cells.

Molecular tools (16s rRNA gene and high throughput sequencing) have been applied to study bacterial/cyanobacterial communities in the field and drinking water treatment plants (Berry et al., 2017; Casero et al., 2019; Eldridge and Wood, 2019; Fortin et al., 2015; Hou et al., 2018; Kim et al., 2018a; Lusty and Gobler, 2020; Pei et al., 2017; Tromas et al., 2017; Xu et al., 2018). Understanding potential selective persistence, shift, and changes within the cyanobacterial community during oxidation can help to select pre-oxidation scenarios (dose and contact time) to dampen the cyanobacteria at water treatment plant intake. Our results in chapter 5 indicate a shift

from *Dolichospermum* at the beginning of the bloom sampling to *Microcystis* at the end of the sampling (during the 4-week temporal analysis). A progressive shift was observed for Cl_2 exposure while $KMnO_4$ and H_2O_2 induced larger changes in bacterial and cyanobacterial community composition. Regardless of the oxidant type, *Dolichospermum sp.90* remains the most dominant species in the beginning of the bloom sampling. *Dolichospermum sp.90* relatively persisted with increasing CTs of Cl_2 and $KMnO_4$, whether it was abundant or not. Same relative persistence was observed for *Microcystis aeruginosa* following soft-ozonation (0 – 0.9 mg.min/L). H_2O_2 pre-oxidation caused an apparent decrease in the relative abundance of all taxa and some species, including toxin-producing taxa of interest, suggesting it can be an efficient barrier against cyanobacteria entering the water treatment plant. The efficiency of H_2O_2 agrees with previous studies (Lusty and Gobler, 2020; Matthijs et al., 2012; Zhou et al., 2013).

This thesis proposed that the most effective pre-oxidant should be selected based on the oxidant's impact on cyanobacterial community composition/diversity as well as other drivers such as disinfection by-products, color and taste and odor compounds.

7.2.1 Variability and reproducibility of the results

In this research study, over 60 metagenomics split samples (in triplicate) were taken. However, due to budget and resource constraints, only one sequencing was performed per sample. To address the issue of repeatability, replicates from the bloom (2019) were taken and analyzed.

Figure 7.4 shows quite similar composition at phylum, order and genus level for the three taken replicate samples. Cyanobacteria was the abundant phylum, followed by proteobacteria and bacteriodetes. At the order level, *Nostocales* was the abundant order. *Dolichospermum* was the abundant genus followed by *Nostoc*. Figure 7.4 confirms the reproducibility of the results.

Also, the progressive shift in the bacterial and cyanobacterial communities and functional (Figure 5.2 and Figure 6.2) response following chlorination (by increasing CT) show a systematic change in the final results following chlorination, considering an increase in the variable of interest (CT). Such a systematic change confirms that the sampling and analysis noise may not plays a role in the final results.

This study is the first to understand the impact of pre-oxidation on the and cyanobacterial bloom composition and functional profile. The experimental design focused on oxidant exposures at

which the shifts happened. The additional studies would be advantageous to extend our results to other drinking water resources.

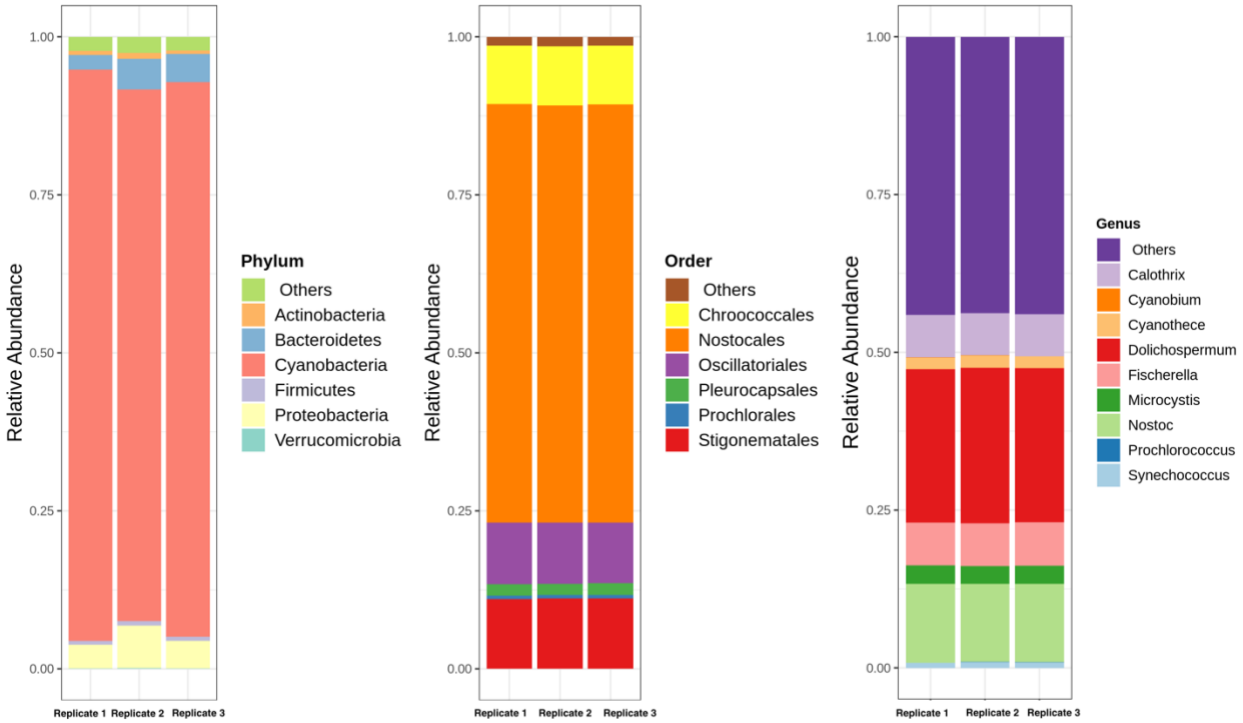

Figure 7.4 Major detected bloom-associated cyanobacterial community members in bloom samples before oxidation, in three replicate samples, at phylum, order, and genus level

7.3 Cyanobacteria functional capacity in response to pre-oxidation

The functional profile can determine how a community may respond and adapt to changing environmental conditions. Despite the efforts to study the functional structure of bacterial and cyanobacterial communities (Hörnlein et al., 2020; Li et al., 2020a; Li et al., 2020b; Lu et al., 2019; Shi et al., 2017; Shilei et al., 2020; Taton et al., 2020; Wang et al., 2018), no study has focused on the functional capacity of cyanobacterial bloom in response to treatment processes, including chemical oxidants. When considering the impact of oxidation, some adaptation may occur, but the changes in functional profiles will also reveal which functions are associated with persistence. Pre-oxidation experiments were conducted with Cl_2, H_2O_2 and $KMnO_4$ using two bloom water samples with distinct bacterial compositions. Bloom samples were retrieved from two different dates: August 1st and August 29th, corresponding to the beginning and the end of the bloom period,

respectively. Analysis of the functional profile presented in chapter 6, shows a shift in the most abundant functional categories from "Carbohydrates", when Proteobacteria is the most abundant phyla in *Dolichospermum*-dominated bloom (on August 1st) to "Protein metabolism" in *Microcystis* dominated bloom (on August 29th), which corresponds to Proteobacteria, Bacteroidetes and Actinobacteria as major bacterial phyla. Genes related to "Metabolism of aromatic compounds", "Carbohydrates", "Stress response" and "Iron acquisition" were clustered with low relative exposure of chlorine and hydrogen peroxide, while high exposure of chlorine and all permanganate samples were clustered together and correlate with "DNA metabolism", "RNA metabolism", "Dormancy and sporulation" and "Cell wall and capsule".

A progressive change in the functional capacity following Cl_2 was observed from the genes related to nutrient/energy metabolism, allowing cells' ability to fulfill normal metabolic processes (e.g. Carbohydrates and iron acquisition) to a relatively high abundance of housekeeping pathways (DNA, RNA and protein metabolism), which is an expected consequence after the synthesis of stress response-associated functions. A further examination into the correlation of cyanobacterial community with both phyla sharing the same bloom and related gene categories was conducted by calculating the Pearson correlation coefficient. On August 1st sample (after Cl_2 oxidation), which corresponds to *Dolichospermum*-dominated bloom, a significant positive correlation was observed between the cyanobacteria and three categories: "Cell division and Cell cycle", "Nitrogen metabolism" and "Photosynthesis". Such results demonstrate the potential of cyanobacteria for growth, Nitrogen fixing and photosynthesis ability following oxidation. Interestingly, cyanobacteria exhibited a negative correlation with Proteobacteria after chlorination. Proteobacteria's functional profile under chemical oxidation (Cl_2) showed a significant positive correlation between the Proteobacteria and energy/nutrient related gene categories: "Carbohydrates", "Iron acquisition and metabolism", "Membrane transport", "Metabolism of aromatic", "Motility and chemotaxis", "Respiration".

To track footsteps of cyanobacteria in the microbial community, our results demonstrate that within *Microcystis*-dominated bloom of August 29th, Cl_2 and $KMnO_4$ oxidation caused limited variation in the relative abundance of the genes related to the selected cyanobacterial biomarkers (RpoD-Like, Heterocyst formation in cyanobacteria and cyanobacteria circadian clock). While, in the presence of *Dolichospermum*-dominated bloom of August 1st, chlorine exposure caused an increase in "RpoD-Like", "Heterocyst formation in cyanobacteria" and "Cyanobacteria circadian clock"

compared to the control condition. H_2O_2 caused a decline in all studied cyanobacteria biomarkers regardless of the abundant genus/species. Such an observation could be related to the drop of the relative abundance of all taxa following H_2O_2, which was shown in our results in chapter 5.

7.4 Management and treatment implications

Previous studies have documented cyanobacteria accumulation, growth and toxin release in clarifiers and filters of drinking water treatment plants (Zamyadi et al., 2013c; Zamyadi et al., 2012b; Zamyadi et al., 2010b).

There are certain evidences that cyanobacterial cell removal by coagulation/flocculation can be improved using pre-oxidation (Ma et al., 2012a; Ma et al., 2012b; Piezer et al., 2020; Qi et al., 2016; Xie et al., 2013). The main mechanisms identified were cell surface damage and the release of organic matter (easy to combine with the coagulant). Also, pre-oxidation has been used to control invasive species and oxidize iron, manganese, taste and odor compounds (Crittenden et al., 2012). Zamyadi et al. (2013c) showed improved cyanobacteria cell removal by clarifiers in a drinking water plant equipped with pre-ozonation (0.3-0.8 mg/L) compared to its twin plant without pre-oxidation (same configuration and water source). Pre-oxidation can be considered a valid option to avoid cyanobacterial cells' accumulation and their associated toxins in sludge and their potential passage in treated water. Pre-oxidation must be capable of injuring the cyanobacterial cells and oxidizing, at least partially, the released cell metabolites, including toxins. Some implications of our findings are as following subsections.

7.4.1 Managing cell damage and release of cell bound organic components during pre-oxidation

Chemical oxidation of cyanobacteria can cause cell degradation, cell bound components and metabolite release into the water. In addition to the morphological changes, the results presented in chapter 4 identified the potential cell bound material release following Cl_2 and O_3 oxidation (e.g. fractions of extracellular organic matter and intracellular organic matter) that might scavenge and hinder the effect that can be seen at a given CT for all oxidants. Also, cell bound organic matter degradation (following $KMnO_4$ and H_2O_2) and release (following Cl_2 and O_3) may hinder the efficient modelling of harmful metabolites degradation (Laszakovits and MacKay, 2019); because the available oxidant to react with cyanotoxins may vary depending on the level of organic matter

released/degraded. Our results showed that ozonation caused an increase (organic carbon) in humic-like substances, biopolymers, building blocks, LMW acids and LMW naturals. The same increasing trend in the organic carbon fractions was observed during chlorination but to a lower extent. Such an increasing pattern could be related to the releasing of the organic matter from the cyanobacteria subjected to oxidation. All organic carbon fractions degraded following oxidation using potassium permanganate (max 43%, LMW naturals) and hydrogen peroxide (max 29%, LMW naturals).

Different morphological changes of cyanobacteria species (depending on oxidant type) may impact metabolite release during pre-oxidation. On the other hand, organic carbon degradation ($KMnO_4$ and H_2O_2) and release (Cl_2 and O_3) highlight the importance of metabolite presence in oxidant dosing calculation and oxidation modeling efficiency. However, for understanding the kinetics, more studies are required to clearly understand the effect of morphological deformation on metabolite release and competition between different organic matter components to consume the oxidant and their impact on oxidation efficiency.

In terms of cell damage, pre-oxidation, even at low soft oxidation dosages, can lead to significant and rapid cell damage. Complete viability loss (100%) was reported following ozonation (0.5-4 mg/L O_3) without any loss of cells (Coral et al., 2013). Similar results in cell viability were observed for ozonation and chlorination by (Fan et al., 2013b). Application of 5 mg/L of $KMnO_4$ caused cell viability loss by 20% and cell number reduction after 2 hours of contact time (Fan et al., 2013b). Oxidation was shown to be more efficient in terms of cell damage for lab grown cyanobacteria in comparison with the natural bloom (Coral et al., 2013; Zamyadi et al., 2015a). We obtained the same results; $KMnO_4$ CT of 456 mg.min/L caused 80 percent cell damage for lab cultured cyanobacteria (Chapter 4) while 80 cell damage for natural bloom was achieved at $KMnO_4$ CT of 565 mg.min/L. In terms of soft oxidation (Cl_2 and O_3) cell damage varies between 14%-30% for soft chlorination and 7%-20% for soft ozonation. Our results showed that soft oxidation might reliably damage cyanobacteria cells (potentially increase cell removal during coagulation/flocculation) while leads to a lower release of cell-bound material (e.g. cyanotoxin) compared to the normal oxidation scenarios.

7.4.2 Management of cell bound and dissolved toxins during pre-oxidation

The oxidation of toxins by various oxidants has been well characterized under varying water quality. Numerous studies have shown that Cl_2, $KMnO_4$, O_3, H_2O_2 can oxidize dissolved toxins such as microcystins, anatoxins, cylindrospermopsin, saxitoxin (Al Momani, 2007; Ding et al., 2010; Fan et al., 2013a; Fan et al., 2013b; Fan et al., 2014b; Jasim and Saththasivam, 2017; Merel et al., 2010b; Nicholson et al., 2003; Onstad et al., 2007; Rodriguez et al., 2007a; Rodriguez et al., 2007b; Rodriguez et al., 2007c; Senogles et al., 2000; Vlad et al., 2014; Xie et al., 2013; Zamyadi et al., 2015a; Zamyadi et al., 2013d; Zhang et al., 2017; Zhou et al., 2013).

When using pre-oxidation, oxidants must first release cell bound toxins by damaging the cells and then proceed to oxidize of the newly released cell bound toxins. Kinetic modelling of these two subsequent steps has been described by a pseudo-first-order reaction to track intracellular metabolic release and subsequent oxidation using chlorine (Fan et al., 2013a; Zamyadi et al., 2013d). However, comparing full-scale oxidation ($KMnO_4$, O_3) results with the model results revealed that lab-based investigations using cultured cells as opposed to natural assemblages can lead to an overestimation of the toxin removal efficiency.

Depending on the dosages applied, insufficient residual oxidant concentrations may be present after the cell bound toxins are released, which could lead to limited or partial toxin removal. Indeed, Fan et al. (2013a) reported 500 ng/L (cell-bound MC) and 2 µg/L (dissolved MC) following CT 1870 mg.min/L ($KMnO_4$ 10 mg/L). Also, results from Zamyadi et al. (2013d) showed that MC-LR might not be completely degraded (3 µg/L cell-bound and 1 µg/L dissolved) following chlorination with 3 mg/L (CT 28 mg.min/L). Our results in chapter 6 oxidation using Cl_2, $KMnO_4$, and H_2O_2 showed a similar trend with a maximum of 34% removal of dissolved MC ($KMnO_4$ with high CT 549 mg.min/L (Figure C.13)). The incomplete oxidation of these low concentrations of MC are not sufficient to conclude on trends. Nevertheless, it is recommended that additional treatment processes should be in place to remove cyanotoxins in the water treatment plant, especially if low pre-oxidation concentration is applied.

7.4.3 Secondary impacts of pre-oxidation

Pre-oxidation can increase cell removal efficiency in coagulation/flocculation. Subsequently, cyanobacteria cell number will increase in the sludge of the clarifier compared to the raw water. Long sludge storage may lead to vesicle damage, cell breakage, cell lysis and subsequently metabolites release into clarifier effluent (Jalili et al., 2021). Besides, pre-oxidation using chlorine and ozone may cause disinfection by-production formation (Coral et al., 2013; Zamyadi et al., 2013d; Zamyadi et al., 2012a). Coral et al. (2013) showed that chlorination by products increased by 174% and 65% for trihalomethanes and haloacetic acids, respectively.

7.4.4 Using genomic markers to predict toxicity in treatment plants

Microcystin encoding genes *mcyD* can be a predictor for MC production and MC concentrations in lake water (Fortin et al., 2015). The correlation between *mcyD* genes MC concentrations can be used as a warning alert of toxic cyanobacterial bloom in the drinking water resources alongside the probe monitoring (phycocyanin) (Zamyadi et al., 2016a). In raw water, our results in chapter 6 showed a significant positive correlation between the *mcyD* gene copies and extracellular MC total (R=0.97), intracellular MC total (R=0.95); such correlations were in accordance with previous studies of the Lake Champlain (Fortin et al., 2010; Fortin et al., 2015). Our results also revealed a significant positive correlation of *mcyD* and intracellular MC total (R=0.98) and intracellular MC-LR (R=0.7) after $KMnO_4$ oxidation. Chlorination results only showed a positive correlation of *mcyD* gene copies with extracellular MC-LR (R=0.55). No correlation between the *mcyD* gene copies and MC was found after H_2O_2 oxidation. These results confirm that the potential toxin concentration in raw water (before oxidation) could be predicted using a quick molecular toxicity test. However, using such a test based on *mcyD* genes does not appear to be appropriate after oxidation because of the different reaction mechanisms of oxidants with cell components. Therefore, the use of a quick toxicity ddPCR based test can be considered as a valid additional tool for cyanobacterial bloom management in the drinking water resources only.

7.4.5 Cost implication of various pre-oxidants

One of the important drivers in pre-oxidation application is cost analysis. Cost estimations of different pre-oxidation are presented in Table 7.2 to compare capital expenditures and operating expenditures.

Table 7.2 Comparison of the pre-oxidation costs based on the (United States Environmental Protection Agency (USEPA), 2003)[i]

Oxidant (dose)	**CAPEX (USD)**	**OPEX(USD)**
Cl_2 (0.6 mg/L)	3,530	7,900
$KMnO_4$ (5 mg/L)[ii]	14,000	7,900
O_3 (0.3 mg/L)	452,000	76,000
H_2O_2 (10mg/L)[iii]	28,000	15,800
No pre-oxidation	Sludge management and potential breakthrough costs	

[i] the prices were updated considering the inflation rate. The cost estimation is based on the maximum flow of the Bedford water treatment plant (64.5 m^3/h).

[ii] the OPEX for $KMnO_4$ was assumed to be equal to Cl_2.

[iii] the CAPEX and OPEX for H_2O_2 oxidation were considered 2 times of $KMnO_4$ due to required contact time (larger reservoir and higher price of H_2O_2), large reservoir increased the operational cost as well.

Table 7.2 shows that pre-oxidation using H_2O_2 has a higher cost compared to Cl_2 and $KMnO_4$. The cost of not using pre-oxidation was not evaluated but merits attention and includes several aspects. Active cyanobacteria cells may accumulate and grow in sludge, constituting a reservoir of cell bound toxins. These cells may reach the clarifier's surface and breakthrough the filtration process. The potential toxin release in such circumstances may result in more frequent filter backwash and cyanobacteria cell breakthrough to the filtered water.

Considering the various impacts of the oxidants on cell viability, toxin release, cyanobacterial abundance, diversity and toxin control, hydrogen peroxide can reduce cell viability, decrease cyanobacteria taxa, the relative abundance of cyanobacteria biomarker and had a low impact on toxin release. However, considering the cost of using only hydrogen peroxide, combining hydrogen peroxide oxidation in advanced oxidation processes (such as UV/H2O2) may optimize the performance and implication costs.

CHAPTER 8 CONCLUSIONS AND RECOMMENDATIONS

8.1 Conclusion

This research project sought to increase our understanding of the cyanobacteria's fate during oxidation using high throughput sequencing technology (shotgun metagenomics) and the new microscopic technique, Enhanced Darkfield Microscopy/Hyper Spectral Imaging. Two different approaches were used: oxidation of cultured-based sample of *Microcystis* and *Dolichospermum* and of cyanobacterial bloom samples (Lake Champlain). Four types of oxidants were used in this research project: Chlorine, Ozone, Permanganate and, Hydrogen peroxide.

The following conclusions were drawn from this research study for the following themes:

(A) Cyanobacteria morphological response to the oxidation:

- Unique shape of spectrum was observed for *Microcystis* and *Dolichospermum* before oxidation.
- Distinct morphological deformations for *Microcystis* and *Dolichospermum* were observed based on the cell wall spectra following chlorination and ozonation.
- Species showed a different morphological deformation based on the cell wall spectra depending the oxidant used.
- Fragmentation of cell links in *Dolichospermum* happened before the cell lysis (cell links were the first targeted points by oxidants).

(B) Impact of pre-oxidation on cyanobacterial community composition:

- Raw water results indicate a shift in the dominant genus/species along the bloom period, from *Dolichospermum/ Dolichospermum Sp.90* on August 1st to *Microcystis/Microcystis aeruginosa* on August 29th.
- Chlorine exposure caused a progressive shift in bacterial and cyanobacterial communities. Potassium permanganate and hydrogen peroxide caused larger changes in bacterial and cyanobacterial community composition compared to chlorine.
- Similar cyanobacterial composition was observed for low exposure of chlorine, permanganate and hydrogen peroxide.

- Some toxin producing species relatively persisted following oxidation; *Dolichospermum* persisted after chlorine and permanganate oxidation, regardless of the dominant genus; *Microcystis* was relatively persisted following soft ozonation (0 – 0.9 mg.min/L).
- Hydrogen peroxide oxidation caused a decline in the relative abundance of all taxa and some toxin-producing species which shows the ability of hydrogen peroxide to prevent entering cyanobacteria to drinking water treatment plants.

(C) Cyanobacteria functional capacity in response to pre-oxidation

- The bacterial functional profile capacity upon oxidation of *Dolichospermum*-dominated bloom (August 1st) and *Microcystis*-dominated bloom (August 29th) are different. For *Dolichospermum*-dominated bloom undergoing oxidation, cyanobacteria phylum seems to be able to accomplish cell growth, Nitrogen/Phosphorus processes and photosynthesis, since significant positive correlation with "Cell division and Capsule", "Nitrogen metabolism", "Phosphorus metabolism", "Photosynthesis" and "Regulation cell signaling" related genes were detected after chlorination. Abundances of proteobacteria are inversely correlated to cyanobacteria associated to *Dolichospermum*-dominated bloom.
- Oxidation had a limited impact on the relative abundance of the cyanobacteria biomarkers when *Microcystis* is the abundant genus. High exposure of hydrogen peroxide caused a dramatic decrease in cyanobacteria biomarkers, regardless of the dominant genus, *Dolichospermum or Microcystis*.

(D) Management and treatment implications

- Ozonation caused an increase in all organic fractions, especially biopolymers. Same pattern was observed for chlorination but to a lower extent. All organic matter fractions decreased following oxidation using permanganate and hydrogen peroxide.
- While ddPCR *mcyD* based toxicity testing can be used to predict potential toxin concentrations before oxidation, such a tool may not be appropriate after oxidation.
- Limited MC removal following soft pre-oxidation demonstrates the requirement of further down flow processes to remove any release cyanotoxins.

8.2 Recommendations

Based on these findings, recommendations for further investigation are:

- Using EDM/HSI on a series of samples to determine the morphological deformation rate during oxidation.
- Integrate the morphological deformation rate into current oxidation models to understand the impact of morphological response on cyanotoxin release.
- Study the kinetics of different fraction of organic matter during cyanobacteria oxidation and their impact on toxin release to improve the oxidation models.
- Study the diversity and shifts in cyanobacterial community during oxidation under different nutrients conditions.
- Evaluate the fate of cyanobacteria during oxidation using meta-transcriptomic analysis to understand the correlation between the gene expression with shifts, diversity, functional profile and metabolite release and degradation.

REFERENCES

Acero, J.L., Rodriguez, E., Majado, M.E., Sordo, A., Meriluoto, J. (2008). Oxidation of microcystin-LR with chlorine and permanganate during drinking water treatment. *Water Supply: Research and Technology-Aqua*, *57*(6), 371-380.

Affe, H.M., Rigonato, J., Nunes, J.M., Menezes, M. (2018). Metagenomic analysis of cyanobacteria in an oligotrophic tropical estuary, South Atlantic. *Frontiers in Microbiology*, *9*, 1393.

Al Momani, F. (2007). Degradation of cyanobacteria anatoxin-a by advanced oxidation processes. *Separation and Purification Technology*, *57*(1), 85-93. https://doi.org/10.1016/j.seppur.2007.03.008

Al-Sammak, M.A., Hoagland, K.D., Cassada, D., Snow, D.D. (2014). Co-occurrence of the cyanotoxins BMAA, DABA and anatoxin-a in Nebraska reservoirs, fish, and aquatic plants. *Toxins (Basel)*, *6*(2), 488-508. https://doi.org/10.3390/toxins6020488

Almuhtaram, H., Cui, Y., Zamyadi, A., Hofmann, R. (2018). Cyanotoxins and cyanobacteria cell accumulations in drinking water treatment plants with a low risk of bloom formation at the source. *Toxins*, *10*, 430. https://doi.org/10.3390/toxins10110430

Alvarez, M., Rose, J., Bellamy, B., (2010) Treating algal toxins using oxidation, adsorption, and membrane technologies, Denver, Colorado, USA, p. 222.

American Public Health Association (APHA), American Water Works Association (AWWA), Water Environment Federation (WEF). (2012). *Standard methods for the examination of water and wastewater* (Vol. 5). American Public Health Association.

American Water Works Association (AWWA). (2010). *M57-Algae source to treatment*.

Andersson, A., Höglander, H., Karlsson, C., Huseby, S. (2015). Key role of phosphorus and nitrogen in regulating cyanobacterial community composition in the northern Baltic Sea. *Estuarine, Coastal and Shelf Science*, *164*, 161-171. https://doi.org/10.1016/j.ecss.2015.07.013

Aust, A.E., Eveleigh, J.F. (1999). Mechanisms of DNA oxidation. *Proceedings of the society for experimental biology and medicine*, *222*(3), 246-252.

Backer, L.C., Landsberg, J.H., Miller, M., Keel, K., Taylor, T.K. (2013). Canine cyanotoxin poisonings in the United States (1920s–2012): Review of suspected and confirmed cases from three data sources. *Toxins*, *5*(9), 1597-1628.

Baker, P.D., Larelle, D.F. (1999). *A guide to the identification of common blue-Green algae (Cyanoprokaryotes) in Australian freshwaters* (Vol. Guide 25). The Cooperative Research Centre for Freshwater Ecology (CRCFE) and Murray-Darling Basin Commission (MDBC).

Bale, N.J., Hennekam, R., Hopmans, E.C., Dorhout, D., Reichart, G.-J., van der Meer, M., Villareal, T.A., Sinninghe Damsté, J.S., Schouten, S. (2019). Biomarker evidence for nitrogen-fixing cyanobacterial blooms in a brackish surface layer in the Nile River plume during sapropel deposition. *Geology*, *47*(11), 1088-1092.

Ballesté, E., Blanch, A.R. (2010). Persistence of Bacteroides species populations in a river as measured by molecular and culture techniques. *Applied and Environmental Microbiology, 76*(22), 7608-7616.

Baxa, D.V., Kurobe, T., Ger, K.A., Lehman, P.W., Teh, S.J. (2010). Estimating the abundance of toxic *Microcystis* in the San Francisco Estuary using quantitative real-time PCR. *Harmful Algae, 9*(3), 342-349. https://doi.org/10.1016/j.hal.2010.01.001

Berry, M.A., Davis, T.W., Cory, R.M., Duhaime, M.B., Johengen, T.H., Kling, G.W., Marino, J.A., Den Uyl, P.A., Gossiaux, D., Dick, G.J., Denef, V.J. (2017). Cyanobacterial harmful algal blooms are a biological disturbance to Western Lake Erie bacterial communities. *Environmental Microbiology*, *19*(3), 1149-1162. https://doi.org/10.1111/1462-2920.13640

Bishop, S.L., Kerkovius, J.K., Menard, F., Murch, S.J. (2018). N-β-methylamino-l-alanine and its naturally occurring isomers in cyanobacterial blooms in Lake Winnipeg. *Neurotox Research*, *33*(1), 133-142. https://doi.org/10.1007/s12640-017-9820-z

Bortoli, S., Oliveira-Silva, D., Krüger, T., Dörr, F.A., Colepicolo, P., Volmer, D.A., Pinto, E. (2014). Growth and microcystin production of a Brazilian Microcystis aeruginosa strain (LTPNA 02) under different nutrient conditions. *Revista Brasileira de Farmacognosia, 24*(4), 389-398. https://doi.org/10.1016/j.bjp.2014.07.019

Brooke, S., Newcombe, G., Nicholson, B., Klass, G. (2006). Decrease in toxicity of microcystins LA and LR in drinking water by ozonation. *Toxicon*, *48*(8), 1054-1059. https://doi.org/10.1016/j.toxicon.2006.08.010

Bui, C.T., Rees, K., Cotton, R.G.H. (2003). Permanganate oxidation reactions of DNA: perspective in biological studies. *Nucleosides, Nucleotides and Nucleic Acids*, *22*(9), 1835-1855.

Bukaveckas, P.A., Lesutienė, J., Gasiūnaitė, Z.R., Ložys, L., Olenina, I., Pilkaitytė, R., Pūtys, Ž., Tassone, S., Wood, J. (2017). Microcystin in aquatic food webs of the Baltic and Chesapeake Bay regions. *Estuarine, Coastal and Shelf Science, 191,* 50-59.

Bullerjahn, G.S., McKay, R.M., Davis, T.W., Baker, D.B., Boyer, G.L., D'Anglada, L.V., Doucette, G.J., Ho, J.C., Irwin, E.G., Kling, C.L. (2016). Global solutions to regional problems: Collecting global expertise to address the problem of harmful cyanobacterial blooms. A Lake Erie case study. *Harmful Algae, 54*, 223-238. https://doi.org/10.1016/j.hal.2016.01.003

Burson, A., Matthijs, H.C.P., de Bruijne, W., Talens, R., Hoogenboom, R., Gerssen, A., Visser, P.M., Stomp, M., Steur, K., van Scheppingen, Y. (2014). Termination of a toxic Alexandrium bloom with hydrogen peroxide. *Harmful Algae, 31,* 125-135.

Buskey, E.J., Hyatt, C.J. (2006). Use of the FlowCAM for semi-automated recognition and enumeration of red tide cells (Karenia brevis) in natural plankton samples. *Harmful Algae, 5*(6), 685-692.

Calle, M.L. (2019). Statistical analysis of metagenomics data. *Genomics & informatics*, *17*(1).

Campinas, M., Rosa, M.J. (2010). Evaluation of cyanobacterial cells removal and lysis by ultrafiltration. *Separation and Purification Technology*, *70*(3), 345-353. https://doi.org/10.1016/j.seppur.2009.10.021

Caporaso, J.G., Lauber, C.L., Walters, W.A., Berg-Lyons, D., Huntley, J., Fierer, N., Owens, S.M., Betley, J., Fraser, L., Bauer, M. (2012). Ultra-high-throughput microbial community analysis on the Illumina HiSeq and MiSeq platforms. *The ISME Journal*, *6*(8), 1621-1624.

Carmichael, W. (2013). *The water environment: algal toxins and health*. Springer Science & Business Media.

Casero, M.C., Ballot, A., Agha, R., Quesada, A., Cirés, S. (2014). Characterization of saxitoxin production and release and phylogeny of *sxt* genes in paralytic shellfish poisoning toxin-producing *Aphanizomenon gracile*. *Harmful Algae*, *37*, 28-37. https://doi.org/10.1016/j.hal.2014.05.006

Casero, M.C., Velázquez, D., Medina-Cobo, M., Quesada, A., Cirés, S. (2019). Unmasking the identity of toxigenic cyanobacteria driving a multi-toxin bloom by high-throughput sequencing of cyanotoxins genes and 16S rRNA metabarcoding. *Science of the Total Environment*, *665*, 367-378. https://doi.org/10.1016/j.scitotenv.2019.02.083

Cataldo, F. (2005). Ozone degradation of ribonucleic acid (RNA). *Polymer Degradation and Stability*, *89*(2), 274-281. https://doi.org/10.1016/j.polymdegradstab.2004.10.020

Cataldo, F. (2006). DNA degradation with ozone. *International journal of biological macromolecules*, *38*(3-5), 248-254.

Celeste, C.M.M., Lorena, R., Oswaldo, A.J., Sandro, G., Daniela, S., Dario, A., Leda, G. (2017). Mathematical modeling of Microcystis aeruginosa growth and [D-Leu^{1}] microcystin-LR production in culture media at different temperatures. *Harmful Algae*, *67*, 13-25. https://doi.org/10.1016/j.hal.2017.05.006

Chaffin, J.D., Mishra, S., Kane, D.D., Bade, D.L., Stanislawczyk, K., Slodysko, K.N., Jones, K.W., Parker, E.M., Fox, E.L. (2019). Cyanobacterial blooms in the central basin of Lake Erie: Potentials for cyanotoxins and environmental drivers. *Journal of Great Lakes Research*, *45*(2), 277-289. https://doi.org/10.1016/j.jglr.2018.12.006

Chen, K., Pachter, L. (2005). Bioinformatics for whole-genome shotgun sequencing of microbial communities. *PLoS Computational Biology*, *1*(2), 106-112. https://doi.org/10.1371/journal.pcbi.0010024

Chen, Y.-T., Chen, W.-R., Lin, T.-F. (2018). Oxidation of cyanobacterial neurotoxin beta-N-methylamino-L-alanine (BMAA) with chlorine, permanganate, ozone, hydrogen peroxide and hydroxyl radical. *Water Research*, https://doi.org/https://doi.org/10.1016/j.watres.2018.05.056

Chen, Y.-T., Chen, W.-R., Liu, Z.-Q., Lin, T.-F. (2017). Reaction pathways and kinetics of a cyanobacterial neurotoxin *β-N*-methylamino-*L*-alanine (BMAA) during chlorination. *Environmental Science & Technology*, *51*(3), 1303-1311. https://doi.org/10.1021/acs.est.6b03553

Cheng, X.L., Shi, H.L., Adams, C.D., Timmons, T., Ma, Y.F. (2009). Effects of oxidative and physical treatments on inactivation of Cylindrospermopsis raciborskii and removal of cylindrospermopsin. *Water Science and Technology*, *60*(3), 689-697.

Cheriaa, J., Rouabhia, M., Maatallah, M., Bakhrouf, A. (2012). Phenotypic stress response of Pseudomonas aeruginosa following culture in water microcosms. *Journal of Water and Health, 10*(1), 130-139.

Chernoff, N., Hill, D.J., Diggs, D.L., Faison, B.D., Francis, B.M., Lang, J.R., Larue, M.M., Le, T.T., Loftin, K.A., Lugo, J.N. (2017). A critical review of the postulated role of the non-essential amino acid, β-N-methylamino-L-alanine, in neurodegenerative disease in humans. *Journal of Toxicology and Environmental Health, Part B, 20*(4), 183-229.

Chia, M.A., Jankowiak, J.G., Kramer, B.J., Goleski, J.A., Huang, I.S., Zimba, P.V., do Carmo Bittencourt-Oliveira, M., Gobler, C.J. (2018). Succession and toxicity of Microcystis and Anabaena (Dolichospermum) blooms are controlled by nutrient-dependent allelopathic interactions. *Harmful Algae, 74*, 67-77.

Chorus, I., Bartram, J., (1999) Toxic cyanobacteria in water: A guide to their public health consequences, monitoring and management / edited by Ingrid Chorus and Jamie Bertram. World Health Organization, Geneva.

Church, M.J., Hutchins, D.A., Ducklow, H.W. (2000). Limitation of bacterial growth by dissolved organic matter and iron in the Southern Ocean. *Applied and Environmental Microbiology, 66*(2), 455-466.

Cissell, E.C., McCoy, S.J. (2020). Shotgun metagenomic sequencing reveals the full taxonomic, trophic, and functional diversity of a coral reef benthic cyanobacterial mat from Bonaire, Caribbean Netherlands. *Science of the Total Environment*, 142719.

Codd, G.A., Jefferies, T.M., Keevil, C.W., Potter, E. (1994). *Detection methods for cynobacterial toxins*. Elsevier.

Coral, L.A., Zamyadi, A., Barbeau, B., Bassetti, F.J., Lapolli, F.R., Prévost, M. (2013). Oxidation of *M. aeruginosa* and *A. flos-aquae* by ozone: Impacts on cell integrity and chlorination by-product formation *Water Research*, *47*(9), 2983–2994. https://doi.org/10.1016/j.watres.2013.03.012

Cox, M.P., Peterson, D.A., Biggs, P.J. (2010). SolexaQA: At-a-glance quality assessment of Illumina second-generation sequencing data. *BMC Bioinformatics, 11*(1), 1-6.

Crittenden, J.C., Howe, K.J., Hand, D.W., Tchobanoglous, G., Trussell, R.R. (2012). *Principles of water treatment*. John Wiley & Sons, Inc.

Daly, R.I., Ho, L., Brookes, J.D. (2007). Effect of chlorination on *Microcystis aeruginosa* cell integrity and subsequent microcystin release and degradation. *Environmental Science and Technology, 41*(12), 4447-4453.

Davis, T.W., Berry, D.L., Boyer, G.L., Gobler, C.J. (2009). The effects of temperature and nutrients on the growth and dynamics of toxic and non-toxic strains of *Microcystis* during cyanobacteria blooms *Harmful Algae*, *8*(5), 715–725. https://doi.org/10.1016/j.hal.2009.02.004

Deborde, M., von Gunten, U. (2008). Reactions of chlorine with inorganic and organic compounds during water treatment--Kinetics and mechanisms: a critical review. *Water Research, 42*(1-2), 13-51.

Ding, J., Shi, H., Timmons, T., Adams, C. (2010). Release and removal of microcystins from microcystis during oxidative, physical, and UV-based disinfection. *Journal of Environmental Engineering*, *136*, 2-11.

Ding, Y., Gan, N., Liu, J., Zheng, L., Li, L., Song, L. (2017). Survival, recovery and microcystin release of Microcystis aeruginosa in cold or dark condition. *Chinese Journal of Oceanology and Limnology*, *35*(2), 313-323.

Dixon, M.B., Falconet, C., Ho, L., Chow, C.W., O'Neill, B.K., Newcombe, G. (2011). Removal of cyanobacterial metabolites by nanofiltration from two treated waters. *Journal of Hazardous Materials*, *188*(1-3), 288-295. https://doi.org/10.1016/j.jhazmat.2011.01.111

Eldridge, S.L.C., Wood, T.M. (2019). Annual variations in microcystin occurrence in Upper Klamath Lake, Oregon, based on high-throughput DNA sequencing, qPCR, and environmental parameters. *Lake and Reservoir Management*, 1-14. https://doi.org/10.1080/10402381.2019.1619112

Falconer, I.R. (2012). *Algal toxins in seafood and drinking water*. Elsevier.

Fan, J., Daly, R., Hobson, P., Ho, L., Brookes, J. (2013a). Impact of potassium permanganate on cyanobacterial cell integrity and toxin release and degradation. *Chemosphere*, *92*(5), 529-534. https://doi.org/10.1016/j.chemosphere.2013.03.022

Fan, J., Ho, L., Hobson, P., Brookes, J. (2013b). Evaluating the effectiveness of copper sulphate, chlorine, potassium permanganate, hydrogen peroxide and ozone on cyanobacterial cell integrity. *Water Research*, *47*(14), 5153-5164. https://doi.org/10.1016/j.watres.2013.05.057

Fan, J., Rao, Chiu, Y.T., Lin, T.F. (2016). Impact of chlorine on the cell integrity and toxin release and degradation of colonial Microcystis. *Water Research*, *102*, 394-404. https://doi.org/10.1016/j.watres.2016.06.053

Fan, J.J., Ho, L., Hobson, P., Daly, R., Brookes, J. (2014a). Application of various oxidants for cyanobacteria control and cyanotoxin removal in wastewater treatment. *Journal of Environmental Engineering*, *140*(7), https://doi.org/10.1061/(ASCE)EE.1943-7870.0000852

Fan, J.J., Hobson, P., Ho, L., Daly, R., Brookes, J. (2014b). The effects of various control and water treatment processes on the membrane integrity and toxin fate of *cyanobacteria*. *Journal of Hazardous Materials*, *264*, 313-322. https://doi.org/10.1016/j.jhazmat.2013.10.059

Farrell, R.E., (2010) RNA Methodologies, A laboratory guide for isolation and characterization, in: Farrell, R.E. (Ed.), *RNA Methodologies (Fourth Edition)*. Academic Press, San Diego, pp. 179-219.

Fortin, N., Aranda-Rodriguez, R., Jing, H., Pick, F., Bird, D., Greer, C.W. (2010). Detection of microcystin-producing cyanobacteria in Missisquoi Bay, Quebec, Canada, using quantitative PCR. *Applied and Environmental Microbiology*, *76*(15), 5105-5112.

Fortin, N., Munoz-Ramos, V., Bird, D., Levesque, B., Whyte, L.G., Greer, C.W. (2015). Toxic cyanobacterial bloom triggers in Missisquoi bay, lake Champlain, as determined by next-generation sequencing and quantitative PCR. *Life (Basel)*, *5*(2), 1346-1380. https://doi.org/10.3390/life5021346

Foster, Z.S., Sharpton, T.J., Grunwald, N.J. (2017). Metacoder: An R package for visualization and manipulation of community taxonomic diversity data. *PLoS Comput Biol*, *13*(2), e1005404. https://doi.org/10.1371/journal.pcbi.1005404

Fu, L., Niu, B., Zhu, Z., Wu, S., Li, W. (2012). CD-HIT: Accelerated for clustering the next-generation sequencing data. *Bioinformatics*, *28*(23), 3150-3152. https://doi.org/10.1093/bioinformatics/bts565

Gad, A.A.M., El-Tawel, S. (2016). Effect of pre-oxidation by chlorine/permanganate on surface water characteristics and algal toxins. *Desalination and Water Treatment*, *57*(38), 17922-17934. https://doi.org/10.1080/19443994.2015.1087337

Gasol, J.M., Comerma, M., García, J.C., Armengol, J., Casamayor, E.O., Kojecká, P., Šimek, K. (2002). A transplant experiment to identify the factors controlling bacterial abundance, activity, production, and community composition in a eutrophic canyon-shaped reservoir. *Limnology and Oceanography*, *47*(1), 62-77.

Gomez-Smith, C.K., Tan, D.T., Shuai, D. (2016). Research highlights: functions of the drinking water microbiome–from treatment to tap. *Environmental Science: Water Research & Technology*, *2*(2), 245-249.

Gong, W., Browne, J., Hall, N., Schruth, D., Paerl, H., Marchetti, A. (2017). Molecular insights into a dinoflagellate bloom. *The ISME Journal*, *11*(2), 439-452.

Gonzalez, A., King, A., Robeson Ii, M.S., Song, S., Shade, A., Metcalf, J.L., Knight, R. (2012). Characterizing microbial communities through space and time. *Current Opinion in Biotechnology*, *23*(3), 431-436.

Gonzalez-Torres, A., Putnam, J., Jefferson, B., Stuetz, R.M., Henderson, R.K. (2014). Examination of the physical properties of Microcystis aeruginosa flocs produced on coagulation with metal salts. *Water Research*, *60*, 197-209. https://doi.org/10.1016/j.watres.2014.04.046

Gray, M.J., Wholey, W.-Y., Jakob, U. (2013). Bacterial responses to reactive chlorine species. *Annual Review of Microbiology*, *67*(1), 141-160. https://doi.org/10.1146/annurev-micro-102912-142520

Greenacre, M. (2018). *Compositional data analysis in practice* (1st edition ed.). CRC Press.

Großkopf, T., Soyer, O.S. (2014). Synthetic microbial communities. *Current Opinion in Microbiology*, *18*, 72-77.

Grutzmacher, G., Bottcher, G., Chorus, I., Bartel, H. (2002). Removal of microcystins by slow sand filtration. *Environmental Toxicology and Chemistry*, *17*(4), 386-394. Research Support, Non-U.S. Gov't. https://doi.org/10.1002/tox.10062

Hakkila, K., Valev, D., Antal, T., Tyystjärvi, E., Tyystjärvi, T. (2019). Group 2 sigma factors are central regulators of oxidative stress acclimation in cyanobacteria. *Plant and Cell Physiology*, *60*(2), 436-447.

Hall, T., Hart, J., Croll, B., Gregory, R. (2000). Laboratory-scale investigations of algal toxin removal by water treatment. *Journal of the Chartered Institution of Water and Environmental Management*, *14*(2), 143-149.

Hamilton, P.B., Ley, L.M., Dean, S., Pick, F.R. (2005). The occurrence of the cyanobacterium *Cylindrospermopsis raciborskii* in Constance Lake: An exotic cyanoprokaryote new to

Canada. *Phycologia*, *44*(1), 17-25. https://doi.org/10.2216/0031-8884(2005)44[17:Tootcc]2.0.Co;2

Hammes, F., Meylan, S., Salhi, E., Köster, O., Egli, T., von Gunten, U. (2007). Formation of assimilable organic carbon (AOC) and specific natural organic matter (NOM) fractions during ozonation of phytoplankton. *Water Research*, *41*(7), 1447-1454.

Harke, M.J., Davis, T.W., Watson, S.B., Gobler, C.J. (2015). Nutrient-controlled niche differentiation of western Lake Erie cyanobacterial populations revealed via metatranscriptomic surveys. *Environmental Science & Technology*, *50*(2), 604-615. https://doi.org/10.1021/acs.est.5b03931

Hawkins, C.L., Pattison, D.I., Whiteman, M., Davies, M.J., (2007) Chlorination and nitration of DNA and nucleic acid components, *Oxidative Damage to Nucleic Acids*. Springer, pp. 14-39.

Hawkins, P.R., Holliday, J., Kathuria, A., Bowling, L. (2005). Change in cyanobacterial biovolume due to preservation by Lugol's Iodine. *Harmful Algae*, *4*(6), 1033-1043.

He, X., Liu, Y.-L., Conklin, A., Westrick, J., Weavers, L.K., Dionysiou, D.D., Lenhart, J.J., Mouser, P.J., Szlag, D., Walker, H.W. (2016). Toxic cyanobacteria and drinking water: Impacts, detection, and treatment. *Harmful Algae*, *54*, 174-193. https://doi.org/10.1016/j.hal.2016.01.001

He, X., Wert, E.C. (2016). Colonial cell disaggregation and intracellular microcystin release following chlorination of naturally occurring Microcystis. *Water Research*, *101*, 10-16. https://doi.org/10.1016/j.watres.2016.05.057

Health Canada, (2018) Guidelines for Canadian drinking water quality: Guideline technical document. Cyanobacterial toxins. Federal-Provincial-Territorial Committee on Drinking Water, Ottawa, ON, CANADA, p. 177.

Health Canada, Federal-Provincial-Territorial Commitee on Drinking Water, (2016) Cyanobacterial toxins in drinking water. Document for public consultation. Guidelines for Canadian Drinking Water Quality: Guideline Technical Document, p. 177.

Henderson, R., Parsons, S.A., Jefferson, B. (2008). The impact of algal properties and pre-oxidation on solid-liquid separation of algae. *Water Research*, *42*(8-9), 1827-1845.

Henderson, R.K., Parsons, S.A., Jefferson, B. (2010). The impact of differing cell and algogenic organic matter (AOM) characteristics on the coagulation and flotation of algae. *Water Research*, *44*(12), 3617-3624. https://doi.org/10.1016/j.watres.2010.04.016

Ho, J.C., Michalak, A.M. (2015). Challenges in tracking harmful algal blooms: A synthesis of evidence from Lake Erie. *Journal of Great Lakes Research*, *41*(2), 317-325. https://doi.org/10.1016/j.jglr.2015.01.001

Ho, L., Dreyfus, J., Boyer, J.e., Lowe, T., Bustamante, H., Duker, P., Meli, T., Newcombe, G. (2012). Fate of cyanobacteria and their metabolites during water treatment sludge management processes. *Science of the Total Environment*, *424*(0), 232-238. https://doi.org/10.1016/j.scitotenv.2012.02.025

Ho, L., Hoefel, D., Saint, C.P., Newcombe, G. (2007). Isolation and identification of a novel microcystin-degrading bacterium from a biological sand filter. *Water Research*, *41*(20), 4685-4695.

Ho, L., Lambling, P., Bustamante, H., Duker, P., Newcombe, G. (2011). Application of powdered activated carbon for the adsorption of cylindrospermopsin and microcystin toxins from drinking water supplies. *Water Research*, *45*(9), 2954-2964.

Ho, L., Onstad, G., von Gunten, U., Rinck-Pfeiffer, S., Craig, K., Newcombe, G. (2006). Differences in the chlorine reactivity of four microcystin analogues. *Water Research*, *40*(6), 1200-1209.

Ho, L., Tanis-Plant, P., Kayal, N., Slyman, N., Newcombe, G. (2009). Optimising water treatment practices for the removal of Anabaena circinalis and its associated metabolites, geosmin and saxitoxins. *Journal of Water and Health*, *7*(4), 544-556.

Hörnlein, C., Confurius-Guns, V., Grego, M., Stal, L.J., Bolhuis, H. (2020). Circadian clock-controlled gene expression in co-cultured, mat-forming cyanobacteria. *Scientific Reports*, *10*(1), 14095. https://doi.org/10.1038/s41598-020-69294-3

Hotto, A.M., Satchwell, M.F., Berry, D.L., Gobler, C.J., Boyer, G.L. (2008). Spatial and temporal diversity of microcystins and microcystin-producing genotypes in Oneida Lake, NY. *Harmful Algae*, *7*(5), 671-681. https://doi.org/10.1016/j.hal.2008.02.001

Hou, L., Zhou, Q., Wu, Q., Gu, Q., Sun, M., Zhang, J. (2018). Spatiotemporal changes in bacterial community and microbial activity in a full-scale drinking water treatment plant. *Science of the Total Environment*, *625*, 449-459.

Huang, T.-L., Zhao, J.-W., Chai, B.-B. (2008). Mechanism studies on chlorine and potassium permanganate degradation of microcystin-LR in water using high-performance liquid chromatography tandem mass spectrometry. *Water Science and Technology*, *58*(5), 1079. 10.2166/wst.2008.460.

Huber, S.A., Balz, A., Abert, M., Pronk, W. (2011). Characterisation of aquatic humic and non-humic matter with size-exclusion chromatography – organic carbon detection – organic nitrogen detection (LC-OCD-OND). *Water Research*, *45*(2), 879-885. https://doi.org/10.1016/j.watres.2010.09.023

Humayun, M.Z. (1998). SOS and Mayday: multiple inducible mutagenic pathways in Escherichia coli. *Molecular Microbiology*, *30*(5), 905-910.

Ininbergs, K., Bergman, B., Larsson, J., Ekman, M. (2015). Microbial metagenomics in the Baltic Sea: recent advancements and prospects for environmental monitoring. *Ambio*, *44*(3), 439-450.

J. Alex, E. (2012). Is the future blue-green? A review of the current model predictions of how climate change could affect pelagic freshwater cyanobacteria. *Water Research*, *46*(5), 1364-1371. https://doi.org/10.1016/j.watres.2011.12.018

Jalili, F., Trigui, H., Guerra Maldonado, J.F., Dorner, S., Zamyadi, A., Shapiro, B.J., Terrat, Y., Fortin, N., Sauvé, S., Prévost, M. (2021). Can Cyanobacterial Diversity in the Source Predict the Diversity in Sludge and the Risk of Toxin Release in a Drinking Water Treatment Plant? *Toxins*, *13*(1), 25.

Janson, S., Vegelius, J. (1981). Measures of ecological association. *Oecologia*, *49*(3), 371-376.

Jasim, S.Y., Saththasivam, J. (2017). Advanced oxidation processes to remove cyanotoxins in water. *Desalination, 406*, 83-87. https://doi.org/10.1016/j.desal.2016.06.031

Kanehisa, M., Goto, S., Sato, Y., Furumichi, M., Tanabe, M. (2012). KEGG for integration and interpretation of large-scale molecular data sets. *Nucleic Acids Research*, *40*(D1), D109-D114.

Kaneko, T., Nakajima, N., Okamoto, S., Suzuki, I., Tanabe, Y., Tamaoki, M., Nakamura, Y., Kasai, F., Watanabe, A., Kawashima, K. (2007). Complete genomic structure of the bloom-forming toxic cyanobacterium Microcystis aeruginosa NIES-843. *DNA Research*, *14*(6), 247-256.

Kardinaal, W.E.A., Janse, I., Kamst-van Agterveld, M., Meima, M., Snoek, J., Mur, L.R., Huisman, J., Zwart, G., Visser, P.M. (2007). Microcystis genotype succession in relation to microcystin concentrations in freshwater lakes. *Aquatic Microbial Ecology*, *48*(1), 1-12.

Kim, D., Hahn, A.S., Wu, S.-J., Hanson, N.W., Konwar, K.M., Hallam, S.J. (2015). *FragGeneScan-Plus for scalable high-throughput short-read open reading frame prediction*. (pp. 1-8).

Kim, J., Lim, J., Lee, C. (2013). Quantitative real-time PCR approaches for microbial community studies in wastewater treatment systems: Applications and considerations. *Biotechnol Adv*, *31*(8), 1358-1373. https://doi.org/10.1016/j.biotechadv.2013.05.010

Kim, K.H., Yoon, Y., Hong, W.-Y., Kim, J., Cho, Y.-C., Hwang, S.-J. (2018a). Application of metagenome analysis to characterize the molecular diversity and saxitoxin-producing potentials of a cyanobacterial community: A case study in the North Han River, Korea. *Applied Biological Chemistry*, *61*(2), 153-161. https://doi.org/10.1007/s13765-017-0342-4

Kim, M.S., Lee, H.-J., Lee, K.-M., Seo, J., Lee, C. (2018b). Oxidation of microcystins by permanganate: pH and temperature-dependent kinetics, effect of DOM characteristics, and oxidation mechanism revisited. *Environmental Science & Technology*. https://doi.org/10.1021/acs.est.8b01447

Kouzminov, A., Ruck, J., Wood, S.A. (2007). New Zealand risk management approach for toxic cyanobacteria in drinking water. *Australian and New Zealand Journal of Public Health*, *31*(3), 275-281. https://doi.org/10.1111/j.1467-842X.2007.00061.x

Krämer, R. (2010). Bacterial stimulus perception and signal transduction: response to osmotic stress. *The Chemical Record*, *10*(4), 217-229.

Krüger, T., Hölzel, N., Luckas, B. (2012). Influence of cultivation parameters on growth and microcystin production of *Microcystis aeruginosa (Cyanophyceae)* isolated from Lake Chao (China). *Microbial Ecology*, *63*(1), 199-209. https://doi.org/10.1007/s00248-011-9899-3

Laszakovits, J.R., MacKay, A.A. (2019). Removal of cyanotoxins by potassium permanganate: Incorporating competition from natural water constituents. *Water Research*, *155*, 86-95.

Latifi, A., Ruiz, M., Zhang, C.C. (2009). Oxidative stress in cyanobacteria. *FEMS Microbiology Reviews*, *33*(2), 258-278. https://doi.org/10.1111/j.1574-6976.2008.00134.x

Lee, C., Marion, J.W., Cheung, M., Lee, C.S., Lee, J. (2015). Associations among human-associated fecal contamination, *Microcystis aeruginosa*, and microcystin at Lake Erie beaches. *International Journal of Environmental Research and Public Health*, *12*(9), 11466-11485. https://doi.org/10.3390/ijerph120911466

Lee, S.J., Jang, M.H., Kim, H.S., Yoon, B.D., Oh, H.M. (2000). Variation of microcystin content of *Microcystis aeruginosa* relative to medium N: P ratio and growth stage. *Journal of Applied Microbiology*, *89*(2), 323-329.

Lévesque, B., Gervais, M.C., Chevalier, P., Gauvin, D., Anassour-Laouan-Sidi, E., Gingras, S., Fortin, N., Brisson, G., Greer, C., Bird, D. (2014). Prospective study of acute health effects in relation to exposure to cyanobacteria. *Science of the Total Environment*, *466–467*(0), 397-403. https://doi.org/10.1016/j.scitotenv.2013.07.045

Lezcano, M.Á., Velázquez, D., Quesada, A., El-Shehawy, R. (2017). Diversity and temporal shifts of the bacterial community associated with a toxic cyanobacterial bloom: An interplay between microcystin producers and degraders. *Water Research*, *125*, 52-61. https://doi.org/10.1016/j.watres.2017.08.025

Li, H., Barber, M., Lu, J., Goel, R. (2020a). Microbial community successions and their dynamic functions during harmful cyanobacterial blooms in a freshwater lake. *Water Research*, 116292.

Li, L., Shao, C., Lin, T.-F., Shen, J., Yu, S., Shang, R., Yin, D., Zhang, K., Gao, N. (2014). Kinetics of cell inactivation, toxin release, and degradation during permanganation of *Microcystis aeruginosa*. *Environmental Science & Technology*, *48*(5), 2885-2892. https://doi.org/10.1021/es405014g

Li, Q., Lin, F., Yang, C., Wang, J., Lin, Y., Shen, M., Park, M.S., Li, T., Zhao, J. (2018). A large-scale comparative metagenomic study reveals the functional interactions in six bloom-forming *Microcystis*-epibiont communities. *Frontiers in Microbiology*, *9*, 746. https://doi.org/10.3389/fmicb.2018.00746

Li, Y., Li, D. (2012). Competition between toxic *Microcystis aeruginosa* and nontoxic *Microcystis wesenbergii* with *Anabaena* PCC7120. *Journal of Applied Phycology*, *24*(1), 69-78.

Li, Y., Xu, C., Zhang, W., Lin, L., Wang, L., Niu, L., Zhang, H., Wang, P., Wang, C. (2020b). Response of bacterial community in composition and function to the various DOM at river confluences in the urban area. *Water Research*, *169*, 115293.

Lin, T.F., Chang, D.W., Lien, S.K., Tseng, Y.S., Chiu, Y.T., Wang, Y.S. (2009). Effect of chlorination on the cell integrity of two noxious cyanobacteria and their releases of odorants. *Journal of water supply : research and technology. AQUA (Print)*, *58*(8), 539-551.

Liu, X., Chen, Z., Zhou, N., Shen, J., Ye, M. (2010). Degradation and detoxification of microcystin-LR in drinking water by sequential use of UV and ozone. *Journal of Environmental Sciences*, *22*(12), 1897-1902. https://doi.org/10.1016/S1001-0742(09)60336-3

Logares, R., Bråte, J., Bertilsson, S., Clasen, J.L., Shalchian-Tabrizi, K., Rengefors, K. (2009). Infrequent marine–freshwater transitions in the microbial world. *Trends in Microbiology*, *17*(9), 414-422.

Lorenzi, A.S., Chia, M.A., Lopes, F.A.C., Silva, G.G.Z., Edwards, R.A., do Carmo Bittencourt-Oliveira, M. (2019). Cyanobacterial biodiversity of semiarid public drinking water supply reservoirs assessed via next-generation DNA sequencing technology. *Journal of Microbiology*, *57*(6), 450-460.

Lu, J., Zhu, B., Struewing, I., Xu, N., Duan, S. (2019). Nitrogen–phosphorus-associated metabolic activities during the development of a cyanobacterial bloom revealed by metatranscriptomics. *Scientific Reports*, *9*(1), 2480. https://doi.org/10.1038/s41598-019-38481-2

Lund, J.W.G. (1959). A simple counting chamber for Nannoplankton. *Limnology and Oceanography*, *4*(1), 57-65. https://doi.org/10.4319/lo.1959.4.1.0057

Lusty, M.W., Gobler, C.J. (2020). The efficacy of hydrogen peroxide in mitigating cyanobacterial blooms and altering microbial communities across four lakes in NY, USA. *Toxins*, *12*(7), 428. https://doi.org/10.3390/toxins12070428

Ma, M., Liu, R., Liu, H., Qu, J. (2012a). Effect of moderate pre-oxidation on the removal of Microcystis aeruginosa by KMnO4–Fe(II) process: Significance of the in-situ formed Fe(III). *Water Research*, *46*(1), 73-81. https://doi.org/10.1016/j.watres.2011.10.022

Ma, M., Liu, R., Liu, H., Qu, J., Jefferson, W. (2012b). Effects and mechanisms of pre-chlorination on Microcystis aeruginosa removal by alum coagulation: Significance of the released intracellular organic matter. *Separation and Purification Technology*, *86*(0), 19-25. https://doi.org/10.1016/j.seppur.2011.10.015

Main, B.J., Bowling, L.C., Padula, M.P., Bishop, D.P., Mitrovic, S.M., Guillemin, G.J., Rodgers, K.J. (2018). Detection of the suspected neurotoxin β-methylamino-l-alanine (BMAA) in cyanobacterial blooms from multiple water bodies in Eastern Australia. *Harmful Algae*, *74*, 10-18. https://doi.org/10.1016/j.hal.2018.03.004

Marinho, M.M., de Oliveira e Azevedo, S.M.F. (2007). Influence of N/P ratio on competitive abilities for nitrogen and phosphorus by *Microcystis aeruginosa* and *Aulacoseira distans*. *Aquatic Ecology*, *41*(4), 525-533. https://doi.org/10.1007/s10452-007-9118-y

Maruyama, T., Kato, K., Yokoyama, A., Tanaka, T., Hiraishi, A., Park, H.D. (2003). Dynamics of microcystin-degrading bacteria in mucilage of Microcystis. *Microbial Ecology*, *46*(2), 279-288.

Matthijs, H.C.P., Visser, P.M., Reeze, B., Meeuse, J., Slot, P.C., Wijn, G., Talens, R., Huisman, J. (2012). Selective suppression of harmful cyanobacteria in an entire lake with hydrogen peroxide. *Water Research*, *46*(5), 1460-1472. https://doi.org/10.1016/j.watres.2011.11.016

McKindles, K.M., Zimba, P.V., Chiu, A.S., Watson, S.B., Gutierrez, D.B., Westrick, J., Kling, H., Davis, T.W. (2019). A multiplex analysis of potentially toxic cyanobacteria in Lake Winnipeg during the 2013 bloom season. *Toxins*, *11*(10), 587. https://doi.org/10.3390/toxins11100587

McMurdie, P.J., Holmes, S. (2013). phyloseq: an R package for reproducible interactive analysis and graphics of microbiome census data. *PLoS ONE*, *8*(4).

McQuaid, N., Zamyadi, A., Prévost, M., Bird, D.F., Dorner, S. (2011). Use of in vivo phycocyanin fluorescence to monitor potential microcystin-producing cyanobacterial biovolume in a

drinking water source. *Journal of Environmental Monitoring*, *13*(2), 455-463. https://doi.org/10.1039/C0EM00163E

Merel, S., Clément, M., Mourot, A., Fessard, V., Thomas, O. (2010a). Characterization of cylindrospermopsin chlorination. *Science of the Total Environment*, *408*(16), 3433-3442. https://doi.org/10.1016/j.scitotenv.2010.04.033

Merel, S., Clement, M., Thomas, O. (2010b). State of the art on cyanotoxins in water and their behaviour towards chlorine. *Toxicon*, *55*(4), 677-691.

Merel, S., Walker, D., Chicana, R., Snyder, S., Baures, E., Thomas, O. (2013). State of knowledge and concerns on cyanobacterial blooms and cyanotoxins. *Environment International*, *59*, 303-327. https://doi.org/10.1016/j.envint.2013.06.013

Miao, H.F., Qin, F., Tao, G.J., Tao, W.Y., Ruan, W.Q. (2010). Detoxification and degradation of microcystin-LR and -RR by ozonation. *Chemosphere*, *79*(4), 355-361.

Mikula, P., Zezulka, S., Jancula, D., Marsalek, B. (2012). Metabolic activity and membrane integrity changes in Microcystis aeruginosa–new findings on hydrogen peroxide toxicity in cyanobacteria. *European Journal of Phycology*, *47*(3), 195-206.

Molica, R.J.R., Oliveira, E.J.A., Carvalho, P.V.V.C., Costa, A.N.S.F., Cunha, M.C.C., Melo, G.L., Azevedo, S.M.F.O. (2005). Occurrence of saxitoxins and an anatoxin-a(s)-like anticholinesterase in a Brazilian drinking water supply. *Harmful Algae*, *4*(4), 743-753. https://doi.org/10.1016/j.hal.2004.11.001

Molnar, C., Gair, J. (2015). Concepts of Biology: 1st Canadian Edition.

Moradinejad, S., Glover, C., Mailly, J., Zadfatollah-Seighalani, T., Peldszus, S., Barbeau, B., Dorner, S., Prévost, M., Zamyadi, A. (2019). Using advanced spectroscopy and organic matter characterization to evaluate the impact of oxidation on cyanobacteria. *Toxins*, *11*(5). https://doi.org/10.3390/toxins11050278

Moradinejad, S., Trigui, H., Guerra Maldonado, J.F., Shapiro, J., Terrat, Y., Zamyadi, A., Dorner, S., Prévost, M. (2020). Diversity Assessment of Toxic Cyanobacterial Blooms during Oxidation. *Toxins*, *12*(11), 728.

Munoz, G., Vo Duy, S., Roy-Lachapelle, A., Husk, B., Sauve, S. (2017). Analysis of individual and total microcystins in surface water by on-line preconcentration and desalting coupled to liquid chromatography tandem mass spectrometry. *Journal of Chromatography A*, *1516*, 9-20. https://doi.org/10.1016/j.chroma.2017.07.096

Naceradska, J., Pivokonsky, M., Pivokonska, L., Baresova, M., Henderson, R.K., Zamyadi, A., Janda, V. (2017). The impact of pre-oxidation with potassium permanganate on cyanobacterial organic matter removal by coagulation. *Water Research*, *114*, 42-49. https://doi.org/10.1016/j.watres.2017.02.029

Ndlela, L.L., Oberholster, P.J., Van Wyk, J., Cheng, P.H. (2016a). An overview of cyanobacterial bloom occurrences and research in Africa over the last decade. *Harmful Algae*, *60*, 11-26.

Ndlela, L.L., Oberholster, P.J., Van Wyk, J.H., Cheng, P.H. (2016b). An overview of cyanobacterial bloom occurrences and research in Africa over the last decade. *Harmful Algae*, *60*, 11-26. https://doi.org/10.1016/j.hal.2016.10.001

Ndong, M., Bird, D., Nguyen-Quang, T., de Boutray, M.L., Zamyadi, A., Vincon-Leite, B., Lemaire, B.J., Prevost, M., Dorner, S. (2014). Estimating the risk of cyanobacterial occurrence using an index integrating meteorological factors: Application to drinking water production. *Water Research*, *56*, 98-108. https://doi.org/10.1016/j.watres.2014.02.023

Newcombe, G., (2009) International guidance manual for the management of toxic cyanobacteria. Global Water Research Coalition and Water Quality Research Australia, London, United Kindgom, p. 44.

Newcombe, G., House, J., Ho, L., Baker, P., Burch, M., (2010) Management strategies for *cyanobacteria* (blue-green algae): a guide for water utilities. The Cooperative Research Centre for Water Quality and Treatment, Adelaïde, South Australia, p. 112.

Newcombe, G., Nicholson, B. (2004). Water treatment options for dissolved cyanotoxins. *Water Supply: Research and Technology-Aqua*, *53*(4), 227-239.

Newton, R.J., Jones, S.E., Eiler, A., McMahon, K.D., Bertilsson, S. (2011). A guide to the natural history of freshwater lake bacteria. *Microbiology and Molecular Biology Reviews*, *75*(1), 14-49.

Nicholson, B.C., Shaw, G.R., Morrall, J., Senogles, P.J., Woods, T.A., Papageorgiou, J., Kapralos, C., Wickramasinghe, W., Davis, B.C., Eaglesham, G.K., Moore, M.R. (2003). Chlorination for degrading saxitoxins (paralytic shellfish poisons) in water. *Environmental Technology*, *24*(11), 1341-1348.

Oksanen, J., Blanchet, F.G., Kindt, R., Legendre, P., Minchin, P.R., O'Hara, R., Simpson, G.L., Solymos, P., Stevens, M.H.H., Wagner, H., (2016) Package 'vegan': Community ecology package, p. 285.

Onstad, G.D., Strauch, S., Meriluoto, J., Codd, G.A., von Gunten, U. (2007). Selective oxidation of key functional groups in cyanotoxins during drinking water ozonation. *Environmental Science and Technology*, *41*(12), 4397-4404.

Ou, H., Gao, N., Wei, C., Deng, Y., Qiao, J. (2012). Immediate and long-term impacts of potassium permanganate on photosynthetic activity, survival and microcystin-LR release risk of *Microcystis aeruginosa*. *Journal of Hazardous Materials*, *219-220*, 267-275. https://doi.org/10.1016/j.jhazmat.2012.04.006

Overbeek, R., Olson, R., Pusch, G.D., Olsen, G.J., Davis, J.J., Disz, T., Edwards, R.A., Gerdes, S., Parrello, B., Shukla, M. (2014). The SEED and the Rapid Annotation of microbial genomes using Subsystems Technology (RAST). *Nucleic Acids Research*, *42*(D1), D206-D214.

Pacheco, A.B., Guedes, I.A., Azevedo, S.M. (2016). Is qPCR a reliable indicator of cyanotoxin risk in freshwater? *Toxins (Basel)*, *8*(6). https://doi.org/10.3390/toxins8060172

Paerl, H.W., Hall, N.S., Calandrino, E.S. (2011). Controlling harmful cyanobacterial blooms in a world experiencing anthropogenic and climatic-induced change. *Science of the Total Environment*, *409*(10), 1739-1745. https://doi.org/10.1016/j.scitotenv.2011.02.001

Paerl, H.W., Paul, V.J. (2012). Climate change: Links to global expansion of harmful cyanobacteria. *Water Research*, *46*(5), 1349-1363. https://doi.org/10.1016/j.watres.2011.08.002

Paine, E.C., Slonecker, E.T., Simon, N.S., Rosen, B.H., Resmini, R.G., Allen, D.W. (2018). Optical characterization of two cyanobacteria genera, Aphanizomenon and Microcystis, with hyperspectral microscopy. *Journal of Applied Remote Sensing, 12*(3), 036013.

Park, J., Kim, Y., Kim, M., Lee, W.H., Park, J., Kim, Y., Kim, M., Lee, W.H. (2018). A novel method for cell counting of Microcystis colonies in water resources using a digital imaging flow cytometer and microscope. *Environmental Engineering Research*, *24*(3), 397-403.

Pazouki, P., Prévost, M., McQuaid, N., Barbeau, B., de Boutray, M.-L., Zamyadi, A., Dorner, S. (2016). Breakthrough of cyanobacteria in bank filtration. *Water Research*, *102*, 170-179. https://doi.org/10.1016/j.watres.2016.06.037

Pearson, K. (1896). VII. Mathematical contributions to the theory of evolution.—III. Regression, heredity, and panmixia. *Philosophical Transactions of the Royal Society of London. Series A, containing papers of a mathematical or physical character*(187), 253-318.

Pei, H., Xu, H., Wang, J., Jin, Y., Xiao, H., Ma, C., Sun, J., Li, H. (2017). 16S rRNA Gene amplicon sequencing reveals significant changes in microbial compositions during cyanobacteria-laden drinking water sludge storage. *Environmental Science & Technology, 51*(21), 12774-12783. https://doi.org/10.1021/acs.est.7b03085

Pessi, I.S., Maalouf, P.D.C., Laughinghouse Iv, H.D., Baurain, D., Wilmotte, A. (2016). On the use of high-throughput sequencing for the study of cyanobacterial diversity in Antarctic aquatic mats. *Journal of Phycology, 52*(3), 356-368. https://doi.org/10.1111/jpy.12399

Pestana, C.J., Reeve, P.J., Sawade, E., Voldoire, C.F., Newton, K., Praptiwi, R., Collingnon, L., Dreyfus, J., Hobson, P., Gaget, V., Newcombe, G. (2016). Fate of cyanobacteria in drinking water treatment plant lagoon supernatant and sludge. *Science of the Total Environment*, *565*, 1192-1200. https://doi.org/10.1016/j.scitotenv.2016.05.173

Piezer, K., Li, L., Jeon, Y., Kadudula, A., Seo, Y. (2020). The Application of Potassium Permanganate to Treat Cyanobacteria-Laden Water. *Process Safety and Environmental Protection*.

Pivokonsky, M., Naceradska, J., Brabenec, T., Novotna, K., Baresova, M., Janda, V. (2015a). The impact of interactions between algal organic matter and humic substances on coagulation. *Water Research*, *84*, 278-285.

Pivokonsky, M., Naceradska, J., Kopecka, I., Baresova, M., Jefferson, B., Li, X., Henderson, R.K. (2015b). The impact of algogenic organic matter on water treatment plant operation and water quality: A review. *Critical Reviews in Environmental Science and Technology, 46*(4), 291-335. https://doi.org/10.1080/10643389.2015.1087369

Planas, C., Guadayol, J.M., Droguet, M., Escalas, A., Rivera, J., Caixach, J. (2002). Degradation of polyethoxylated nonylphenols in a sewage treatment plant. Quantitative analysis by isotopic dilution-HRGC/MS. *Water Research*, *36*(5), 982-988.

Planas, D., Desrosiers, M., Groulx, S.R., Paquet, S., Carignan, R. (2000). Pelagic and benthic algal responses in eastern Canadian Boreal Shield lakes following harvesting and wildfires. *Canadian Journal of Fisheries and Aquatic Sciences*, *57*, 136-145. https://doi.org/10.1139/cjfas-57-S2-136

Plummer, J., Edzwald, J.K. (2002). Effects of chlorine and ozone on algal cell properties and removal of algae by coagulation. *Journal of Water Supply: Research and Technology—AQUA*, *51*(6), 307-318.

Polek, B., Godočíková, J. (2012). The effect of some factors of polluted environment on catalase responses and resistance of microbial isolates against toxic oxidative stress. *Current Microbiology*, *65*(4), 345-349.

Qi, J., Lan, H., Miao, S., Xu, Q., Liu, R., Liu, H., Qu, J. (2016). KMnO4–Fe(II) pretreatment to enhance *Microcystis aeruginosa* removal by aluminum coagulation: Does it work after long distance transportation? *Water Research*, *88*, 127-134. https://doi.org/10.1016/j.watres.2015.10.004

Qian, F., Dixon, D.R., Newcombe, G., Ho, L., Dreyfus, J., Scales, P.J. (2014). The effect of pH on the release of metabolites by cyanobacteria in conventional water treatment processes. *Harmful Algae*, *39*(0), 253-258. https://doi.org/10.1016/j.hal.2014.08.006

Quince, C., Lanzén, A., Curtis, T.P., Davenport, R.J., Hall, N., Head, I.M., Read, L.F., Sloan, W.T. (2009). Accurate determination of microbial diversity from 454 pyrosequencing data. *Nature Methods*, *6*(9), 639-641.

Raes, J., Bork, P. (2008). Molecular eco-systems biology: towards an understanding of community function. *Nature Reviews Microbiology*, *6*(9), 693-699.

Raivo, K., (2019) Pheatmap: pretty Heatmaps. R package version 1.0.12.

Randolph, K., Wilson, J., Tedesco, L., Li, L., Pascual, D.L., Soyeux, E. (2008). Hyperspectral remote sensing of cyanobacteria in turbid productive water using optically active pigments, chlorophyll a and phycocyanin. *Remote Sensing of Environment*, *112*(11), 4009-4019.

Ranjan, R., Rani, A., Metwally, A., McGee, H.S., Perkins, D.L. (2016). Analysis of the microbiome: Advantages of whole genome shotgun versus 16S amplicon sequencing. *Biochemical and biophysical research communications*, *469*(4), 967-977.

Rapala, J., Robertson, A., Negri, A.P., Berg, K.A., Tuomi, P., Lyra, C., Erkomaa, K., Lahti, K., Hoppu, K., Lepistö, L. (2005). First report of saxitoxin in Finnish lakes and possible associated effects on human health. *Environmental Toxicology*, *20*(3), 331-340. https://doi.org/10.1002/tox.20109

Rinta-Kanto, J.M., Konopko, E.A., DeBruyn, J.M., Bourbonniere, R.A., Boyer, G.L., Wilhelm, S.W. (2009). Lake Erie Microcystis: Relationship between microcystin production, dynamics of genotypes and environmental parameters in a large lake. *Harmful Algae*, *8*(5), 665-673. https://doi.org/10.1016/j.hal.2008.12.004

Rodriguez, E., Majado, M.E., Meriluoto, J., Acero, J.L. (2007a). Oxidation of microcystins by permanganate: reaction kinetics and implications for water treatment. *Water Research*, *41*(1), 102-110.

Rodriguez, E., Onstad, G.D., Kull, T.P.J., Metcalf, J.S., Acero, J.L., von Gunten, U. (2007b). Oxidative elimination of cyanotoxins: comparison of ozone, chlorine, chlorine dioxide and permanganate. *Water Research*, *41*(15), 3381-3393.

Rodriguez, E., Sordo, A., Metcalf, J.S., Acero, J.L. (2007c). Kinetics of the oxidation of cylindrospermopsin and anatoxin-a with chlorine, monochloramine and permanganate. *Water Research*, *41*(9), 2048-2056.

Rositano, J., Newcombe, G., Nicholson, B., Sztajnbok, P. (2001). Ozonation of NOM and algal toxins in four treated waters. *Water Research*, *35*(1), 23-32.

Roy-Lachapelle, A., Duy, S.V., Munoz, G., Dinh, Q.T., Bahl, E., Simon, D.F., Sauvé, S. (2019). Analysis of multiclass cyanotoxins (microcystins, anabaenopeptins, cylindrospermopsin and anatoxins) in lake waters using on-line SPE liquid chromatography high-resolution Orbitrap mass spectrometry. *Analytical Methods*. https://doi.org/10.1039/c9ay01132c

Sabart, M., Crenn, K., Perrière, F., Abila, A., Leremboure, M., Colombet, J., Jousse, C., Latour, D. (2015). Co-occurrence of microcystin and anatoxin-a in the freshwater lake Aydat (France): Analytical and molecular approaches during a three-year survey. *Harmful Algae*, *48*, 12-20. https://doi.org/10.1016/j.hal.2015.06.007

Scherer, P.I., Millard, A.D., Miller, A., Schoen, R., Raeder, U., Geist, J., Zwirglmaier, K. (2017). Temporal dynamics of the microbial community composition with a focus on toxic cyanobacteria and toxin presence during harmful algal blooms in two South German lakes. *Frontiers in Microbiology*, *8*, 2387. https://doi.org/10.3389/fmicb.2017.02387

Schindler, D.W., Hecky, R.E., McCullough, G.K. (2012). The rapid eutrophication of Lake Winnipeg: Greening under global change. *Journal of Great Lakes Research*, *38*(Supplement 3), 6-13. https://doi.org/10.1016/j.jglr.2012.04.003

Senogles, P., Shaw, G., Smith, M., Norris, R., Chiswell, R., Mueller, J., Sadler, R., Eaglesham, G. (2000). Degradation of the cyanobacterial toxin cylindrospermopsin, from Cylindrospermopsis raciborskii, by chlorination. *Toxicon*, *38*(9), 1203-1213.

Senogles, P., Smith, M., Shaw, G. (2002). *Physical, chemical and biological methods for the degradation of the Cyanobacterial toxin, Cylindrospermopsin*. American Water Works Association-Water Quality Technology Conference Seattle, Washington, USA (pp. 14).

Senogles-Derham, P.-J., Seawright, A., Shaw, G., Wickramisingh, W., Shahin, M. (2003). Toxicological aspects of treatment to remove cyanobacterial toxins from drinking water determined using the heterozygous P53 transgenic mouse model. *Toxicon*, *41*(8), 979-988.

Sharma, N., Kumar, J., Abedin, M.M., Sahoo, D., Pandey, A., Rai, A.K., Singh, S.P. (2020). Metagenomics revealing molecular profiling of community structure and metabolic pathways in natural hot springs of the Sikkim Himalaya. *BMC Microbiology*, *20*(1), 1-17.

Shi, L., Cai, Y., Li, P., Yang, H., Liu, Z., Kong, L., Yu, Y., Kong, F. (2009). Molecular identification of the colony-associated cultivable bacteria of the cyanobacterium *Microcystis aeruginosa* and their effects on algal growth. *Journal of Freshwater Ecology*, *24*(2), 211-218. https://doi.org/10.1080/02705060.2009.9664285

Shi, L., Huang, Y., Zhang, M., Yu, Y., Lu, Y., Kong, F. (2017). Bacterial community dynamics and functional variation during the long-term decomposition of cyanobacterial blooms in-vitro. *Science of the Total Environment*, *598*, 77-86.

Shilei, Z., Yue, S., Tinglin, H., Ya, C., Xiao, Y., Zizhen, Z., Yang, L., Zaixing, L., Jiansheng, C., Xiao, L. (2020). Reservoir water stratification and mixing affects microbial community

structure and functional community composition in a stratified drinking reservoir. *Journal of Environmental Management*, *267*, 110456.

Šimek, K., Horňák, K., Jezbera, J., Nedoma, J., Vrba, J., Straškrábová, V., Macek, M., Dolan, J.R., Hahn, M.W. (2006). Maximum growth rates and possible life strategies of different bacterioplankton groups in relation to phosphorus availability in a freshwater reservoir. *Environmental Microbiology*, *8*(9), 1613-1624.

Simis, S.G., Peters, S.W.M., Gons, H.J. (2005). Remote sensing of the cyanobacterial pigment phycocyanin in turbid inland water. *Limnology and Oceanography*, *50*(1), 237-245.

Song, H.-K., Song, W., Kim, M., Tripathi, B.M., Kim, H., Jablonski, P., Adams, J.M. (2017). Bacterial strategies along nutrient and time gradients, revealed by metagenomic analysis of laboratory microcosms. *FEMS Microbiology Ecology*, *93*(10), fix114.

Sorlini, S., Gialdini, F., Collivignarelli, C. (2013). Removal of cyanobacterial cells and Microcystin-LR from drinking water using a hollow fiber microfiltration pilot plant. *Desalination*, *309*, 106-112. https://doi.org/https://doi.org/10.1016/j.desal.2012.09.028

Srivastava, A., Summers, M.L., Sobotka, R. (2020). Cyanobacterial sigma factors: Current and future applications for biotechnological advances. *Biotechnology Advances*, *40*, 107517.

Stanier, R.Y., Cohen-Bazire, G. (1977). Phototrophic prokaryotes: the cyanobacteria. *Annual Review of Microbiology*, *31*(1), 225-274.

Taton, A., Erikson, C., Yang, Y., Rubin, B.E., Rifkin, S.A., Golden, J.W., Golden, S.S. (2020). The circadian clock and darkness control natural competence in cyanobacteria. *Nature communications*, *11*(1), 1688. https://doi.org/10.1038/s41467-020-15384-9

Tatusov, R.L., Galperin, M.Y., Natale, D.A., Koonin, E.V. (2000). The COG database: a tool for genome-scale analysis of protein functions and evolution. *Nucleic Acids Research*, *28*(1), 33-36.

Teixeira, M.R., Sousa, V., Rosa, M.J. (2010). Investigating dissolved air flotation performance with cyanobacterial cells and filaments. *Water Research*, *44*(11), 3337-3344. https://doi.org/https://doi.org/10.1016/j.watres.2010.03.012

Théoret, T., Wilkinson, K.J. (2017). Evaluation of enhanced darkfield microscopy and hyperspectral analysis to analyse the fate of silver nanoparticles in wastewaters. *Analytical Methods*, *9*(26), 3920-3928.

Theruvathu, J.A., Flyunt, R., Aravindakumar, C.T., von Sonntag, C. (2001). Rate constants of ozone reactions with DNA, its constituents and related compounds. *Journal of the Chemical Society, Perkin Transactions 2*(3), 269-274.

Tromas, N., Fortin, N., Bedrani, L., Terrat, Y., Cardoso, P., Bird, D., Greer, C.W., Shapiro, B.J. (2017). Characterising and predicting cyanobacterial blooms in an 8-year amplicon sequencing time course. *ISME Journal*, *11*(8), 1746-1763. https://doi.org/10.1038/ismej.2017.58

United States Environmental Protection Agency (USEPA), (2003) Technologies and costs for control of microbial contaminants and disinfection byproducts. The Cadmus Group, Inc. and Malcolm Pirnie, Inc, Washington, DC, USA, p. 235.

United States Environmental Protection Agency (USEPA), (2009) Federal Register. Drinking water contaminant candidate list 3 (Final), Washington, DC, USA.

United States Environmental Protection Agency (USEPA), (2015) Recommendations for public water systems to manage cyanotoxins in drinking water, p. 70.

Vadde, K.K., Feng, Q., Wang, J., McCarthy, A.J., Sekar, R. (2019). Next-generation sequencing reveals fecal contamination and potentially pathogenic bacteria in a major inflow river of Taihu Lake. *Environmental Pollution*, *254*, 113108. https://doi.org/10.1016/j.envpol.2019.113108

Van Wichelen, J., Vanormelingen, P., Codd, G.A., Vyverman, W. (2016). The common bloom-forming cyanobacterium Microcystis is prone to a wide array of microbial antagonists. *Harmful Algae*, *55*, 97-111. https://doi.org/https://doi.org/10.1016/j.hal.2016.02.009

Vézie, C., Rapala, J., Vaitomaa, J., Seitsonen, J., Sivonen, K. (2002). Effect of nitrogen and phosphorus on growth of toxic and nontoxic Microcystis strains and on intracellular microcystin concentrations. *Microbial Ecology*, *43*(4), 443-454. https://doi.org/10.1007/s00248-001-0041-9

Villacorte, L.O., Ekowati, Y., Neu, T.R., Kleijn, J.M., Winters, H., Amy, G., Schippers, J.C., Kennedy, M.D. (2015). Characterisation of algal organic matter produced by bloom-forming marine and freshwater algae. *Water Research*, *73*, 216-230.

Vincent, R.K., Qin, X., McKay, R.M.L., Miner, J., Czajkowski, K., Savino, J., Bridgeman, T. (2004). Phycocyanin detection from LANDSAT TM data for mapping cyanobacterial blooms in Lake Erie. *Remote Sensing of Environment*, *89*(3), 381-392.

Vlad, S., Anderson, W.B., Peldszus, S., Huck, P.M. (2014). Removal of the cyanotoxin anatoxin-a by drinking water treatment processes: A review. *Journal of Water and Health*, *12*(4), 601-617. https://doi.org/10.2166/wh.2014.018

Wacklin, P., Hoffmann, L., Komárek, J. (2009). Nomenclatural validation of the genetically revised cyanobacterial genus Dolichospermum (Ralfs ex Bornet et Flahault) comb. nova. *Fottea*, *9*(1), 59-64. https://doi.org/10.5507/fot.2009.005

Wagner, J.R., Cadet, J. (2010). Oxidation reactions of cytosine DNA components by hydroxyl radical and one-electron oxidants in aerated aqueous solutions. *Accounts of chemical research*, *43*(4), 564-571.

Walter, J.M., Lopes, F.A.C., Lopes-Ferreira, M., Vidal, L.M., Leomil, L., Melo, F., de Azevedo, G.S., Oliveira, R., Medeiros, A.J., Melo, A.S.O. (2018). Occurrence of harmful cyanobacteria in drinking water from a severely drought-impacted semi-arid region. *Frontiers in Microbiology*, *9*, 176.

Wang, H., Ho, L., Lewis, D.M., Brookes, J.D., Newcombe, G. (2007). Discriminating and assessing adsorption and biodegradation removal mechanisms during granular activated carbon filtration of microcystin toxins. *Water Research*, *41*(18), 4262-4270. https://doi.org/10.1016/j.watres.2007.05.057

Wang, K., Mao, H., Li, X. (2018). Functional characteristics and influence factors of microbial community in sewage sludge composting with inorganic bulking agent. *Bioresource Technology*, *249*, 527-535.

Watson, S.B. (2004). Aquatic taste and odor: a primary signal of drinking-water integrity. *Journal of Toxicology and Environmental Health, Part A*, *67*(20-22), 1779-1795.

Wells, M.L., Trainer, V.L., Smayda, T.J., Karlson, B.S.O., Trick, C.G., Kudela, R.M., Ishikawa, A., Bernard, S., Wulff, A., Anderson, D.M., Cochlan, W.P. (2015). Harmful algal blooms and climate change: Learning from the past and present to forecast the future. *Harmful Algae*, *49*, 68-93. https://doi.org/10.1016/j.hal.2015.07.009

Wert, E.C., Dong, M.M., Rosario-Ortiz, F.L. (2013). Using digital flow cytometry to assess the degradation of three cyanobacteria species after oxidation processes. *Water Research*, *47*(11), 3752-3761. https://doi.org/10.1016/j.watres.2013.04.038

Wert, E.C., Korak, J.A., Trenholm, R.A., Rosario-Ortiz, F.L. (2014). Effect of oxidant exposure on the release of intracellular microcystin, MIB, and geosmin from three cyanobacteria species. *Water Res*, *52*, 251-259. https://doi.org/10.1016/j.watres.2013.11.001

Westrick, J.A., Szlag, D.C., Southwell, B.J., Sinclair, J. (2010). A review of cyanobacteria and cyanotoxins removal/inactivation in drinking water treatment. *Analytical and Bioanalytical Chemistry*, *397*(5), 1705-1714. https://doi.org/10.1007/s00216-010-3709-5

Willis, A., Woodhouse, J.N. (2020). Defining Cyanobacterial Species: Diversity and Description Through Genomics. *Critical Reviews in Plant Sciences*, 1-24.

Wood, S.A., Rueckert, A., Hamilton, D.P., Cary, S.C., Dietrich, D.R. (2011). Switching toxin production on and off: intermittent microcystin synthesis in a Microcystis bloom. *Environmental Microbiology Reports*, *3*(1), 118-124. https://doi.org/10.1111/j.1758-2229.2010.00196.x

Woodhouse, J.N., Kinsela, A.S., Collins, R.N., Bowling, L.C., Honeyman, G.L., Holliday, J.K., Neilan, B.A. (2015). Microbial communities reflect temporal changes in cyanobacterial composition in a shallow ephemeral freshwater lake. *The ISME Journal*, *10*, 1337. Original Article. https://doi.org/10.1038/ismej.2015.218

Wright, S.J.L., Thompson, R.J. (1985). Bacillus volatiles antagonize cyanobacteria. *FEMS microbiology letters*, *30*(3), 263-267.

Xagoraraki, I., Zulliger, K., Harrington, G.W., Zeier, B., Krick, W., Karner, D.A. (2005). CT values required for degradation of microcystin-LR by free chlorine. *Water Supply: Research and Technology-Aqua*, *55*(4), 233-245.

Xiao, X., Sogge, H., Lagesen, K., Tooming-Klunderud, A., Jakobsen, K.S., Rohrlack, T. (2014). Use of high throughput sequencing and light microscopy show contrasting results in a study of phytoplankton occurrence in a freshwater environment. *PLoS ONE*, *9*(8), e106510.

Xie, P., Chen, Y., Ma, J., Zhang, X., Zou, J., Wang, Z. (2016). A mini review of preoxidation to improve coagulation. *Chemosphere*, *155*, 550-563. https://doi.org/10.1016/j.chemosphere.2016.04.003

Xie, P., Ma, J., Fang, J., Guan, Y., Yue, S., Li, X., Chen, L. (2013). Comparison of permanganate preoxidation and preozonation on algae containing water: Cell integrity, characteristics, and chlorinated disinfection byproduct formation. *Environmental & Science Technology*, *47*(24), 14051-14061. https://doi.org/10.1021/es4027024

Xing, W., Xie, L.-r., Zeng, X., Yang, Y., Zhang, C.-C. (2020). Functional Dissection of Genes Encoding DNA Polymerases Based on Conditional Mutants in the Heterocyst-Forming Cyanobacterium Anabaena PCC 7120. *Frontiers in Microbiology*, *11*, 1108.

Xu, H., Pei, H., Jin, Y., Ma, C., Wang, Y., Sun, J., Li, H. (2018). High-throughput sequencing reveals microbial communities in drinking water treatment sludge from six geographically distributed plants, including potentially toxic cyanobacteria and pathogens. *Science of the Total Environment*, *634*, 769-779. https://doi.org/10.1016/j.scitotenv.2018.04.008

Yan, B., Cai, J., Ma, R., Gao, J., Liu, Y., Chen, T., Bao, F. (2012). Modified Macroporous Polystyrene Matrices as Highly Efficient Adsorption Material for Cyanobacteria Control. *Polymer-Plastics Technology and Engineering*, *51*(14), 1451-1459. https://doi.org/10.1080/03602559.2012.709298

Yan, S., Jia, A., Merel, S., Snyder, S.A., O'Shea, K.E., Dionysiou, D.D., Song, W. (2016). Ozonation of cylindrospermopsin (cyanotoxin): Degradation mechanisms and cytotoxicity assessments. *Environmental Science & Technology*, *50*(3), 1437-1446. https://doi.org/10.1021/acs.est.5b04540

Yang, Q., Xu, J., Qian, X., Zhang, K., Lei, X. (2006). Eliminating nucleic acids contaminants by hydrogen peroxide-induced free radicals during the preparation of proteins. *Biochemical Engineering Journal*, *29*(1-2), 23-26.

Yao, W., Qu, Q., von Gunten, U., Chen, C., Yu, G., Wang, Y. (2017). Comparison of methylisoborneol and geosmin abatement in surface water by conventional ozonation and an electro-peroxone process. *Water Research*, *108*, 373-382. https://doi.org/10.1016/j.watres.2016.11.014

Yilmaz, M., Phlips, E.J. (2011). Diversity of and selection acting on cylindrospermopsin cyrB gene adenylation domain sequences in Florida. *Applied and Environmental Microbiology*, *77*(7), 2502-2507. https://doi.org/10.1128/AEM.02252-10

Zambrano, M.M., Siegele, D.A., Almiron, M., Tormo, A., Kolter, R. (1993). Microbial competition: Escherichia coli mutants that take over stationary phase cultures. *Science*, *259*(5102), 1757-1760.

Zamyadi, A. (2011). *The value of in vivo monitoring and chlorination for the control of toxic Cyanobacteria in drinking water production* [Ph.D., Ecole Polytechnique de Montréal].

Zamyadi, A. (2014). Emerging toxic cyanobacterial issues in freshwater sources: influence of climate change. *Seafood and Freshwater Toxins: Pharmacology, Physiology, and Detection*, 105.

Zamyadi, A., Choo, F., Newcombe, G., Stuetz, R., Henderson, R.K. (2016a). A review of monitoring technologies for real-time management of cyanobacteria: Recent advances and future direction. *TrAC Trends in Analytical Chemistry*, *85*, 83-96. https://doi.org/10.1016/j.trac.2016.06.023

Zamyadi, A., Coral, L.A., Barbeau, B., Dorner, S., Lapolli, F.R., Prévost, M. (2015a). Fate of toxic cyanobacterial genera from natural bloom events during ozonation. *Water Research*, *73*, 204-215. https://doi.org/10.1016/j.watres.2015.01.029

Zamyadi, A., Coral, L.A., Barbeau, B., Prévost, M. (2013a). *Pre-ozonation a solution to prevent toxic cyanobacteria cell breakthrough into water treatment plants*. American Water Works Association-Water Quality Technology Conference and Exposition (WQTC), Long Beach, CA, USA (pp. 22).

Zamyadi, A., Dorner, S., Ellis, D., Bolduc, A., Bastien, C., Prévost, M. (2013b). Species-dependence of *cyanobacteria* removal efficiency by different drinking water treatment processes. *Water Research*, *47*(8), 2689–2700. https://doi.org/10.1016/j.watres.2013.02.040

Zamyadi, A., Dorner, S., Ndong, M., Ellis, D., Bolduc, A., Bastien, C., Prévost, M. (2013c). Low-risk cyanobacterial bloom sources: Cell accumulation within full-scale treatment plants. *Journal American Water Works Association*, *102*(11), E651-E663. https://doi.org/10.5942/jawwa.2013.105.0141

Zamyadi, A., Fan, Y., Daly, R.I., Prévost, M. (2013d). Chlorination of *Microcystis aeruginosa*: Toxin release and oxidation, cellular chlorine demand and disinfection by-products formation. *Water Research*, *47*(3), 1080–1090. https://doi.org/10.1016/j.watres.2012.11.031

Zamyadi, A., Greenstein, K.E., Glover, C.M., Adams, C., Rosenfeldt, E., Wert, E.C. (2020). Impact of hydrogen peroxide and copper sulfate on the delayed release of microcystin. *Water*, *12*(4), 1105. https://doi.org/10.3390/w12041105

Zamyadi, A., Henderson, R., Stuetz, R., Hofmann, R., Ho, L., Newcombe, G. (2015b). Fate of geosmin and 2-methylisoborneol in full-scale water treatment plants. *Water Research*, *83*, 171-183. https://doi.org/10.1016/j.watres.2015.06.038

Zamyadi, A., Henderson, R.K., Stuetz, R., Newcombe, G., Newtown, K., Gladman, B. (2016b). Cyanobacterial management in full-scale water treatment and recycling processes: Reactive dosing following intensive monitoring. *Environmental Science: Water Research & Technology*, *2*(2), 362-375. 10.1039/C5EW00269A. https://doi.org/10.1039/C5EW00269A

Zamyadi, A., Ho, L., Newcombe, G., Bustamante, H., Prévost, M. (2012a). Fate of toxic cyanobacterial cells and disinfection by-products formation after chlorination. *Water Research*, *46*(5), 1524 -1535. https://doi.org/10.1016/j.watres.2011.06.029

Zamyadi, A., Ho, L., Newcombe, G., Daly, R.I., Burch, M., Baker, P., Prévost, M. (2010a). Release and oxidation of cell-bound saxitoxins during chlorination of *Anabaena circinalis* cells. *Environmental Science and Technology*, *44*(23), 9055-9061. https://doi.org/10.1021/es102130b

Zamyadi, A., MacLeod, S., Fan, Y., McQuaid, N., Dorner, S., Sauvé, S., Prévost, M. (2012b). Toxic cyanobacterial breakthrough and accumulation in a drinking water plant: A monitoring and treatment challenge. *Water Research*, *46*(5), 1511-1523. https://doi.org/10.1016/j.watres.2011.11.012

Zamyadi, A., Romanis, C., Mills, T., Neilan, B., Choo, F., Coral, L.A., Gale, D., Newcombe, G., Crosbie, N., Stuetz, R., Henderson, R.K. (2019). Diagnosing water treatment critical control points for cyanobacterial removal: Exploring benefits of combined microscopy, next-

generation sequencing, and cell integrity methods. *Water Research, 152*, 96-105. https://doi.org/10.1016/j.watres.2019.01.002

Zamyadi, A., Wang, Y., Fan, Y., Newcombe, G., Ho, L., Prévost, M. (2010b, Oct 30-Nov 2). *Chlorination as a barrier against toxic cyanobacterial breakthrough: Validation of laboratory findings in a drinking water treatment plant*. 14th Canadian National Conference and 5th Policy Forum on Drinking Water, Saskatoon, SK, Canada (pp. 22).

Zhang, C.C., Laurent, S., Sakr, S., Peng, L., Bédu, S. (2006). Heterocyst differentiation and pattern formation in cyanobacteria: a chorus of signals. *Molecular Microbiology*, *59*(2), 367-375.

Zhang, H., Dan, Y., Adams, C.D., Shi, H., Ma, Y., Eichholz, T. (2017). Effect of oxidant demand on the release and degradation of microcystin-LR from *Microcystis aeruginosa* during oxidation. *Chemosphere*, *181*, 562-568. https://doi.org/10.1016/j.chemosphere.2017.04.120

Zhang, S., Lin, T., Chen, H., Chen, W., Xu, H., Tao, H. (2020). DNA pyrimidine bases in water: Insights into relative reactivity, byproducts formation and combined toxicity during chlorination. *Science of the Total Environment*, *717*, 137205.

Zhang, X.-j., Chen, C., Ding, J.-q., Hou, A., Li, Y., Niu, Z.-b., Su, X.-y., Xu, Y.-j., Laws, E.A. (2010). The 2007 water crisis in Wuxi, China: analysis of the origin. *Journal of Hazardous Materials*, *182*(1-3), 130-135.

Zhang, X.-W., Fu, J., Song, S., Zhang, P., Yang, X.-H., Zhang, L.-R., Luo, Y., Liu, C.-H., Zhu, H.-L. (2014). Interspecific competition between *Microcystis aeruginosa* and *Anabaena* flos-aquae from Taihu Lake, China. *Zeitschrift für Naturforschung C*, *69*(1-2), 53-60. https://doi.org/10.5560/ZNC.2012-0155

Zhang, Y., Shao, Y., Gao, N., Chu, W., Sun, Z. (2016). Removal of microcystin-LR by free chlorine: Identify of transformation products and disinfection by-products formation. *Chemical Engineering Journal*, *287*, 189-195. https://doi.org/10.1016/j.cej.2015.10.111

Zhaxybayeva, O., Gogarten, J.P., Charlebois, R.L., Doolittle, W.F., Papke, R.T. (2006). Phylogenetic analyses of cyanobacterial genomes: quantification of horizontal gene transfer events. *Genome Research*, *16*(9), 1099-1108.

Zhou, S., Shao, Y., Gao, N., Deng, Y., Qiao, J., Ou, H., Deng, J. (2013). Effects of different algaecides on the photosynthetic capacity, cell integrity and microcystin-LR release of *Microcystis aeruginosa*. *Science of the Total Environment*, *463*, 111-119. https://doi.org/10.1016/j.scitotenv.2013.05.064

Zhou, S., Sun, Y., Yu, M., Shi, Z., Zhang, H., Peng, R., Li, Z., Cui, J., Luo, X. (2020). Linking Shifts in Bacterial Community Composition and Function with Changes in the Dissolved Organic Matter Pool in Ice-Covered Baiyangdian Lake, Northern China. *Microorganisms*, *8*(6), 883.

Zhu, L., Zuo, J., Song, L., Gan, N. (2016). Microcystin-degrading bacteria affect *mcyD* expression and microcystin synthesis in *Microcystis* spp. *Journal of Environmental Sciences*, *41*, 195-201. https://doi.org/10.1016/j.jes.2015.06.016

APPENDICES

Appendix A SUPPLEMENTARY INFORMATION, ARTICLE 1

Journal: *Toxins*

Title: Using advanced spectroscopy and organic matter characterization to evaluate the impact of oxidation on cyanobacteria

Authors: Saber Moradinejad, Caitlin M. Glover, Jacinthe Mailly, Tahere Zadfathollah Seighalani, Sigrid Peldszus, Benoit Barbeau, Sarah Dorner, Michèle Prévost, Arash Zamyadi

Table A.1 First-order decay rates for chlorination and resulting CT

Oxidant dose and contact time		k (min^{-1})	R^2	CT (mg-min/L)
Chlorine	1 mg/L, 10 min	1.43×10^{-5}	0.98	5.2
	1 mg/L, 20 min	1.36×10^{-5}	0.99	6.9
	2 mg/L, 10 min	1.18×10^{-5}	0.95	11.7
	2 mg/L, 20 min	7.1×10^{-3}	0.98	21.4
	2 mg/L, 30 min	6.7×10^{-3}	0.99	21.7
	3 mg/L, 10 min	6.8×10^{-3}	0.92	25.9
	3 mg/L, 20 min	6.3×10^{-3}	0.98	35.9
	3 mg/L, 30 min	7.0×10^{-3}	0.94	37.5
Ozone	2 mg/L, 5 min	8.64×10^{-3}	0.84	2.94
	2 mg/L, 10 min	1.70×10^{-3}	0.94	2.15
$KMnO_4$	2 mg/L, 120 min	9.89×10^{-5}	0.98	172
	5 mg/L, 120 min	7.99×10^{-5}	0.98	456
H_2O_2	5 mg/L, 6 hr	8.29×10^{-5}	0.95	837
	10 mg/L, 6 hr	5.17×10^{-5}	0.99	2168

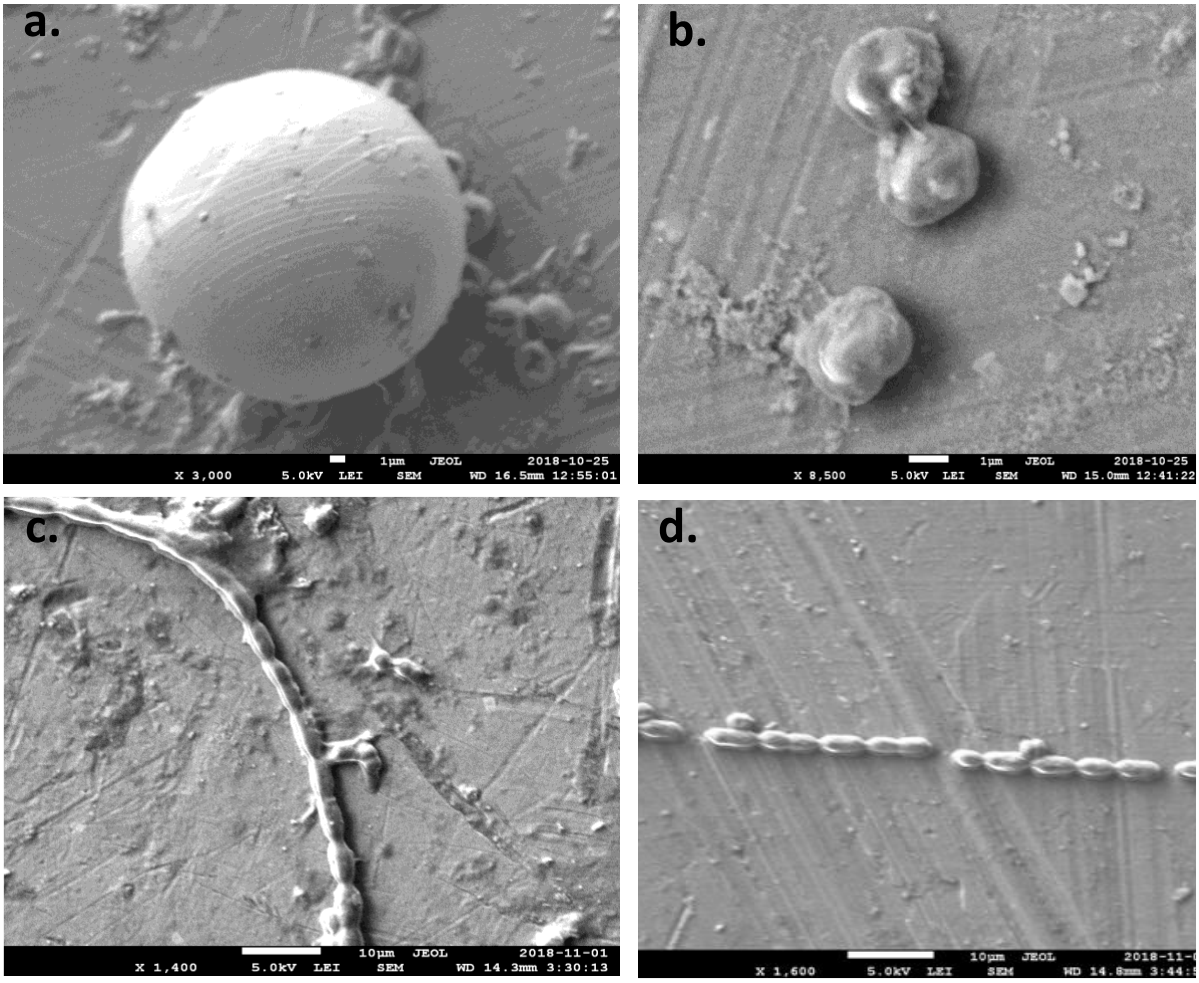

Figure A.1 SEM images of the cyanobacteria morphology both before and after chlorination (CT of 37.5 mg-min/L): a) *Microcystis* in control (3000X) b) chlorinated *Microcystis* cells (8500X), c) *Dolichospermum* cells in control (1400X), and d) chlorinated *Dolichospermum* cell (1600X).

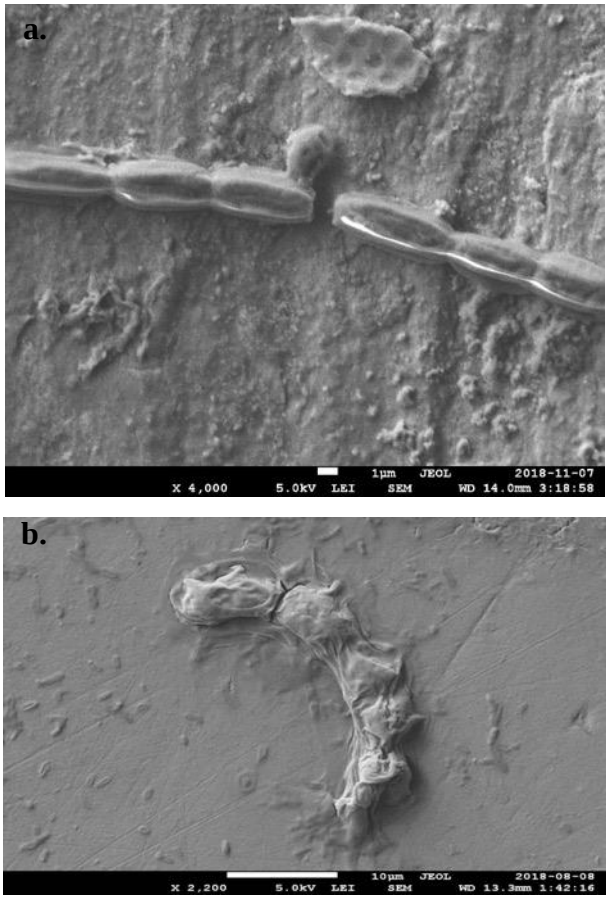

Figure A.2 SEM image of cyanobacteria after a) ozonation of both *Microcystis* and *Dolichospermum* (0.5 mg/L, 5 min exposure at 4,000X) and b) hydrogen peroxide application on *Dolichospermum* (837 mg-min/L at 2,200X)

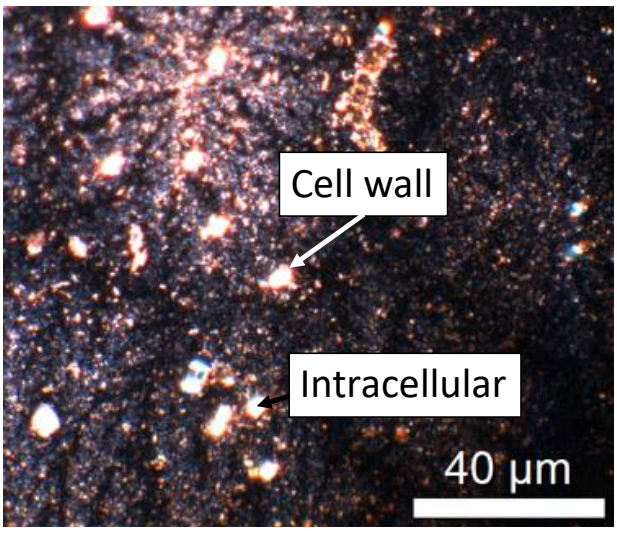

Figure A.3 EDM image of un-oxidized *Microcystis* with cell wall and intracellular material identified

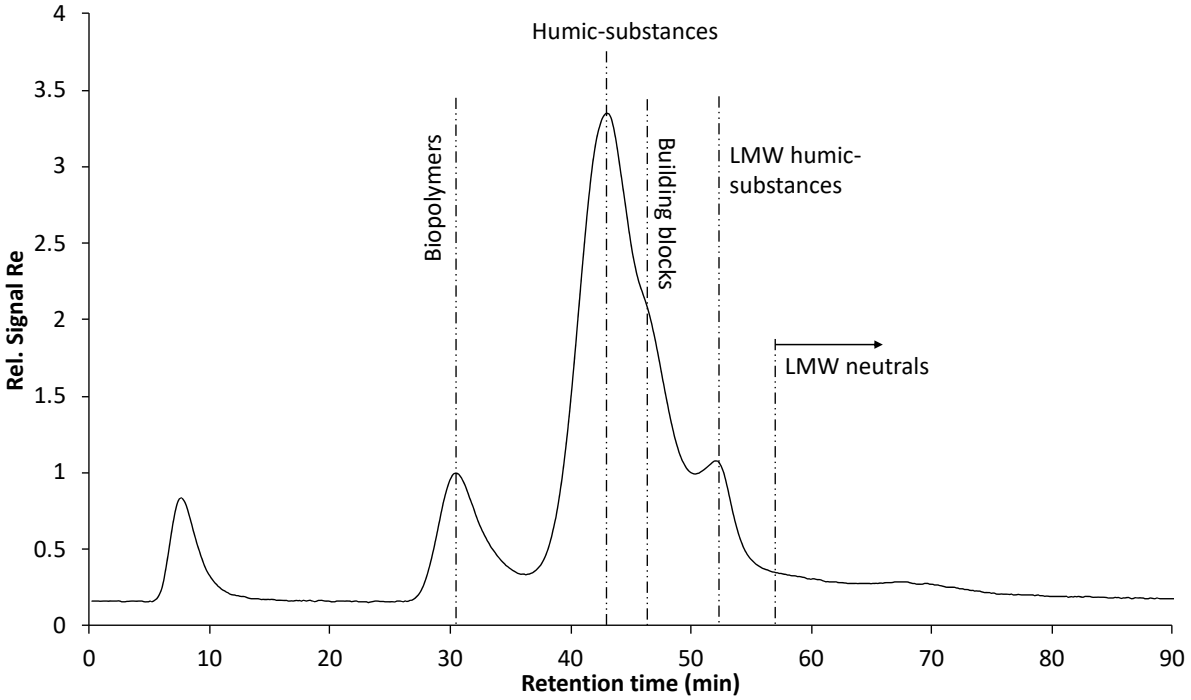

Figure A.4 LC-OCD chromatogram of the un-oxidized control cyanobacteria sample. The water was filtered (0.45 μm) *Microcystis* and *Dolichospermum* spiked into Lake Champlain water

Table A.2 Impact of oxidation on organic carbon fractions with LC-OCD-OND-UVD

	Concentration (µg C/L)					
	Total DOC	**Bio-polymer**	**Humic-substances**	Building blocks	LMW acids	LMW neutrals
Chlorine control	5184	556	2677	757	145	411
Chlorine (3 mg/L, 30 min)	5216	583	2583	866	145	496
Ozone control	5632	402	3335	706	131	481
Ozone (2 mg/L, 10 min)	6382	547	3440	810	167	630
$KMnO_4$ and H_2O_2 control	6134	383	3146	884	140	796
KMnO4 (5 mg/L, 120 min)	5533	271	3131	735	131	448
H_2O_2 (5 mg/L, 6 hr)	5913	380	3308	825	114	565

Table A.3 Cont. Impact of oxidation on organic carbon fractions with LC-OCD-OND-UVD

	Bio-polymer DON (µg N/L)	**Bio-polymer N/C (µg/µg)**	**Humic-substances DON (µg N/L)**	**Humic-substance N/C (µg/µg)**	**Humic-substances SUVA (L $mg^{-1}m^{-1}$)**	**Humic-substances Molecular Weight (M_n-g/mol)**
Chlorine control	61	0.11	147	0.05	3.93	624
Chlorine (3 mg/L, 30 min)	47	0.08	133	0.05	3.25	626
Ozone control	56	0.14	136	0.04	3.99	626
Ozone (2 mg/L, 10 min)	216	0.40	140	0.04	2.84	583
$KMnO_4$ and H_2O_2 control	13	0.03	108	0.03	4.45	701
KMnO4 (5 mg/L, 120 min)	21	0.09	101	0.03	3.93	638
H_2O_2 (5 mg/L, 6 hr)	54	0.14	121	0.04	4.34	570

LMW = low molecular weight. Building blocks = low molecular weight humic-like substances. Biopolymer = high molecular weight (> 10 kDa) polysaccharides, proteins, amino-acids, and other components in extracellular polymeric substances

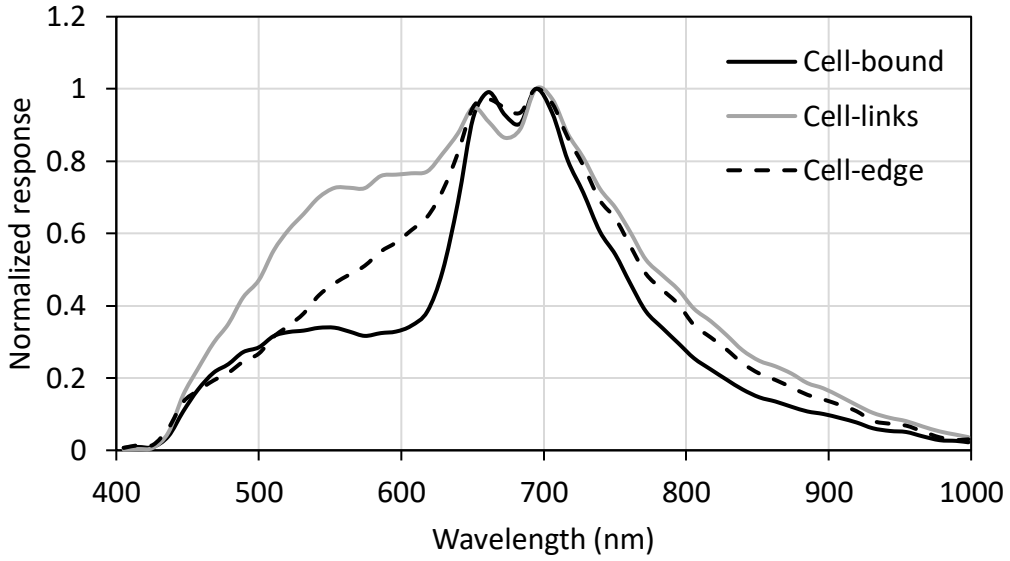

Figure A.5 HSI responses of cell-bound, cell-wall, and cell-links for *Dolichospermum*. Instrument responses were normalized to the maximum value of each spectra for comparison

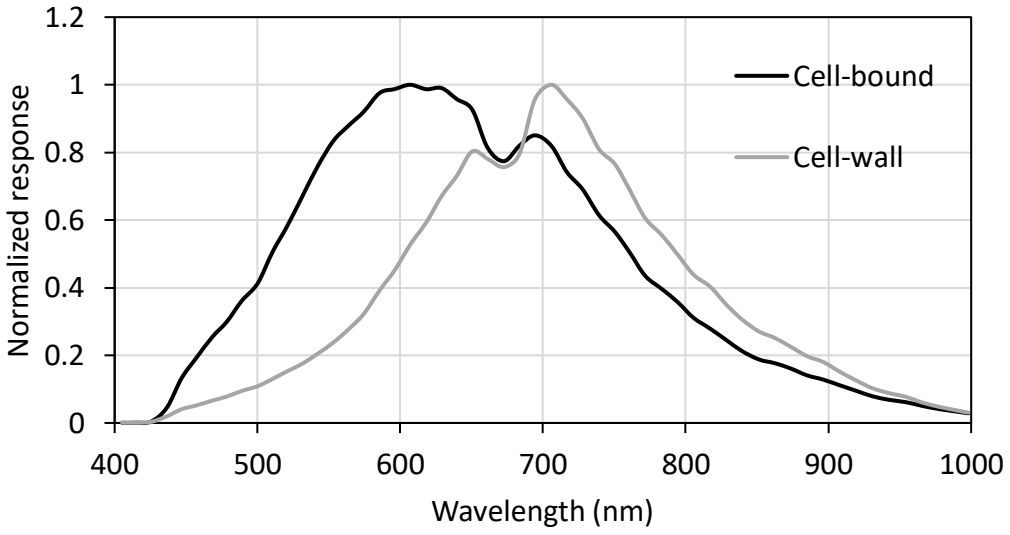

Figure A.6 HSI responses of cell-bound and cell-wall for *Microcystis*. Instrument responses were normalized to the maximum value of each spectra for comparison

Appendix B SUPPLEMENTARY INFORMATION, ARTICLE 2

Journal: *Toxins*

Title: Diversity assessment of the toxic cyanobacterial bloom during oxidation

Authors: Saber Moradinejad, Hana Trigui, Juan Francisco Guerra Maldonado, Jesse Shapiro, Yves Terrat, Arash Zamyadi, Sarah Dorner, Michèle Prévost

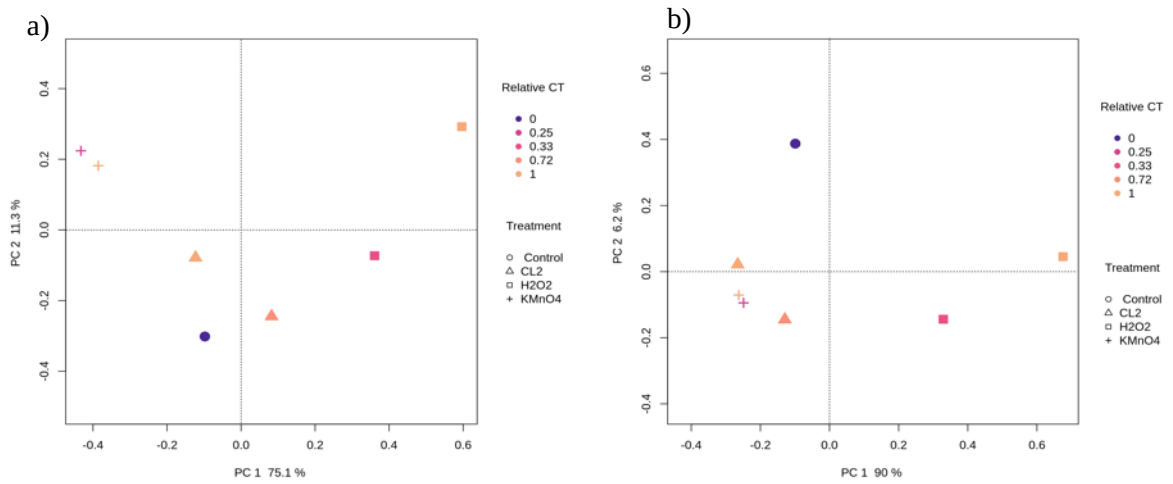

Figure B.1 Principal components analysis (PCA) of the normalized relative abundance of comparative metagenomics reads in 29 August 2018 sample. Data are plotted following the genus-level classification (a) PCA analysis of bacterial community following oxidation using different CT (b) PCA of the cyanobacterial community following oxidation using different CT.

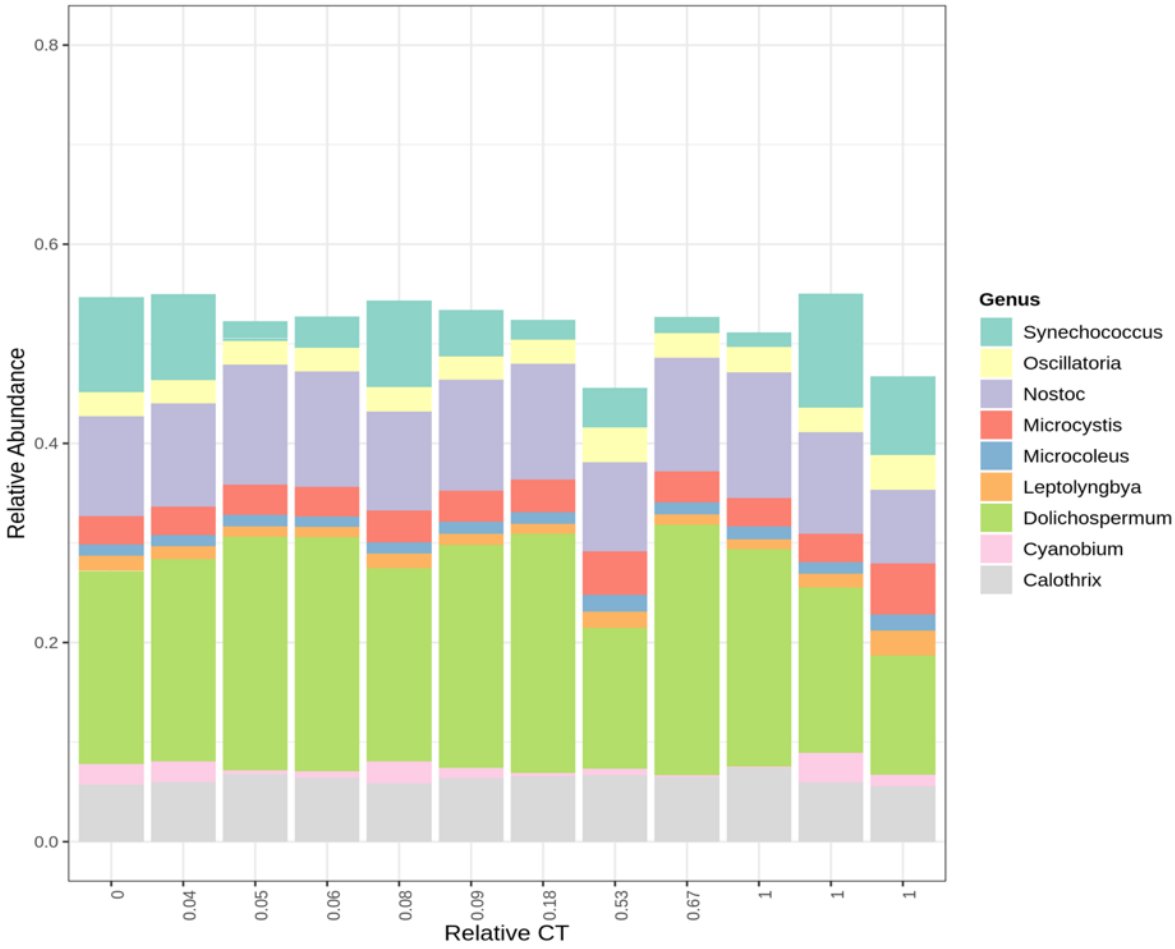

Figure B.2 Relative abundance of the most abundant genus following the oxidation using Cl_2, $KMnO_4$, H_2O_2 (1 August 2018 abundant: *Dolichospermum*).

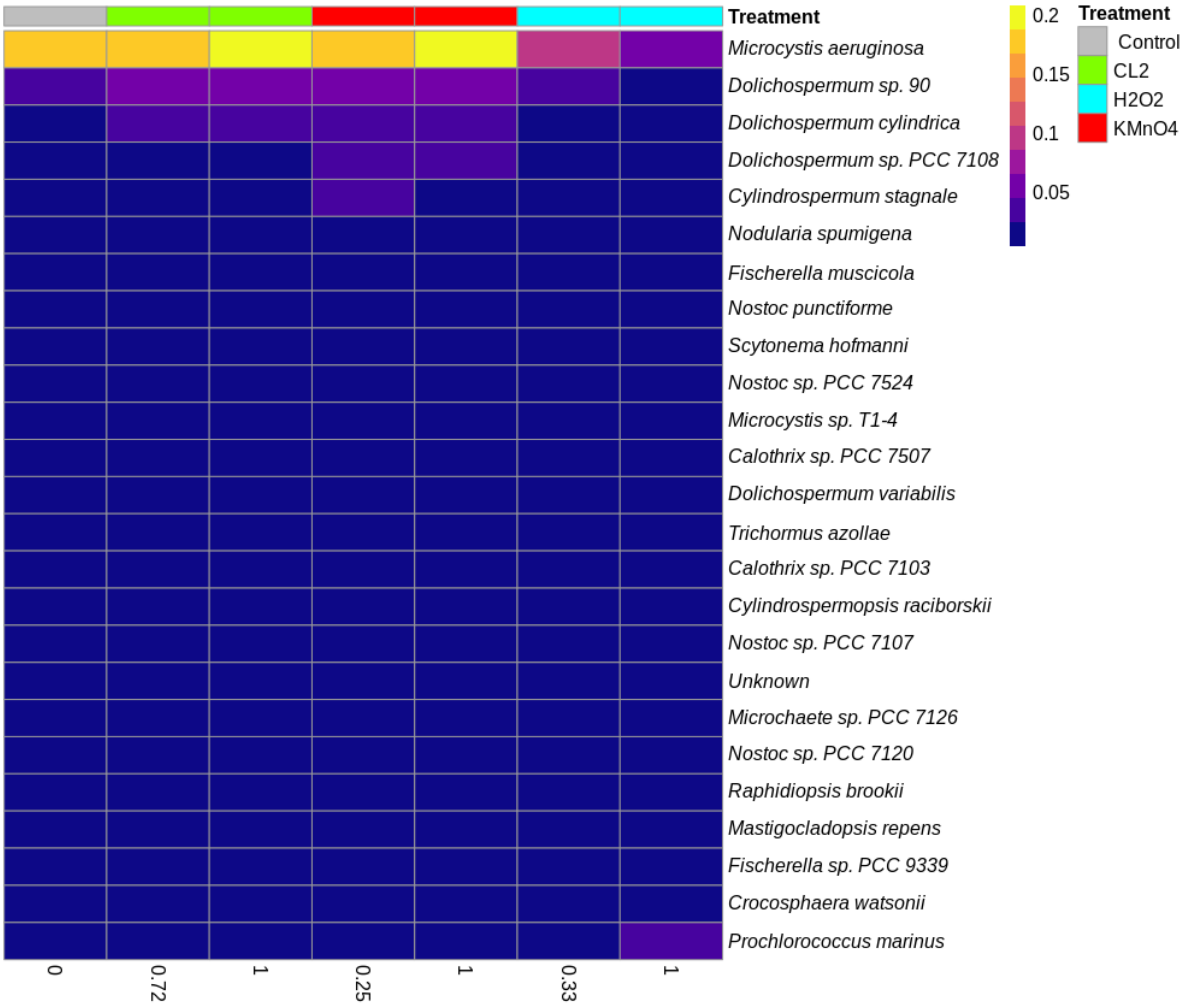

Figure B.3 Cyanobacterial species heat map following the oxidation using Cl_2, $KMnO_4$, H_2O_2 (29 August 2018 abundant: *Microcystis*).

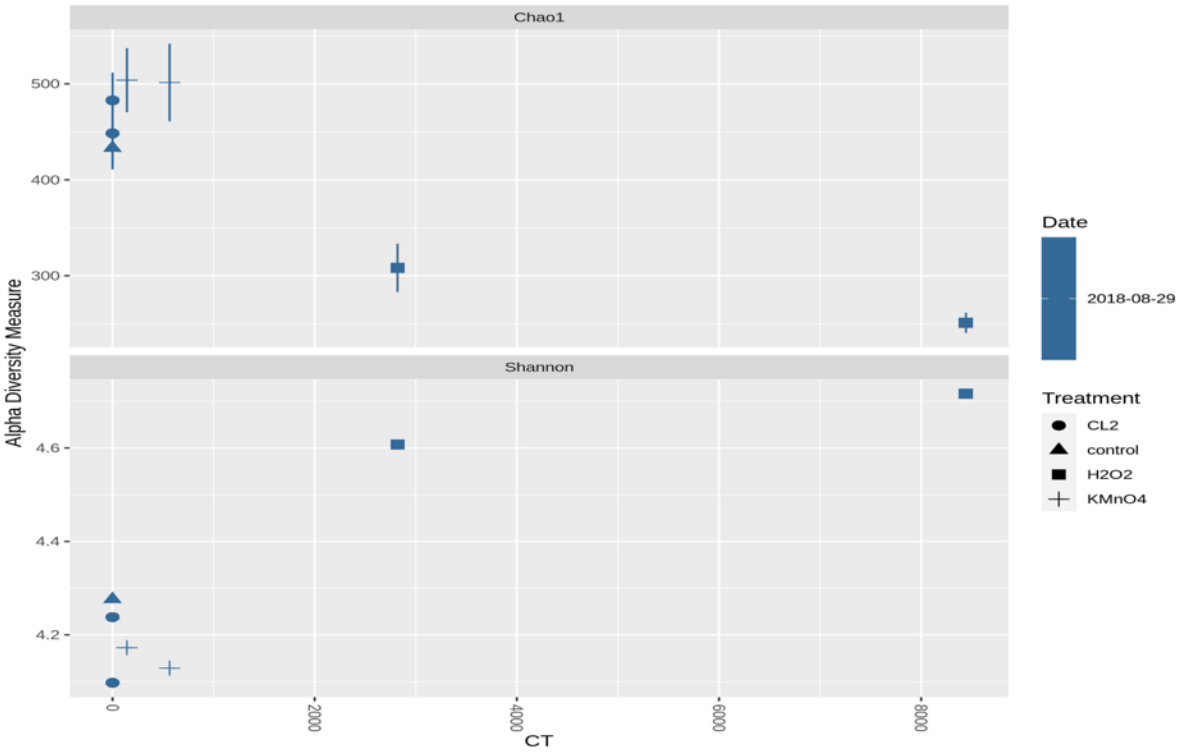

Figure B.7 Alpha diversity measures of cyanobacterial community following oxidation Cl_2, $KMnO_4$, H_2O_2 (29 August 2018, abundant genus: *Microcystis*).

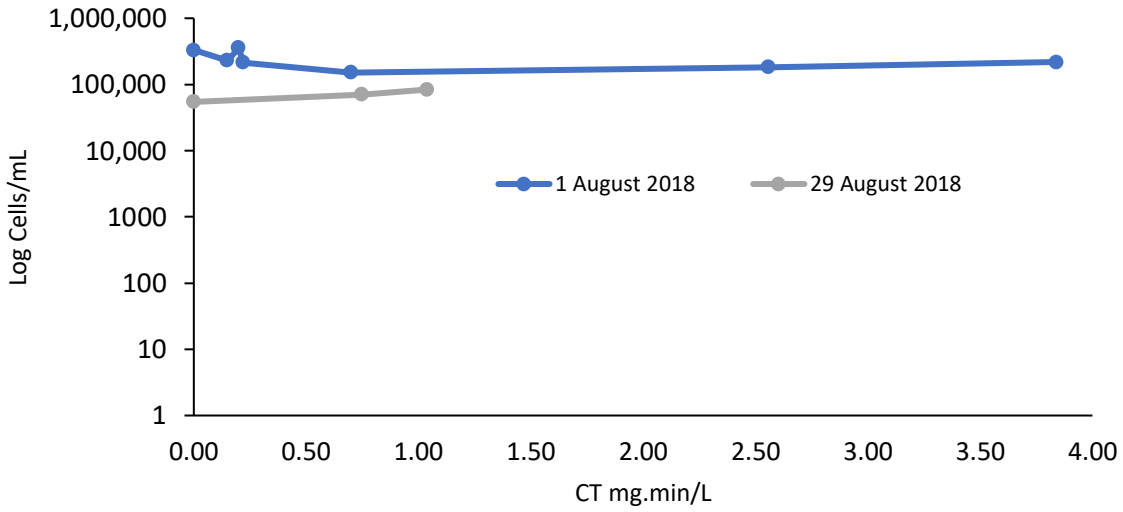

Figure B.5 Total cyanobacteria cell counts following chlorination for 1 August 2018 trial and 29 August 2018 trial.

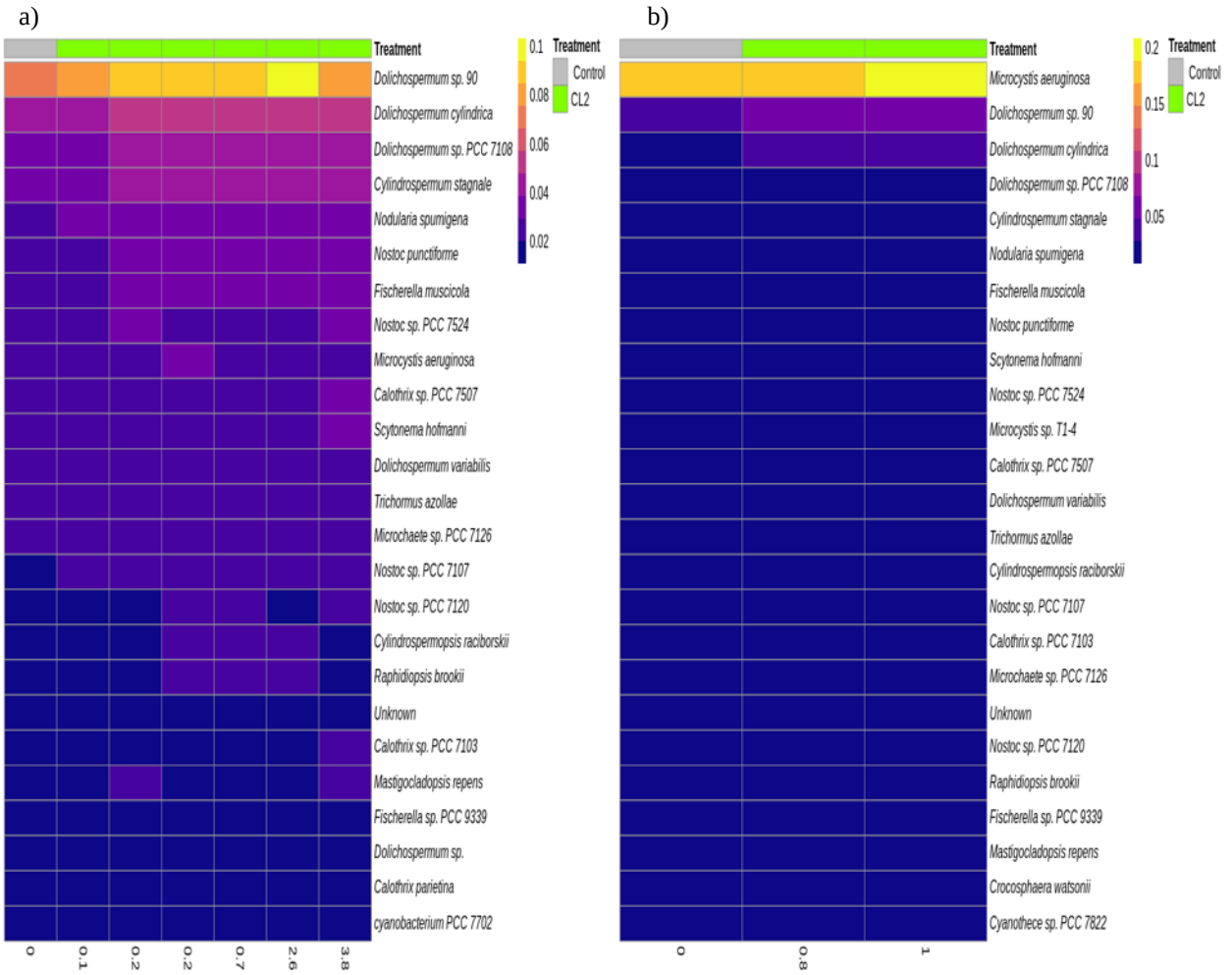

Figure B.6 Cyanobacterial species heat map following the chlorination (a) 1 August 2018 trial, (b) 29 August 2018 trial.

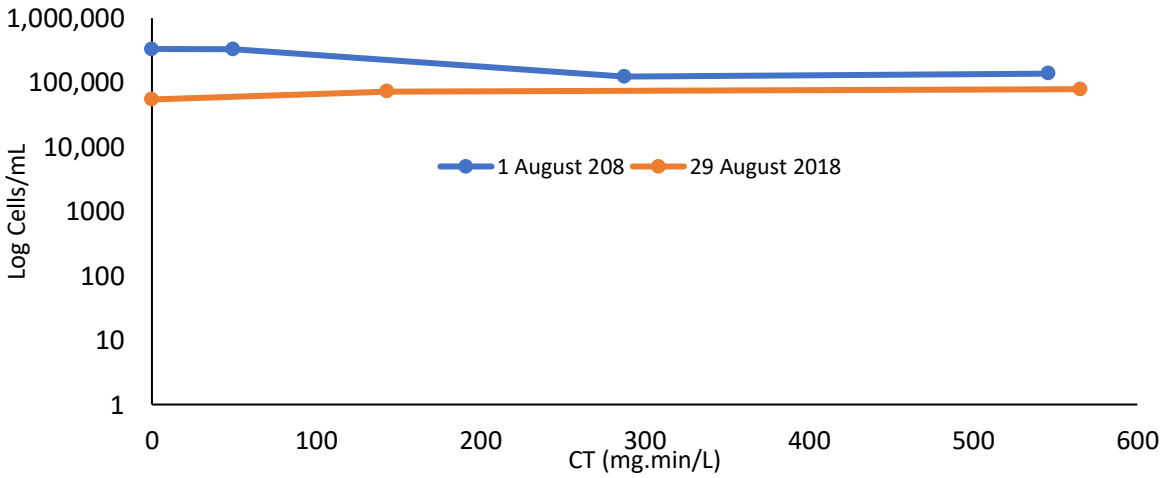

Figure B.7 Total cyanobacteria cell counts following the permanganate oxidation for 1 August 2018 trial and 29 August 2018 trial.

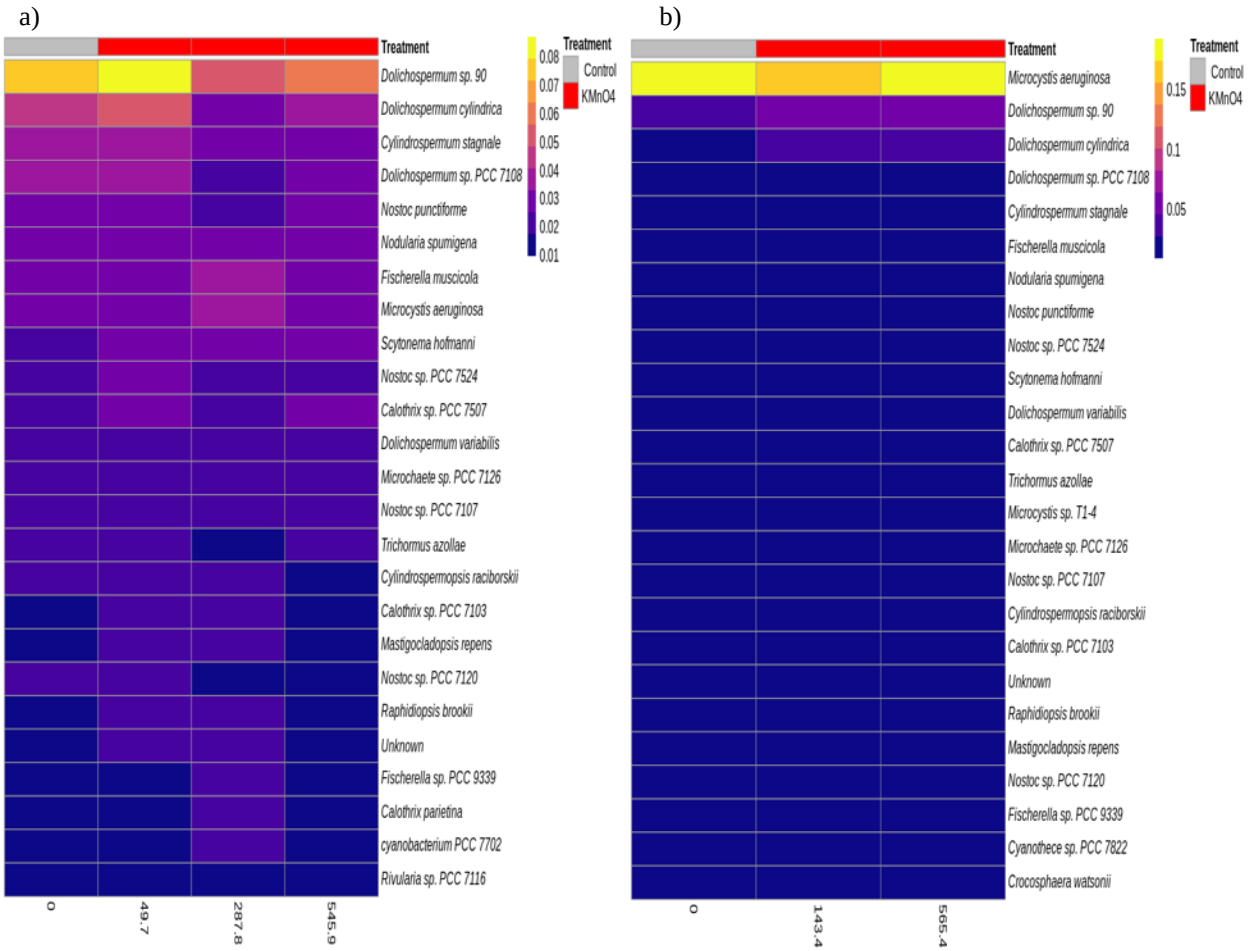

Figure B.8 Cyanobacterial Species heat map following the oxidation using $KMnO_4$ (a) 1 August 2018 trial, (b) 29 August 2018 trial

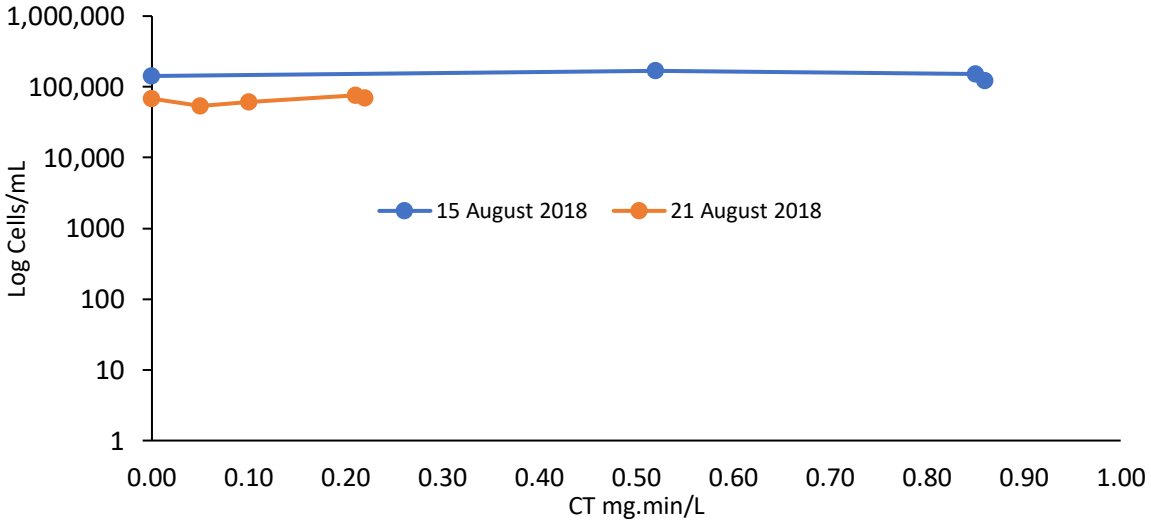

Figure B.9 Total cyanobacteria cell counts following the O_3 oxidation for 15 August 2018 trial and 21 August 2018 trial.

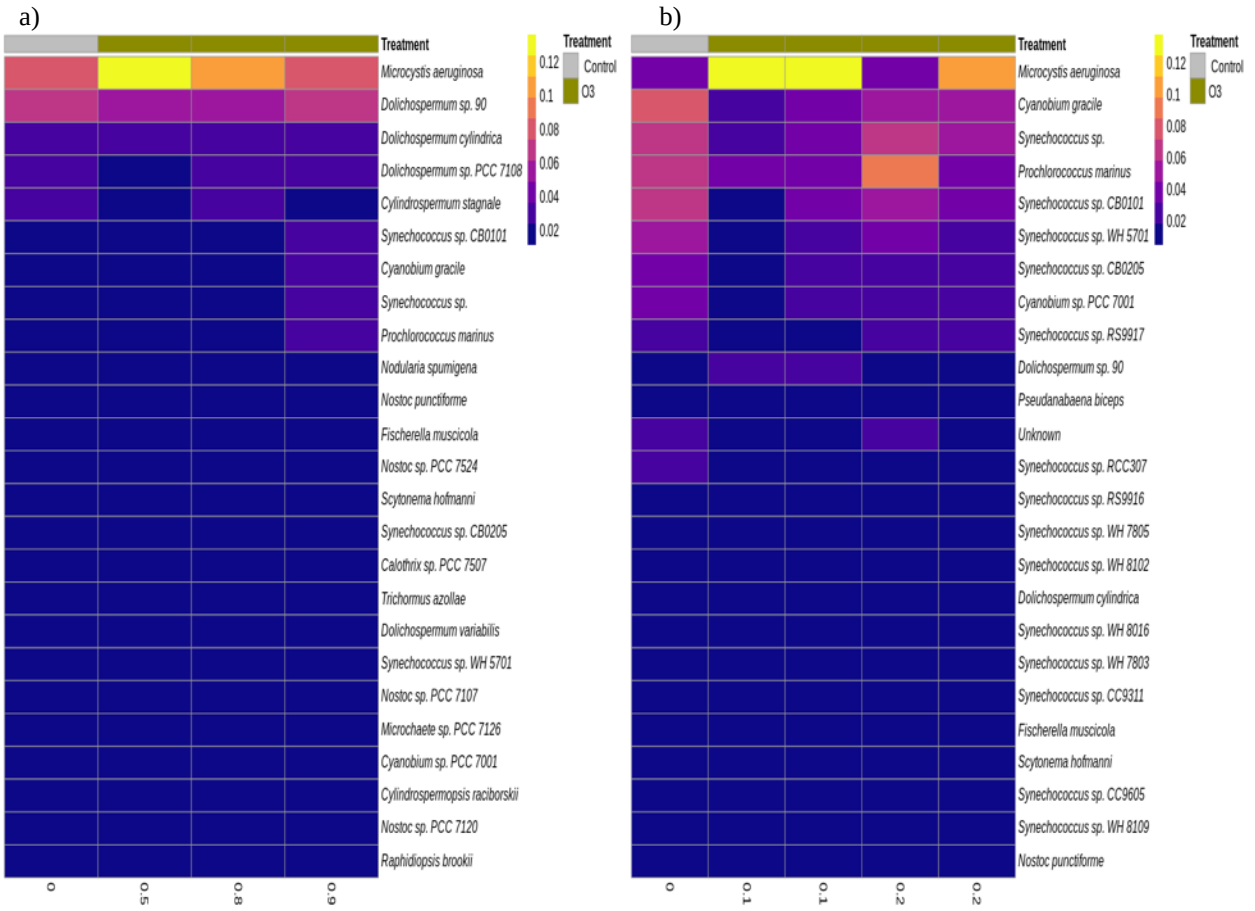

Figure B.10 Cyanobacterial Species heat map following the oxidation using O_3 (a) 15 August 2018 trial, (b) 21 August 2018 trial.

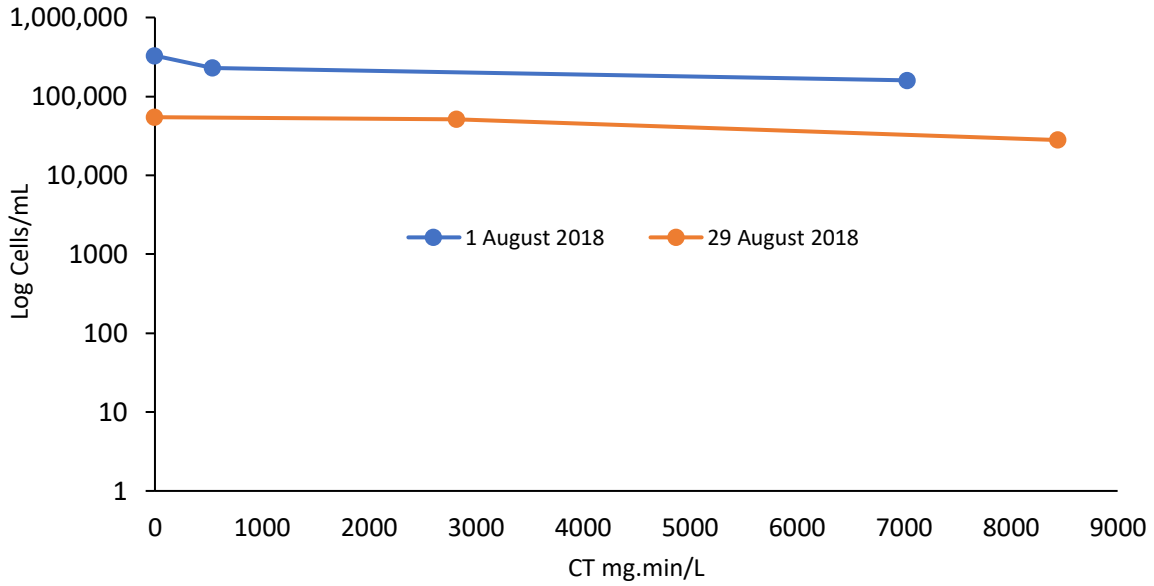

Figure B.11 Total cyanobacteria cell counts following the H_2O_2 oxidation for 1 August 2018 trial and 29 August 2018 trial.

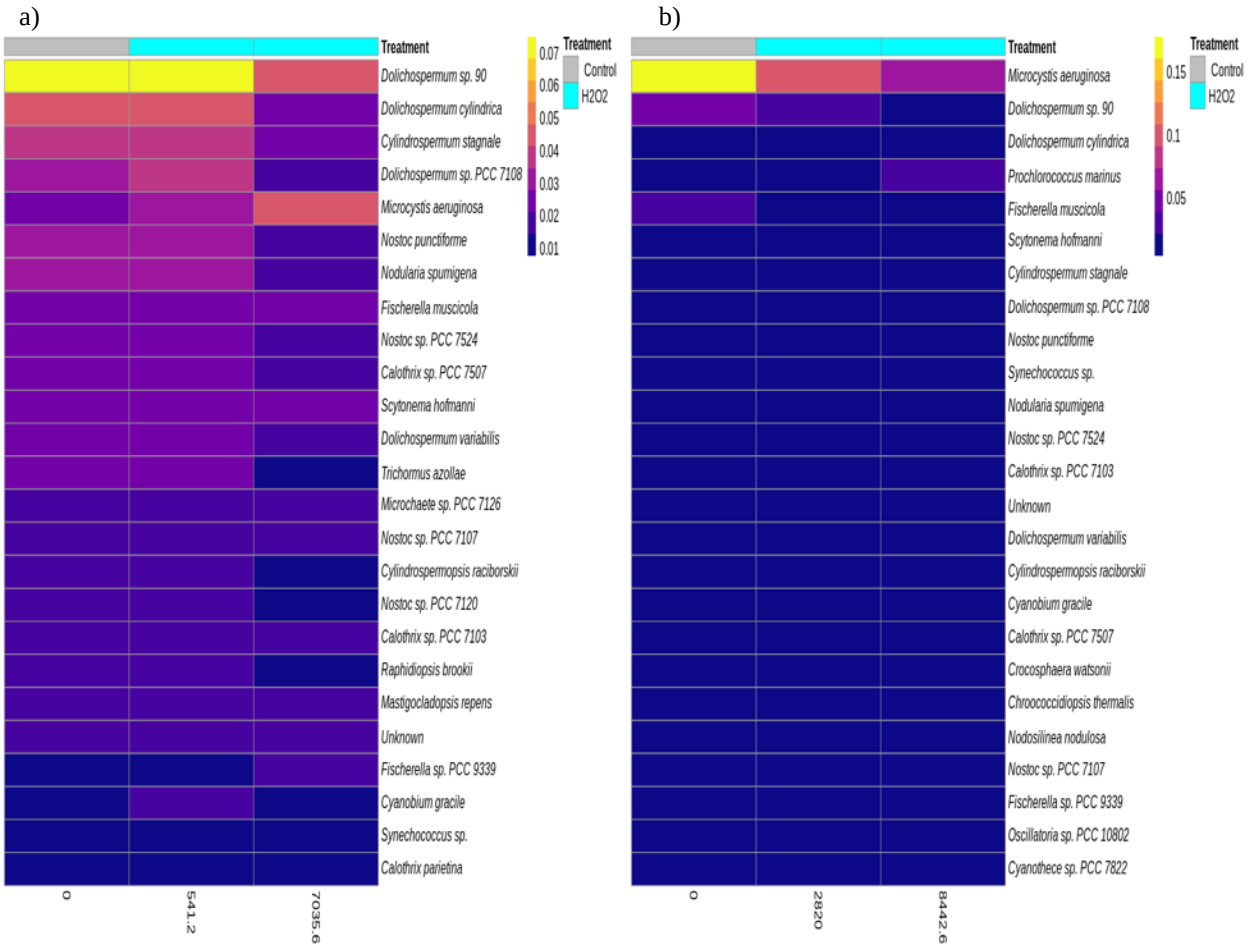

Figure B.12 Cyanobacterial Species heat map following the oxidation using H_2O_2 (a) 1 August 2018 trial (b) 29 August 2018 trial.

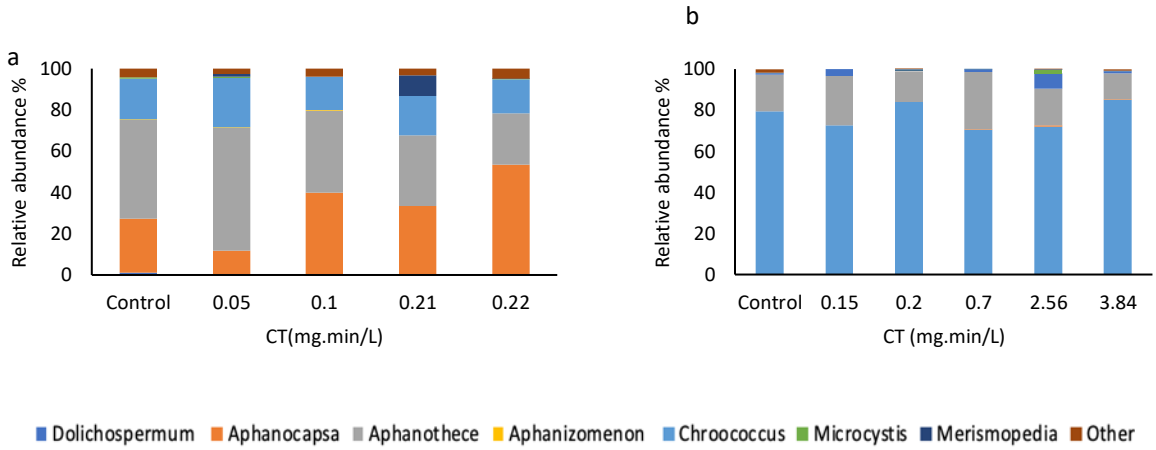

Figure B.13 Relative abundance of cyanobacteria species (via light Microscopy) following oxidation (a) O_3 second trial (15 August 2018) (b) Cl_2 first trial (1 August 2018).

Appendix C SUPPLEMENTARY INFORMATION, ARTICLE 3

Journal: *Chemical Engineering Journal Advances*

Title: Evaluation of functional capacity of a cyanobacterial bloom during oxidation

Authors: Saber Moradinejad, Hana Trigui, Juan Francisco Guerra Maldonado, B. Jesse Shapiro, Yves Terrat, Sébastien Sauvé, Nathalie Fortin, Arash Zamyadi, Sarah Dorner, Michèle Prévost

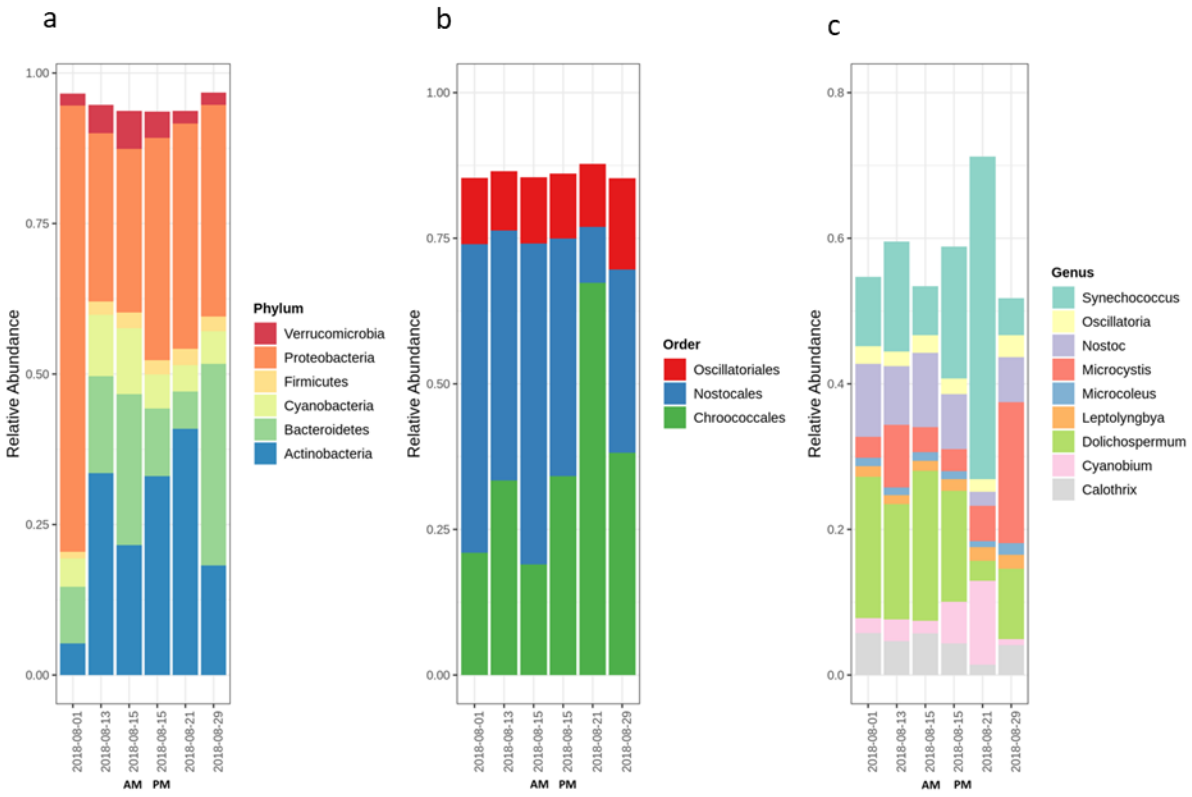

Figure C.1 Bloom-associated cyanobacterial members observed at the intake of the drinking water production plant in Missisquoi Bay, Lake Champlain during the month of August, 2018: a) phylum, b) orders belonging to cyanobacterial phylum, c) genera belonging to the *Nostocales*, *Chrooccocales* and, *Oscillatoriales* orders adapted from (Moradinejad et al., 2020).

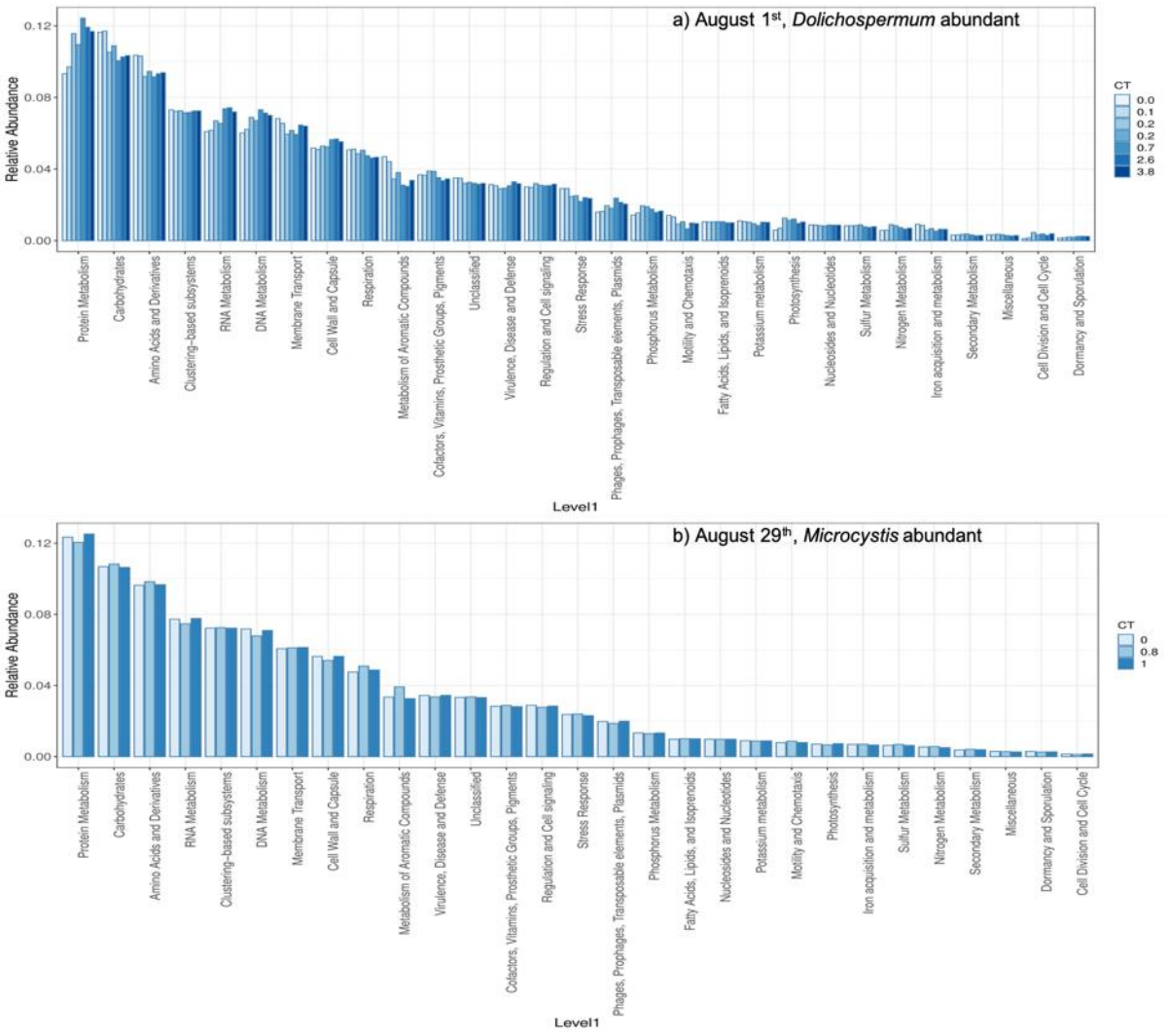

Figure C.2 Functional capacity of the cyanobacterial bloom during Cl_2, oxidation, a) August 1st, *Dolichospermum* was the most abundant genus, b) August 29th, *Microcystis* was the most abundant genus. The analysis was generated from the metagenomics dataset.

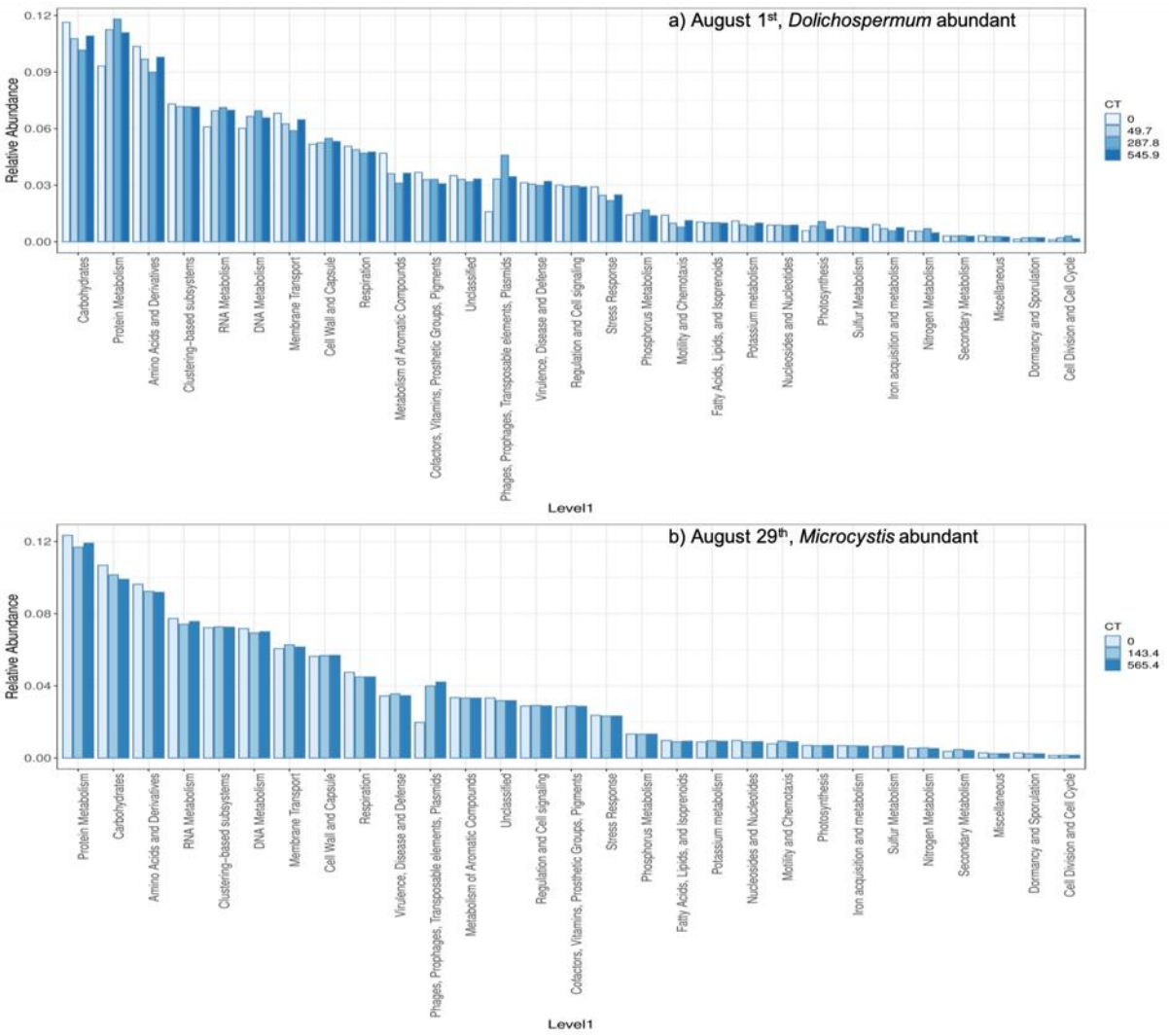

Figure C.3 Functional capacity of the cyanobacterial bloom during $KMnO_4$ oxidation, a) August 1st, *Dolichospermum* was the most abundant genus, b) August 29th, *Microcystis* was the most abundant genus. The analysis was generated from the metagenomics dataset.

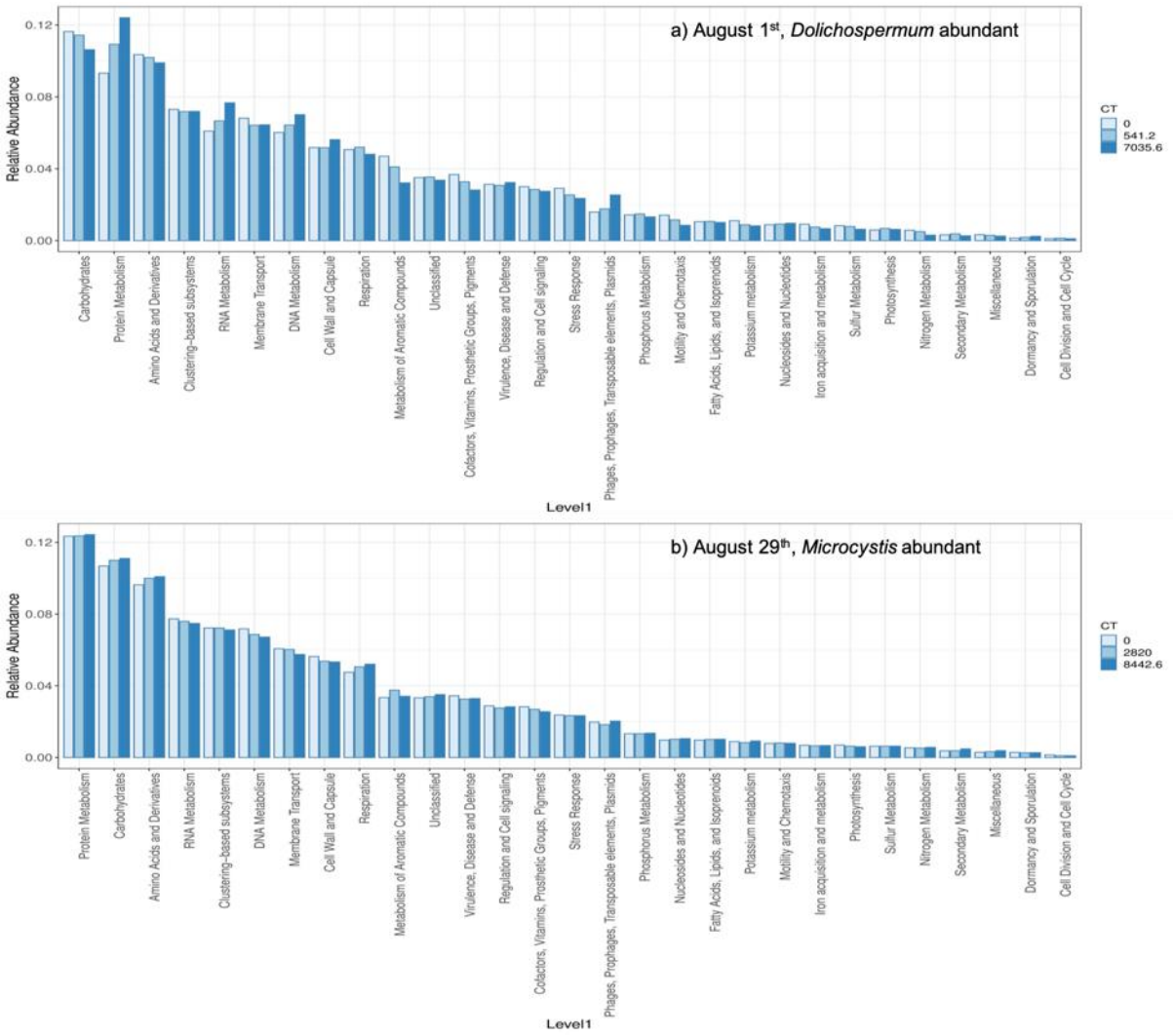

Figure C.4 Functional capacity of the cyanobacterial bloom during H_2O_2 oxidation, a) August 1st, *Dolichospermum* was the most abundant genus, b) August 29th, *Microcystis* was the most abundant genus. The analysis was generated from the metagenomics dataset.

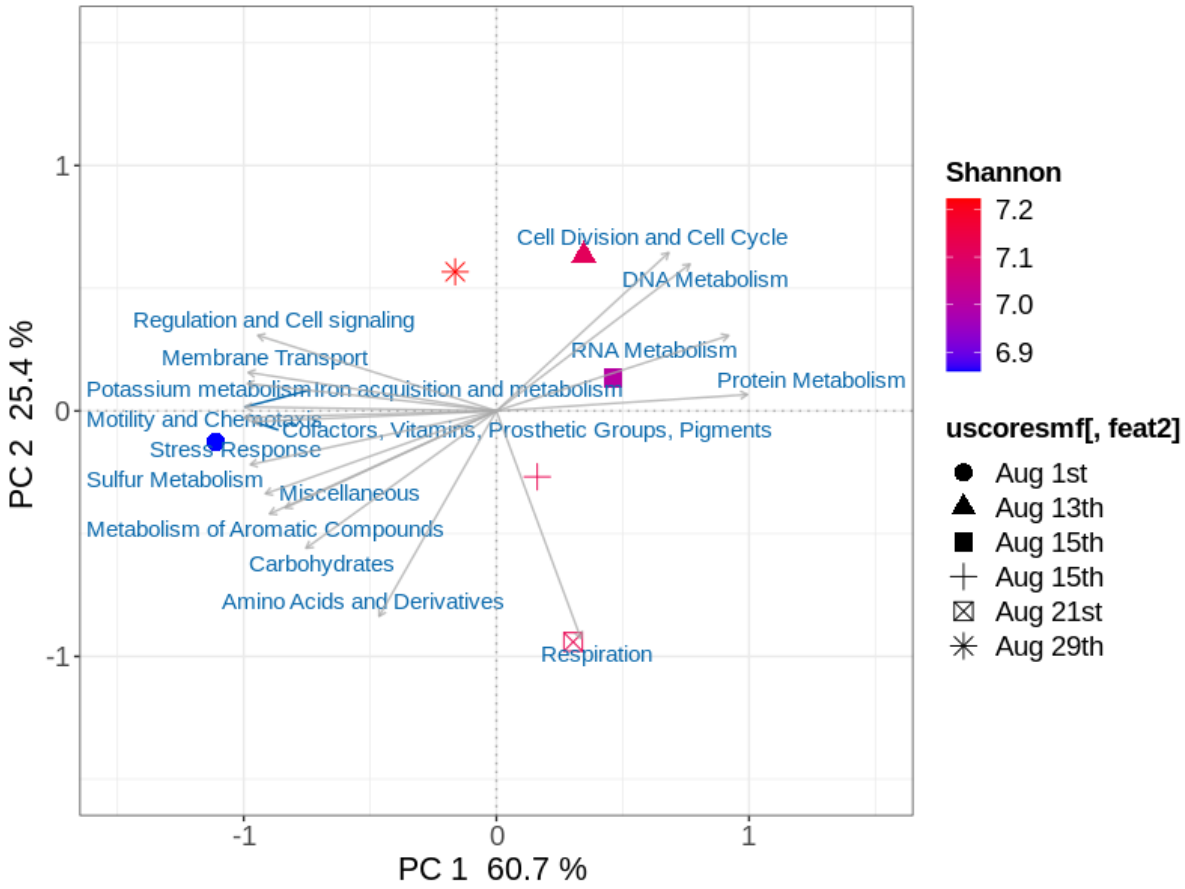

Figure C.5 PCA functional profiles of cyanobacterial bloom samples collected at the intake of the drinking water production plant in Missisquoi Bay, Lake Champlain during the month of August 2018. The analysis was generated from the metagenomics dataset.

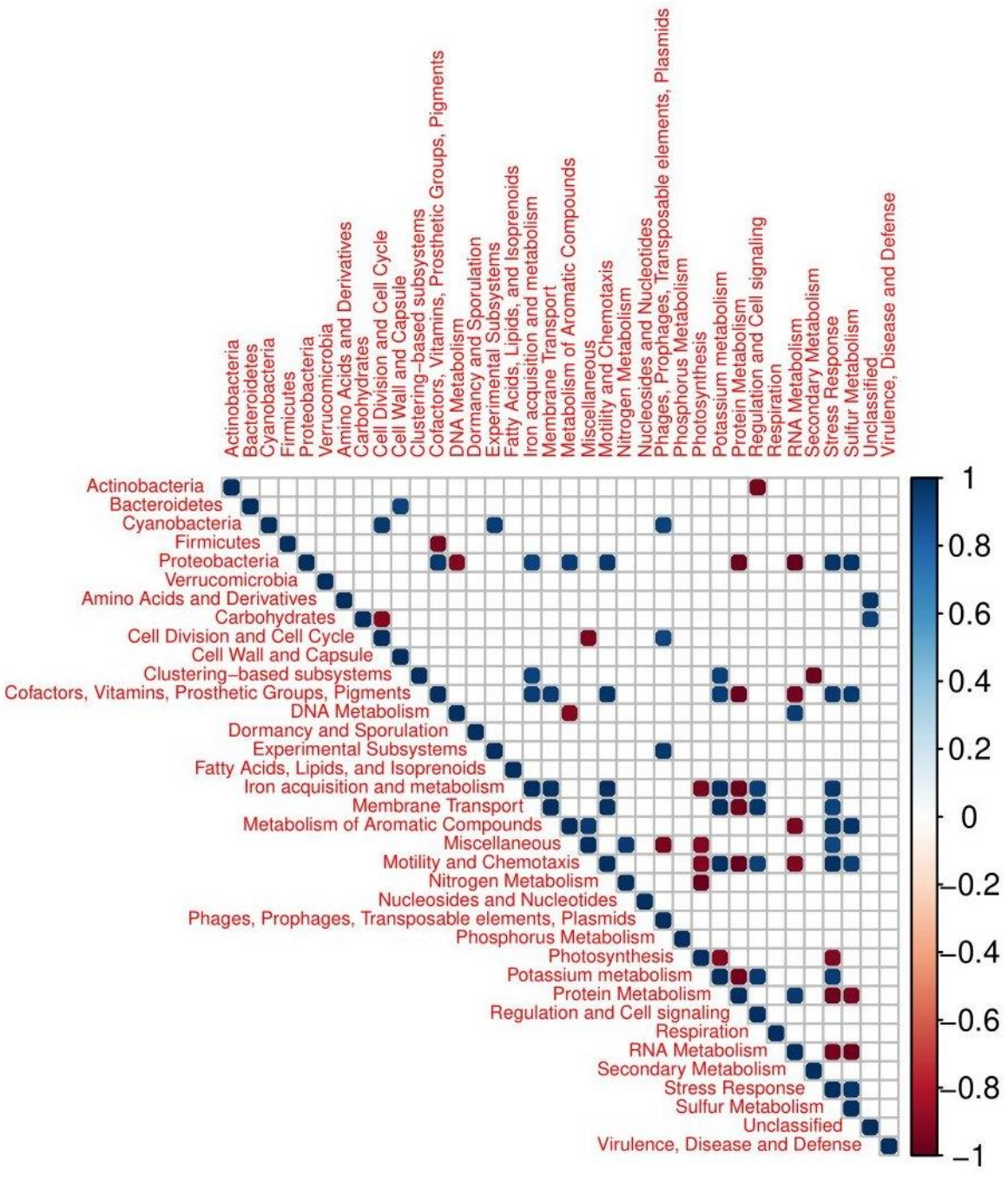

Figure C.6 Analysis of correlations between functional and taxonomic profiles identified in the cyanobacterial bloom at the intake of the drinking water production plant in Missisquoi Bay, Lake Champlain during the month of August 2018.

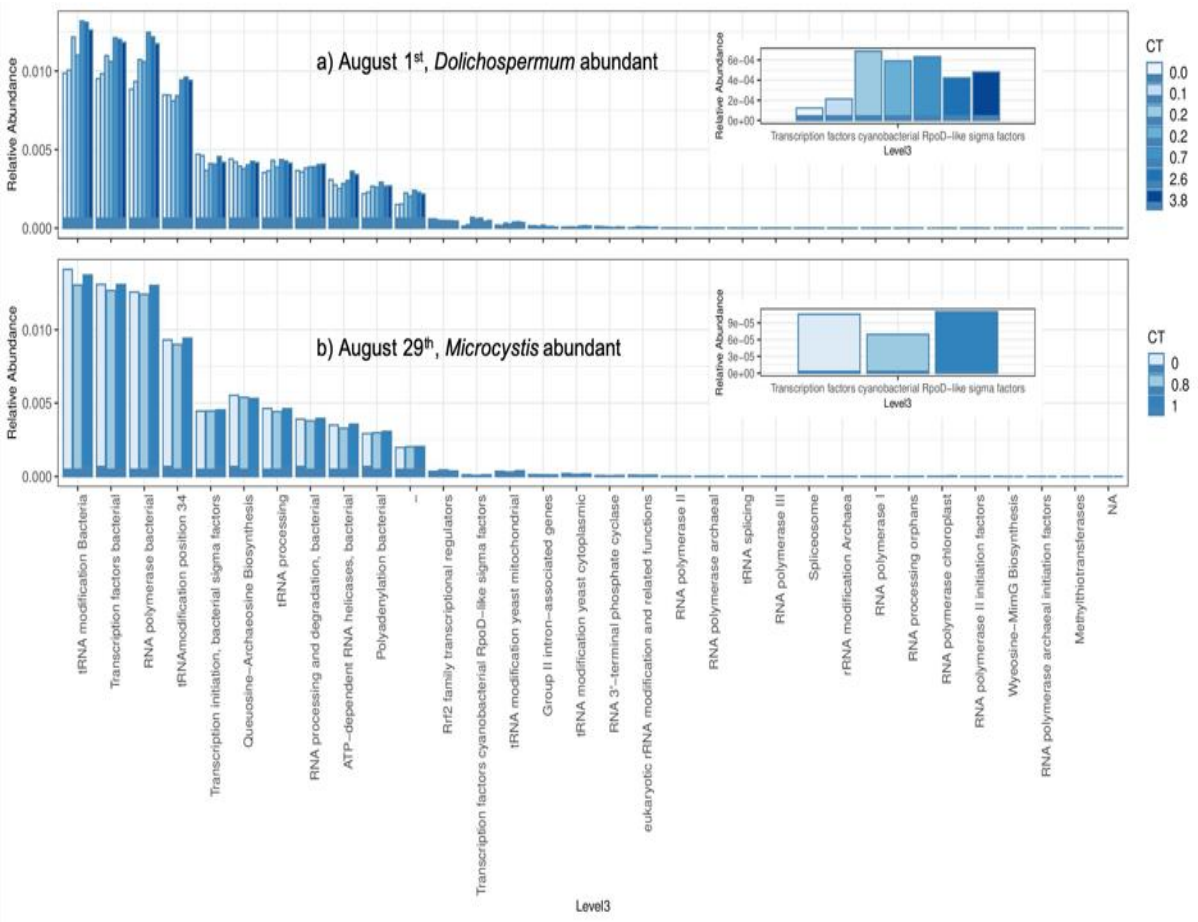

Figure C.7 Impact of oxidation stress on RNA Metabolism includes rpoD-Like biomarker following Cl_2 oxidation, a) August 1st, *Dolichospermum* was the most abundant genus, b) August 29th, *Microcystis* was the most abundant genus. The analysis was generated from the metagenomics dataset.

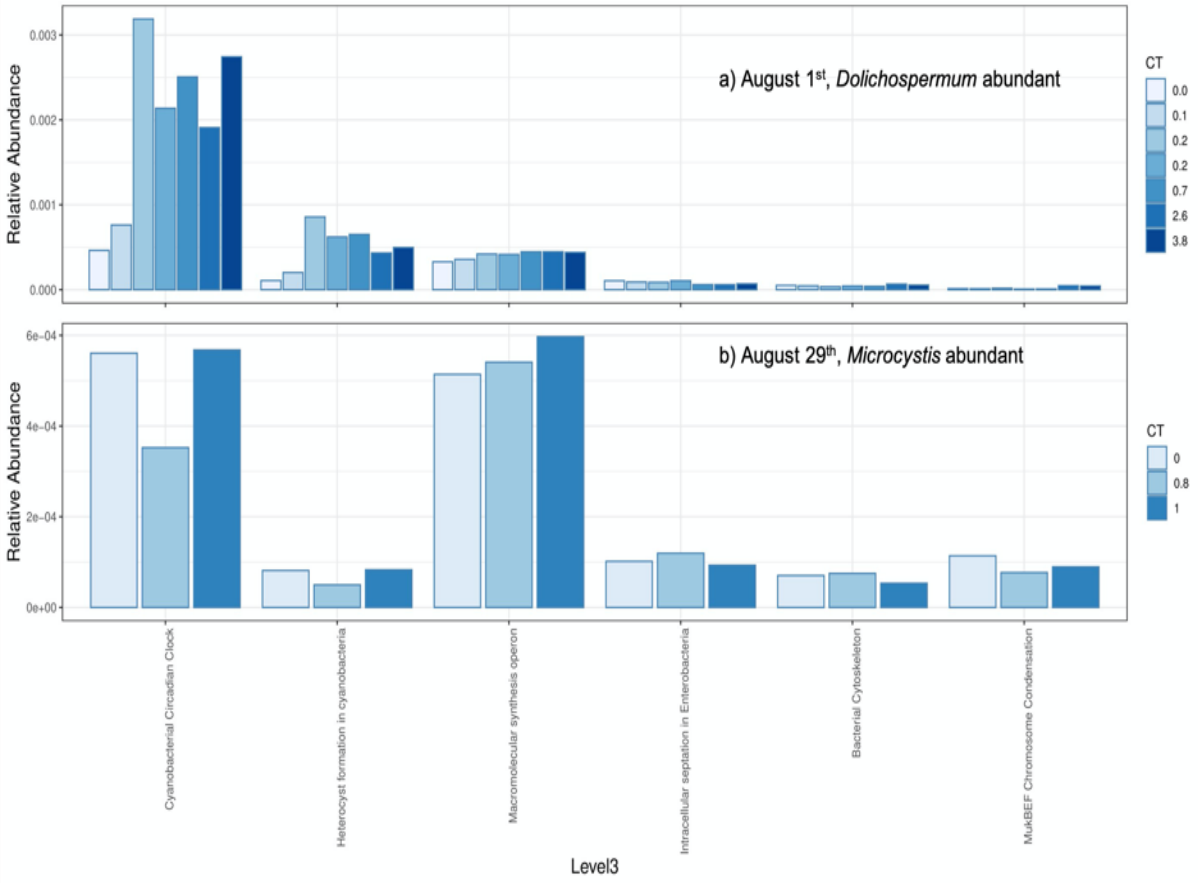

Figure C.8 Impact of oxidation stress on cyanobacterial cell division and cell cycle subsystems following Cl_2 oxidation, a) August 1st, *Dolichospermum* was the most abundant genus, b) August 29th, *Microcystis* was the most abundant genus. The analysis was generated from the metagenomics dataset.

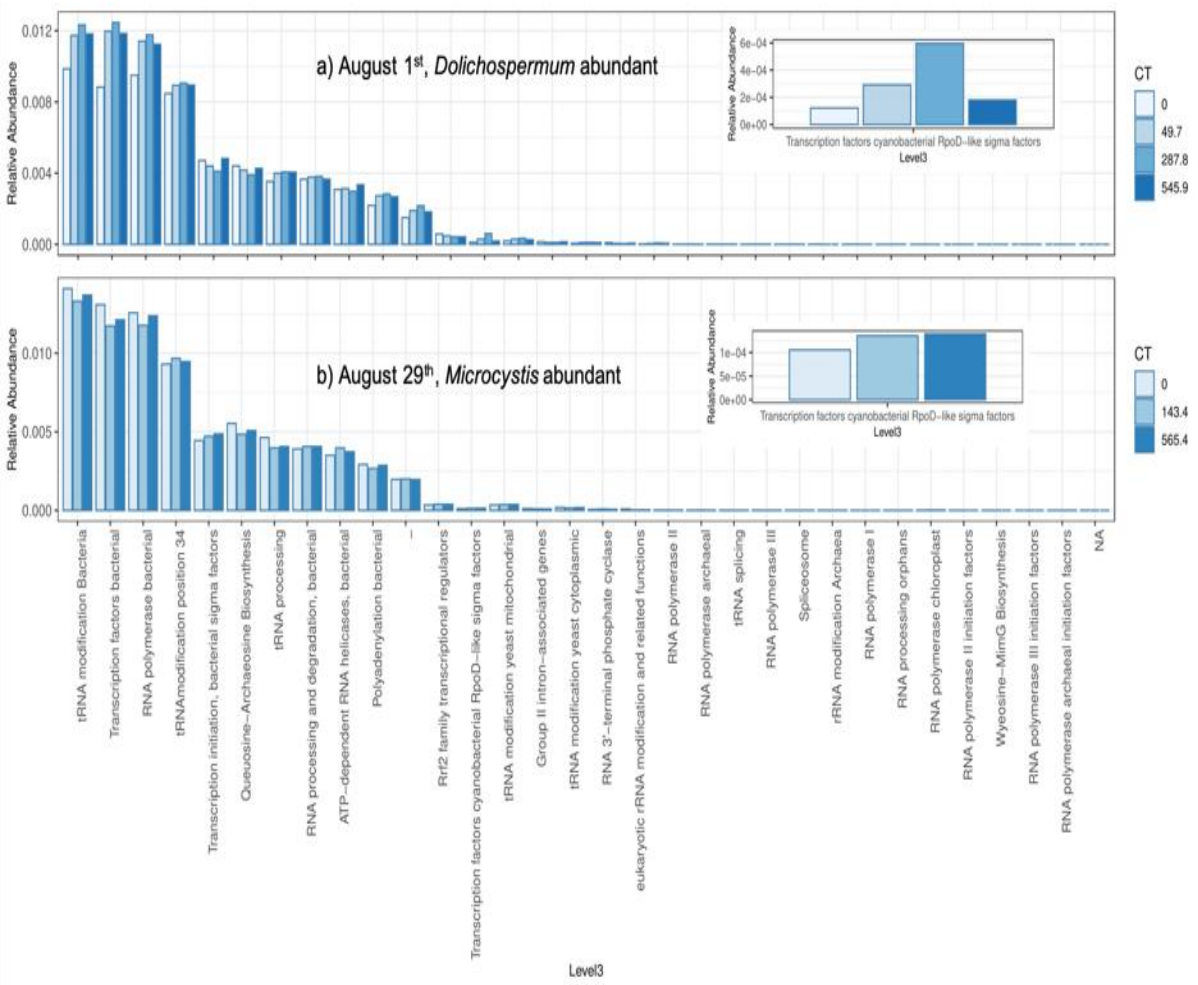

Figure C.9 Impact of oxidation stress on RNA Metabolism includes rpoD-Like biomarker following $KMnO_4$ oxidation, a) August 1st, *Dolichospermum* was the most abundant genus, b) August 29th, *Microcystis* was the most abundant genus. The analysis was generated from the metagenomics dataset.

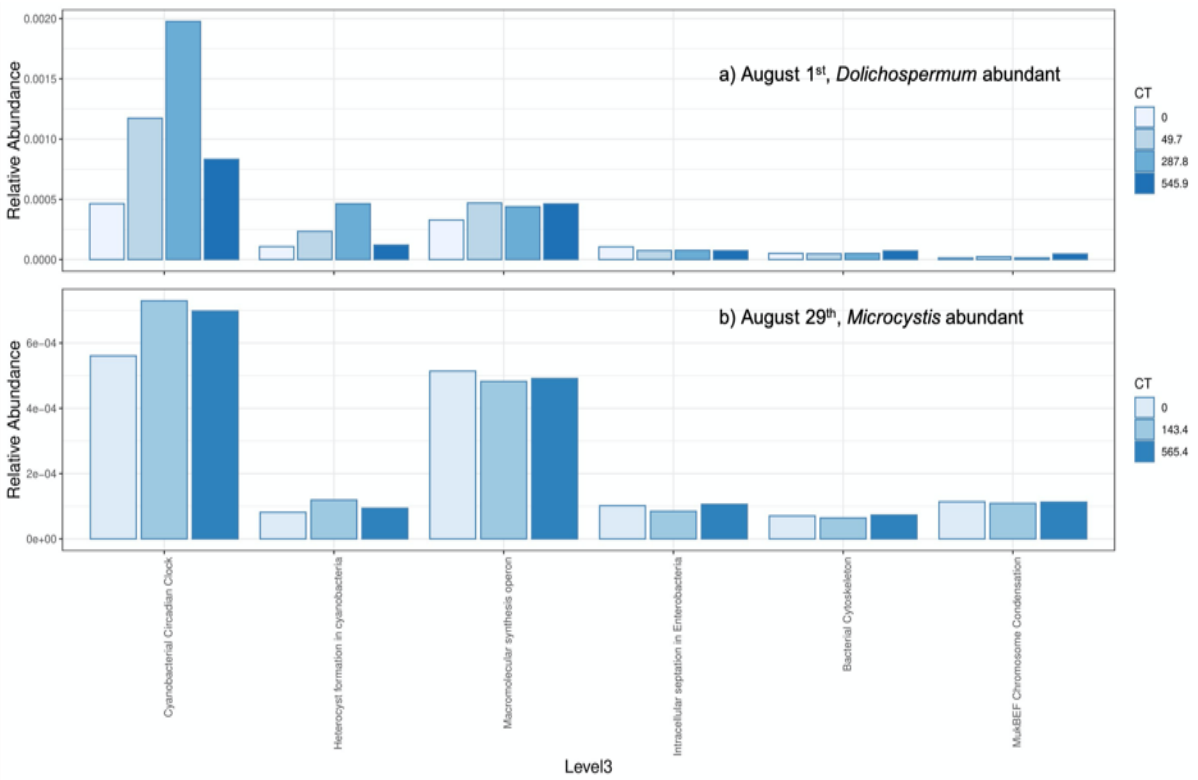

Figure C.10 Impact of oxidation stress on cyanobacterial cell division and cell cycle subsystems following $KMnO_4$ oxidation, a) August 1st, *Dolichospermum* was the most abundant genus, b) August 29th, *Microcystis* was the most abundant genus. The analysis was generated from the metagenomics dataset.

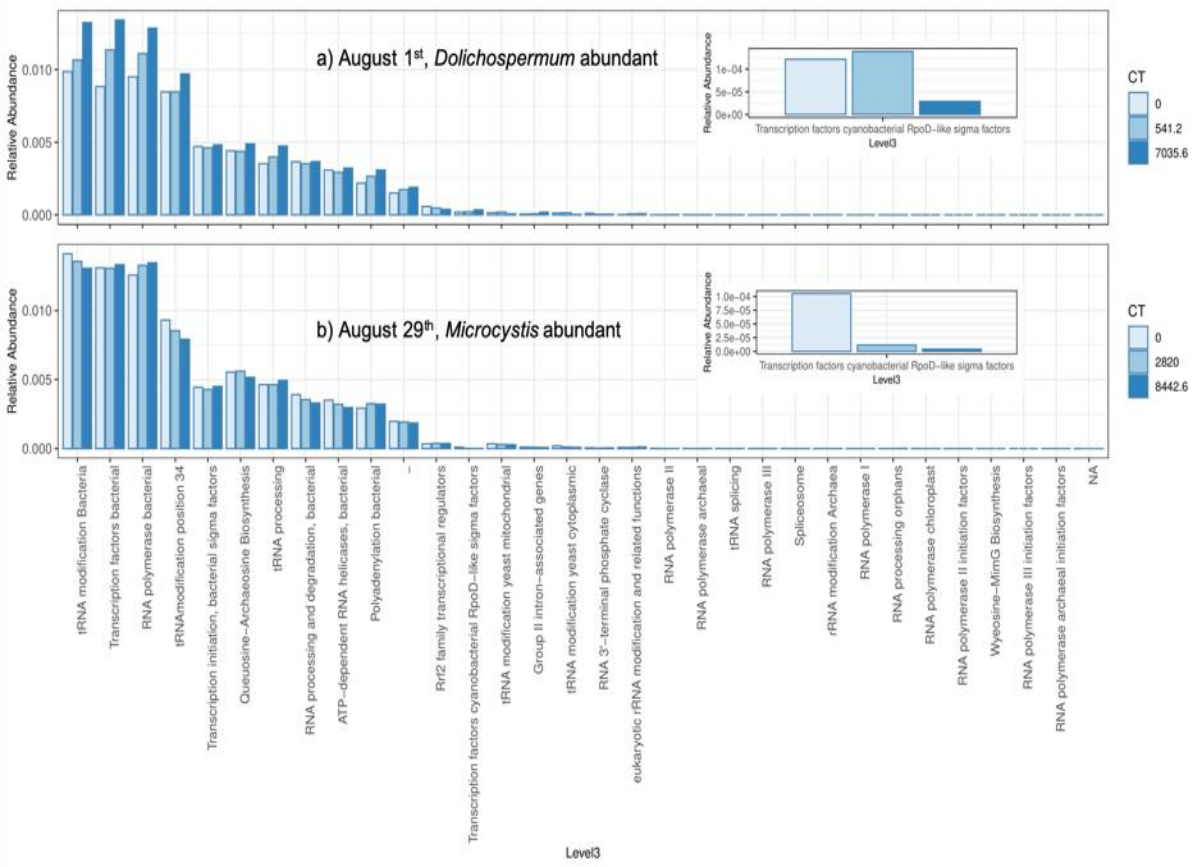

Figure C.11 Impact of oxidation stress on RNA Metabolism includes rpoD-Like biomarker following H_2O_2 oxidation, a) August 1st, *Dolichospermum* was the most abundant genus, b) August 29th, *Microcystis* was the most abundant genus. The analysis was generated from the metagenomics dataset.

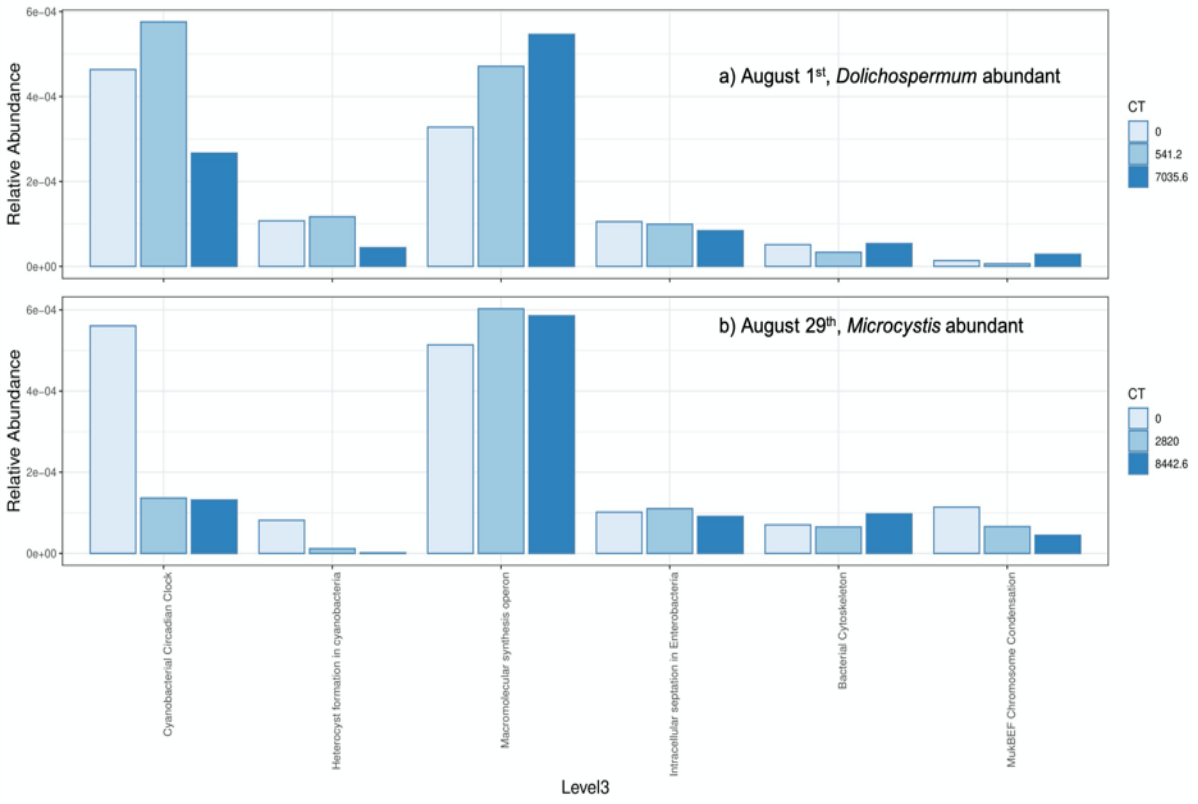

Figure C.12 Impact of oxidation stress on cyanobacterial cell division and cell cycle subsystems following H_2O_2 oxidation, a) August 1st, *Dolichospermum* was the most abundant genus, b) August 29th, *Microcystis* was the most abundant genus. The analysis was generated from the metagenomics dataset.

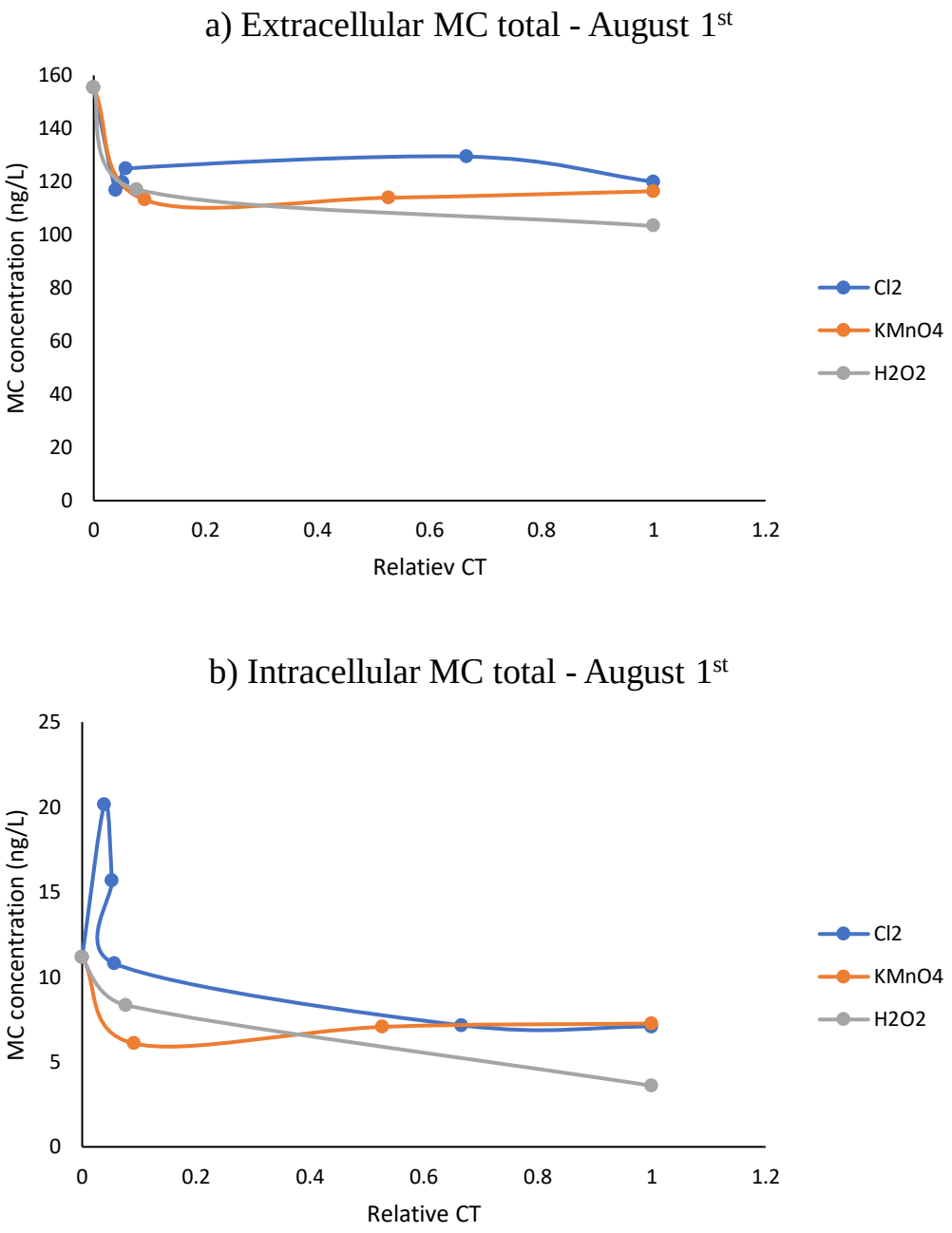

Figure C.13 Microcystin concentrations following oxidation with Cl_2, $KMnO_4$ and H_2O_2 on August 1st, 2018 a) Extracellular microcystin, b) Intracellular microcystin.

RNA integrity following oxidation

Table C.1 The experimental design for RNA integrity during oxidation

Oxidant	Water type	Cyanobacteria Species	Oxidant dose	Contact time
Cl_2	Natural water (SJSR)	Mix of *Microcystis* (50%) and *Dolichospermum* (50%) 200,000 cell/mL each	3 mg/L	2 min 5 min 30 min 1 h 2 h
$KMnO_4$			10 mg/L	30 min 1 h 2 h 4 h